TESIS CARRERA DE DOCTORADO EN FÍSICA

MODELOS DE HIGGS COMPUESTO PARA FÍSICA DE SABOR Y ANOMALÍAS DE MESONES B

Federico Lamagna
Doctorando

Dr. Leandro Da Rold
Director

Miembros del Jurado
Dr. Diego Harari (Instituto Balseiro)
Dr. Aníbal Medina (Instituto de Física La Plata)
Dr. Esteban Roulet (Centro Atómico Bariloche)
Dr. Alejandro Szynkman (Instituto de Física La Plata)

Noviembre de 2022

Física de Partículas – Centro Atómico Bariloche

Instituto Balseiro
Universidad Nacional de Cuyo
Comisión Nacional de Energía Atómica
Argentina

A mi familia por el apoyo incondicional, y a los amigos que están siempre.

Agradecimientos

Como primera instancia quisiera agradecer a Leandro por todo lo que aprendí en estos años. Por su calidad profesional y por ser una excelente persona. Y en particular en cuanto al presente trabajo, por la minuciosa lectura del manuscrito, y por discusiones muy enriquecedoras.

En cuanto a mi estadía en el Instituto, quisiera agradecer a todos los colegas, docentes y amigos del Centro Atómico Bariloche. Quisiera mencionar al Fresco, por todas las charlas sobre física y matemática que sirvieron para mejorar mi entendimiento sobre algunos tópicos presentes en esta tesis. Además por tener siempre la buena voluntad y disposición para ayudar en lo que sea.

Además quisiera agradecer al ICAS por darme la oportunidad de realizar una estadía en el mismo. Puntualmente a Ezequiel Álvarez y a Manuel Szewc, quienes resultaron excelentes colaboradores y personas, siempre mostrando la máxima motivación y energía para encarar cualquier cuestión.

A Conicet, por brindarme la oportunidad de formarme estos años. Al Instituto Balseiro, al Centro Atómico Bariloche y puntualmente al Grupo de Partículas y Campos por brindar un excelente lugar para esto mismo.

Contents

List of Figures

List of Tables

Resumen

Los modelos de Higgs Compuesto, donde una teoría de campos fuertemente interactuante genera al Higgs como un pseudo bosón de Nambu-Goldstone, son capaces de resolver el Problema de la Jerarquía de la escala electrodébil, asi como proveer una explicación para el problema de la pequeña jerarquía, naturalmente ubicando la escala de nueva física en unos pocos TeV. En estos modelos la estructura de sabor emerge a bajas energías, teniendo potencialmente un impacto grande en la física de sabor. En la presente tesis exploramos la habilidad de los modelos de Higgs Compuesto para explicar un conjunto de desviaciones en decaimientos de mesones B medidas recientemente en diversos experimentos, así como nuevos escenarios compatibles con resonancias a la escala TeV. Consideramos la descripción efectiva de estas teorías, determinada por el patrón de ruptura de simetrías y trabajamos con los primeros niveles de resonancias.

Las llamadas anomalías de la física del B son un conjunto de mediciones experimentales expresadas en términos de cocientes de decaimientos de mesones B que, estando en tensión con la predicción del Modelo Estándar, podrían indicar la existencia de nueva física a la escala del TeV. Asimismo, como requieren nueva física mayormente acoplada a la tercera generación de fermiones, resulta natural buscar una explicación común de las anomalías-B junto con el Problema de la Jerarquía con modelos de Higgs compuesto. Proponemos y exploramos diversos modelos que contienen leptoquarks compuestos que pueden proveer los operadores apropiados para explicar las anomalías. Eligiendo el patrón de ruptura de simetría global obtenemos: un modelo con un leptoquark escalar S_3, un modelo con dos leptoquarks escalares, S_1 y S_3, y un modelo con un leptoquark vectorial U_1. Si bien el modelo con S_3 no es capaz de explicar simultáneamente todas las anomalías-B, los otros dos modelos sí lo son. Mostramos como esto es naturalmente posible gracias a la estructura obtenida con acoplamientos anárquicos en el sector compuesto. Además obtenemos estados adicionales en el espectro de escalares: un cuadruplete de $\mathrm{SU}(2)_L$ que puede dar contribuciones a parámetros de precisión electrodébil, o un singlete del grupo de gauge del Modelo Estándar que puede ser un candidato a materia oscura. Calculamos el potencial que es generado dinámicamente, obteniendo las masas de los escalares, incluido el bosón de Higgs. Estudiamos los principales límites en cada modelo, donde encontramos cierta tensión, por ejemplo desviaciones en acoplamientos del bosón Z a quarks b o a neutrinos, así como en acoplamientos al bosón

W, o desviaciones en decaimientos del τ.

En una dirección diferente, construimos un modelo de sabor que combina Froggatt-Nielsen con composición parcial. Estudiamos los diferentes límites dados por física de sabor, donde encontramos supresión con respecto a composición parcial anárquica para algunos de los más rigurosos: en la contribución de quiralidad mixta a la mezcla $K^0-\bar{K}^0$ y en operadores dipolares de quarks encontramos una supresión de una y dos potencias del ángulo de Cabibbo, λ_C, respectivamente.

Palabras clave: INSTITUTO BALSEIRO, TESIS DOCTORAL, FÍSICA MÁS ALLÁ DEL MODELO ÉSTANDAR, HIGGS COMPUESTO, LEPTOQUARKS, ANOMALÍAS B, FÍSICA DE SABOR

Abstract

Composite Higgs models, where a strongly coupled field theory develops the Higgs as a pseudo Nambu-Goldstone boson, are able to solve the Hierarchy Problem of the electroweak scale, as well as to provide an explanation for the little hierarchy problem, naturally pushing the scale of new physics to a few TeV. In these models the structure of flavor emerges at low energies, with a large potential impact on flavor physics. In the present thesis we explore the ability of Composite Higgs models to explain a set of deviations in B-meson decays recently measured in several experiments, as well as new scenarios compatible with resonances at the TeV scale. We consider the effective description of these theories, determined by the pattern of symmetry breaking and working with the first levels of resonances.

The so called B-physics anomalies are a set of experimental measurements expressed in terms of ratios of decays of B-mesons that, being in tension with the Standard Model prediction, could signal the existence of new physics at the TeV scale. Moreover, since they require new physics mostly coupled to the third generation of fermions, it is natural to look for a common explanation of the B-anomalies as well as the Hierarchy Problem in Composite Higgs models. We propose and explore different models containing composite leptoquarks which can provide the right operators for accommodating the anomalies. By choosing the pattern of global symmetry breaking we obtain: a model with a scalar leptoquark S_3, a model with two scalar leptoquarks, S_1 and S_3, and a model with a vector leptoquark U_1. While the model with S_3 is not able to simultaneously explain all the B-anomalies, the other two models are. We show how the structure of couplings given by anarchic partial compositeness is naturally able to do so. We also obtain additional states in the scalar spectrum: a $\mathrm{SU}(2)_L$-fourplet which can give contributions to electroweak precision tests parameters, or a Standard Model gauge singlet which can be a candidate for dark matter. We compute the potential that is generated dynamically, obtaining the masses of the scalar states, including the Higgs boson. We study the main constraints in each model, finding certain tension, like deviations with Z couplings to b-quarks or neutrinos, as well as W-violating couplings, or deviations in tau decays.

In a different direction, we build a flavor model which combines Froggatt-Nielsen with partial compositeness. We study the different flavor constraints, finding suppres-

sion with respect to anarchic partial compositeness for some of the most stringent ones: in the mixed-chirality contribution to $K^0 - \bar{K}^0$ mixing and in the quark dipole operators we find a suppression of one and two powers of the Cabibbo angle, λ_C, respectively.

Keywords: INSTITUTO BALSEIRO, DOCTORAL THESIS, BEYOND THE STANDARD MODEL PHYSICS, COMPOSITE HIGGS, LEPTOQUARKS, B ANOMALIES, FLAVOR PHYSICS

Chapter 1

Introduction

Our current understanding of subatomic interactions is described by the Standard Model of particle physics (SM). This model includes all known particles and their interactions. It uses the language of Quantum Field Theory (QFT), a framework that allows to model relativistic fields and the interactions between their quantum excitations, among which are the known particles. Since its inception, the Standard Model has been successful in explaining the observed particle physics phenomenology, in some cases by the inclusion of new fundamental particles. The last of which has been the Higgs boson, an integral piece of the puzzle since it plays a central role in the spontaneous breaking of the Electro-Weak gauge symmetry [2–7]. It is through this mechanism that the W and Z bosons acquire masses, as do the elementary fermions, via their interactions with the Higgs. However, the Higgs sector is not without issues, and in the SM so far there is no known, fundamental origin for its potential.

There are a few well established reasons that suggest that the SM is not the most fundamental theory of Nature. For one, the Standard Model does not include gravity, for which we do not yet have a complete high-energy description. Attempting to bring the framework of QFT into Einstein's equations raises problems with renormalization and unitarity [8]. More involved scenarios like String Theory or Loop Quantum Gravity exist, but they have their own unresolved issues, and no precise way to merge one of these schemes with the SM exists so far. The Standard Model also fails to provide an explanation to the observed matter-antimatter asymmetry, neither does it account for the observed dark matter and dark energy in the universe [9, 10], nor does its current formulation include neutrino masses and their oscillations [11]. On the other hand, there are theoretical shortcomings related to the idea of "Naturalness", which is concerned with the natural, as opposed to fine tuned, size of the coefficients of the theory. Here we can mention the strong CP problem, or why no CP violation coming from the strong sector in the SM has been observed, as there is no actual reason this symmetry should be preserved [12]. Another discrepancy is that between the observed cosmological constant

and what is predicted on simple grounds by quantum field theory [13]. Finally, the one that concerns us here, and one of the main motivations for our work is the so called Hierarchy Problem. We proceed by briefly describing how this problem emerges, and what its possible solution entails for potential new physics (NP).

In the Standard Model, the Higgs is the only fundamental scalar in its spectrum. Moreover, it has a mass which has been measured at $m_h \approx 125$ GeV [14, 15], which in the SM arises from the spontaneous breaking of the EW symmetry. As far as the SM is concerned, the Higgs field H presents a quartic potential, parametrized as

$$V(H) = -\mu^2 H^\dagger H + \lambda_H (H^\dagger H)^2 \ , \tag{1.1}$$

where we included an explicit sign in the quadratic term, in order for the Higgs to acquire a non-trivial vacuum expectation value (VEV). This quadratic term, and its parameter μ is central to the whole discussion of the Hierarchy Problem. Its value is related to the observed Higgs mass, being $\mu^2 = (m_h^2)/2 \simeq (89 \text{ GeV})^2$. The Higgs quadratic term is particularly special, as it involves the only dimensional parameter in the theory.

As previously discussed, the SM cannot be a theory of everything, as it is lacking in several respects. Thus, it is only reasonable to think of the SM as an effective field theory, and one possible justification for this point lies in the partial inclusion of gravity as a quantum field theory. When trying to quantize general relativity, in what is termed the semiclassical expansion, one finds that the theory has a natural cutoff scale around the Planck mass $M_P \simeq 10^{19}$ GeV, at which the perturbative description of the theory is no longer valid and some more fundamental description of quantum gravity must arise. The SM has then a finite cutoff Λ_{SM} at which non-SM particles and interactions have to be included, with $\Lambda_{\text{SM}} \leq M_P$. However this does not necessarily mean that the first sector of Beyond the Standard Model (BSM) physics that needs to emerge is the one addressing the issue of quantum gravity, nor that it has to arise at the Planck scale, hence the inequality above. Assuming the existence of a physical cutoff for the theory, beyond which new physics appear, is a crucial piece in our formulation of the Hierarchy Problem. It is important to note that without this cutoff, the Standard Model would be a valid theory up to arbitrary high scales [16].

We can now formulate the Hierarchy Problem by using the language of effective field theories (EFT). In an EFT, the main prescription is to include all interaction terms which are allowed by the symmetries, involving the known particle content. An effective theory description, then, has an infinite number of local gauge invariant operators with energy dimensions "d". On dimensional grounds alone, as the Lagrangian is of dimension 4, the scaling of the coefficients of these operators are proportional to $1/\Lambda_{\text{SM}}^{d-4}$. Thus, it gives a rationale for ordering the different terms, as their effect on low-energy

observables has a suppression of order $(E/\Lambda_{\rm SM})^{d-4}$. This is why in the language of EFT, operators with $d > 4$ are termed "irrelevant", as with regard to energies under the cutoff their effects are power-law suppressed, with a power of $d-4$. The renormalizable SM Lagrangian, which involves only $d \leq 4$ terms, is capable of describing a huge set of experimental data collected over the last few decades [17]. However, as we mentioned above in our discussion of the Higgs potential, the quadratic term in Eq. (1.1) is the only $d < 4$ operator found in the SM, with $d = 2$. By the same scaling arguments discussed in the context of EFTs, the coefficient μ must then be enhanced by Λ^2. That is:

$$\mu^2 H^\dagger H \equiv c_\mu \Lambda_{\rm SM}^2 H^\dagger H \ , \tag{1.2}$$

where c_μ is some numerical coefficient. The Hierarchy Problem, then, is concerned with the perceived smallness of this coefficient. Now, as $\mu^2 \simeq (89 \text{ GeV})^2$, this observation pushes down the cutoff scale of the SM to ~ 100 GeV to a few TeV. Otherwise, if no new physics were present up to high scales, say $\Lambda_{\rm SM} \sim M_{\rm GUT} = 10^{15}$ GeV, this suggests an enormous unexplained hierarchy exists between the electroweak scale and the SM cutoff:

$$\frac{\mu^2}{\Lambda_{\rm SM}^2} \sim 10^{-28} \ll 1 \ . \tag{1.3}$$

Besides this naive, dimensional analysis argument, there are stronger lines of reasoning that suggest the EW scale must have an origin at not extremely high energies. Here we can mention the apparent instability of the Higgs potential under QFT effects. When one calculates 1-loop corrections to the quadratic term in Eq. (1.1), we find that when considering either top-quark, EW bosons, or Higgs loop diagrams, all three are quadratically divergent [18]. This means that if one considers the SM as an EFT valid up to a cutoff scale $\Lambda_{\rm SM}$, these corrections are of order:

$$\delta\mu^2 \simeq \Lambda_{\rm SM}^2 \ , \tag{1.4}$$

and once again, there is an enormous hierarchy $\mu^2/\delta\mu^2 \ll 1$ as long as $\Lambda_{\rm SM}$ is a high enough scale. Moreover, as the Higgs mass has been measured and thus has the scale of μ, this means that the eventual NP contributions that arise at energies higher than $\Lambda_{\rm SM}$ need to be extremely fine tuned in order to cancel those coming from the SM loop corrections. For a high enough cutoff $\Lambda_{\rm SM}$, there would have to be a cancellation between two a priori unrelated terms, the contributions to the Higgs mass coming from the SM and those coming from the new physics sector Beyond the Standard Model:

$$m_h^2 = \delta_{\rm SM}\, m_h^2 + \delta_{\rm BSM}\, m_h^2 \ . \tag{1.5}$$

An example of such a cancellation would be in a supersymmetric (SUSY) extension of

the SM, where for each of the loop diagrams there is a corresponding one with a supersymmetric partner inside the loop. This, in an unbroken SUSY scenario, guarantees an exact cancellation. As no supersymmetry has been observed in nature so far, this means that it has to be broken, which trades the UV scale sensitivity for a sensitivity with the scale of breaking of SUSY [19].

Another line of reasoning is to assume the Higgs has a microscoping origin. In this case, it is reasonable to search for it in scales of order few TeV, where the amount of fine tuning is small enough and thus the theory has some predictability. For BSM physics with $\Lambda_{\rm SM}$ of order $M_{\rm GUT}$, this cancellation means that the level of accuracy needed to calculate such a contribution is of about 24 digits [18], which then has the same level of predictability as if we took m_h as a given input parameter of the SM. Furthermore, as current and future particle accelerators will probe these scales first, it is only practical that one searches for NP solutions at this scale, which have reasonable chances to be tested.

Other, smaller hierarchies which are present in the SM are those of the quark and lepton masses, which have their origin in the Yukawa couplings between these fermions and the Higgs. Being $d = 4$ operators, they do not suffer from a scaling problem as did the Higgs mass term, as their loop corrections are only logarithmically divergent, instead of quadratically divergent. However, these Yukawa couplings do present us with an interesting puzzle and one that must guide our search for NP theories. We can describe the SM flavor puzzle in what follows. In our current understanding of particle physics, there are three generations, or flavors, of quarks and leptons. Each generation functions as pretty much exact copies, in which all their quantum numbers and thus their gauge interactions are universal. The only place where they differ in the SM Lagrangian is in their Yukawa interactions with the Higgs, which give rise to their masses and mixings. Without these Yukawa couplings, the SM fermions would remain massless, and a global symmetry $\mathrm{U}(3)^5$, or flavor symmetry, would be present as an accidental symmetry. This group arises from the existence of 5 distinct representations under the SM gauge symmetry $\mathrm{G_{SM}} \equiv \mathrm{SU}(3)_C \times \mathrm{SU}(2)_L \times \mathrm{U}(1)_Y$:

$$\begin{cases} q_L & = (\mathbf{3}, \mathbf{2})_{1/6} \\ u_R & = (\mathbf{3}, \mathbf{1})_{2/3} \\ d_R & = (\mathbf{3}, \mathbf{1})_{-1/3} \\ l_L & = (\mathbf{1}, \mathbf{2})_{-1/2} \\ e_R & = (\mathbf{1}, \mathbf{1})_{-1} \end{cases}$$

where each of these representations comes in three copies or flavors, hence the $\mathrm{U}(3)^5$ symmetry. However, this symmetry is broken in Nature, since quark and leptons are

massive particles. Moreover, the patterns present in the Yukawa matrices Y^u, Y^d, Y^e, which give rise to such a spectrum of masses, have no microscopic origin to provide them with a rationale in the SM. In other words, if one looks at the fermions, we find that in the quark sector, there is a a hierarchy of values $m_u \ll m_c \ll m_t$, and $m_d \ll m_s \ll m_b$, where the lightest quarks have masses of a $\sim$ few MeV, and the heaviest, the top, weighs ≈ 170 GeV [17]. We find thus a span of 5 orders of magnitude. A similar scenario is present in the charged leptons, with $m_e \ll m_\mu \ll m_\tau$, with the electron weighing 0.5 MeV, and the heaviest, the tau lepton at 1.7 GeV. Again we find 4 orders of magnitude between the lightest and heaviest flavor. And this is not even taking into account the neutrino sector, which have masses measured at sub eV values, and in some models they present with an inverted hierarchy with respect to the charged leptons [20, 21].

The subject of flavor, however, acquires an interesting new dimension when considering BSM physics. In the SM, the only source of flavor violation is the Yukawa sector, but New Physics could have completely generic flavor structures. Yet in reality, these NP will be constrained by experimental bounds on flavor transitions, some of which are quite stringent. For example, we can consider $\Delta F = 2$ operators which contribute to the physics of meson mixing, where we encode the effects of the NP in the Wilson Coefficients (WC) of $d = 6$ four-fermion operators which we generically write as:

$$\mathcal{L}^{\Delta F=2} \simeq \sum_T \sum_{i \neq j} \frac{c_{ij}}{\Lambda^2} (\bar{f}_i T f_j)^2 \ , \tag{1.6}$$

where the c_{ij} are numerical matrices in flavor space, Λ is the scale of the NP, and T accounts for the different γ matrices which may be present depending on the chiral structure. It turns out that when considering the different meson systems (K, B_d, B_s, D), these operators put very strong constraints on either the scale Λ of the NP for generic coefficients (*i.e.* $c_{ij} = 1$), or they require an extremely non-generic flavor structure c_{ij} for $\Lambda = 1$ TeV. In Table 1.1, taken from Ref. [22], we show the size of these bounds for either Λ or c_{ij} for the operators of different chiralities. When limits exist coming from CP violating and CP conserving observables, we only quote the strongest of these constraints.

Operator	Λ [TeV] (for $c_{ij} = 1$)	c_{ij} (for $\Lambda = 1$ TeV)	Observables
$(\bar{s}_L\gamma^\mu d_L)^2$	1.6×10^4	3.4×10^{-9}	Δm_K; ϵ_K
$(\bar{s}_R d_L)(\bar{s}_L d_R)$	3.2×10^5	2.6×10^{-11}	Δm_K; ϵ_K
$(\bar{c}_L\gamma^\mu u_L)^2$	2.9×10^3	1.0×10^{-7}	Δm_D; $\lvert q/p\rvert$, ϕ_D
$(\bar{c}_R u_L)(\bar{c}_L u_R)$	1.5×10^4	1.1×10^{-8}	Δm_D; $\lvert q/p\rvert$, ϕ_D
$(\bar{b}_L\gamma^\mu d_L)^2$	9.3×10^2	1.0×10^{-6}	Δm_{B_d}; $S_{\psi K_S}$
$(\bar{b}_R d_L)(\bar{b}_L d_R)$	3.6×10^3	1.7×10^{-7}	Δm_{B_d}; $S_{\psi K_S}$
$(\bar{b}_L\gamma^\mu s_L)^2$	1.1×10^2	7.6×10^{-5}	Δm_{B_s}
$(\bar{b}_R s_L)(\bar{b}_L s_R)$	3.7×10^2	1.3×10^{-5}	Δm_{B_s}

Table 1.1: Bounds on representative $d = 6$ $\Delta F = 2$ operators, on either the scale Λ if the operator couples with a coefficient $1/\Lambda^2$, or over the respective c_{ij} if Λ is fixed at 1 TeV. CP violating observables are separated by a semicolon from the CP conserving ones. Regardless, we only keep the strongest bound in each cell.

Motivated by the search of NP able to provide an origin to the EW scale, we see that for $\Lambda = 1$ TeV the bounds on flavor space are particularly restrictive, hence whatever model one constructs must respect a certain structure in flavor space. It certainly cannot be arbitrary, yet at the same time it would be preferable for a theory to offer some kind of rationale for such a pattern of coefficients, without their simply having *ad-hoc* values which pass the flavor constraints. Minimal Flavor Violation (MFV) provides such an option, in which all operators in the new theory have as the only source of flavor violation the Yukawa matrices of the SM. This greatly reduces the constrains from flavor violating processes. Another related, but deeper question is that of building a flavor model. That is, a scheme in which the patterns of the SM Yukawas, as well as the physics of flavor in some eventual NP sector, are explained. In the present work we will be looking at some models that can fulfill this role.

Besides the concrete shortcomings of the SM which we mentioned above, recently there have been some experimental signals which also suggest that some New Physics may arise at the TeV scale. Some anomalies have been observed in semileptonic B decays, which seem to point out to Lepton Flavor Universality (LFU) violation. LFU refers to how in the SM, apart from the Higgs sector, all three charged leptons have identical interactions. There are several observables which are measured to test LFU in the SM. Here we can focus on two ratios of semileptonic decays of B mesons, which are bound states containing one b quark. These B mesons can decay through charged currents to a D meson, or through neutral currents to a K meson. D mesons are those containing one c quark, whereas K mesons (or kaons) contain one s quark. By measuring ratios of these decays involving different lepton flavors, LFU can be tested.

One of these experimental ratios, measuring possible deviations from τ/μ and τ/e

universality in $b \to c\ell\bar{\nu}$ charged currents, is defined as:

$$R_{D^{(*)}} = \left. \frac{\mathrm{Br}\left(B \to D^{(*)}\tau\bar{\nu}\right)}{\mathrm{Br}\left(B \to D^{(*)}\ell\bar{\nu}\right)} \right|_{\ell \in \{e,\mu\}} , \tag{1.7}$$

and an excess has been measured with respect to its SM predicted value, by BaBar, Belle and LHCb [23–27]. The most recent averages of the two ratios R_D and R_{D^*}, when combined, give an excess of $\approx 3.08\,\sigma$ [28].

Regarding the neutral current $b \to s\ell^+\ell^-$, a similar ratio is defined, which tests μ/e universality:

$$R_{K^{(*)}}^{[q_1^2,q_2^2]} = \frac{\mathrm{Br}'\left(B \to K^{(*)}\mu\mu\right)}{\mathrm{Br}'\left(B \to K^{(*)}ee\right)} , \tag{1.8}$$

with Br$'$ referring to a partial branching ratio by taking the invariant mass squared of the outgoing leptons in the interval $[q_1^2, q_2^2]$. In this case, these ratios, measured by Belle and LHCb, have been found to be lower than in the SM [29–33]. The values reported by LHCb are in tension with the SM by $\approx 3.1\,\sigma$ for R_K, and $\approx 2.5\,\sigma$ in the case of R_{K^*}.

The observation that both $R_{D^{(*)}}$ and $R_{K^{(*)}}$ are in excess and deficit, respectively, from their predicted values is commonly referred to as B-anomalies, and will be another guiding tenet in our search for new physics. While there is no evidence of a common origin for these B-anomalies, several attempts at combined explanations have been proposed [34–59]. Interestingly enough, these anomalies seem to suggest physics which couple preferentially to third generation quarks and leptons, with smaller couplings to the lighter generations [44, 60, 61]. Moreover, these anomalies can be well fitted by including semileptonic effective operators with the scale of NP set at the TeV [34–39]. There are different ways of generating these effective operators with BSM physics, one of them involves colorless $\mathrm{SU}(2)_L$-triplets (W',B') [34, 50], another one involves leptoquarks, which are hypothetical new particles which have both baryon and lepton numbers, thus having interaction vertices involving both quarks and leptons [44, 60]. Various leptoquarks (LQ) can be defined depending on their $\mathrm{G_{SM}}$ transformation properties, and they have been thoroughly classified according to their interactions with the SM particles [62]. There are some of these leptoquarks whose interactions can produce the right operators that are able to explain either of the ratios $R_{K^{(*)}}$ or $R_{D^{(*)}}$. Fewer are those that can also simultaneously pass other semileptonic constraints. Several studies have been made, with particular emphasis on being able to accommodate both B-anomalies with either single or multi-leptoquark models. We show a summary of this in Table 1.2, taken from Ref. [44].

Model	$R_{K^{(*)}}$	$R_{D^{(*)}}$	$R_{K^{(*)}}$ & $R_{D^{(*)}}$
S_1	✗	✓	✗
R_2	✗	✓	✗
$\widetilde{R}_2$	✗	✗	✗
S_3	✓	✗	✗
U_1	✓	✓	✓
U_3	✓	✗	✗

Table 1.2: Summary of leptoquarks which are able to accommodate either $R_{K^{(*)}}$, $R_{D^{(*)}}$, or both simultaneously (first, second and third columns respectively), without inducing other phenomenological problems.

We see that the vector LQ U_1 can provide the most economical solution, whereas a combination of two scalar LQ like S_1 and R_2, or S_1 and S_3 may also accommodate both anomalies. It is worthy of mention that most of these fits require a particular structure of fermion couplings to LQs, with often first generation couplings being set to zero, as well as couplings to right handed fermions. When working with BSM models, it is often desirable to have such non-generic structures motivated by some underlying mechanism.

Guided by the Hierarchy Problem of the EW scale, one idea that can serve as an explanation for the nature of the Higgs boson is that of the composite Higgs scenario. In the SM, apart from the Higgs, all other known scalar particles arise as bound states of quantum chromodynamics (QCD). QCD, being a strongly interacting theory, has a confining scale at which different composite resonances emerge as a product of this confinement. At energies above this confinement scale, the constituents of these mesons are the quarks. At lower energies, however, the effective theory of mesons is a valid description of the experiments [7].

In a completely analogous manner, one can postulate that the Higgs is a composite state of another, strongly coupled field theory (SCFT), with a composite scale m_* of order few TeV [63–65]. In this framework, the problem of fine tuning related to its quadratic term loses importance, as the effective scale where the NP starts to be present is much closer to the EW scale: $\mu \lesssim \Lambda_{\text{SM}}$ in Eq. (1.3). Similarly to QCD, this confinement scale can be exponentially smaller than the UV scale due to the breaking of scale invariance by renormalization effects, a phenomenon known as dimensional transmutation [66].

Eventually this composite scale can be pushed up towards ~ 10 TeV due to flavor constraints, with this reintroducing a certain fine tuning with respect to the EW scale. At this composite scale m_* other resonances are expected to arise as a product of the confinement, of either scalar, vectorial, and fermionic nature. Whereas certain attempts have been made at obtaining a high energy description of the composite sector [67, 68],

we are interested in the effective description. To this end, it suffices to model that the field content of the theory belongs in either of two sectors. One is the elementary sector, which contains all the fields of the SM minus the Higgs, with all interactions given by gauge-invariant terms that are therefore universal for all three generations of each fermion representation. The other is the composite sector, which contains the Higgs and other composite resonances. The way to model the composite sector is with a certain global symmetry group G, which contains the SM gauge group G_{SM} but in principle can be larger. Product of the strong dynamics, there is a spontaneous symmetry breaking of G into a subgroup H, which also has G_{SM} as a subgroup. This global symmetry breaking is responsible for massless scalars to arise in the theory, among which the composite Higgs will be present, as given by the Nambu Goldstone theorem. In absence of elementary-composite interactions, these are exact Nambu Goldstone bosons (NGB), and would remain massless. However, both the gauging of the SM gauge group, and the interactions between fermions and the composite sector are responsible for an explicit breaking of the global symmetry. To generate a large scale separation, as in QCD with dimensional transmutation, it is assumed that at some high UV scale the SCFT is approximately scale invariant (usually conformally invariant), it is at this UV scale where some fermionic operators have linear couplings to the elementary fermions. Scale invariance allows one to characterize the SCFT operators according to their anomalous dimensions [69]. This assumption, called Partial Compositeness, allows for the large hierarchy present in the physical fermion masses to be generated via running of the renormalization group equations, from $\mathcal{O}(1)$ differences in the composite operators dimensions. In this way, physical fermions now become partially composite, as they are linear combinations of elementary fermions and the SCFT resonances. The partial compositeness hypothesis is extremely powerful, since then all couplings between physical fermions and resonances are driven by their compositeness fractions, thus providing a rationale for all flavor matrices present in the theory. The simplest ansatz within partial compositeness is that of Anarchic Partial Compositeness (APC), under which all flavor structure in the composite sector is taken to be anarchic. That is, all flavor matrices can be written in terms of some common factor multiplied by dimensionless couplings c_{ij} of the same $\mathcal{O}(1)$ size. Under such an assumption, all flavor transitions between resonances are of the same order, and the mechanism of partial compositeness is the one responsible for the correct flavor patterns to arise between the physical states.

It is the explicit breaking of the symmetry by the elementary sector which is responsible for the NGB of acquiring a radiative potential. These pseudo-NGB (pNGB) then acquire masses which have a 1-loop factor suppression with respect to the typical masses of the composite sector m_*. This gap in the mass spectrum is beneficial for the phenomenology, as the scale of the composite resonances cannot be arbitrarily light, given that none have been observed yet. The calculation of this radiative potential and

the conditions for its finiteness will be discussed in more detail in Chapter 2.

In the present work, we are interested in studying composite Higgs models, and also the viability of having leptoquarks coming from the composite sector, such that the B-anomalies can simultaneously be addressed. Some models in this direction have already been proposed [70–72]. As we have already mentioned, leptoquarks require a non-generic structure of couplings with the different fermion generations. This structure tends to favor couplings to the third generation, and Left-handed over Right-handed couplings. This pattern of couplings can be obtained in a fairly simple way by Anarchic Partial Compositeness, a fact that makes composite leptoquarks a natural idea. Moreover, the scale for leptoquarks solutions to the B-anomalies is of roughly the same TeV order as a theory of composite Higgs requires for addressing the Hierarchy Problem. We are thus interested in trying to merge both LQs and Composite Higgs into a single model. We explore different composite models in order to deliver the appropriate LQ in the spectrum for accommodating the B-anomalies.

This work is organized as follows: In Chapter 2 we are concerned with the fundamentals of Composite models. It is in this chapter where most of the ideas common to all studied composite models are presented. We delve into the basics of the Higgs as a pseudo Nambu Goldstone, and we concern ourselves with how to model the spontaneous symmetry breaking of the composite sector to obtain the pNGB, how to model their interactions, and how to then obtain the Coleman-Weinberg potential at 1-loop. We review the main ideas of APC, which allows for a rationale for flavor to be obtained. We then examine some basic flavor constraints, which put bounds on the composite scales m_* and the Goldstone decay constant f of the theory. These bounds are important as they tend to require larger m_*, which then may be in tension with the necessary leptoquark masses for the B-anomalies explanations. We also look into how to model in very simple terms a theory of resonances. This allows for some of the form factors involved in the calculation of the Higgs potential to be explicitly obtained, and this way equip the models with better predictability.

In Chs. 3, 4 and 5 we are concerned with explicit composite Higgs models involving leptoquarks. We consider the different groups G and H needed to obtain different LQs in the spectrum. In Ch. 3, we are concerned with obtaining S_3 as a composite pNGB from a simple group, along with the Higgs. Other scalar particles, like another LQ and a colorless $\mathrm{SU}(2)_L$ fourplet are present in the spectrum. We are able to calculate the potential of the pNGBs, up to quartic order, by an explicit modeling of the first sector of resonances. We also are able to calculate the potential for the EM-neutral Higgs and fourplet VEVs, up to all orders in these VEVs, and study EWSB in detail. We also show how the presence of this leptoquark is able to account for the anomalies in $R_{K^{(*)}}$, yet not simultaneously those of $R_{D^{(*)}}$.

In Ch. 4, we study the presence of vector LQ U_1 in a composite Higgs model. This

too allows for a simple group to be considered. We show how the inclusion of this state alone can account for the anomalies in both ratios $R_{K^{(*)}}$ and $R_{D^{(*)}}$, yet this forces the scale m_* to be somewhat lower, or causes a certain tension with constraints from flavor-violating processes and from Z-couplings to be present. We also show how, by explicitly modeling the first two sets of composite resonances of the theory, we can calculate the pNGB potential. In the pNGB spectrum, another scalar leptoquark and a $\mathrm{G_{SM}}$ singlet, which can be a dark matter candidate, are also present. We discuss some of their phenomenology as well.

In Ch. 5, we go back to scalar leptoquarks in the pNGB spectrum, this time by considering both S_1 and S_3. We show how the smallest group that can provide exactly the two LQs plus the Higgs is however not a simple group. We once again calculate the potential at quartic order, but without an explicit modeling of the resonances of the composite sector. We are interested in looking at the combined $S_1 - S_3$ model and its compatibility with APC. We thus study their contributions to the B-anomalies, as well as an exhaustive look to the contributions coming from a number of flavor observables. We show how this solution can account for the anomalous ratios, while respecting all flavor constraints, without being in an excessively tuned sector of parameter space. We also briefly discuss the phenomenology of other vector and spinorial resonances present in the composite sector.

In Ch. 6 we distance ourselves from LQs and B-anomalies, and we instead take a closer look at the APC hypothesis. We are interested in studying a different approach to flavor, one that mixes partial compositeness with a $\mathrm{U}(1)_F$ flavor symmetry in the composite sector. We show how this approach, which is modeled after the Froggatt-Nielsen (FN) mechanism, is able to interpolate between APC and FN. We revisit the flavor constraints to APC in the light of this new model, and we show how some suppression in certain observables can be obtained in a natural way. This theory, having a spontaneous breaking of a U(1) symmetry, has an axion present in its spectrum, whose phenomenology may be interesting to study.

Finally, in Ch. 7 we summarize most of the work and include some conclusions, together with possible future outlooks.

A few of the more technical details are relegated to the appendices.

Chapter 2

Theoretical Framework

2.1. Higgs as a pNGB

The way composite Higgs models work around the Hierarchy problem is by making the Higgs no longer be a fundamental scalar, but a bound state of some new physics sector, which works in analogy to QCD bound states. In this work we will not concern ourselves with a fundamental description of said new physics sector, but work in an effective field theory description, similar to how pions are described in chiral perturbation theory [7]. A specific mechanism that the composite Higgs will be dependent on is that of the Nambu-Goldstone theorem, which we will describe in this chapter.

The Nambu-Goldstone theorem states that massless spin-0 states arise whenever there is a global continuous symmetry that is spontaneously broken [73, 74]. This can be stated in a more formal way. We follow Ref. [18] in most of the elements presented in this Chapter. Suppose our composite sector is characterized by a global symmetry group G, which contains a smaller subgroup H, that is large enough to contain the Standard Model gauge group: $\mathrm{G_{SM}}$. If we use T^A to denote the generators of the algebra of G, then we can choose a basis in which these generators can be split up as:

$$T^A = \{T^a,\ \hat{T}^{\hat{a}}\} \tag{2.1}$$

where T^a will now denote the generators of the algebra of H, and the remaining generators are said to be in the coset G/H. Those latter generators are the ones identified with the Nambu-Goldstone bosons, the multiplicity of these given by the difference in dimensionalities between G and H. This is,

$$\dim(\mathrm{G/H}) = \dim(\mathrm{G}) - \dim(\mathrm{H}) \tag{2.2}$$

The transformation properties of these NG bosons can be obtained by looking at the commutators between T^a and $\hat{T}^{\hat{a}}$. This can be deduced from the algebra of G, which we

decompose as commutators among H generators, among generators in the coset, and the action of H on elements of the coset, which defines the transformation properties of the NG bosons.

$$\begin{aligned}\left[T^a, T^b\right] &= i f_c^{ab} T^c \\ \left[\hat{T}^{\hat{a}}, \hat{T}^{\hat{b}}\right] &= i f_c^{\hat{a}\hat{b}} T^c + i f_{\hat{c}}^{\hat{a}\hat{b}} \hat{T}^{\hat{c}} \\ \left[T^a, \hat{T}^{\hat{b}}\right] &= i f_{\hat{c}}^{a\hat{b}} \hat{T}^{\hat{c}} \equiv (t_\pi^a)_{\hat{c}}^{\hat{b}} \hat{T}^{\hat{c}}\end{aligned} \tag{2.3}$$

We will usually denote the NG bosons with the symbol Π. Here we see that the elements in the coset transform in a certain representation of H, whose generators we denoted by t_π. These set of commutation relations tells us how the adjoint representation of G is split up in terms of representation of the unbroken subgroup:

$$\mathbf{Adj}(\mathrm{G}) \to \mathbf{Adj}(\mathrm{H}) + \mathbf{r}_\Pi \tag{2.4}$$

This coset representation can be either irreducible or reducible under the group H, and also under $\mathrm{G_{SM}}$. By a proper choice of groups G, H and identification of $\mathrm{G_{SM}}$ within H, the model can contain components which transform as the Higgs particle. One such model is the Minimal Composite Higgs Model, or MCHM, where the coset is SO(5)/SO(4) and delivers exactly four states transforming as the Higgs [65]. For larger or more complex groups, the coset will also contain other states as well [75].

In the case of an exact G → H spontaneous global symmetry breaking, the NG bosons are massless, having no potential at all. Thus, all vacuum expectation values of these fields, $\langle\Pi\rangle$, are equivalent, and can be set to zero by a symmetry transformation. However, this is not the case when the G symmetry is broken, as is the case with the introduction of the elementary sector. The gauging of the electroweak group G_{EW}, which is contained in H, introduces an explicit breaking of the global symmetry. This is also the case with the elementary fermions of the theory, which will not transform in full representations of the group G, thus also being a source of explicit symmetry breaking. This explicit breaking of the symmetry causes the NG bosons to acquire a potential, thus their VEVs are no longer equivalent. They cease to be exact NG bosons and they become pseudo-NG bosons (pNGB). The potential for these pNGB can be calculated as the sum of all 1-loop contributions, all of which necessarily involve states of the elementary sector, which are the responsible for the explicit breaking of this symmetry. This 1-loop potential is named after Coleman and Weinberg, and will be described in more detail later in this chapter.

In order to write the interactions between the pNGB and the elementary fields, we resort to the following parametrization, following the construction by Callan, Coleman,

Wess and Zumino (CCWZ)[76, 77]:

$$U\left[\Pi\right] \equiv e^{\frac{i\Pi_{\hat{a}}(x)\hat{T}^{\hat{a}}}{f}} \tag{2.5}$$

where f denotes the Goldstone decay constant, or sometimes called the Higgs decay constant, and represents the typical scale of the G/H spontaneous symmetry breaking. This matrix can be understood as an element of the group G, however, it is not the most general element since it involves only broken generators. It is usually called the Goldstone matrix. It has a particular transformation property under G. Under a group transformation g of the Goldstone fields $\Pi(x) \to \Pi^{(g)}(x)$, the matrix does not transform as one could expect, $U \to gUg^{-1}$, but in the following way:

$$U[\Pi] \to U[\Pi^{(g)}] = g \cdot U[\Pi] \cdot h^{-1}[\Pi; g] \tag{2.6}$$

where now h is a group transformation of the unbroken subgroup H, which has an implicit dependence on both g and Π. This expression can be deduced from the more basic property that a generic element g of the group G can always be decomposed as the following product in a unique way:

$$g[\alpha_A] = e^{i\alpha_A T^A} = e^{if_{\hat{a}}[\alpha]\hat{T}^{\hat{a}}} \cdot e^{if_a[\alpha]T^a} \tag{2.7}$$

where the parameters of the two exponentials are functions of the transformation $g[\alpha]$. As the generators T^a form a subgroup, the second factor is a subgroup element h. The commutation relations in Eq. (2.3) can be used to show that if the transformation g is picked as an element of the subgroup H, g_H, the transformation of $U[\Pi]$ is such that the fields transform under the coset representation $\mathbf{r}_\Pi$. That is,

$$\Pi_{\hat{a}} \to \Pi_{\hat{a}}^{(g_H)} = \left(e^{i\alpha_a t_\pi^a}\right)_{\hat{a}}^{\hat{b}} \Pi_{\hat{b}} \ , \tag{2.8}$$

where the α_a parametrize the transformation $g_H \in$ H. However, under a more general transformation which includes the broken generators, there is no closed expression for the way Π transform, not even in the infinitesimal level, except under very simple coset examples. However, as the action of the group on the Goldstone matrices is simple enough, this object $U[\Pi]$ can be used to construct invariants.

It is useful to define the Maurer-Cartan form, by using the covariant derivative D_μ of the Goldstone matrix, and splitting it into the broken and unbroken components as

$$iU^\dagger D_\mu U = d_{\mu,\hat{a}}\hat{T}^{\hat{a}} + e_{\mu,a}T^a \ , \tag{2.9}$$

where the covariant derivative includes the gauge fields of the Standard Model sym-

metry group G_{SM}. It can be shown that, under a transformation of the full group G, the Maurer-Cartan form will transform linearly with a transformation of the unbroken group H. This allows us to build G-invariants by combining these symbols d_μ and e_μ, in a simple manner. This is the CCWZ construction, after Callan-Coleman-Wess-Zumino. The simplest combination one can build is by using two insertions of d_μ:

$$\mathcal{L}^{(2)} \supset \frac{f^2}{2} d_{\mu,\hat{a}}[\Pi, A] d^{\mu,\hat{a}}[\Pi, A] \ , \tag{2.10}$$

where we denote the dependence of d_μ on both Goldstones Π and gauge fields A. This Lagrangian includes at the lowest order, the kinetic term for the Goldstone fields,

$$\frac{f^2}{2} d_{\mu,\hat{a}}[\Pi, A] d^{\mu,\hat{a}}[\Pi, A] \supset \frac{1}{2} \partial_\mu \Pi_{\hat{a}} \partial^\mu \Pi^{\hat{a}} + \sum_n \mathcal{O}\left(\left\{ (\partial \Pi)^2 + f^2 A^2 \right\} \cdot \frac{\Pi^n}{f^n} \right) \tag{2.11}$$

where we schematically wrote all higher order interactions with two derivatives of the Goldstone fields, and interactions between the gauge fields and the Goldstones. These latter interactions, after the Higgs acquired a VEV, will be responsible for the gauge boson mass terms. Depending on the particularities, or details of the coset choice and thus the representation $\mathbf{r}_\Pi$, more than one way to combine the $d_\mu^{\hat{a}}$ into an invariant may exist. However the invariant specified in Eq. (2.10) is always present due to the Goldstone representation being real.

In the Standard Model, the Higgs sector has an approximate global symmetry, which receives the name of custodial symmetry [78]. This is an SO(4) symmetry of the Higgs potential, broken by the VEV to an $SO(3)_c$ subgroup, which is exact in the limit where both the gauging of the hypercharge, as well as the Yukawas, are set to zero. Its effect is best seen in the ρ parameter, which encodes the ratio of strengths of the neutral to charged currents:

$$\rho = \left(\frac{g^2}{c_W^2 M_Z^2} \right) \left(\frac{g^2}{M_W^2} \right)^{-1} = \frac{M_W^2}{c_W^2 M_Z^2} \tag{2.12}$$

where $c_W \equiv \cos\theta_W = g/\sqrt{g^2 + g'^2}$ is the cosine of the Weinberg angle. This parameter is equal to 1 at tree level in the SM, due to the custodial symmetry. In extensions to the SM this symmetry is often included in the NP sector, as too large contributions to this parameter would be ruled out by electroweak precision tests (EWPT). It is usual to work with the difference $\rho - 1 \equiv \alpha_{\text{em}} T \equiv \hat{T}$, which is one of the Peskin-Takeuchi parameters, the other being S and U [79–81].

Equation (2.11), when evaluated at the electromagnetic-neutral VEV, gives rise to mass terms for the SM gauge bosons. Depending on the particularities of the groups in question, this leads to an expression for the matching of the Standard Model Higgs

VEV in terms of the pNGB Higgs. As an example, in the simplest coset SO(5)/SO(4) present in the MCHM [65], one has:

$$v_{\rm SM}^2 = f^2 \sin^2\left(\frac{v}{f}\right) \tag{2.13}$$

This model is minimal in the sense that it exactly delivers the Higgs and no other scalars, and contains a custodial symmetry group. In fact, the coset SO(5) /SO(4) has the property that for any pair of embeddings of SO(4) $\subset$ SO(5), their intersection always contains an SO(3) subgroup. This ensures that the Higgs VEV always preserves a custodial $\mathrm{SO}(3)_c$. That is, a vacuum misalignment can occur if the group preserved by the vacuum, $\mathrm{SO}(4)_{\rm vac}$, is different from that which is gauged by the SM, $\mathrm{SO}(4)_g$. However, two SO(4)'s embedded in SO(5) will always share a common $\mathrm{SO}(3)_c$ subgroup [75].

We can see from the above equation that if $v \ll f$, $v_{\rm SM} \sim v$. As a matter of fact, the limit of $f \to \infty$, with fixed v, is such that the rest of the resonances of the composite sector decouple from the elementary sector, with only the NGB remaining in the spectrum. In this limit the Higgs acts effectively as an elementary state. One can show, for example, how in the quadratic NGB Lagrangian in Eq. (2.10) all higher dimension terms are effectively suppressed by powers of f, going to zero in this limit. A quantity that is usually defined in composite Higgs models, is the ξ parameter:

$$\xi \equiv \frac{v_{\rm SM}^2}{f^2} \tag{2.14}$$

This will be typically $\xi \ll 1$, in order to pass electroweak precision tests. This often serves as an expansion parameter, and as a way of quantifying the amount of tuning of the theory.

2.1.1. Fermion sector

So far we have not specified how the SM fermions are introduced in the theory, and how their interactions with the pNGBs, particularly with the Higgs, can be written down. In order to do this, we need to discuss the idea of partial fermion compositeness. In this framework, all the SM fermions are external to the composite sector, and will couple linearly to fermionic operators $\mathcal{O}_F^{L,R}$ of the SCFT (see Ref. [82] for a model with fully composite Right-handed top quarks). This interaction between the elementary fermions and the composite sector will be written down at a scale $\Lambda_{\rm UV}$,

$$\mathcal{L}_{\rm UV} = \sum_\psi \left\{ \frac{\omega_L^\psi}{\Lambda_{\rm UV}^{\Delta_L^\psi - 5/2}} \bar{\psi}_L \mathcal{O}_L^\psi + \frac{\omega_R^\psi}{\Lambda_{\rm UV}^{\Delta_R^\psi - 5/2}} \bar{\psi}_R \mathcal{O}_R^\psi \right\} \tag{2.15}$$

where the sum is over the different SM fermions ψ. There is also a sum over different generations of fermions, but for now we omit such indices, leaving the topic of flavor structure for later. Each $\mathcal{O}_L^\psi$ has the same SM quantum numbers as the elementary fermion it couples to, and for simplicity we assume that a single composite operator couples to each elementary fermion. If more than one composite operator were coupled to each elementary fermion, the one with the smallest operator dimension would dominate, as we will see shortly. As the composite sector is also characterized by a group symmetry G, these operators are inside representations of G. However, as the elementary fermions do not transform under G, these interaction terms constitute an explicit breaking of G, and along with the gauging of $\mathrm{G_{SM}}$ are one of the two sources of explicit breaking and are responsible for the generation of the scalar potential, as we will later see. A way of parametrizing this breaking is with spurions, by making the elementary fermions $\psi_{L,R}$ into representations of the group G, with non-dynamical spurion fields in all entries not transforming with the proper ψ SM quantum numbers. These non-dynamical entries are later set to zero in the calculation. We will resort to this when writing an effective Lagrangian for the elementary fields and the interaction with the pNGB.

We assume that this strongly coupled field theory has a dynamical scale m_* at around the TeV, where it confines, generating resonances of vectorial, scalar, and fermionic type. Particularly the operators $\mathcal{O}_{L,R}^\psi$ will generate fermionic resonances with the same quantum numbers as the SM fermions. At energies over the TeV, the strong sector will be near a conformal fixed point, and thus we will consider that the running of these couplings ω^ψ are driven by the operator dimensions $\Delta_{L,R}^\psi$. With this in mind, the interaction between the elementary fermions, and the lightest composite resonances Φ_ψ at the scale m_* will be proportional to a renormalized coupling:

$$\omega_{L,R}^\psi[m_*] \equiv \lambda_{L,R}^\psi \sim \omega_{L,R}^\psi \left(\frac{m_*}{\Lambda_{\mathrm{UV}}}\right)^{\Delta_{L,R}^\psi - 5/2} \tag{2.16}$$

This relation allows for a hierarchy of couplings to be generated from operators' dimensions that are naturally of the same order, provided the scale separation is large enough. For example, for $m_* \sim$ TeV, and Λ_{UV} of the GUT scale, $\sim 10^{15}$ GeV, the ratio $m_*/\Lambda_{\mathrm{UV}} \sim 10^{-12}$ is such that different $\Delta_{L,R} \gtrsim 5/2$ will produce a hierarchy in the couplings λ^ψ. This mechanism will allow for the generation of a hierarchy in the masses and the mixings of SM fermions.

The Lagrangian involving the interaction between elementary and composite fermions now has the form

$$\mathcal{L}_{\mathrm{el-cp}} = \sum_\psi \left\{ i\bar{\psi}\not{\partial}\psi + \lambda^\psi f\, \bar{\psi}\, \Phi_\psi + m_* \bar{\Phi}_\psi\, \Phi_\psi \right\} \ , \tag{2.17}$$

where the sum is over the different elementary fermions, with each fermion having a specific partner Φ_ψ, and a linear coupling λ^ψ depending on the chirality of the fermion. Moreover, with the coupling λ^ψ being dimensionless, there is an extra factor of $f = m_*/g_*$ in the elementary-composite interaction. That is, the elementary fermions are chiral, whereas each composite resonance is a vectorial fermion. This is better illustrated by picking a single quark generation, let's say the third, and thus writing the Lagrangian:

$$\mathcal{L}_{\text{el}-\text{cp}} \supset i\left(\bar{q}_L \not{\partial} q_L + \bar{t}_R \not{\partial} t_R\right) + \lambda^q f\, \bar{q}_L Q + m_* \bar{Q} Q + \lambda^t f\, \bar{t}_R T + m_* \bar{T} T \tag{2.18}$$

where Q, T are the massive resonances corresponding to the elementary fermions q, t_R. For simplicity both their masses are taken to be equal to m_*. We can now see where the name "partial" compositeness comes from, as the physical fermions will now be linear combinations of both elementary and composite fermions. After a diagonalization of the mass matrices, one gets

$$\begin{aligned}
|q_{L,\text{phys}}\rangle &= \cos(\theta_q)\,|q_{L,\text{el}}\rangle + \sin(\theta_q)\,|q_{L,\text{cp}}\rangle \\
|t_{R,\text{phys}}\rangle &= \cos(\theta_t)\,|t_{R,\text{el}}\rangle + \sin(\theta_t)\,|t_{R,\text{cp}}\rangle \\
|Q_{L,\text{phys}}\rangle &= -\sin(\theta_q)\,|q_{L,\text{el}}\rangle + \cos(\theta_q)\,|q_{L,\text{cp}}\rangle \\
|T_{R,\text{phys}}\rangle &= -\sin(\theta_t)\,|t_{R,\text{el}}\rangle + \cos(\theta_t)\,|t_{R,\text{cp}}\rangle
\end{aligned} \tag{2.19}$$

with the angles given by

$$\sin(\theta_x) = \frac{\lambda_x}{\sqrt{\left(\frac{m_*}{f}\right)^2 + \lambda_x^2}} \simeq \frac{\lambda_x f}{m_*} \equiv \epsilon_x, \qquad (x = q, t) \tag{2.20}$$

where the last equality is for $\lambda \ll m_*/f$, which will generally be valid for light fermions, with the top quark potentially being the exception as it has a larger coupling than other flavors. These compositeness fractions we will usually denote with the symbol ϵ, specifying the chirality and the generation in a compact manner, for example ϵ_{q1} for the left handed first generation quarks, ϵ_{u1} for the up-quark, etc.

These compositeness fractions will control how the physical states couple to the Higgs, which after EWSB will be the one responsible for the generation of their masses. We can estimate these Yukawa couplings, which will be given by the product of the compositeness fractions of both left and right-handed quarks, and the coupling between composite resonances g_*. The size of their Yukawa couplings can be estimated as:

$$y \sim g_*\, \epsilon_L\, \epsilon_R \tag{2.21}$$

This can be pictured in Fig. 2.1. In this way, we can see how the hierarchy in the masses of the Standard Model fermions is inherited, through the compositeness fractions, by the hierarchy in the elementary composite couplings $\lambda^{\psi}_{L,R}$. And this large hierarchy is created through a running of the Renormalization Group (RG) equations along a large separation of scales. In other words, in the UV scale where the original elementary-composite couplings are written, there is no large hierarchy, and we can expect all the couplings and the dimensions of operators to be of the same order. We will later review this in more depth when we touch the subject of Anarchic Partial Compositeness.

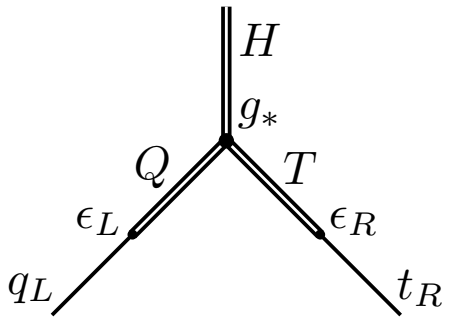

Figure 2.1: Yukawa couplings as generated in the composite theory, through the mixing of the elementary fermions with the composite resonances Q and T, for the top quark.

2.1.2. Effective Field Theory

We are now ready to write the effective interaction between the elementary states and the pNGB. The way to do this, as in every effective field theory construction, is to allow for all interactions that are compatible with the spacetime and internal symmetries to exist. It is useful to embed the elementary fields inside full representations of G, to write the Lagrangian in a G-invariant way. For doing so we must find representations $\mathbf{R}_f$ of G that include components with the same SM quantum numbers of the physical fermions. More than one representation $\mathbf{R}_f$ may be needed for the different fermions f, and within a single representation, there may be more than one multiplet that interacts with the elementary fermions. Moreover, each representation $\mathbf{R}_f$ of G decomposes as a particular sum of representations $\mathbf{r}$ of H: $\mathbf{R}_f \sim \oplus_{\mathbf{r}} \mathbf{r}$. All those components of the elementary fermions with SM quantum numbers that are different than those of the physical fermions will be non-dynamical spurions, an artifact to write the interactions in a simple way, but that will be set to zero in the end. This way, it can be seen how it is the explicit breaking of the symmetry that is responsible for the generation of a potential for the NGB. With the fermions being in representations of G, they can be "dressed" by the action of the Goldstone matrix, which transforms in a special manner, $U \to gUh^{-1}$. Thus, for a multiplet Ψ transforming in a representation under G,

we construct the product

$$\widetilde{\Psi} = U^\dagger \cdot \Psi \tag{2.22}$$

This ensures that for a transformation $g \in \mathrm{G}$, $\Psi \to g\Psi$, the dressed fermion transforms only under a particular $h \in \mathrm{H}$ group element. This h, although being a complicated function of both g and the Goldstones Π, ensures this dressed fermion can be thought of in terms of its different multiplets or representations $\mathbf{r}$ of H, and the group acts only over each of these multiplets in block-diagonal form, without mixing the different components. That is, if the representation $\mathbf{R}_f$ of G splits as a sum of representations $\mathbf{r}$ of H, the dressed multiplet $\widetilde{\Psi}_f$ transforms under G as

$$\widetilde{\Psi}_f \to \oplus_{\mathbf{r}}\, h^{(\mathbf{r})} \hat{P}_{\mathbf{r}} \widetilde{\Psi}_f \tag{2.23}$$

where $\hat{P}_{\mathbf{r}}$ is a projector that selects the multiplet inside $\mathbf{R}_f$ that transforms as $\mathbf{r}$ under H, with $h^{(\mathbf{r})}$ being the transformation h in that particular representation. These projectors allow us to treat each of the representations of H on a different footing, as we are describing the interactions after the spontaneous breaking of $\mathrm{G} \to \mathrm{H}$ has taken place. We can then construct an effective Lagrangian involving the elementary fermions and the pNGB, up to quadratic order in Ψ, as:

$$\begin{aligned}\mathcal{L}^{\psi}_{\text{eff}} = &\sum_f \Psi_f Z_f \not{p} \Psi_f \\ &+ \sum_{f,f'} \sum_{\mathbf{r}} \left[\Pi^{\mathbf{r}}_{ff'}(p) \left(\bar{\Psi}_f U\right) \hat{P}_{\mathbf{r}} \left(U^\dagger \Psi_{f'}\right) + \Pi^{\mathbf{r}}_{ff'^c}(p) \left(\bar{\Psi}_f U\right) \hat{P}_{\mathbf{r}} \left(U^\dagger \Psi_{f'}\right)^c \right] + \text{h.c.}\end{aligned} \tag{2.24}$$

The first term in this expression is the elementary kinetic term, with Z_f the field normalization, taken to 1 in all numerical calculations. The second term contains the contributions from the composite sector, where the sums of f, f' are over the different elementary fermions. The superindex c refers to charge conjugation of the fermions, which may be necessary in order to construct certain independent terms, depending on the field content of the coset. For a minimal coset containing the Higgs alone, this leads to the same invariants as those without the charge conjugation, and thus can be omitted. The other sum is over the representations $\mathbf{r}$ of H that are contained in the representations $\mathbf{R}_f$. The symbols $\Pi^{\mathbf{r}}_{ff'}$ are functions of momenta, or correlators, that encode the short distance dynamics that have been integrated out. Their explicit form depends on the specifics of the theory of resonances, which will be a subject of sections to follow. In this expression, for $f \neq f'$, the two fermions may not be embedded in the same representation of the group G. If this is the case, that is: $\mathbf{R}_f \neq \mathbf{R}_{f'}$, then the remaining sum is over representations of H common to both, $\mathbf{r} \in (\mathbf{R}_f \cap \mathbf{R}_{f'})$. For

cases where $\mathbf{R}_f = \mathbf{R}_{f'}$, we can see another property of this Lagrangian which is when $\Pi^{(\mathbf{r})}_{ff'}$ are independent of $\mathbf{r}$, the sum over representations $\mathbf{r}$ is such that $\sum_{\mathbf{r}} \hat{P}_{\mathbf{r}} = \mathbb{1}$, and thus as the Goldstone matrix is unitary, this interaction becomes independent of the pNGB. In this case the Goldstones have decoupled from the elementary fermions, this is because by making all correlators $\Pi^{\mathbf{r}}_{ff'}$ equal we have not allowed for the breaking of G. A simple consequence of the unitarity of U is that for all the different invariants that can be formed for each $\mathbf{r}$, not all are linearly independent, as the sum of them is equal to one. For $f,\ f'$ of the same chirality, $\Pi^{\mathbf{r}}_{ff'}$ are proportional to $\not{p}$, in those cases we trade $\Pi^{\mathbf{r}}_{ff'} \to \not{p}\Pi^{\mathbf{r}}_{ff'}$. We will assume this factorization has been done in what follows.

Another property of these correlators is that as the interactions between the elementary and composite sector that are dominant are assumed to be linear, after the integration of the heavier states, the dependence of $\Pi^{\mathbf{r}}_{ff'}$ on the compositeness fractions ϵ_f can be factorized as $\Pi^{\mathbf{r}}_{ff'} = \epsilon_f \epsilon_{f'} \widetilde{\Pi}^{\mathbf{r}}_{ff'}$, with $\widetilde{\Pi}$ only depending on momentum and the parameters of the composite sector. We can see that as a consequence, only the fermions with the largest compositeness will contribute to the effective Lagrangian and to the NGB potential in a substantial manner.

The next ingredient in the effective theory is the interaction between gauge fields and Goldstone fields. For this, we embed the physical gauge fields within multiplets transforming as the adjoint representation of G, filling the rest of entries with nondynamical spurions. We call this G multiplet A^μ, which contains both the elementary gauge fields a^μ as well as spurions $\widetilde{a}^\mu$. As with fermions, the gauge fields multiplets are then dressed with the Goldstone matrices. This allows us to write the interactions, quadratic in the gauge fields, as:

$$\mathcal{L}^g_{\text{eff}} = \frac{1}{2} P_{\mu\nu} \left\{ \sum_a \left[-Z_a p^2 a^\mu a^\nu \right] + \sum_{\mathbf{r}} \Pi^{\mathbf{r}}_G(p) \left(A^\mu U \right) \hat{P}_{\mathbf{r}} \left(U^\dagger A^\nu \right) \right\} \tag{2.25}$$

where the sum over $a = g, w, b$ indexes the SM gauge fields of each factor $\mathrm{SU}(3)_c \times \mathrm{SU}(2)_L \times \mathrm{U}(1)_Y$ respectively. The field normalization is taken as $Z_a = 1/(g_{0,a})^2$, with $g_{0,a}$ denoting each elementary gauge coupling, and the Lorentz structure taken as $P_{\mu\nu} = \eta_{\mu\nu} - p_\mu p_\nu / p^2$. Once again the $\Pi^{\mathbf{r}}_G$ represent correlators encoding the short-distance dynamics after integrating out the resonances of the composite sector.

The Goldstone matrices used in the previous expressions cannot always be explicitly calculated for arbitrary group cosets, as the exponential of an arbitrary matrix will involve a series that may not always be easily summated. However, it is useful to consider the case in which only the Higgs field has a VEV, setting the rest of the NGB fields to zero. In this case, the effective Lagrangian can be put into a simpler form,

after keeping only the dynamical fermionic and gauge degrees of freedom:

$$\mathcal{L}_{\text{eff}}\Big|_v \supset \sum_{f=u,d,e} \left[\bar{f}_L M_f(v,p) f_R + \text{h.c.}\right] + \sum_{f=u,d,e,\nu} \sum_{Q=L,R} \bar{f}_Q \not{p} \left[Z_{f_Q} + \Pi_{f_Q}(v,p)\right] f_Q$$
$$+ \frac{1}{2}\left\{ \sum_{a=g,w,b} a_\mu \left[-Z_a p^2 + \Pi_a(v,p)\right] a^\mu + 2\,\Pi_{wb}(v,p)\, w_\mu^3\, b^\mu \right\} \tag{2.26}$$

The field ν_R can be included just as well, here we do not, as it depends on a choice for the realization of the neutrino masses. In the case of $f = \nu$, therefore, the only chirality included is $Q = L$. We use indices i, j to denote the components of the algebra for each gauge factor, *i.e.*: w^i for $i \in [1,3]$, g^i for $i \in [1,8]$. The functions Π_a, Π_{wb}, Π_{f_Q}, and M_f, now represent sums of invariants, which are functions of v, weighted by the correlators, which are functions of momenta. In the gauge sector there is an off-diagonal term involving bosons w_μ^3 and b_μ, which accounts for the mixing of these two gauge bosons due to the presence of the Higgs VEV. We can write the factorization of these correlators in the case of the gauge sector, as

$$\Pi_a(v,p) = \sum_{\mathbf{r}} i_a^{\mathbf{r}}(v) \Pi_G^{\mathbf{r}}(p) \qquad a = g, w, b, wb \tag{2.27}$$

And for the fermionic sector M_f and Π_{f_L/f_R} are given by

$$\begin{aligned} M_f &= \sum_{\mathbf{r}} j_f^{\mathbf{r}} \Pi_{qf}^{\mathbf{r}}, \quad \Pi_{f_R} = \sum_{\mathbf{r}} i_{f_R}^{\mathbf{r}} \Pi_f^{\mathbf{r}}, \quad \Pi_{f_L} = \sum_{\mathbf{r}} i_{f_L}^{\mathbf{r}} \Pi_q^{\mathbf{r}}, \quad (f = u, d)\ , \\ M_e &= \sum_{\mathbf{r}} j_e^{\mathbf{r}} \Pi_{le}^{\mathbf{r}}, \quad \Pi_{e_R} = \sum_{\mathbf{r}} i_{e_R}^{\mathbf{r}} \Pi_e^{\mathbf{r}}, \quad \Pi_{f_L} = \sum_{\mathbf{r}} i_{f_L}^{\mathbf{r}} \Pi_l^{\mathbf{r}}, \quad (f = e, \nu)\ , \end{aligned} \tag{2.28}$$

where we have omitted the dependence on $\{v, p\}$. The functions $i_f^{\mathbf{r}}$, $j_f^{\mathbf{r}}$ and $i_a^{\mathbf{r}}$ can be expressed in terms of trigonometric functions of v/f, as they arise from the different invariants formed for each representation $\mathbf{r}$, and the Goldstone matrix is an exponential function of the Higgs VEV. As an example, we can show the invariants that arise in the Minimal Composite Higgs Model, coset SO(5)/SO(4), and as well as a family of larger groups with the simple coset structure SO(N)/SO(N−1), with N ≥ 5, where the custodial SO(4) is contained in the unbroken subgroup SO(N − 1), and the fermions are included in the adjoint representation. This will be the case for some of the models considered in the present work. We list the most relevant invariants for this coset in Table 2.1, as functions of $s_v \equiv \sin(v/f)$, $c_v \equiv \cos(v/f)$.

SO(N)	SO(N−1)	i_{u_L}	i_{d_L}	i_{u_R}	i_{ν_L}	i_{e_L}	j_u	i_g	i_w
$\frac{\mathbf{(N-1)N}}{\mathbf{2}}$	$\frac{\mathbf{(N-2)(N-1)}}{\mathbf{2}}$	$1-s_v^2/2$	1	s_v^2	$1-s_v^2/2$	1	$ic_vs_v/\sqrt{2}$	1	$1-s_v^2/2$
	$\mathbf{N-1}$	$s_v^2/2$	0	c_v^2	$s_v^2/2$	0	$-ic_vs_v/\sqrt{2}$	0	$s_v^2/2$

Table 2.1: Invariants $i_f^{\mathbf{r}}$ and $j_f^{\mathbf{r}}$ of the kinetic and mass terms, in the background of the Higgs VEV. We have used $s_v = \sin v/f$ and $c_v = \cos v/f$. We only show the invariants of the fields that have a non-negligible degree of compositeness and contribution to the potential.

We can see how invariants for different representations are not independent: for each diagonal one, the sum $\sum_{\mathbf{r}} i_{f/g}^{\mathbf{r}} = 1$, and for the fermion mass terms, $\sum_{\mathbf{r}} j_f^{\mathbf{r}} = 0$, due to the orthogonality for fermions of different representations. Here $\frac{\mathbf{(N-1)N}}{\mathbf{2}}$ and $\frac{\mathbf{(N-2)(N-1)}}{\mathbf{2}}$ are the adjoint representations of SO(N) and SO(N − 1), respectively. The Higgs transforms in the coset representation $\mathbf{N-1}$. We see how the gluon has invariants i_g independent of v, due to the fact that the Higgs is colorless, and the gluons are $\mathrm{SU}(2)_L \times \mathrm{U}(1)_Y$ singlets. Some of the invariants have been omitted, we only show those corresponding to the elementary states with the most sizeable contributions to the potential. In the case of fermions, as the form factors are proportional to the compositeness fractions, in our framework the Left-handed states will dominate over the Right-handed ones, and particularly those of the third generation. This pattern of mixings is required for accommodating the B-anomalies, as we will later show. In the case of gauge fields, their contribution to the potential is weighted by the elementary gauge couplings $g_{0,a}$ through their field normalization factors Z_a. For this reason, in the table above and in this work we will ignore contributions of the hypercharge gauge boson to the potential. We will find a particular example including these invariants with the coset structure SO(12) /SO(11) in Chapter 4.

The spectrum of fermions, both physical states and heavier resonances of the theory, can be obtained by computing the equations of motion from the effective Lagrangian of Eq. (2.26):

$$p^2(Z_{f_L} + \Pi_{f_L}(v,p))(Z_{f_R} + \Pi_{f_R}(v,p)) - |M_f(v,p)|^2 = 0 \tag{2.29}$$

The masses of the physical fermions are obtained by the values of momenta corresponding to the smallest zeros of this expression. We see how in the absence of a Higgs VEV, as $M_f(v) = 0$ the smallest zero is at $p = 0$, thus without EWSB the dynamical fermions are massless. The spectrum of heavier resonances that have the same quantum numbers as the physical fermions corresponds to the heavier zeros of this equation. However, there may also be exotic states in the composite sector, this is, states that have quantum numbers different from the SM fermions. These states are contained in the multiplets of G, however, they are not directly coupled to elementary fermions.

The masses of these resonances will be given by the poles of this equation, with $Z_f = 0$ as there is no corresponding elementary state.

2.1.3. Calculation of pNGB potential

Having already written the effective interaction in terms of the elementary states, one can proceed by computing the potential for the NG bosons. This potential is dynamically generated, and can be easily calculated at 1 loop. This potential arises as the sum of all one-particle irreducible diagrams, or 1PI. This potential arises exclusively because of the elementary states being in incomplete representations of the group G, thus being a source of explicit breaking of the symmetry group of the composite sector. We can write this effective potential as an integral in momentum space:

$$V(\Pi) = \frac{1}{2}\int \frac{d^4p}{(2\pi)^4}\left\{-\log \mathrm{Det}\left(\frac{\mathcal{K}_f}{\mathcal{K}_f^0}\right) + \log \mathrm{Det}\left(\frac{\mathcal{K}_a}{\mathcal{K}_a^0}\right)\right\} \ , \tag{2.30}$$

where $\mathcal{K}_f$ and $\mathcal{K}_a$ are the fermionic and bosonic matrices in the quadratic effective Lagrangian over elementary fields:

$$\mathcal{L}_{\text{eff}} \supset \bar{f}\,\mathcal{K}_f(\Pi)\,f + \frac{1}{2}a\,\mathcal{K}_a(\Pi)\,a \ , \qquad f^t = (u_L, d_L, \nu_L, e_L, u_R, d_R, e_R) \ , \ a^t = (g^k, w^i, b) \ . \tag{2.31}$$

This Lagrangian is simply a rewriting of Eqs. (2.24) and (2.25) in compact form, where all dependence in the scalar fields is contained in these matrices $\mathcal{K}_f$ and $\mathcal{K}_a$, Lorentz indices have been omitted, and the fields have been packed in vectors f and a. If one considers a single generation of fermions, taking into account the color multiplicities in $u_{L/R}$ and $d_{L/R}$, the matrix $\mathcal{K}_f$ is 15-by-15, and matrix $\mathcal{K}_a$ is 12-by-12. In most of the present work we will focus on the contributions of the third generation of fermions to the potential, as their degrees of compositeness are larger than those of the lighter generations. Similarly, in our approach the compositeness of the Right-handed bottom quark, and tau lepton are smaller than that of the top quark. For this reason, d_R, e_R can usually be dropped from the calculations, as can the weak hypercharge boson B, whose compositeness is proportional to the gauge coupling g'. The potential in Eq. (2.30) has been normalized by subtracting a constant term in the Goldstones, this removes an infinite volume divergent term. The superindex 0, in these matrices, means the NGBs are set to zero: $\mathcal{K}^0_{f/a} \equiv \mathcal{K}_{f/a}(\Pi = 0)$. The difference in relative sign between the fermionic and bosonic contributions to the potential is related to the anticommuting nature of fermions, *i.e.* the minus sign in Eq. (2.30). For an arbitrary coset and all the Goldstone fields at nonzero values, computing these matrices to all orders in Π may not be a feasible task. However, if only the Higgs acquires a VEV, we have shown how the effective Lagrangian is taken to the form in Eq. (2.26). The matrix K_f in this case

takes a block diagonal form, where for a given fermion each block reads:

$$\left[\bar{u}_L,\ \bar{u}_R\right] \cdot \mathcal{K}_f^{(u)} \cdot \begin{bmatrix} u_L \\ u_R \end{bmatrix} = \left[\bar{u}_L,\ \bar{u}_R\right] \cdot \begin{pmatrix} \not{p}\,(Z_q + \Pi_{u_L}) & M_u \\ M_u^* & \not{p}\,(Z_{u_R} + \Pi_{u_R}) \end{pmatrix} \cdot \begin{bmatrix} u_L \\ u_R \end{bmatrix} \quad (2.32)$$

Here we are showing the block that corresponds to the up-quark, as the top quark has the largest compositeness, and as such the effect of either Π_{u_R} or M_u cannot be ignored. For other fermions with smaller masses, their compositeness fractions will be such that mostly the Left-handed correlator Π_{f_L} will have an appreciable effect. In those cases only the term coming from the elementary fermion and corresponding to its Right-handed chirality will be present: $Z_{f_R}\not{p}$. As the potential involves the Determinant of the whole matrix $\mathcal{K}_f$, this factorizes as the product of the Determinant of each block. The spinor multiplicity will only contribute to a factor of 4 in the potential, after taking the log function. The same will occur with the color multiplicity, as the Higgs is colorless and does not mix between different components. Taking these things into consideration, the potential can now be expressed as:

$$\begin{aligned} V(v) \simeq \int \frac{d^4p}{(2\pi)^4} \Big\{ & \frac{9}{2} \log\left[-Z_w p^2 + \Pi_w\right] - 2\log\left[p^2 Z_{e_R}\left(Z_l + \Pi_{e_L}\right)\right] - 2\log\left[p\left(Z_l + \Pi_{\nu_L}\right)\right] \\ & - 2N_c \log\left[p^2 Z_{d_R}\left(Z_q + \Pi_{d_L}\right)\right] - 2N_c \log\left[p^2\left(Z_q + \Pi_{u_L}\right)\left(Z_{u_R} + \Pi_{u_R}\right) - |M_u|^2\right] \Big\} \\ & - V(v=0)\ . \end{aligned} \quad (2.33)$$

We have written explicitly factors such as $p^2 Z_{e_R}$ or $p^2 Z_{d_R}$ that are however removed after subtracting the constant term, as without the inclusion of a mass term, Left and Right chiralities are factored. This is only an approximation, using the fact that the smaller degree of compositeness makes such form factor Π_{f_R} smaller than its Left counterpart. In this expression we have not considered the presence of a Right-handed neutrino. The gluons only contribute with a constant term to the potential, as Π_g is independent of v, and has been omitted in the equation above as such a constant term gets subtracted.

One can see how each term in the potential is given by the log of the equations of motion of each matter field, with a factor given by the multiplicity of said field. For instance, for $\mathrm{SU}(2)_L$ bosons, we get a 9 for three helicities of massive bosons, times three generators. For Dirac fermions, a factor of 4 (times a prefactor of $\frac{1}{2}$) corresponds to the degrees of freedom. For a fermion of a single chirality, as could be the case of ν_L, one has to consider the E.O.M. quadratic in momentum inside the log. In that case, one gets a term $\log\left[p^2\left(Z_l + \Pi_{\nu_L}\right)^2\right]$, the degrees of freedom being 2 for a fermion of a single chirality.

In order to study EWSB, it is useful to resort to a power expansion. By looking at

Table 2.1, we see that the potential can be expanded in terms of $s_v \equiv \sin(v/f)$, which, for small enough $v \ll f$, is a good approximation. We have, up to fourth order [83]:

$$V(v) \simeq -\alpha s_v^2 + \beta s_v^4 + \mathcal{O}\left(s_v^6\right) \ , \tag{2.34}$$

where we have chosen an explicit sign for the quadratic term in the potential. The actual sign of α however depends on the specific values of the correlators, which in turn depend on microscopic parameters of the theory of resonances. The cases where there is EWSB correspond to $\alpha > 0,\ \beta > 0$. We can give an estimate for a natural size of these parameters, as they are given by 1 loop integrals of such correlators, whose size is driven by the compositeness of the heaviest fermions, ϵ_f. We have [84]:

$$\alpha \sim \frac{N_c}{(4\pi)^2} m_*^4 \epsilon_f^2, \qquad \beta \sim \frac{N_c}{(4\pi)^2} m_*^4 \epsilon_f^4 \ , \tag{2.35}$$

where ϵ_f will be the dominant mixing, typically q or u_R of the third generation. The value of the Higgs VEV can be found by computing the minimum of Eq. (2.34), ignoring all higher order terms, we get:

$$s_v^2 \simeq \frac{\alpha}{2\beta} \ . \tag{2.36}$$

For this coset structure, the matching equation is that of Eq. (2.13). For a large dominant mixing $\epsilon_f \sim 1$, as can be expected for the top quark, one has $\alpha \sim \beta$. We see that in order to get a Higgs VEV of order $v_{\rm SM}^2/f^2 = s_v^2 \ll 1$, a tuning of this order is needed in these parameters. Moreover, for $\epsilon_f < 1$, the tuning is worsened by a factor of $1/\epsilon_f^2$, which is usually termed "double tuning" [84].

Computing the second order derivative at the minimum, we can get an estimate for the Higgs mass,

$$m_h^2 \simeq \frac{8}{f^2}\frac{\alpha(\beta-\alpha)}{\beta} \sim \frac{N_c}{2\pi^2} g_*^4 \epsilon_f^4 v_{\rm SM}^2 \simeq \left[380 \text{ GeV} \left(\frac{g_*}{4}\right)^2 \left(\frac{\epsilon_f}{1/2}\right)^2\right]^2 \ . \tag{2.37}$$

This equation also shows that some tuning is required in order to get a Higgs mass of order $m_h \approx 125$ GeV. For the top quark Yukawa, $y_t \sim g_* \epsilon_{q3} \epsilon_{u3} g_* \sim 1$, if we take similar mixings for both chiralities, and $g_* \approx 4$[1], we obtain $\epsilon_{q3/u3} = 0.5$. In this case, Eq. (2.37) shows some tension with the physical value of the Higgs mass. There are however ways this tension can be alleviated, as for example a calculation of both α and β will show the presence of Clebsch-Gordan coefficients in different combinations, usually these numbers can help the m_h to approach the physical value. We will later show an explicit calculation of these parameters, in Chapter 5. Calculations in explicit models of resonances, as for example in extra-dimensions [65, 83] and discrete composite

[1] From QCD one gets an estimate of $g_* \approx 4$, where from $\rho \to \pi\pi$ one gets $g_{\rho\pi\pi} \sim 4-6$ [85].

Higgs models [86, 87], have shown that this mass can be correlated with the presence of light fermionic resonances, usually $\lesssim 1$ TeV, also called custodians.

In the framework where one coupling g_* and one scale m_* completely characterize the first level of resonances, fixing m_* and g_* (and thus $f = m_*/g_*$) one can obtain a lower bound for the tuning associated to the Higgs VEV. For $f \sim$ TeV, the tuning required in s_v^2 is of order $\sim 6\,\%$. However, if $m_* \gtrsim 10 - 30$ TeV, as required by contributions of gluon resonances to ϵ_K [88], the estimate $g_* \approx 4$ leads to a tuning in the VEV at least of order $(1 - 0.1)\,\%$.

If the potential is dominated by the fermionic contributions, when the fermionic resonances are lighter than the spin-1 resonances, some amount of tuning associated to Eq. (2.37) can be alleviated, since in this case the Higgs potential can be regulated by a lighter fermionic state [84]. Trading $m_* \to m_\psi = g_\psi f$, amounts to changing g_* by g_ψ in (2.37), that for $g_\psi = k_\psi g_*$, leads to a suppression factor k_ψ^2. In this case the two distinct couplings $g_{*/\psi}$ are accounting for the scale separation between fermionic and bosonic resonances. For $k_\psi \simeq 0.5$ one can expect a Higgs mass of $\mathcal{O}(100$ GeV). On the other hand, the tuning from Eq. (2.36) depends on the relative size of α and β, thus it is not expected to decrease with k_ψ, instead in the present model for $\epsilon_f < 1$ one obtains a problem of double tuning. It is known that in this case the double tuning helps reducing the Higgs mass [84].

As we previously mentioned, computing $\mathcal{K}(\Pi)$ to all orders in the Goldstone fields is not usually possible. However, the Goldstone matrix can be computed up to any specific order in a trivial manner, as it is the exponential of a matrix, defined through its Taylor series. This allows us to define a perturbative $\mathcal{K}$ matrix. In order to expand in powers of the NGB, we introduce an accompanying factor ω in these scalar fields, such that $\Pi \to \omega\Pi$. This is only an auxiliary factor, to be later set to 1. We thus have, by definition of the Goldstone matrix:

$$U(\Pi;\omega) \equiv e^{i\omega\Pi/f} = \sum_{n\geq 0} \frac{i^n \omega^n}{n! f^n} \Pi^n \ . \tag{2.38}$$

This allows us to compute a fermionic invariant, for example, at a given order L:

$$\begin{aligned} &\frac{\partial^L}{\partial \omega^L} \left[\left(\bar{\Psi}_f U(\Pi;\omega)\right) \hat{P}_{\mathbf{r}} \left(U^\dagger(\Pi;\omega)\Psi_f\right) \right] \Big|_{\omega=0} \\ &\qquad = \frac{i^L}{f^L} \sum_{\ell=0}^{L} \frac{1}{\ell!(L-\ell)!} \left(\bar{\Psi}_f \Pi^\ell\right) \hat{P}_{\mathbf{r}} \left(\left(-\Pi^\dagger\right)^{L-\ell} \Psi_f \right) \ , \end{aligned} \tag{2.39}$$

where we consider here two fermionic multiplets belonging to representation $\mathbf{R}_f$, thus the Goldstone matrices are expressed in terms of generators in the same representation. Notice that the projector $\hat{P}_{\mathbf{r}}$ does not commute with the matrix insertions, thus in

general, $L+1$ terms have to be computed independently. This procedure allows us to obtain the fermionic $\mathcal{K}_f$ perturbatively, an equivalent expression applies to those terms involving gauge fields. We can thus define, for either fermionic or bosonic matrices, their perturbative expansions:

$$\mathcal{K}(\Pi) \equiv \sum_{n\geq 0} \omega^n \mathcal{K}_n \ . \tag{2.40}$$

This allows us to perturbatively compute the NGB potential. The integrand of the potential involves, schematically, $V(\Pi) \sim \int d^4p\, \mathcal{V}(p,\Pi)$, where $\mathcal{V} = \log \mathrm{Det}(\mathcal{K}/\mathcal{K}_0)$ and we are omitting both the loop factor and the fermionic/bosonic identification and sign. Here we have to make use of the following operator identity:

$$\mathcal{V}(\Pi) = \log \mathrm{Det}\left(\mathcal{K}(\Pi)\mathcal{K}_0^{-1}\right) = \mathrm{Tr}\log\left(\mathcal{K}(\Pi)\mathcal{K}_0^{-1}\right) = \mathrm{Tr}\log\left(1+\sum_{n\geq 1}\omega^n \mathcal{K}_n\mathcal{K}_0^{-1}\right) \ . \tag{2.41}$$

We are now ready to expand the potential in powers of ω. Defining $\widetilde{\mathcal{K}}_n = \mathcal{K}_n\mathcal{K}_0^{-1}$ we have,

$$\begin{aligned}\mathrm{Tr}\log\left(\mathcal{K}(\Pi)\mathcal{K}_0^{-1}\right) \simeq\ & \omega\,\mathrm{Tr}\left(\widetilde{\mathcal{K}}_1\right) + \omega^2\,\mathrm{Tr}\left(\widetilde{\mathcal{K}}_2 - \frac{\widetilde{\mathcal{K}}_1^2}{2}\right) + \omega^3\,\mathrm{Tr}\left(\widetilde{\mathcal{K}}_3 - \widetilde{\mathcal{K}}_1\widetilde{\mathcal{K}}_2 + \frac{\widetilde{\mathcal{K}}_1^3}{3}\right) \\ & + \omega^4\,\mathrm{Tr}\left(\widetilde{\mathcal{K}}_4 - \widetilde{\mathcal{K}}_1\widetilde{\mathcal{K}}_3 - \frac{\widetilde{\mathcal{K}}_2^2}{2} + \widetilde{\mathcal{K}}_1^2\widetilde{\mathcal{K}}_2 - \frac{\widetilde{\mathcal{K}}_1^4}{4}\right) + \mathcal{O}(\omega^5) \ .\end{aligned} \tag{2.42}$$

We see how by having an expansion of the $\mathcal{K}$ matrix we can compute the potential up to a given order by a trace of products and sums of matrices alone. Here we have truncated up to fourth order, at this order one can begin to characterize the spontaneous symmetry breaking, if it occurs. Typically the shape of the potential in terms of the Goldstones can be constructed by looking at their SM quantum numbers alone: one can see what combination of fields form invariants under $\mathrm{SU}(3)_c\times\mathrm{SU}(2)_L\times\mathrm{U}(1)_Y$:

$$V(\Pi) \simeq \mu_H^2|H|^2 + \lambda_H\left(|H|^2\right)^2 + \sum_{\Pi\neq H}\left\{\mu_\Pi^2|\Pi|^2 + \lambda_\Pi\left(|\Pi|^2\right)^2 + \lambda_{H\Pi}|H|^2|\Pi|^2\right\} + \dots \tag{2.43}$$

Depending on the specifics of the coset there may also be cubic or linear terms, if for example a singlet is present. There may also be more than one way to combine the fields into a quartic invariant in a way that is linearly independent. We will see this later on with explicit examples of cosets. By performing the computation of $\mathcal{V}(\Pi)$ in Eq. (2.42), and matching at $\omega = 1$ with Eq. (2.43), we get the coefficients of the potential as momentum integrals of combinations of fermionic and bosonic form factors $\Pi^{\mathbf{r}}_{ff'}$ and $\Pi^{\mathbf{r}}_{g}$. By modeling the theory of resonances, one can compute the shape of these

correlators and thus perform the integrals in momenta. Examples of this will be shown in later sections. Without an explicit model of resonances, or even specifying the coset, we can still estimate the size of these coefficients by dimensional analysis alone. We have, for the quadratic and quartic terms, the following estimates

$$\mu_\Pi^2 \sim \epsilon_f^2 \frac{m_*^4}{(4\pi)^2 f^2}, \qquad \lambda_\Pi \sim \epsilon_f^2 \frac{m_*^4}{(4\pi)^2 f^4} \ , \tag{2.44}$$

where the fractions ϵ_f correspond to the fields with the largest compositeness, usually third generation quarks, where an extra factor N_c of color multiplicity can be present or not, depending on whether the pNGB field Π has color and the specifics of the invariant.

2.2. Anarchic Partial Compositeness

So far we have discussed the hypothesis of Partial Compositeness and how it allows the generation of a hierarchy of masses via small differences in the composite operator scaling dimensions, and the running of the elementary-composite couplings through a large separation of scales. However we now turn to the task of describing how this simple tool is applied to the SM flavor structure. That is, how one can generate the actual spectrum of fermions, and their mixings, in a way that does not require a particular tuning of the parameters of the theory. A simple scheme that is able to generate the flavor structure of the SM and requires very few hypotheses is the one called Anarchic Partial Compositeness (APC). We will briefly describe it, together with the main experimental constraints on it, and the limitations it faces. A starting point is considering Eq. (2.15) with generation indices added to it:

$$\mathcal{L}_{\text{UV}} = \sum_{i,j=1,2,3} \left\{ \frac{\omega_{q_L}^{ij}}{\Lambda_{\text{UV}}^{\Delta_{q_L}^j - 5/2}} \bar{q}_L^i \mathcal{O}_{q_L}^j + \frac{\omega_{d_R}^{ij}}{\Lambda_{\text{UV}}^{\Delta_{d_R}^j - 5/2}} \bar{d}_R^i \mathcal{O}_{d_R}^j + \frac{\omega_{u_R}^{ij}}{\Lambda_{\text{UV}}^{\Delta_{u_R}^j - 5/2}} \bar{u}_R^i \mathcal{O}_{u_R}^j \right\} \ , \tag{2.45}$$

where we concentrate on the quark sector, which has both a hierarchical spectrum of masses and of mixing angles in the Cabibbo-Kobayashi-Maskawa (CKM) matrix. The lepton sector requires a choice for the modeling of the neutrino masses, and the Pontecorvo–Maki–Nakagawa–Sakata (PMNS) matrix differs from the CKM in that it has large mixing angles. We are now considering that for a particular fermion, all three generations couple with the three composite operators with the same quantum numbers. The composite operators $\mathcal{O}^{\psi,i}$ are characterized by their scaling dimensions Δ_ψ^i, which we assume are different. These fermionic operators are defined in the UV where the global symmetry G is unbroken, and as such these operators are contained within full representations of this symmetry group. We shall assume that the same

representation is being used for the three generations. The coupling of this composite operators with the elementary fermions does however explicitly break this symmetry, by selecting the part of the full representation which has the same SM quantum numbers. The structure of matrices ω_ψ^{ij} is said to be anarchic, as in all entries, including the off-diagonal ones, are of the same order. At lower energies, the composite sector confines and the lightest fermionic resonances appear. At this scale the couplings are modified via their running under the RG equations:

$$\lambda_\psi^{ij} \equiv \omega_\psi^{ij}[m_*] = \omega_\psi^{ij} \left(\frac{m_*}{\Lambda_{\rm UV}}\right)^{\Delta_\psi^j - 5/2} \equiv \widetilde{\lambda}_\psi \, c_\psi^{ij} \, \zeta_\psi^j \ , \tag{2.46}$$

where in the last equality we have factored this matrix into an overall normalization, $\widetilde{\lambda}_\psi$, an anarchic matrix c_ψ^{ij} with entries of order one, and the vector ζ^j, whose components

$$\zeta_\psi^j = \left(\frac{m_*}{\Lambda_{\rm UV}}\right)^{\Delta_\psi^j - 5/2} \ , \tag{2.47}$$

will be hierarchical for composite operators with different scaling dimensions, and a large scale separation $m_* \ll \Lambda_{\rm UV}$. We assume the operators have been ordered such that $\zeta^1 \ll \zeta^2 \ll \zeta^3$, this demands that $\Delta_\psi^i > \Delta_\psi^j$ for $i < j$. At this lower energy scale, the interaction between the elementary fermions and the composite operators, and consequently between the elementary sector and the fermionic resonances Φ_ψ excited by these operators, will be given by these matrices λ_ψ^{ij}:

$$\mathcal{L}_{\rm int}[m_*] \sim \sum_{\psi = q_L, u_R, d_R} c_\psi^{ij} \, \widetilde{\lambda}_\psi \, f \, \zeta_\psi^j \, \bar{\psi}^i \, \Phi_\psi^j \tag{2.48}$$

Whereas at high energies the composite operators of different generations have different scaling dimensions, which can be understood as different quantum numbers under the full symmetry group, once we are working with the effective theory of resonances, the conformal symmetry has been broken and all fermionic resonances have dimension 3/2. This means that for a specific fermion species ψ we can now perform a rotation that mixes the different fermionic resonances Φ_ψ^j. In order to do so, we can first state a very simple theorem on the singular value decomposition of a matrix [18]. Starting with a matrix with the following form:

$$M_{ij} \equiv \zeta_L^i c^{ij} \zeta_R^j \tag{2.49}$$

with c^{ij} an anarchic matrix, with $\mathcal{O}(1)$ coefficients, and $\zeta_{L,R}$ vectors which are ordered $\zeta_L^i \leq \zeta_L^j$ for $i < j$ and likewise for ζ_R^i. The theorem is useful when either one or both the $\zeta_{L,R}$ have a hierarchic ordering, that is, $\zeta^i \ll \zeta^j$ for $i < j$. Following a singular

value decomposition of the matrix M, we get

$$M^{ij} = U_L^{ik} m^{kl} (U_R^\dagger)^{lj} \ , \tag{2.50}$$

with m being a real diagonal matrix with entries of order given by

$$m^{ii} \sim \zeta_L^i \zeta_R^i \ , \tag{2.51}$$

and the elements of each unitary transformation are:

$$U_L^{ij} \sim \begin{cases} \zeta_L^i / \zeta_L^j & \text{for} \quad i < j \\ 1 & \text{for} \quad i = j \\ \zeta_L^j / \zeta_L^i & \text{for} \quad i > j \end{cases} \ , \tag{2.52}$$

with the same structure being present in U_R. The result is non-trivial only for hierarchical ζ_L or ζ_R. In this case the diagonal entries of m will also be hierarchical $m^{11} \ll m^{22} \ll m^{33}$, and the rotations corresponding to the hierarchical vectors will be close to unity.

Applying this theorem for the couplings matrix in Eq. (2.48), we have a non-hierarchical, order one ζ_L and a strongly hierarchical $\zeta_R = \zeta_\psi$. Thus, performing rotations of both elementary and composite fields can take this matrix to a diagonal form. The rotation of the elementary fields involves anarchic $\mathcal{O}(1)$ entries, whereas the rotation of composite fermions is hierarchical. The interaction Lagrangian now takes a diagonal form:

$$\mathcal{L}_{\text{int}}[m_*] \sim \sum_{\psi = q_L, u_R, d_R} \widetilde{\lambda}_\psi^i \, f \, \bar{\psi}^i \, \Phi_\psi^i \tag{2.53}$$

with $\widetilde{\lambda}_\psi^i = \widetilde{\lambda}_\psi \, \zeta_\psi^i$. If more than one multiplet of resonances in the composite sector couple to the elementary sector, the interaction Lagrangian will have more than one term present for a single species of fermions ψ, all of which in general will not assume a diagonal form. As the diagonalization procedure requires the elementary fermions to be rotated, for such a situation where multiple couplings are present, only the mixings of a single set of composite fermions can be diagonalized. In certain models, however, multiple mixings are required in order to obtain a realistic scenario. This can involve further hypotheses to be demanded, as for instance an alignment to be present among the couplings with different composite multiplets [89].

With the structure of the elementary-composite couplings of fermions at hand, we can look into the generation of masses and mixings present in the standard model. Focusing on the quark sector, we are confronted with reproducing the structure of the Left-handed mixings, that conform the V_{CKM} matrix, along with a particular spectrum

of masses. We will see how this translates into a particular hierarchy for the elementary-composite couplings and thus the compositeness fractions. As the Higgs now belongs to the composite sector, with a $\mathcal{O}(g_*)$ (with $g_* \gg 1$) anarchic coupling to fermionic resonances, the Yukawa coupling to physical fermions will involve two insertions of the elementary-composite couplings λ^i_ψ. We can write the Yukawa matrices for the quarks as

$$y_u^{ij} = \frac{\lambda^i_{q_L}\lambda^j_{u_R}}{g_*} c_u^{ij} \ , \qquad y_d^{ij} = \frac{\lambda^i_{q_L}\lambda^j_{d_R}}{g_*} c_d^{ij} \tag{2.54}$$

Matrices c_u and c_d represent couplings in the composite sector among the different generations of composite quarks. Their structure depends on the details of the composite sector. In anarchic partial compositeness, there is no flavor structure in the composite sector, and thus one has both c_u and c_d with all entries of the same order:

$$c_u^{ij} \sim c_d^{ij} \sim 1, \tag{2.55}$$

As the spectrum of masses and mixings of quarks is indeed hierarchical, this structure has to be inherited from the elementary-composite mixings λ^i_ψ. We have seen how, for different operator dimensions, these couplings are in general strongly ordered, due to the running of the renormalization group equation, and a large separation of scales. We consider $\lambda^1_\psi \ll \lambda^2_\psi \ll \lambda^3_\psi$, for $\psi = q_L$, u_R, d_R. In order to find the spectrum we can use the theorem stated above, where now both ζ_L and ζ_R are hierarchical. These Yukawa matrices are taken into diagonal form

$$y_u = U_L y_u^D U_R^\dagger, \qquad y_d = D_L y_d^D D_R^\dagger \ , \tag{2.56}$$

where the diagonalized Yukawas have entries of order

$$y_u^{D,ii} \sim \frac{\lambda^i_{q_L}\lambda^i_{u_R}}{g_*}, \qquad y_d^{D,ii} \sim \frac{\lambda^i_{q_L}\lambda^i_{d_R}}{g_*} \ , \tag{2.57}$$

and the rotations are close to the identity, with off diagonal entries given by the ratios of the λ^i_ψ couplings:

$$U_L^{ij} \sim \begin{cases} \lambda^i_{q_L}/\lambda^j_{q_L} & \text{for} \quad i<j \\ 1 & \text{for} \quad i=j \\ \lambda^j_{q_L}/\lambda^i_{q_L} & \text{for} \quad i>j \end{cases} \tag{2.58}$$

and similarly for U_R, and $D_{L,R}$.

It is useful to write these expressions in terms of the compositeness fractions

ϵ_{qi}, ϵ_{ui}, ϵ_{di} which, for small λ_ψ are defined as

$$\epsilon_{\psi,i} = \frac{\lambda_\psi^i}{g_*} \ . \tag{2.59}$$

In this case, the Yukawas are now given by $y_{u,d} \sim \epsilon_q \, g_* \, \epsilon_{u,d}$, and the mixing matrices by the ratios of these ϵ. The $V_{\rm CKM}$ matrix is defined as the product of both Left-handed rotation matrices:

$$V_{\rm CKM} = U_L^\dagger D_L \tag{2.60}$$

which, as both rotations are of the same size, implies that lacking any artificial alignment, CKM has entries of the same order:

$$V_{\rm CKM}^{ij} \sim V_{\rm CKM}^{ji} \sim \frac{\epsilon_{q,i}}{\epsilon_{q,j}} \qquad \text{for} \quad i < j \ . \tag{2.61}$$

Now, as the elementary-composite mixings are free parameters of the theory, their hierarchies being inherited by the values of the scaling dimensions of composite operators in the strongly coupled sector, we can see how the choice of these parameters can reproduce the specific spectrum and mixings of the quark sector.

In order to reproduce the $V_{\rm CKM}$ matrix, we look at the following parametrization:

$$V_{\rm CKM} \sim \begin{pmatrix} 1-\lambda_C^2 & \lambda_C & \lambda_C^3 \\ \lambda_C & 1-\lambda_C^2 & \lambda_C^2 \\ \lambda_C^3 & \lambda_C^2 & 1 \end{pmatrix} \tag{2.62}$$

where we express the size of the entries in terms of the sine of the Cabibbo angle, $\lambda_C = \sin(\theta_C) \simeq 0.225$. It can be thought of as a simplification of the Wolfenstein parametrization, at $\mathcal{O}(\lambda_C^3)$, where we disregard $\mathcal{O}(1)$ parameters and phases. Reproducing the CKM matrix, then, involves fixing the hierarchy of Left-handed compositeness fractions, in terms of the Cabibbo angle [18, 88, 90, 91]:

$$\frac{\epsilon_{q1}}{\epsilon_{q3}} \sim \lambda_C^3, \qquad \frac{\epsilon_{q2}}{\epsilon_{q3}} \sim \lambda_C^2 \ . \tag{2.63}$$

For the Right-handed compositeness, one must reproduce the spectrum of masses. We get, in terms of the SM Yukawas:

$$\begin{aligned} \epsilon_{u1} &\sim \frac{y_u^{\rm SM}}{\lambda_C^3 g_* \epsilon_{q3}} \ , & \epsilon_{u2} &\sim \frac{y_c^{\rm SM}}{\lambda_C^2 g_* \epsilon_{q3}} \ , & \epsilon_{u3} &\sim \frac{y_t^{\rm SM}}{g_* \epsilon_{q3}} \ , \\ \epsilon_{d1} &\sim \frac{y_d^{\rm SM}}{\lambda_C^3 g_* \epsilon_{q3}} \ , & \epsilon_{d2} &\sim \frac{y_s^{\rm SM}}{\lambda_C^2 g_* \epsilon_{q3}} \ , & \epsilon_{d3} &\sim \frac{y_b^{\rm SM}}{g_* \epsilon_{q3}} \ , \end{aligned} \tag{2.64}$$

where the Yukawas can be written in terms of the particle masses as $y_f^{\rm SM} \sim m_f / v_{\rm SM}$.

With these conditions all free parameters are fixed, except the compositeness of the third generation, of which only the product is fixed. Because of this, all parameters have been written in terms of ϵ_{q3}.

So far, we have focused on the quark sector. Regarding the lepton sector, besides the spectrum one has to reproduce the mixings contained in the PMNS matrix. However, we have not chosen a specific realization of the neutrinos in our composite model, as such, not all elementary-composite mixings can be fixed. The mass spectrum of charged leptons does put conditions on the product of Left and Right-handed compositeness fractions. The Right-handed ones can be written in terms of the Yukawas and the left handed ones as

$$\epsilon_{e1} \sim \frac{y_e^{\rm SM}}{g_* \epsilon_{l1}} \ , \qquad \epsilon_{e2} \sim \frac{y_\mu^{\rm SM}}{g_* \epsilon_{l2}} \ , \qquad \epsilon_{e3} \sim \frac{y_\tau^{\rm SM}}{g_* \epsilon_{l3}} \ . \tag{2.65}$$

For example, a choice one can make is a Left-Right symmetric scenario for the compositeness fractions, which fixes each generation to be of size

$$\epsilon_{l1} \sim \epsilon_{e1} \sim \sqrt{\frac{y_e^{\rm SM}}{g_*}} \ , \qquad \epsilon_{l2} \sim \epsilon_{e2} \sim \sqrt{\frac{y_\mu^{\rm SM}}{g_*}} \ , \qquad \epsilon_{l3} \sim \epsilon_{e3} \sim \sqrt{\frac{y_\tau^{\rm SM}}{g_*}} \ , \tag{2.66}$$

and, as we will later see, in specific models one can deviate from this structure. In the L-R symmetric case, as the masses of charged leptons are $m_e \ll m_\mu \ll m_\tau$, then the mixings themselves inherit this hierarchy. This in turn means that the matrices diagonalizing the charged lepton mass matrices are hierarchical ($U_{e_L}^{ij} \sim \epsilon_{li}/\epsilon_{lj}$, $U_{e_R}^{ij} \sim \epsilon_{ei}/\epsilon_{ej}$, for $i < j$). As the PMNS matrix has large mixing angles, this forces its structure to be generated by the neutrino sector [18, 92, 93].

2.2.1. Constraints to APC

We are now ready to examine the main flavor constrains to APC. In this section we will be looking at the main processes contributing to flavor violation in the SM, which operators give contributions to these processes and what the experimental limits are. Finally we will provide estimates in APC for the Wilson Coefficients of said observables, and we will look at how this translates to limits on the mass scale of the composite sector. We organize this section by considering both flavor and CP violating processes, dividing it into $\Delta F = 2$, $\Delta F = 1$ and $\Delta F = 0$.

$\Delta F = 2$

The main contributions to these processes arise from 4-fermion contact interactions. One can write a Lagrangian for interactions of this kind as:

$$\mathcal{L}_{\Delta F=2} \sim \frac{\lambda_i \lambda_j \lambda_k \lambda_l}{g_*^2 m_*^2} (\bar{f}_i \gamma_\mu f_j)(\bar{f}_k \gamma^\mu f_l) \tag{2.67}$$

By use of Fierz identities, these interactions can be reduced into a basis of 8 operators, whose Wilson Coefficients are bounded by the different flavor violating processes involving meson mixings. This basis of operators we denote by Q_k^{ij}, with i, j being labels for the different quark flavors, with $k = 1, \dots 5$, and $\widetilde{Q}_k^{ij}$ with $k = 1, \dots 3$. We can write these operators as:

$$Q_1^{ij} = (\bar{f}_{iL}^{\alpha} \gamma_\mu f_{jL}^{\alpha})(\bar{f}_{iL}^{\beta} \gamma^\mu f_{jL}^{\beta}) \tag{2.68}$$
$$Q_2^{ij} = (\bar{f}_{iR}^{\alpha} f_{jL}^{\alpha})(\bar{f}_{iR}^{\beta} f_{jL}^{\beta}) \tag{2.69}$$
$$Q_3^{ij} = (\bar{f}_{iR}^{\alpha} f_{jL}^{\beta})(\bar{f}_{iR}^{\beta} f_{jL}^{\alpha}) \tag{2.70}$$
$$Q_4^{ij} = (\bar{f}_{iR}^{\alpha} f_{jL}^{\alpha})(\bar{f}_{iL}^{\beta} f_{jR}^{\beta}) \tag{2.71}$$
$$Q_5^{ij} = (\bar{f}_{iR}^{\alpha} f_{jL}^{\beta})(\bar{f}_{iL}^{\beta} f_{jR}^{\alpha}) \tag{2.72}$$

where the $\widetilde{Q}_k^{ij}$ are obtained by flipping the chiralities of the quarks. We see how operator Q_1 involves only Left-handed quarks, and the rest $Q_2 \dots Q_5$ involving two Left- and two Right-handed quarks. By flipping the chiralities, $\widetilde{Q}_1$ will involve only Right-handed quarks.

The constraints on the WC of these operators come from considering flavor violating processes involving meson mixing. For example, the Kaon system provides constraints for coefficients involving the first and second generation of down quarks. The mixing of the K^0 resonance with its anti-particle $\bar{K}^0$ provides the main flavor-violating effect, which are usually encoded in two observables Δm_K and ϵ_K. The experiments, then, by measuring these observables put constraints on the coefficients that accompany these operators in the effective Lagrangian. That is, we can write

$$\mathcal{L}_{\Delta F=2} = \sum \frac{C(Q_k)}{\Lambda^2} Q_k \tag{2.73}$$

with Λ being the mass scale at which these coefficients are defined. This can be chosen to be $\Lambda = 1$ TeV, which is of the same order of the usual scale for the new physics in composite Higgs models. By doing so, one can keep the effects of running of the renormalization group equations under control. We can focus on operators Q_1, Q_2 and Q_4, as these provide us with the strongest constraints on the new physics. The

constraints can be expressed as [94, 95]:

$$\begin{aligned} |\mathrm{Re}(C_1^{sd})| &\lesssim 9.0\times10^{-7}, & |\mathrm{Im}(C_1^{sd})| &\lesssim 3.4\times10^{-9}, \\ |\mathrm{Re}(C_2^{sd})| &\lesssim 1.9\times10^{-8}, & |\mathrm{Im}(C_2^{sd})| &\lesssim 1.0\times10^{-10}, \\ |\mathrm{Re}(C_4^{sd})| &\lesssim 6.9\times10^{-9}, & |\mathrm{Im}(C_4^{sd})| &\lesssim 2.6\times10^{-11}\ , \end{aligned} \tag{2.74}$$

where the bounds for $\widetilde{C}_2$ are the same as those for C_2. The contributions to these WC coming from APC can be easily estimated. For each insertion of an elementary quark, a corresponding factor of compositeness ϵ_{fi} has to be inserted. For example, for C_1^{sd}, we have four Left-handed down quarks, two of the first generation, and two of the second:

$$C_1^{sd} \sim \left(\frac{g_*}{m_*}\right)^2 \epsilon_{q1}^2 \epsilon_{q2}^2\ .$$

Now we rewrite this expression in terms of the third generation compositeness, according to the hierarchy in Eq. (2.63) in order to reproduce the CKM matrix:

$$C_1^{sd} \sim \left(\frac{g_*}{m_*}\right)^2 \epsilon_{q3}^4 \lambda_C^{10}\ .$$

Finally, using that the top quark mass can be written as $m_t = g_* v \epsilon_{q3}\epsilon_{u3}/\sqrt{2}$, we insert the adequate powers of v and ϵ_{u3}, to get:

$$C_1^{sd} \sim \left(\frac{\sqrt{2}m_t}{v}\right)^2 \left(\frac{\epsilon_{q3}}{\epsilon_{u3}}\right)^2 \lambda_C^{10} \frac{1}{m_*^2}\ . \tag{2.75}$$

This expression depends on the ratio $\epsilon_{q3}/\epsilon_{u3}$ which is a free parameter of the model, as only the product of the two are fixed by the top Yukawa, is usually denoted as x_t. It also depends on the scale of the composite resonances, m_*. By using the same procedure we can write the remaining estimates as

$$\begin{aligned} C_2^{sd} &\sim \left(\frac{g_*}{m_*}\right)^2 (\epsilon_{d2}\epsilon_{q1})^2 \sim \left(\frac{\sqrt{2}m_s}{v}\right)^2 \lambda_C^2 \frac{1}{m_*^2}\ , \\ \widetilde{C}_2^{sd} &\sim \left(\frac{g_*}{m_*}\right)^2 (\epsilon_{d1}\epsilon_{q2})^2 \sim \left(\frac{\sqrt{2}m_d}{v}\right)^2 \lambda_C^{-2} \frac{1}{m_*^2}\ , \\ C_4^{sd} &\sim \left(\frac{g_*}{m_*}\right)^2 \epsilon_{q1}\epsilon_{q2}\epsilon_{d1}\epsilon_{d2} \sim \frac{\sqrt{2}m_d}{v}\frac{\sqrt{2}m_s}{v}\frac{1}{m_*^2}\ . \end{aligned} \tag{2.76}$$

Each of these expressions is up to $\mathcal{O}(1)$, with an indeterminate phase. To derive the constraints on the mass scale m_*, we have to use the experimental limits on the WC given in Eq. (2.74). For each Wilson Coefficient, one gets a constraint for m_*, which

in the case of Q_1 also depends on the relative compositeness of the third generation x_t. We can thus utilize the bounds on both real and imaginary part of each coefficient, and as the phase is not determined, whichever is smaller will provide the strongest constraint on m_*. In all cases the bounds on the imaginary part are more stringent. We get:

$$\begin{aligned} m_* &\gtrsim 6\, x_t \,\text{TeV} \qquad \text{for} \quad \text{Im}\left(C_1^{sd}\right) \,, \\ m_* &\gtrsim 5 \,\text{TeV} \qquad \text{for} \quad \text{Im}\left(C_2^{sd}\right) \,, \\ m_* &\gtrsim 6 \,\text{TeV} \qquad \text{for} \quad \text{Im}\left(\widetilde{C}_2^{sd}\right) \,, \\ m_* &\gtrsim 10 \,\text{TeV} \qquad \text{for} \quad \text{Im}\left(C_4^{sd}\right) \,, \end{aligned} \tag{2.77}$$

where we see that the strongest constraint coming from the Kaon system is from C_4^{sd}.

With an analogous derivation, one can obtain similar bounds corresponding to flavor violating processes involving B_d and B_s and D mesons. The observables involved are Δm_{B_d}, Δm_{B_s}, Δm_D, as well as other CP-violating ones like $S_{\psi K_S}$, ϕ_D, $|q/p|$. (See Ref. [22] for a more detailed description of these observables). Taking into account each of the operators we can derive lower bounds for m_* coming from each meson system, and for each of the operators. We sum up these bounds in Table 2.2 [18]

WC	$\text{Re}(C_k^{ij})$	$\text{Im}(C_k^{ij})$
C_1^{sd}	$0.4\, x_t$ TeV	$6\, x_t$ TeV
C_2^{sd}	0.4 TeV	5 TeV
$\widetilde{C}_2^{sd}$	0.4 TeV	6 TeV
C_4^{sd}	0.6 TeV	10 TeV
C_1^{bd}	$5\, x_t$ TeV	$7\, x_t$ TeV
C_2^{bd}	1.4 TeV	2 TeV
C_4^{bd}	0.6 TeV	0.8 TeV
C_1^{bs}	$5\, x_t$ TeV	$8\, x_t$ TeV
C_2^{bs}	0.6 TeV	1 TeV
C_4^{bs}	0.5 TeV	1 TeV
C_1^{cu}	$0.5\, x_t$ TeV	$1.2\, x_t$ TeV
C_2^{cu}	1.4 TeV	3 TeV
C_4^{cu}	0.5 TeV	1.1 TeV

Table 2.2: Lower bounds on the mass scale of the composite sector m_*, from $\Delta F = 2$ processes. They are organized according to constraints on the real or imaginary part of operators Q_K^{ij}, where we only keep those with the most stringent bounds. Bounds from operator Q_1 are expressed in terms of the free parameter x_t.

$\Delta F = 1$

We can continue by looking at transitions with $\Delta F = 1$, where we will mainly consider operators of three kinds that contribute to these processes. The first of those is the dipole operator, arising at dimension 5, which we can write in the EW broken phase as

$$\mathcal{L}_{\Delta F=1,\text{dip}} \sim \left(\frac{g_*}{4\pi}\right)^2 \frac{\lambda_i \lambda_j}{g_*} \frac{v}{m_*^2} \bar{f}_i \sigma_{\mu\nu} g_{\text{SM}} F_{\text{SM}}^{\mu\nu} f_j \tag{2.78}$$

where the SM collectively stands for the standard model fields $F^{\mu\nu}$ and couplings g_{SM}, which after EWSB is either the electromagnetic or the chromomagnetic gauge fields. In the kind of composite model we consider in this work, these dipole operators originate at loop level, hence the factor of $g_*^2/16\pi^2$. This loop factor provides an extra suppression with respect to a tree level operator, as the typical coupling between resonances g_* can be large but the theory still remains perturbative $1 \ll g_* < 4\pi$. Constraining these Wilson coefficients will provide bounds for $m_*/g_* \equiv f$, the decay constant of the pNG bosons of the composite theory.

The second kind of operators are those that contribute through penguin operators to modifications to the Z boson couplings. We can write dimension 6 operators involving two insertions of the Higgs field, as

$$\mathcal{L}_{\Delta F=1,\text{peng}} \sim \frac{\lambda_i \lambda_j}{m_*^2} \bar{f}_i \gamma^\mu f_j i H^\dagger \overset{\leftrightarrow}{D}_\mu H \tag{2.79}$$

where we are using the notation $H^\dagger \overset{\leftrightarrow}{D}_\mu H \equiv H^\dagger D_\mu H - (D_\mu H)^\dagger H$ for the derivatives of the Higgs fields.

Finally, the third class of operators are those modifying the W boson couplings. Among these, the operators which induce transitions involving Right-handed quarks are the most relevant. We can write them as

$$\mathcal{L}_{\Delta F=1,W} \sim \frac{\lambda_i \lambda_j}{m_*^2} \bar{u}_R^i \gamma^\mu d_R^j i H^{c\dagger} D_\mu H \tag{2.80}$$

where we are using the notation for the charge-conjugated doublet: $H^c \equiv i\sigma_2 H^*$.

Apart from these classes of operators, there are others that induce subleading effects to the gauge boson couplings. These can come from dimension-6 operators containing multiple derivatives. The Z boson coupling can be modified by operators involving two quarks and a derivative of the field strength $F_{\mu\nu}$. These operators are suppressed by a factor of $(g_{\text{SM}}/g_*)^2$ with respect to penguin operators [96]. The W boson couplings, are however modified by operators involving two derivatives of the elementary quark. They thus arise at a fourth order in elementary/composite mixings, contrasted to those of quadratic order coming from Eq. (2.80). Thus they are subleading as long as there is no

vanishing of the leading operators, for example via discrete symmetries being present in the composite sector.

Electromagnetic and Chromomagnetic dipoles

The most stringent contributions of the dipole operator comes from the $b \to s\gamma$ process. However, we can treat all electro- and chromo-magnetic operators together and check the size of the experimental bounds. In order to define the Wilson Coefficients, the operators are put together into the following effective Hamiltonian [97]

$$\mathcal{H}_{\text{dip,eff}} = -\sum_{q,i,j,V} \left\{ C_{q_i q_j V} Q_{q_i q_j V} + C'_{q_i q_j V} Q'_{q_i q_j V} \right\} \tag{2.81}$$

where i, j label the different flavors, $q = u, d$, and $V = \gamma, g$, either of the gauge fields. The difference between Q and Q' is which chiralities are involved in the transition. The operators are of the form of Eq. (2.78), with normalizations given by

$$\begin{aligned} Q_{q_i q_j \gamma} &= \frac{e\, m_{q_i}}{16\pi^2} \left(\bar{q}_j \sigma^{\mu\nu} P_R q_i\right) F_{\mu\nu} \,, \qquad Q_{q_i q_j g} &= \frac{g_s\, m_{q_i}}{16\pi^2} \left(\bar{q}_j \sigma^{\mu\nu} T^a P_R q_i\right) G_{a,\mu\nu} \,, \\ Q'_{q_i q_j \gamma} &= \frac{e\, m_{q_i}}{16\pi^2} \left(\bar{q}_j \sigma^{\mu\nu} P_L q_i\right) F_{\mu\nu} \,, \qquad Q'_{q_i q_j g} &= \frac{g_s\, m_{q_i}}{16\pi^2} \left(\bar{q}_j \sigma^{\mu\nu} T^a P_L q_i\right) G_{a,\mu\nu} \,. \end{aligned} \tag{2.82}$$

QCD corrections introduce a mixing of these two sets of operators $Q_\gamma^{(\prime)}$ and $Q_g^{(\prime)}$, through renormalization effects. Thus, the WC of both sets of operators are modified according to RG equations. Running from a NP energy scale to the scale of the top-quark mass and lower, the electromagnetic dipole coefficients receive contributions of both electro and chromo-magnetic operators:

$$\begin{pmatrix} C_\gamma(\mu_l) \\ C_g(\mu_l) \end{pmatrix} = \begin{pmatrix} \eta_{\gamma\gamma} & \eta_{\gamma g} \\ 0 & \eta_{gg} \end{pmatrix} \begin{pmatrix} C_\gamma(\mu_h) \\ C_g(\mu_h) \end{pmatrix} \,. \tag{2.83}$$

Numerical estimates of these coefficients can be obtained, via evolving first from some higher energy scale μ_h to m_t, and then from m_t to some lower energy scale μ_l, taking into consideration how the number of active quarks change at different thresholds.

The experimental constraints here come from limits on Flavor Changing Neutral Currents (FCNC), mainly coming from down-sector processes: $b \to s\gamma/g$, $b \to d\gamma/g$. Bounds on these operators are obtained from B decay processes. Constraints on charmed FCNC can be obtained by measuring the CP asymmetry between $D \to KK$ and $D \to \pi\pi$. An upper bound on this can be related to the chromomagnetic dipole Q'_{cug}. Flavor changing processes containing top quarks are not yet strongly constrained, however they will in the future through top decays $t \to u\gamma/g$, $t \to c\gamma/g$. Constraints on flavor changing decays $s \to d\gamma/g$ are also less strongly constrained, with long-distance dominance of K mesons making it difficult to relate the observables to their short-

distance contributions. Still, limits over the WC of $s \to dg$ processes can be related to measurements on the parameter ϵ'/ϵ.

Each of these constraints on the electro- and chromo-magnetic dipole operators for flavor transitions puts a lower bound on the scale $f \sim m_*/g_*$ of the composite theory. We summarize these constraints in Table 2.3, where the bounds are taken from Ref. [97]. As the contributions to the WC coming from the composite theory have $\mathcal{O}(1)$ coefficients, the resulting phase is indeterminate. However, the experiments provide bounds for the WC which depend on the value of these phases. We only show the bounds coming from either real or imaginary part of the coefficients, picking the largest of bounds for each coefficient.

WC	Re(C)	Im(C)
$C_{bs\gamma}$	2.81 TeV	1.44 TeV
C_{bsg}	1.34 TeV	0.69 TeV
$C'_{bs\gamma}$	1.41 TeV	1.31 TeV
C'_{bsg}	0.68 TeV	0.68 TeV
$C_{bd\gamma}$	3.74 TeV	2.91 TeV
C_{bdg}	1.79 TeV	1.4 TeV
$C'_{bd\gamma}$	2.37 TeV	2.37 TeV
C'_{bdg}	1.14 TeV	1.14 TeV
$C^{(\prime)}_{sdg}$	—	2.80 TeV
$C^{(\prime)}_{sdg}$	—	2.14 TeV

Table 2.3: Bounds on the scale $f = m_*/g_*$ derived from constraints on $\Delta F = 1$ dipole operators. Bounds are exhibited in terms of constraints over the real or imaginary parts of the Wilson coefficients. In the case of transitions $s \to d$ and $c \to u$, only a constraint coming from the imaginary part is shown.

Modifications to Z couplings

The general structure of operators contributing to these flavor violating currents are given by Eq. (2.79). By integrating out Z, we obtain four fermion operators with a structure given by

$$\frac{\lambda_i \lambda_j}{m_*^2} \bar{f}_i \gamma^\mu f_j J_\mu^{(Z)} \ , \tag{2.84}$$

with $J^{(Z)}$ representing the SM four-current:

$$J_\mu^{(Z)} = \sum_{f_i} \bar{f}_i \gamma_\mu \left[T_L^3 (1 - \gamma_5) - 2q \sin^2 \theta_w \right] f_i \ , \tag{2.85}$$

where T_L^3 represents the third generator of the weak $\mathrm{SU}(2)_L$ group, and q the electric charge of each fermion f_i.

The flavor violating processes coming from penguin operators that are the most strongly constrained are those involving down-type quarks, especially $b \to s$ and $s \to d$ transitions. The way to encode new physics contributions to $b \to s$ transitions is through the following effective Hamiltonian:

$$\mathcal{H}_{b\to s} = \frac{G_F}{\sqrt{2}} V_{tb} V_{ts}^* \frac{e^2}{4\pi^2} \left[C_{10} (\bar{s}_L \gamma^\mu b_L)(\bar{\ell}\gamma_\mu \gamma^5 \ell) + C'_{10} (\bar{s}_R \gamma^\mu b_R)(\bar{\ell}\gamma_\mu \gamma^5 \ell) \right] . \tag{2.86}$$

The contributions of these WC in a composite model can be estimated by using Eq. (2.84), as

$$\begin{aligned} C_{10} &\sim \frac{4\pi^2}{G_F e^2} \frac{\lambda_C^2}{V_{tb} V_{ts}^*} \frac{1}{m_*^2} \frac{m_t}{v} g_* x_t \, , \\ C'_{10} &\sim \frac{4\pi^2}{G_F e^2} \frac{\lambda_C^2}{V_{tb} V_{ts}^*} \frac{1}{m_*^2} \frac{m_t}{v} \frac{g_*}{x_t} \left(\frac{m_s m_b}{\lambda_C^4 m_t^2} \right) . \end{aligned} \tag{2.87}$$

These WC can be bounded by studying $b \to s\ell^+\ell^-$ decays. We have [98, 99]:

$$|C_{10}| \lesssim 2.6 \, , \qquad |C'_{10}| \lesssim 3.1 \, . \tag{2.88}$$

Among these two limits, it is the one on the Left-handed operator, C_{10}, which provides the strongest bound on the mass scale

$$m_* \gtrsim 3\sqrt{g_* x_t}\, \text{TeV} \, , \tag{2.89}$$

whereas the bound coming from the Right-handed operator is further suppressed by the last factor in Eq. (2.87), $\left(\frac{m_s m_b}{\lambda_C^4 m_t^2}\right) \sim 2 \times 10^{-3}$.

Regarding $s \to d$ transitions, the strongest constraint comes from $K_L \to \mu^+\mu^-$, although similar bounds can be obtained via the decay $K^+ \to \pi^+ \nu\bar{\nu}$, and from measurements of $\text{Re}(\epsilon'_K/\epsilon_K)$. The NP can be encoded in the following Lagrangian, which involves flavor-violating interactions of the Z boson:

$$\mathcal{L}_{s\to d} = -\frac{g}{c_w} Z_\mu \left(\delta g_L^{ds} \bar{d}_L \gamma^\mu s_L + \delta g_R^{ds} \bar{d}_R \gamma^\mu s_R + \text{h.c.} \right) . \tag{2.90}$$

Once again we can estimate these coefficients from Eq. (2.84):

$$\delta g_L^{ds} \sim \frac{m_t v}{\sqrt{2}} \frac{1}{m_*^2} g_* x_t \lambda_C^5 , \qquad \delta g_R^{ds} \sim \frac{m_t v}{\sqrt{2}} \frac{1}{m_*^2} \frac{g_*}{x_t} \lambda_C^5 \left(\frac{m_d m_s}{\lambda_C^{10} m_t^2} \right) , \tag{2.91}$$

where we see that Right-handed transitions are suppressed by a factor $\left(\frac{m_d m_s}{\lambda_C^{10} m_t^2}\right) \sim 0.02$ with respect to the Left-handed ones. The experimental measurements provide a bound

on these flavor violating couplings, [100]

$$|\delta g^{ds}_{L,R}| \lesssim 6 \times 10^{-7} \ . \tag{2.92}$$

We can thus derive from this constraint a lower limit on the mass scale m_*, by limiting the Left-handed transition δg^{ds}_L:

$$m_* \gtrsim 4.7\sqrt{g_* x_t}\ \text{TeV} \ , \tag{2.93}$$

whereas the Right-handed transition δg^{ds}_R is further suppressed, but has an inverse dependence with x_t

$$m_* \gtrsim 0.7\sqrt{\frac{g_*}{x_t}}\ \text{TeV} \ . \tag{2.94}$$

Finally, this penguin operator can also give contribution to flavor-conserving quantities. In this case, the couplings of the Z boson to third generation quarks are among the most relevant modifications. Experimentally, the coupling to the bottom quark is the one most strongly constrained, at the per mil level. From Eq. (2.79) one can derive expressions for the deviations of these Z boson couplings:

$$\begin{aligned} \delta g_{b_L} &\simeq \frac{\lambda^2_{q3}}{2m^2_*} v^2 \simeq \frac{1}{m^2_*}\frac{m_t v}{\sqrt{2}} g_* x_t \ , \\ \delta g_{b_R} &\simeq \frac{\lambda^2_{d3}}{2m^2_*} v^2 \simeq \frac{1}{m^2_*}\frac{m_t v}{\sqrt{2}}\frac{g_*}{x_t}\left(\frac{m_b}{m_t}\right)^2 \ . \end{aligned} \tag{2.95}$$

The Left-handed coupling deviation is more relevant than the Right-handed one, which is much smaller than the experimental precision. To get a rough estimate which is independent of the model, we can impose a limit on the size δg_{b_L} of the size of the precision, which is 10^{-3}. With this, a limit on m_* can be derived,

$$m_* \gtrsim 5\sqrt{g_* x_t}\ \text{TeV} \ , \tag{2.96}$$

which is roughly of the same size as those coming from flavor violating couplings.

In a model dependent way, there are ways of protecting some of these couplings via discrete symmetries [101]. There are two possible symmetries that can forbid the penguin operators in Eq. (2.79), these are P_{LR} or P_C. The action of the first is an exchange of the $\text{SU}(2)_L$ and $\text{SU}(2)_R$ generators inside the SO(4), in the case of the MCHM. In larger groups one still identifies both $\text{SU}(2)_L$ and $\text{SU}(2)_R$ inside the unbroken subgroup H. The symmetry P_C, on the other hand, is defined through its action on the eigenstates of $\text{SU}(2)_L \times \text{SU}(2)_R$, and acts by flipping the sign of its charges. This way, a typical example of an eigenstate of P_C is a current which has $t^3_L = t^3_R = 0$. In the case of P_{LR}, a way of respecting this symmetry is by embedding the elementary

fermions in multiplets that respect $t_L^3 = t_R^3$. This presents a singular problem in the case of Left-handed fermions, as they forcibly belong to the same $\mathrm{SU}(2)_L$ multiplet and thus only one of the pair can have its couplings protected. This will typically be the bottom quark, as the experimental limits are more sensitive than those of the top quark. That is, the symmetry will usually be used to protect Zb_Lb_L, whereas the modifications of Zt_Lt_L will be allowed by the larger uncertainties. The deviation to the couplings with Right-handed quarks can sometimes be protected by the P_C symmetry, by having embeddings that have $t_{L,R}^3 = 0$.

Modifications to W couplings

The class of operators in Eq. (2.80) lead to modifications of the W couplings. One way of constraining these modifications is through their contributions to $b \to s\gamma$ transitions [102, 103]. In APC, as the elementary/composite couplings of the third generation are the largest, the most important contribution to $b \to s\gamma$ will be through modified couplings to the t_R quark. Thus, in APC the most important effects will be those of Wt_Rb_R, which modifies the dipole WC $C_{bs\gamma}$, and the Wt_Rs_R coupling, modifying the opposite chirality coefficient $C'_{bs\gamma}$. These WC must be calculated at one loop, which involves both a t_R coupling and a W in the loop. The contribution to the W couplings are given by

$$\begin{cases} \frac{gv^2}{2\sqrt{2}} \frac{\lambda_{u3}\lambda_{d3}}{m_*^2} (\bar{t}_R \not{W} b_R) \\ \frac{gv^2}{2\sqrt{2}} \frac{\lambda_{u3}\lambda_{d2}}{m_*^2} (\bar{t}_R \not{W} s_R) \end{cases}$$

Their contributions to the dipole WC involve the loop function $A_7(m_t^2/m_W^2) \simeq -0.8$ [103]:

$$\begin{aligned} C_{bs\gamma} &\sim \frac{1}{\sqrt{2}} m_t g_* v \frac{1}{x_t m_*^2} A_7(m_t^2/m_W^2) \ , \\ C'_{bs\gamma} &\sim \frac{1}{\sqrt{2}} m_t g_* v \frac{1}{x_t m_*^2} \left(\frac{m_s}{m_b \lambda_C^4} \right) A_7(m_t^2/m_W^2) \ . \end{aligned} \tag{2.97}$$

We see that one WC is enhanced by a factor $\left(\frac{m_s}{m_b\lambda_C^4}\right) \sim 8$ with respect to the other one. One can then constrain m_* from the bounds on these dipole operators:

$$\begin{aligned} m_* &\gtrsim 0.3 \sqrt{\frac{g_*}{x_t}} \ \text{TeV} \ , \\ m_* &\gtrsim 0.5 \sqrt{\frac{g_*}{x_t}} \ \text{TeV} \ , \end{aligned} \tag{2.98}$$

coming from $C_{bs\gamma}$ and $C'_{bs\gamma}$ respectively.

$\Delta F = 0$

Here we have to consider the constraints coming from the measurements of the neutron electric dipole moment EDM d_n. The largest NP contributions come from flavor-conserving electro- and chromo-magnetic dipole operators, like those defined in Eq. (2.82). As the neutron EDM is generated only by the CP-violating effects of the dipole operators, only the imaginary part of their WC gives a contribution to d_n. The main constraints coming from the neutron EDM are to the first generation quarks, where we can obtain the following lower bounds for the scale f [97] :

$$\begin{aligned} f &\gtrsim 1.08 \text{ TeV} \quad \text{from} \quad C_{uu\gamma}, \\ f &\gtrsim 1.45 \text{ TeV} \quad \text{from} \quad C_{uug} \ , \\ f &\gtrsim 3.11 \text{ TeV} \quad \text{from} \quad C_{dd\gamma} \ , \\ f &\gtrsim 3.79 \text{ TeV} \quad \text{from} \quad C_{ddg} \ . \end{aligned} \tag{2.99}$$

There are also constraints coming from dipole operators involving second and third generation quarks. These stem from QCD running effects, and although weaker, the bounds coming from these operators are not insignificant. The following bounds on f can be derived [97]:

$$\begin{aligned} f &\gtrsim 1.22 \text{ TeV} \quad \text{from} \quad C_{ccg} \ , \\ f &\gtrsim 0.67 \text{ TeV} \quad \text{from} \quad C_{bbg} \ , \\ f &\gtrsim 0.30 \text{ TeV} \quad \text{from} \quad C_{ttg} \ . \end{aligned} \tag{2.100}$$

In this section we gave an account on the main constraints to the flavor scheme given by APC, particularly regarding the sector of quarks. In APC, the flavor violating processes are suppressed by the same small mixings that generate the hierarchical structure of masses and mixings of the SM [90, 104–107]. This suppression is enough in many of the bounds, which are consistent with m_* of order TeV. However, a few observables, particularly those coming from transitions in the Kaon sector, and from dipole operators, can push the scale of m_* to $\mathcal{O}(10 - 100)$ TeV.

Regarding the lepton sector, the most stringent constraints come from the electron EDM and from $\mu \to e\gamma$ decay [18, 107]. The bounds can be obtained by a similar analysis, and they can be even stronger than those coming from the quark sector. If operators are loop induced, one can get a lower limit on f of order $\mathcal{O}(25 - 40)$ TeV.

Simply increasing the scale m_* reintroduces a hierarchy with the Higgs scale, as we described in Sec. 2.1.2 regarding the tuning necessary for reproducing v_{SM} and m_h. Another way to avoid these bounds is by considering flavor as well as CP symmetries in the SCFT, in both quark and lepton sectors [89, 102, 108–112]. Other possibilities

are the presence of different dynamical scales for different flavors [113], the inclusion of tiny bilinear interactions [93], or the existence of extended color symmetries in the SCFT [114, 115], to name a few. We will choose the scale m_* of order $\sim$ few TeV to $\mathcal{O}(10)$ TeV, with one of the abovementioned alternative, which one will depend on the specific model.

2.3. B-physics anomalies

Observables $R_{D^{(*)}}$

The SM prediction [116–119] and the experimental values of $R_{D^{(*)}}$, averaging results from BaBar [23], LHCb [26, 27], and Belle [24, 25] are [28]:

$$\begin{aligned} R_D^{\text{exp}} &= 0.340 \pm 0.03 \ , \qquad & R_{D^*}^{\text{exp}} &= 0.295 \pm 0.014 \ , \\ R_D^{\text{SM}} &= 0.299 \pm 0.003 \ , \qquad & R_{D^*}^{\text{SM}} &= 0.258 \pm 0.005 \ , \end{aligned} \tag{2.101}$$

which, when combined, the pair of observables have a discrepancy of about $\approx 3.08\sigma$ with respect to their SM values [28]. As the NP contributions which we study in the present work give symmetric contributions to both R_D and R_{D^*}, it is useful to give the average of both ratios, with respect to their SM values, as:

$$R_{D^{(*)}} \equiv \frac{R_{D^{(*)}}^{\text{exp}}}{R_{D^{(*)}}^{\text{SM}}} = 1.135 \pm 0.055 \ , \tag{2.102}$$

noting that this ratio is equal to 1 in absence of NP contributions. There are different dimension six operators which are capable of generating these semi-leptonic decays via charged currents. We can write the following effective Lagrangian [44]:

$$\begin{aligned} \mathcal{L}_{\text{eff}}^{R_D} = -2\sqrt{2} G_F V_{ud} \Big[& (1 + g_{V_L})(\bar{u}_L \gamma_\mu d_L)(\bar{\ell}_L \gamma^\mu \nu_L) + g_{V_R}(\bar{u}_R \gamma_\mu d_R)(\bar{\ell}_L \gamma^\mu \nu_L) \\ & + g_{S_L}(\bar{u}_R d_L)(\bar{\ell}_R \nu_L) + g_{s_R}(\bar{u}_L d_R)(\bar{\ell}_R \nu_L) + g_T(\bar{u}_R \sigma_{\mu\nu} d_L)(\bar{\ell}_R \sigma^{\mu\nu} \nu_L) \Big] + \text{h.c.} \end{aligned} \tag{2.103}$$

where the different couplings g_{V_L}, g_{V_R}, g_{s_L}, g_{s_R}, g_T encode the NP contributions, and flavor indices have been omitted. There can be different BSM states responsible for these couplings [44, 60]. The left handed current g_{V_L} alone can accommodate for the deviation in $R_{D^{(*)}}$, where at first order in this coupling we have $R_{D^{(*)}} \simeq 1 + g_{V_L}$. In the models we will consider, composite leptoquarks being responsible for generating this operator, and anarchic couplings in the composite sector, we get

$$g_{V_L} \simeq \frac{x_{b\tau}^* x_{c\tau} v_{\text{SM}}^2}{2 M_{\text{LQ}}^2 V_{cb}} \sim \frac{g_*^2 v_{\text{SM}}^2 \epsilon_{q3}^2 \epsilon_{l3}^2}{2 M_{\text{LQ}}^2} \ , \tag{2.104}$$

where x_{ql} represent LQ couplings, $M_{\rm LQ}$ the LQ mass, and in the second equality we are assuming APC. The overall factor depends on the spin of the LQ state generating the operator, and anarchic $\mathcal{O}(1)$ coefficients have been omitted. For $\epsilon_{q3} \sim 1$, $M_{\rm LQ} \sim 1$ TeV, and $g_* \sim 2-4$, compositeness of the Left-handed leptons of order $\mathcal{O}(0.5-1)$ give a coefficient of the right size for $R_{D^{(*)}}$, $g_{V_L} \sim 0.1$. This suggests that composite LQ along with APC can generate the right couplings in order to accommodate the charged current B-anomaly. We will be giving more precise statements about this when working with actual LQ models.

Observables $R_{K^{(*)}}$

In the case of the neutral current ratios $R_{K^{(*)}}$, they have been measured by Belle [29] and LHCb [30–33]. In this case the observables are defined in terms of partial branching ratios taken in a range of the dilepton invariant mass. We can quote for R_K the latest value reported by LHCb [33], which is the most accurate up to date:

$$R_K^{[1.0,\ 6.0]} = 0.846 \pm 0.044 \ , \tag{2.105}$$

where the interval for q^2 is in units of GeV^2. The central value coincides with their previous measurement [32], but with smaller uncertainties. This reported value is in tension with the SM value of approximate unity [120, 121] by a factor of $\approx 3.1\,\sigma$. Previous combined measurements obtained an average for this anomaly which stood at $\approx 2.5\,\sigma$ [32].

In the case of R_{K^*}, results by LHCb [31] cite the following values

$$R_{K^*}^{[0.045,\ 1.1]} = 0.66 \pm 0.11 \ , \qquad R_{K^*}^{[1.1,\ 6.0]} = 0.69 \pm 0.11 \ , \tag{2.106}$$

for the low-q^2 and central-q^2 bins. In both bins the difference with the SM value $\simeq 1$ stands at $\approx 2.5\,\sigma$. A later report by Belle, which measured this ratio in both B^0 and B^+ decays, obtained a combined average which stands compatible with the predicted SM value [29].

When studying fits to these neutral current anomalies, the most relevant contributions come from the following $b \to s\ell\ell$ operators:

$$\begin{aligned}
\mathcal{H}_{\rm eff}^{R_K} &= -\frac{4G_F}{\sqrt{2}} V_{tb}V_{ts}^* \left\{ \sum_{K=9,10} C^K_{\ell_i\ell_j bs}\mathcal{O}^K_{\ell_i\ell_j bs} + \left(C^K_{\ell_i\ell_j bs}\right)' \left(\mathcal{O}^K_{\ell_i\ell_j bs}\right)' \right\} + \text{h.c.} \ , \\
\mathcal{O}^9_{\ell_i\ell_j bs} &= \frac{\alpha_{\rm em}}{4\pi} \left(\bar{s}\gamma^\mu P_L b\right) \left(\bar{\ell}_i\gamma_\mu \ell_j\right) \ , \\
\mathcal{O}^{10}_{\ell_i\ell_j bs} &= \frac{\alpha_{\rm em}}{4\pi} \left(\bar{s}\gamma^\mu P_L b\right) \left(\bar{\ell}_i\gamma_\mu\gamma_5 \ell_j\right) \ ,
\end{aligned} \tag{2.107}$$

with operators $\mathcal{O}'^{9/10}$ involving the Right-handed quarks. Several references have fitted $R_{K^{(*)}}$ using these operators, as well as electromagnetic dipolar operators [122–124]. One preferred scheme is that given by a purely Left-handed contribution, which implies the relation $\Delta C^9_{\mu\mu} = -\Delta C^{10}_{\mu\mu}$ over their WCs. Here we can cite Ref. [123] which performs this fit including the latest R_K measurement by LHCb, where they find, for Left-handed NP:

$$\Delta C^9_{\mu\mu} = -\Delta C^{10}_{\mu\mu} = -0.49 \pm 0.07 \ , \tag{2.108}$$

where the ΔC refers to the BSM contribution to the coefficients.

In the LQ models we will consider in the present work, with Left-handed couplings, we can get a prediction for these WCs:

$$\Delta C^9_{\mu\mu} = -\Delta C^{10}_{\mu\mu} \simeq \frac{\pi v^2_{\rm SM}}{V_{tb}V^*_{ts}\alpha_{\rm em}} \frac{x_{b\mu}x^*_{s\mu}}{M^2_{\rm LQ}} \sim \frac{g^2_*\pi v^2_{\rm SM}}{\alpha_{\rm em} M^2_{\rm LQ}} \epsilon^2_{q3}\epsilon^2_{l2} \ , \tag{2.109}$$

where in the second estimate we use APC, and we are omitting $\mathcal{O}(1)$ coefficients. From this expression, it can be seen how for a LQ mass of $\sim$ TeV, a degree of compositeness for the third generation Left-handed quarks $\epsilon_{q3} \sim 1$, and $g_* \sim 4$, the required contribution to these WCs fixes the value for ϵ_{l2}. We get a degree of compositeness for the second generation Left-handed leptons of the same order as that obtained for the L-R symmetric case in Eq. (2.66), of about $\mathcal{O}(10^{-2})$.

2.4. Models of Resonances

In this Section we detail how one can achieve a description of the sector of resonances, in a way that allows to make calculations over all observed quantities of the theory starting from some input parameters. There exists a variety of options when wanting to describe a theory with composite resonances. An example of this can be extra dimensional theories with a warped spacetime, where the compactification of the fifth dimension brings about a tower of Kaluza Klein states from each of the 5d fields. This description is useful for its theoretical simplicity, and low number of parameters, although there exists some freedom as to how the Higgs field is represented. In this kind of extra dimensional theory, the spacetime metric is a slice of AdS, between two branes, usually called the "UV" and "IR" branes [125]. The AdS warp factor of the metric allows the hierarchy of the Yukawas and spectrum, along with the Higgs mass, to be easily explained. The Higgs field can be either a 5d scalar, or a scalar entirely localized in the "IR" or "TeV" brane, or a pNGB obtained as the fifth component of a gauge field in the bulk [96, 126–128]. In some models, the masses of the 5d fermion fields control their shapes in the extra dimension and thus their couplings. They act as the compositeness fractions ϵ_{fi} [90].

While having theoretical simplicity and a huge power of description, the extra dimensional models involve more complex computations, for instance having to deal with solutions to differential equations and zeroes of special functions. We will focus on a simpler class of models which in some cases can be thought of as a discretization of an extra dimension, although the structure of couplings can be generalized over a simple discretization. These discrete models are valid alternatives to a full 5d description of the sector or resonances, as they are still highly predictive, yet the computations gain in simplicity. These discrete model theories receive the name of N-site theories, and in the following we will be working with either two-, or three-site theories, depending on how many "sites" of resonances are present [87, 129]. We will first proceed to describe a three-site theory, as a theory of only two sites shares many of the features and can be thought of as a limit.

A property of a three site model is that the pNGB potential at one-loop is automatically finite [129]. A simple way to show an N-site model is through a "moose diagram", we show one such diagram for the three site model in Fig. 2.2. Site-0 contains the elementary fermions and gauge fields of the SM, while the other two sites contain the lightest set of resonances of the composite theory. The fields are denoted with capital letters, with subindices indicating the site, and Ψ_f representing the elementary fermions in site-0. Site-1 has a local symmetry $\mathrm{G}_1 = \mathrm{G}$, along with massive Dirac fermions that transform in irreducible representations of G_1. Site-2 has also massive Dirac fermions transforming as irreducible representations of a now global symmetry $\mathrm{G}_2 = \mathrm{G}$, whereas only the subgroup $\mathrm{H}_2 = \mathrm{H}$ is gauged on this site. For each pair of neighboring sites j and $j+1$, there is a σ-model that is based on the coset $\mathrm{G}_j \times \mathrm{G}_{j+1}/\mathrm{G}_{j+(j+1)}$, this being represented by a solid line in the moose diagram, with the field $\Omega_j = e^{i\Pi_j/f_j}$ parametrizing the coset, and transforming linearly under $\mathrm{G}_j \times \mathrm{G}_{j+1}$.

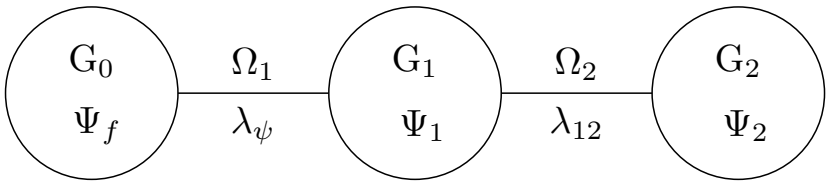

Figure 2.2: Moose diagram of the three-site theory.

Following the idea described in section 2.1.2, the elementary fields will be promoted into full multiplets of G by the use of spurions, which are later set to zero at the end of the calculations. Thus, a_μ will represent the embedding of the gauge fields into G, and Ψ_f that of the elementary fermions, with $f = q, u, d, l, e$. With this in mind, we can begin by writing the Lagrangian for the bosonic sector:

$$\mathcal{L}_{\mathrm{b}} = -\frac{1}{4g_0^2} f^a_{\mu\nu} f^{a,\mu\nu} + \sum_{j=1,2} \left[-\frac{1}{4g_j^2} F^a_{j,\mu\nu} F^{a,\mu\nu}_j + \frac{f_j^2}{4} \mathrm{Tr}\left(|D_\mu \Omega_j|^2 \right) \right] \tag{2.110}$$

where $f_{\mu\nu}$ and $F_{j,\mu\nu}$ represent the field strength on site-0 and j respectively, and $D_\mu\Omega_j = \partial_\mu\Omega_j + iA_{j-1,\mu}\Omega_j - i\Omega_j A_{j,\mu}$, with $A_{0,\mu} \equiv a_\mu$, the four-vector of the zeroth site. The normalization of the kinetic term for the scalar fields is related to normalization for the generators, in order to obtain the expected kinetic term for a scalar. In this particular example, $\mathrm{Tr}(T^a T^b) = 2\delta^{ab}$ The gauge couplings of each site are labeled by g_j, with $g_{\rm SM} \ll g_1,\ g_2 \ll 4\pi$. A matching of the unbroken diagonal subgroup gives $g_{\rm SM}^{-2} = g_0^{-2} + g_1^{-2} + g_2^{-2}$, which fixes the value of g_0. Its size can be readily estimated as $g_0 \sim g_{\rm SM}$, for $g_1,\ g_2 \gg g_{\rm SM}$. An additional subindex of $g_{\rm SM}$, as well as of g_0 must be understood, which distinguishes the different factors of the SM gauge symmetry.

The σ-model fields provide a number of NGBs, in this case as $\mathrm{G}_1 = \mathrm{G}_2 = \mathrm{G}$, this will be equal to twice the dimension of the adjoint of G. In the unitary gauge, a subset of these will become the longitudinal degrees of freedom of all site-1 spin one resonances, and all of the resonances corresponding to the gauged H_2 subgroup in site-2. Thus, a remainder of $\dim(\mathbf{Adj}(\mathrm{G})) - \dim(\mathbf{Adj}(\mathrm{H})) = \dim(\mathbf{r}_\Pi)$ remain as NGB in the spectrum. By going to the unitary gauge, one can obtain the decay constant of the physical NGB: f, as:

$$\frac{1}{f^2} = \frac{1}{f_1^2} + \frac{1}{f_2^2} \tag{2.111}$$

We can write the Lagrangian for the fermionic sector, as

$$\begin{aligned}\mathcal{L}_{\rm f} = &\sum_f i\bar{\Psi}_f \not{D}\Psi_f + \bar{\Psi}_1^{\mathbf{R}}(i\not{D} - m_1^{\mathbf{R}})\Psi_1^{\mathbf{R}} + i\bar{\Psi}_2^{\mathbf{R}}\not{D}\Psi_2^{\mathbf{R}} + \sum_{\mathbf{r}} m_{2,\mathbf{r}}^{\mathbf{R}}\bar{\Psi}_{2,\mathbf{r}}^{\mathbf{R}}\Psi_{2,\mathbf{r}}^{\mathbf{R}} \\ &+ f_1\sum_f \lambda_f^{\mathbf{R}}\bar{\Psi}_f\Omega_1\Psi_1^{\mathbf{R}} + \lambda_{1,2}^{\mathbf{R}} f_2\bar{\Psi}_1^{\mathbf{R}}\Omega_2\Psi_2^{\mathbf{R}} + \text{h.c.}\ , \\ &f = q, u, d, l, e\ ,\end{aligned} \tag{2.112}$$

where we have omitted an additional index for labeling generations. The superindex $\mathbf{R}$ refers to the G representation of the corresponding fermions. Depending on the particulars of the model, all fermions could be fitted into a specific representation, or more generally a combination of representations. The first line of Eq. (2.112) contains the kinetic terms of the elementary fermions f, along with the kinetic and mass terms for fermions on sites 1 and 2. The last term of the first line contains masses for fermions on site-2, where $\mathbf{r}$ labels the representations obtained after decomposing Ψ_2 under $\mathrm{H}_2 = \mathrm{H}$. These terms, giving different masses to each H multiplet of fermions, are allowed because on site-2 the global symmetry has already been broken by the gauging of $\mathrm{H}_2 \subset \mathrm{G}_2$. The second line contains the mixings between fermions located at different sites, they are gauge invariant thanks to the transformation properties of the NGB matrices. The mixing parameters are dimensionless, the mass dimensions being carried by the factors $f_{1,2}$. The parameters λ_f also span a hierarchy of values, as they are responsible for generating the mixings and spectrum of the SM fermions. The masses

for site-1 and site-2 fermions are taken as $m_1 \sim g_1 f_1$ and $m_{2,\mathbf{r}} \sim g_2 f_2$, such that fermionic and bosonic resonances have masses of the same size.

One can then diagonalize the bosonic and fermionic mass matrices, before EWSB, with the massless eigenstates corresponding to the SM states. This allows for the definition of degrees of compositeness of the SM states in terms of the parameters of the model. For bosons, as the structure of representations in the adjoint is quite generic for different groups, one can express results that are quite independent of the particulars of the group. If one decouples the site-0 with the rest of the theory, by making $g_0 = 0$, then one gets a multiplet in the representation $\mathbf{r}_\Pi$ of H, located in site-1, with mass $g_1\sqrt{(f_1^2+f_2^2)/2}$ that does not mix with any other state in this limit, as site-2 has only gauge-fields for the group H, which are in representation $\mathbf{Adj}$(H). The fields belonging in that representation, belonging to both site-1 and site-2 are mixed by the action of f_2. This mixing can be diagonalized, in the limit $f_1 = f_2$ and $g_1 = g_2$, one finds that the mass eigenstates have masses: $\simeq g_1 f_1/2$ and $\simeq g_1 f_1$. Turning on g_0, elementary and composite states are now mixed. It is by diagonalizing this mixing, and before EWSB, that the SM gauge fields are defined as the massless eigenstates. The degree of compositeness of the massless states, ϵ_g can be defined as

$$\epsilon_g^2 = 1 - \frac{g_1^2 g_2^2}{g_0^2 g_1^2 + g_0^2 g_2^2 + g_1^2 g_2^2} \simeq g_0^2 \left(\frac{1}{g_1^2} + \frac{1}{g_2^2}\right) + \mathcal{O}\left(\frac{g_0}{g_i}\right)^4 , \tag{2.113}$$

which is obtained by computing the massless eigenstate after diagonalization of the mass matrix, before EWSB. This ϵ_g can be defined as $\epsilon_g = \sqrt{1 - x_{g,\mathrm{el}}^2}$, where $x_{g,\mathrm{el}}$ is the projection of the massless eigenstate onto the elementary one.

For the fermions, there is usually more freedom in the representations that can be chosen for the embedding of the SM fermions and their corresponding composite resonances. The different representations will have different decompositions, product rules, and Clebsch-Gordan coefficients, for which the mass matrices will in general differ. One can also here perform a diagonalization of the mass matrices, before EWSB, with the massless eigenstates corresponding to the SM fermions. This allows, as in the case of bosons, to define the degree of compositeness in terms of the parameters of the model. Generally, before turning on the elementary-composite mixings, and at the limit $\lambda_{1,2} \sim g_1 \sim g_2$, the mass of these fermionic resonances is expected to be of order $g_i f_i$, that is the same as the spin one resonances. After mixing with the elementary states, the masses of the resonances will be shifted. Especially among the resonances belonging in the same G multiplet as the SM fermions but with different SM quantum numbers, these shifts can be such that their masses will be lowest. These light fermionic resonances, of typically $\lesssim 1$ TeV, are also called custodians, and they have been shown in some models to be correlated with a lighter Higgs mass.

An integration of all resonances in sites 2 and 3 is possible, leading to an effective

Lagrangian involving only elementary fields and the NGB fields. This integration allows for explicit expressions of the form factors $\Pi_{f,f'}$ as defined in section 2.1.2. These form factors, when expressed in terms of the parameters of the discrete theory, make the potential calculable.

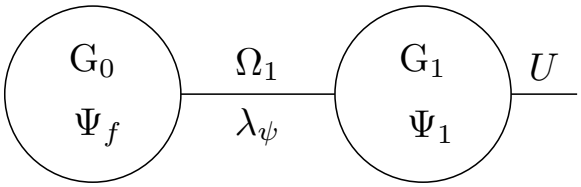

Figure 2.3: Moose diagram for the two-site theory.

Let us now turn our attention to a two site model. This amounts to a few modifications to the three-site model described above. We show the moose diagram for the two site model in Figure 2.3. In this case, the outermost site, now site-1, has a $\mathrm{G}_1 = \mathrm{G}$ local symmetry, which will provide the massive spin one resonances. Thus, we need to keep the second $\sigma-$model to account for the NGBs of the G/H symmetry breaking. In this case we use the notation $U(\Pi)$ for this NGB matrix, as described in Sec. 2.1. Regarding the bosonic Lagrangian of the two-site theory, one must add a kinetic term for the NGB fields, as in Eq. (2.9), where now the covariant derivative involves the gauge fields of $\mathrm{G}_1 = \mathrm{G}$.

$$\mathcal{L}_{\rm b}^{\rm 2site} = -\frac{1}{4g_0^2} f^a_{\mu\nu} f^{a,\mu\nu} - \frac{1}{4g_1^2} F^a_{1,\mu\nu} F_1^{a,\mu\nu} + \frac{f_1^2}{4}\mathrm{Tr}\left(|D_\mu \Omega_1|^2\right) + \frac{f_2^2}{2} d_{\mu,\hat{a}} d^{\mu,\hat{a}} \ , \tag{2.114}$$

here the difference in normalization for the kinetic terms for Ω_1 and U are again related to normalization of generators. In the case of the symbols $d^{\mu,\hat{a}}$ of the Maurer-Cartan form, these are independent of the generator normalization.

In the case of Spin 1/2 states, the Lagrangian takes the following form:

$$\begin{aligned}\mathcal{L}_{\rm f}^{\rm 2site} =& \sum_f i\bar{\Psi}_f \not{D} \Psi_f + \bar{\Psi}_1^{\mathbf{R}}(i\not{D} - m_1^{\mathbf{R}})\Psi_1^{\mathbf{R}} \\ &+ f_1 \sum_f \lambda_f^{\mathbf{R}} \bar{\Psi}_f \Omega_1 \Psi_1^{\mathbf{R}} + \sum_r y_{\mathbf{r}}^{\Psi} \left(\bar{\Psi}_{1,L}^{\mathbf{R}} U\right) \hat{P}_{\mathbf{r}} \left(U^\dagger \Psi_{1,R}'^{\mathbf{R}}\right) + \text{h.c.} \ , \\ & f = q, u, d, l, e \ ,\end{aligned} \tag{2.115}$$

where, as in Eq. (2.112), it includes elementary fermions at site 0, and massive Dirac fermions at site-1. The σ model Ω_1 connects sites 0 and 1. And the second σ model, U, is responsible for interactions between fermions at site-1. Particular emphasis must be put in this last term, where Ψ refers to the field associated to a Left-handed elementary fermion, and Ψ' to that associated to a Right-handed elementary fermion. Including only this chiral structure, and not other similar terms which are however allowed by the

symmetry, is needed to ensure the finiteness of the potential at one loop [86, 87, 129]. This term involves a projector $\hat{P}_{\mathbf{r}}$ over the different representations of the subgroup H, and hence the couplings $y_{\mathbf{r}}$ can have different values. It is the NG bosons which allow different multiplets inside the fields Ψ, Ψ' to be connected. It is important to note that this extra field Ψ' is needed, even if there is a single representation which can fit both Left and Right handed fields. If that is the case, two multiplets transforming under the same representation are needed. This can be contrasted to the 3-site theory, where if the group theory allows it, a single multiplet Ψ can contain the degrees of freedom of both Left- and Right-handed counterparts of elementary fermions. From a point of view of counting the degrees of freedom, both theories are somewhat equivalent: In a 3-site theory where, focusing only on the top quark, one can fit both chiralities inside a certain representation, one has two fermions Ψ_1 and Ψ_2. In the 2-site variant, one is forced to use Ψ_U and Ψ_Q at site 1, in order to write the allowed interaction at site 1.

Without this required "LR" chiral structure, the potential would be logarithmically divergent at one loop. However, the finiteness of the potential is always spoiled if one increases the number of loops, for this reason these computations must be understood in an effective field theory sense. In an extra-dimensional theory, the Higgs potential can be calculated and is finite at 1-loop. One has to understand these discrete models as effective ways to model the sector of resonances, where only certain interactions are allowed. The finiteness of the potential in an extra dimensional theory is related to locality. As the Higgs mass term is generated via interactions through the fifth dimension, and the spontaneous and explicit symmetry breaking occur in different branes, such integrals cannot be contracted into a point and are therefore finite. Following this logic, a discretized theory only including nearest neighbor interactions can be thought of as mimicking this extra dimensional property. In this case, for two sites one can have a 1-loop logarithmically divergent potential if all interactions are allowed at site-1, for three sites this finiteness is recovered.

Just as in the three site model, in this model one can perform an integration of the composite resonances, leading to expressions for the form factors of the effective theory involving only the elementary fields and the NGBs. We will see an explicit example of form factors for a two site model in Chapter 3, and for a three site model in Chapter 4. These description of resonances, while retaining a relatively low number of parameters, have a certain predictability which makes them useful for the purposes of our work.

In this Chapter we have displayed most of the elements surrounding the idea of Composite Higgs which will be needed in the present work. We will come back to many of the concepts and equations described here, in certain cases with minor variations which will be properly pointed out. In what follows, we will focus on the specifics of each model, making use of this Chapter and its content whenever necessary.

Chapter 3

A model with leptoquark S_3 for $R_{K^{(*)}}$

In this Chapter we construct a model to study the anomalies in semileptonic B decays. We propose a composite grand unified theory, based on a simple group that contains the custodial and Standard Model gauge symmetries. This model contains a set of composite pseudo Nambu-Goldstone bosons, among which the Higgs field is contained. Besides these scalar composite states, the model also contains both fermionic and vectorial states. Being interested in studying solutions to the B-anomalies that involve leptoquarks, we find a group that is capable of delivering an $\mathrm{SU}(2)_L$ triplet S_3 among the pNGB. This state is interesting because it can generate the adequate contributions in the Wilson Coefficients capable of explaining the deviations in $R_{K^{(*)}}$, especially for sizeable couplings with third and second generation fermions, as Table 1.2 shows. Alongside this triplet, the model has other pNGB present in the coset: a colorless $\mathrm{SU}(2)_L$-fourplet, and two other leptoquark doublets. By assuming anarchic partial compositeness, we find representations for the composite fermions that allow for the Higgs Yukawa couplings to be generated, as well as leptoquark interactions of the right size that are able to explain deviations in $R^{\mu e}_{K^{(*)}}$. Just as the mechanism for anarchic partial compositeness is able to generate the right masses and mixings for SM fermions, the couplings of the elementary fermions of the third generation to the LQs are favored. Regarding the scale of the New Physics, a benefit of the leptoquark being a pNGB is that its mass is suppressed with respect to the rest of the resonances of the composite sector, this way preventing a bunch of new states at the TeV conflicting with precision observables.

The mixing between elementary and composite sectors generates a potential at one loop that can trigger EW symmetry breaking and generate leptoquark masses dynamically. Moreover, with the global symmetry G being a simple group, unification provides a highly predictive scenario as it relates the Higgs and the leptoquark sectors.

In order to make precise predictions, we consider a description of the resonances of the SCFT in terms of a two-site theory, that provides a weakly coupled description of the composite dynamics. In this way, we can compute the potential at one loop and show that there are regions of the parameter space where EW symmetry breaking (EWSB) occurs dynamically. This allows us to obtain the masses of the would-be NGBs. As the spectrum of NGB includes another colorless state, a fourplet of $\mathrm{SU}(2)_L$, the matching of the Higgs SM vacuum expectation value is modified, and with this may arise some issues related with EW precision tests, as the ρ parameter and corrections to $Zb_L\bar{b}_L$. These are also studied in some detail.

As we have previously mentioned the ability of the leptoquark triplet S_3 to explain the deviations in $R_{K^{(*)}}$, we also consider the possibility of explaining $R_{D^{(*)}}$ with the leptoquark content of the theory. However, we show that bounds from processes as: lepton flavor universality violation in τ decays, as well as $B \to K\nu\bar{\nu}$, are not compatible with $R_{D^{(*)}}$, in agreement with results from the literature [44, 60]. A solution to this puzzle could be generated by including a leptoquark $S_1 \sim (\bar{\mathbf{3}}, \mathbf{1})_{1/3}$, or $R_2 \sim (\bar{\mathbf{3}}, \mathbf{2})_{7/6}$. It is very simple to include scalar states with those charges, but as ordinary resonances, expected to be heavier than the NGBs. A model also addressing $R_{D^{(*)}}$ requires an extension of our model, including S_1 or R_2 as pNGBs as well. The model presented in this Chapter represents a first step towards that solution, in terms of an effective theory of resonances.

This Chapter is organized as follows: in Sec. 3.1 we describe the specifics of this SCFT based on symmetry principles. We discuss its global symmetry group and the pattern of spontaneous symmetry breaking leading to NGBs, containing the Higgs and S_3. We also select representations of the fermionic operators of the SCFT that allow to obtain suitable Yukawa couplings. We briefly discuss some properties of the global symmetries related with physics constraints. In Sec. 3.2 we describe the effective theory obtained after integration of the heavy states of the model, that contains the SM degrees of freedom and the NGBs. This effective theory allows us to compute the potential, and study the conditions that lead to an appropriate vacuum. The results concerning the potential and spectrum are shown in Sec. 3.3. Finally, a study of the phenomenology of the leptoquarks is included in Sec. 3.4, whereas we end the Chapter with a summary of results and some discussions in Sec. 3.5.

3.1. Leptoquarks and Higgs as composite pNGBs

We consider a composite-Higgs model with characteristics as outlined in Chapter 2. There is a sector of elementary fields, containing the same degrees of freedom as the SM, except the Higgs, that is not present in this sector. There is also a new strongly interacting sector, that produces bound states, or resonances, at a scale m_* of a few

TeV. The resonances interact with couplings collectively denoted as g_*, that will be assumed to be perturbative, in the range: $g_{\rm SM} \lesssim g_* < 4\pi$. This sector has a global symmetry G, which in this model is taken to be a simple group, that contains the SM gauge symmetry. G is spontaneously broken by the strong dynamics to a subgroup H, generating a set of NGBs that can be parametrized by the broken generators in G/H. We will focus here on the case where the set of NGBs contains, at least, the Higgs as well as a leptoquark $S_3 = (\bar{\mathbf{3}}, \mathbf{3})_{1/3}$. The NGBs decay constant is of order: $f \sim \sqrt{2} m_*/g_*$. We assume that there are fermionic resonances transforming in irreducible representations of G. It is also straightforward to include spin-one resonances transforming with the adjoint representation of G (they can be excited by the Noether currents of the SCFT associated to the symmetry G). The SCFT sector will be taken flavor anarchic, thus all the Yukawa couplings of the fermion resonances are of the same order. APC provides with a natural explanation for both the hierarchy of masses and the mixings of the SM fermions, by fixing the pattern of elementary-composite couplings as in Eqs. (2.63), (2.64) and (2.65). This will also generate the appropriate couplings to the leptoquark S_3, as we will show.

The elementary sector and the composite sector interact with each other: the elementary gauge fields weakly gauge a subgroup of G, whereas the elementary fermions have linear interactions with the SCFT. These linear interactions are defined in terms of composite operators $\mathcal{O}^{\rm SCFT}$ at a UV scale: $\mathcal{L}_\Lambda \supset \omega\, \bar{\psi} \mathcal{O}^{\rm SCFT}$. These operators, being defined at a scale $\Lambda \gg f$, transform linearly with irreducible representations of G. These representations are not fixed, leaving room for model-building, we will discuss the conditions they must satisfy, selecting a suitable set of them, in Sec. 3.1.1.

We assume the model is equipped with the mechanism of Anarchic Partial Compositeness, as was laid out in Sec. 2.2.

3.1.1. The global symmetry of the SCFT

We can list several conditions that guide us in the choice of the symmetries of the composite sector, particularly of groups G and H. This choice is driven by several things. H must contain the SM gauge group, $\rm G_{SM}$, and G must be such that the coset G/H contains a state with the SM quantum numbers of the Higgs, as well as the leptoquark triplet S_3. Also, we are demanding that the group G must be simple, and not a product of group factors. However we can further refine these conditions as follows:

First, the subgroup H must contain a custodial group $\rm SO(4) \simeq SU(2)_L \times SU(2)_R$, this helps avoid large contributions to the T-parameter. Thus, since it must also contain the SM gauge symmetry, H contains a subgroup which we call $\rm H_{min}$, such that $\rm H \supset H_{min} \equiv SU(3)_c \times SU(2)_L \times SU(2)_R \times U(1)_X$. The SM hypercharge is given by the linear combination $Y = T^3_R + \alpha X$, with α a real constant to be fixed later. Notice that, whereas

the Higgs is taken as a bidoublet of SO(4), the $\mathrm{SU}(2)_R$ charge of the other resonances is not fixed. For example, only the linear combination corresponding to hypercharge is fixed for S_3: $Y = 1/3$.

As discussed in Chapter 2, we will use the following notation for group representations: capital **R** will denote G representations, whereas **r** will denote those of the unbroken subgroup H, and alternatively r for those of $\mathrm{H}_{\mathrm{min}}$. Also they will generally be denoted by their dimensions, with the use of a bar to distinguish a representation and its complex conjugate. For irreducible representations of SU(2) a small **n** will be used. We can sum up the pattern of group embeddings, and the corresponding notation for their representations as follows:

$$\begin{array}{ccccccc} \mathrm{G} & \to & \mathrm{H} & \supset & \mathrm{H}_{\mathrm{min}} & \supset & \mathrm{G}_{\mathrm{SM}} \\ \uparrow & & \uparrow & & \uparrow & & \\ \mathbf{R} & & \mathbf{r} & & r & & \end{array} \tag{3.1}$$

As a second condition, then, we demand that the coset G/H contain a set of generators transforming as $r_H = (\mathbf{1}, \mathbf{2}, \mathbf{2})_0$ and $r_{S_3} = (\bar{\mathbf{3}}, \mathbf{3}, \mathbf{n}_R)_X$ under $\mathrm{H}_{\mathrm{min}}$, that will correspond to the Higgs and the leptoquark S_3, respectively. That is:

$$\mathrm{G/H} \sim \mathbf{r}_\Pi \sim r_H \oplus r_{S_3} \oplus \dots \tag{3.2}$$

where the second relation stands for the decompositions of the coset representation $\mathbf{r}_\Pi$ under $\mathrm{H}_{\mathrm{min}}$. The dots are present because there could be other NGB states in G/H, besides H and S_3.

We found as a suitable choice of groups G and H the one given by

$$\begin{aligned} \mathrm{G} &\simeq \mathrm{SO}(13)\ , \\ \mathrm{H} &\simeq \mathrm{SO}(6)\times\mathrm{SU}(2)^3\ . \end{aligned} \tag{3.3}$$

This embedding of H in G can be further understood by the following breaking patterns:

$$\begin{aligned} \mathrm{G} \equiv \mathrm{SO}(13) &\to \mathrm{SO}(6)\times\mathrm{SO}(7) \\ \mathrm{SO}(7) &\to \mathrm{SU}(2)_1\times\mathrm{SU}(2)_2\times\mathrm{SU}(2)_R\ , \end{aligned} \tag{3.4}$$

where $\mathrm{H}_{\mathrm{min}}$ is contained in H in the following way: first identifying $\mathrm{SU}(2)_L \equiv \mathrm{SU}(2)_{1+2}$, the diagonal subgroup contained in the product of the first and second SU(2) factors, and also by decomposing $\mathrm{SO}(6) \simeq \mathrm{SU}(4) \supset \mathrm{SU}(3)_c \times \mathrm{U}(1)_X$.

Once G and H are chosen, and the embedding of $\mathrm{H}_{\mathrm{min}}$ in H is determined, it is straightforward to obtain the NGBs. The representation of the Goldstones, $\mathbf{r}_\Pi$, can be

written in terms of irreducible representations of H as:

$$\mathbf{r}_\Pi = \mathbf{r}_S \oplus \mathbf{r}_R \oplus \mathbf{r}_H = (\mathbf{6},\mathbf{3},\mathbf{1},\mathbf{1}) \oplus (\mathbf{6},\mathbf{1},\mathbf{2},\mathbf{2}) \oplus (\mathbf{1},\mathbf{3},\mathbf{2},\mathbf{2}) \ . \tag{3.5}$$

In order to find the decomposition under $\mathrm{H}_{\mathrm{min}}$, we need to know the decomposition of some of the lowest dimensional irreducible representations of SO(6) under SU(3)×U(1):

$$\begin{aligned} \mathbf{4} &\sim \mathbf{3}_{-1} \oplus \mathbf{1}_3 \ , & \mathbf{6} &\sim \mathbf{3}_2 \oplus \bar{\mathbf{3}}_{-2} \ , \\ \mathbf{10} &\sim \mathbf{6}_2 \oplus \bar{\mathbf{3}}_{-2} \oplus \mathbf{1}_{-6} \ , & \mathbf{15} &\sim \mathbf{8}_0 \oplus \bar{\mathbf{3}}_4 \oplus \mathbf{3}_{-4} + \mathbf{1}_0 \ , \end{aligned} \tag{3.6}$$

where some of these decompositions, even though not needed for decomposing $\mathbf{r}_\Pi$, will be needed later. By using this, we obtain that under $\mathrm{H}_{\mathrm{min}}$ the NGBs transform as

$$\begin{aligned} r_S &= (\bar{\mathbf{3}},\mathbf{3},\mathbf{1})_{-2} + \text{c.c.} \ , \\ r_R &= (\bar{\mathbf{3}},\mathbf{2},\mathbf{2})_{-2} + \text{c.c.} \ , \\ r_H \oplus r_{H_4} &\sim (\mathbf{1},\mathbf{2},\mathbf{2})_0 \oplus (\mathbf{1},\mathbf{4},\mathbf{2})_0 \ , \end{aligned} \tag{3.7}$$

where c.c. stands for the complex conjugate representations, and where we have used that, for SU(2): $\mathbf{2} \otimes \mathbf{3} \sim \mathbf{2} \oplus \mathbf{4}$. [1]

In order to obtain the proper hypercharge of S_3, we need to fix the parameter $\alpha = -1/6$, thus obtaining:

$$Y = T^{3R} - X/6 \ . \tag{3.8}$$

Having fixed α, now we can get the G_{SM} quantum numbers of the remaining leptoquarks. The $\mathrm{H}_{\mathrm{min}}$ representation r_R decomposes as the sum of two representations, corresponding to leptoquark doublets with hypercharges differing in one unit: $Y_R = -1/3 \pm 1/2$. Therefore, besides the usual SM Higgs H, in the NGB spectrum we can find a colorless fourplet H_4, and the leptoquarks S_3, $\tilde{R}_2$ and $\hat{R}_2$:

$$\begin{aligned} H &\sim (\mathbf{1},\mathbf{2})_{1/2} \ , & H_4 &\sim (\mathbf{1},\mathbf{4})_{1/2} \ , & \\ S_3 &\sim (\bar{\mathbf{3}},\mathbf{3})_{1/3} \ , & \tilde{R}_2 &\sim (\mathbf{3},\mathbf{2})_{1/6} \ , & \hat{R}_2 &\sim (\mathbf{3},\mathbf{2})_{-5/6} \ . \end{aligned} \tag{3.9}$$

Thus, although SO(13) is the smallest simple group that we found that fulfills the conditions of containing $\mathrm{H}_{\mathrm{min}}$, and being able to deliver S_3 and H as NGBs, we see that it also contains an extra pair of leptoquark doublets, as well as an extra colorless fourplet. With these additional states being present in the spectrum, their influence on the different constraints of the theory must be assessed.

[1] We have used the subindex R for the second line of Eq. (3.7) because, as we will show below, it leads to the leptoquarks usually denoted with the letter R, see for example the notation of Ref. [62].

Representations of the fermions

The SCFT operators $\mathcal{O}^{\rm SCFT}$ are in irreducible representations of G, whereas the elementary fermions only transform under $\mathrm{G_{SM}}$. The elementary-composite couplings explicitly break $\mathrm{G_{SM}}\times\mathrm{G}$ to the diagonal subgroup. In order to understand several properties of this breaking, it is useful to add spurionic degrees of freedom in the elementary sector, embedding the SM fermions in the same irreducible representations of SO(13) as the operators of the SCFT mixing with them. [2] In order to find the right choices of SO(13) representations for the embedding of these fermions, there are several conditions that these representations must satisfy. To avoid an explicit breaking of $\mathrm{G_{SM}}$, they must contain components in the same representations under $\mathrm{G_{SM}}$ as the SM fermions, besides we require that they allow the usual Yukawa couplings with the Higgs, and finally we also require Yukawa interactions leading to $S_3\bar{q}^c l$, with q and l the quark and lepton doublets. This last condition is necessary in order to explain deviations in $R_{K^{(*)}}$.

We find that the smallest representations of SO(13) in which the SM fermions can be embedded, are the following ones:

$$\begin{aligned} \mathbf{R}_q &= \mathbf{286} \supset (\mathbf{6},\mathbf{3},\mathbf{2},\mathbf{2}) = \mathbf{r}_q \ , & \mathbf{R}_{u,d} &= \mathbf{286} \supset (\mathbf{6},\mathbf{1},\mathbf{1},\mathbf{3}) = \mathbf{r}_{u,d} \ , \\ \mathbf{R}_l &= \mathbf{78} \supset (\mathbf{1},\mathbf{3},\mathbf{2},\mathbf{2}) = \mathbf{r}_l \ , & \mathbf{R}_e &= \mathbf{78} \supset (\mathbf{1},\mathbf{1},\mathbf{1},\mathbf{3}) = \mathbf{r}_e \ , \end{aligned} \tag{3.10}$$

where we have specified the component under H containing the SM fermions. For each fermion, all three generations are embedded in the same representation. A more detailed description of the lowest dimensional representations of SO(13), and their decompositions under H and $\mathrm{H_{min}}$ can be found in Ap. A.1.

The following embedding also contains a state with the same quantum numbers as q: $\mathbf{R}_q = \mathbf{286} \supset \mathbf{r}_{q'} = (\mathbf{15},\mathbf{1},\mathbf{2},\mathbf{2})$. This can be derived from the fact that **15** contains an SU(3) triplet, as Eq. (3.6) shows. However, unless u and d are embedded in higher dimensional representations of SO(13), $\mathbf{r}_{q'}$ does not allow for the usual Yukawa couplings. Besides, it also induces LQqq interactions that, as we will discuss in Sec. 3.1.1, can induce proton decay. [3] For this reason we will assume that the mixing with the component (**15**,**1**,**2**,**2**) is very small, and we will not consider it in our analysis (However, in Ap. A.3 we show its contributions to the potential). The size of this mixing being negligible does not depend on tuning, but can be simply attributed to the running of this parameter. That is, its composite operator has a larger scaling dimension Δ than that of the operator mixing with the multiplet $\mathbf{r}_q$.

There are smaller irreducible representations in which to embed the SM fermions,

[2] These new elementary fermions, added to furnish complete representations of SO(13), are spurions, they do not correspond to propagating degrees of freedom.

[3] We are using LQ to generically denote any leptoquark state.

but they not satisfy all the conditions discussed in the beginning of this section. It is also possible to embed l in $\mathbf{286} \supset (\mathbf{1},\mathbf{3},\mathbf{2},\mathbf{2})$, but for simplicity we will only work with the embeddings of Eq. (3.10).

As described in Chapter 2, in the effective theory we use the notation Ψ_f, with $f = q, u, d, l, e$, to denote the chiral fermion obtained after the embedding of the elementary fermion f into a representation of SO(13). For example: Ψ_q represents an elementary Left-handed fermion in the representation **286**, where only the components corresponding to the SM quark doublet, *i.e.*: in the representation $(\mathbf{3},\mathbf{2})_{1/6}$ of the SM group, are dynamical, and the other components are non-dynamical spurions.

A symmetry to forbid baryon decay

The interactions involving two quarks and one leptoquark can induce baryon decay. In our model there are LQqq interactions at the TeV scale that make the theory phenomenologically unacceptable. However these interactions can be forbidden by imposing a Z_2-symmetry from SO(13), as: $P = e^{iT_P\pi/2}$, with T_P a generator of the SO(6) subgroup (see Ap. A.1 for more details). In the representation **13** of SO(13), choosing a suitable basis, P can be written as a block diagonal matrix: $P = \mathrm{diag}(I_7, -I_6)$, where I_6 and I_7 are the identity in SO(6) and SO(7), respectively. [4] As an example, fields in the fundamental representation of SO(6) are odd under P, as the quarks in $\mathbf{r}_{q,u,d}$ and the leptoquarks, whereas fields in the singlet or adjoint representation of SO(6) are even, as the leptons and the quarks in $\mathbf{r}_{q'}$. This symmetry then forbids the interactions LQqq and LQ$q'q'$, however it allows interactions LQ$q'q$, with q a quark in $\mathbf{r}_{q,u,d}$ and q' in $\mathbf{r}_{q'}$. To forbid transitions mediated by the last operator, the projection on $\mathbf{r}_{q'}$ must be suppressed, thus we take $\lambda_{q'} = 0$ and neglect its effect in what follows.

3.1.2. Flavor

Regarding flavor, we follow the construction detailed on Chapter 2, specifically in Sec. 2.2, where we describe Anarchic Partial Compositeness. This mechanism allows for the masses and mixings of the SM fermions to be explained appropriately, if the mixings ϵ_f obey the relations in Eq. (2.63,2.64) and Eq. (2.65) for quarks and leptons respectively. However if the elementary fermions interact with several operators of the SCFT, as could be the case if both $\mathbf{r}_q$ and $\mathbf{r}_{q'}$ are included, there can be more freedom regarding these relations [18, 88]. In our case we only consider a single elementary-composite mixing per quark per generation, which at low energies is a good approximation if the two composite operators have different scaling dimensions: $\Delta_q \neq \Delta_{q'}$. When this is the case, fixing the quark masses and the CKM matrix leaves only a single free parameter, ϵ_{q3}. Regarding the sector of leptons, their linear couplings cannot be fixed as in the

[4] See [71] for a similar symmetry in a factorizable group.

quark sector, as a mechanism generating neutrino masses must be chosen first, and we have not done so in the present work. We then consider a Left-Right symmetric scheme, where $\epsilon_{li} \sim \epsilon_{ei}$, as in Eq. (2.65) which has been shown to minimize flavor constraints [18]. In this case the unitary matrices diagonalizing the charged lepton mass matrix have hierarchical angles, thus the angles of the PMNS matrix have to be generated in the neutrino sector, see Refs. [18, 92, 93] for these scenarios.

3.1.3. Constraints

We consider first the most important effects on the oblique parameters and $Zb\bar{b}$ couplings related with composite grand unification. As we will discuss, due to the presence of an extended scalar sector, there are new contributions to the $\hat{T}$-parameter, that are absent in the MCHM containing a single scalar. However we will show that these contributions are suppressed for small ξ. [130]

As mentioned in Sec. 2.1, the MCHM preserves the custodial symmetry, which is a property of its coset, SO(5) /SO(4). In the present model the color singlets H_2 and H_4 are in the coset SO(7)/[SO(4)×SO(3)], they transform as a $(\mathbf{4},\mathbf{3})$ of the invariant subgroup. The SM gauges (a subgroup of) an $[\mathrm{SO}(4)\times\mathrm{SO}(3)]_g$ subgroup of SO(7), generating a potential for the NGB and eventually misaligning the vacuum. The misalignment happens if the group preserved by the vacuum, $[\mathrm{SO}(4)\times\mathrm{SO}(3)]_{\mathrm{vac}}$, is different from $[\mathrm{SO}(4)\times\mathrm{SO}(3)]_g$. We find three possibilities for the misalignment, that depend on which subgroup is shared by these two groups: (a) an SO(3) subgroup, in this case only H_2 has a VEV, (b) an SO(2) subgroup, in this case $\langle H_4\rangle$ is annihilated by the same generator as $\langle H_2\rangle$, and both VEVs have the same charge under T^3_L, and (c) the trivial subgroup, as happens for generic VEVs $\langle H_2\rangle$ and $\langle H_4\rangle$ that do not satisfy the conditions of case (b). Case (a) is the most favorable one, containing a custodial symmetry, whereas case (c) is not compatible with the phenomenology, since there is no massless photon in the spectrum. In Sec. 3.3.1 we will show that, in our model, case (b) is realized, since the presence of the Higgs VEV triggers a VEV of the neutral component of H_4: v_4 [130]. Case (c) is also possible in our model. A non-vanishing v_4 modifies the ρ-parameter as: $\rho \simeq 1 - 6v_4^2/v^2$. Ref. [130] has shown that the constraints on ρ require, at 3 σ level, $v_4 \lesssim 2.5$ GeV. [5] We will show that v_4 is suppressed compared with v by: $v_4 \sim \xi v/2$, leading to $\rho \sim 1 + \mathcal{O}(\xi^2)$. By considering just this contribution to ρ, and neglecting corrections to other EW parameters, $\xi \lesssim 0.02 - 0.04$, increasing the amount of tuning compared with the usual MCHM, that requires $\xi \lesssim 0.1 - 0.3$.

As we will show, the VEV of H_4 is generated by a term in the potential of the form $(H_2^2 H_2^\dagger H_4^\dagger)$. We have searched for symmetries that could prohibit this term, relaxing

[5] It has also shown that there are positive contributions to ρ induced by the splitting of the H_4 components.

the bounds from ρ. An example would be a parity transformation such that H_2 and H_4 have different eigenvalues under this operation, for example ± 1. We have found that there is no non-trivial element in the algebra of SO(7) having H_2 and H_4 as eigenvectors. Since the exponential map is surjective for SO(7), this result covers all the possibilities. Thus there are no symmetries inside SO(7) that could forbid the cited term in the potential. Extending the group to O(7) does not offer new solutions.

Corrections from new physics to $Zb_L\bar{b}_L$ coupling cannot be larger than $\sim 0.25\,\%$. In composite Higgs models with partial compositeness, in the simple framework of one scale and one coupling in the sector of resonances, the tree-level corrections can be estimated as $\delta g_{b_L}/g \sim \xi\epsilon_{q3}^2$. For $f \sim 800$ GeV, δg_{b_L} is usually too large. However it is possible to protect the Z-couplings with a discrete subgroup of the custodial symmetry, a parity P_{LR}, ensuring that δg_{b_L} is sufficiently suppressed [101]. This symmetry requires embedding q_L in a $(\mathbf{2},\mathbf{2})_{2/3}$ of $\mathrm{SU}(2)_L{\times}\mathrm{SU}(2)_R{\times}\mathrm{U}(1)_X$. From Eqs. (3.8) and (3.10), one can see that, by choosing $\mathbf{R}_q = \mathbf{286}$, q_L is embedded in a $(\mathbf{2},\mathbf{2})_{-1/3}$ of $\mathrm{SU}(2)_L{\times}\mathrm{SU}(2)_R{\times}\mathrm{U}(1)_X$. Thus extra tuning could be needed, with this choice of $\mathbf{R}_q$, to pass the constraints from $Zb\bar{b}$.

In Secs. 3.3 and 3.4 we will show the prediction of v_4 and δg_{b_L} in our model, as well as the tuning.

One possibility to avoid too large δg_{b_L} is to find an $\mathbf{R}_q$ containing a $(\mathbf{2},\mathbf{2})_{2/3}$ for the Left-handed quarks. The smallest SO(13) representation that we have found with this property is: $\mathbf{R}_q = \overline{\mathbf{715}}$, that contains an $\mathbf{r}_q = (\mathbf{15},\mathbf{3},\mathbf{2},\mathbf{2})$, allowing the proper embedding of q_L. In this case one can choose, for example, $\mathbf{R}_u = \mathbf{78}$, leading to the right Yukawa coupling with the Higgs. Given the large dimension of $\mathbf{R}_q$, we have not pursued this analysis.

Other strong constraints in this kind of theories arise from neutron-antineutron oscillations. This process is induced by operators of dimension 9, involving six quarks of the first generation [131]. However it has been shown that in the framework of anarchic partial compositeness, with a compositeness scale in the range of few TeV, the Wilson coefficients of these operators are sufficiently suppressed. [71]

In Sec. 3.4 we will comment on other phenomenological constraints, as direct searches at colliders, flavor transitions and lepton flavor universality violation.

3.2. Effective theory

At energies below m_* the heavy resonances of the SCFT can be integrated-out, leading to an effective theory with the SM degrees of freedom, plus the NGBs. Given the symmetries and the fermionic representations, many properties of this effective low energy description are fixed. We follow the ideas outlined in Sec. 2.1, where many of the same concepts will be extended to a coset that now includes other scalar states apart

from the Higgs. By using the CCWZ formalism, one can build an effective Lagrangian that, although superficially looks only H-invariant, is G-invariant after embedding the SM fermions in representations of G. As a central building block, we have the Goldstone Matrix U, as defined in Eq. (2.5). A small point in which this model differs from the MCHM, is that, since $\{T^{\hat{a}}\}$ spans a reducible representation of H (see Eq. (3.5)), there are three independent decays constants: f_S, f_R and f_H, one associated with each irreducible representation. As described in Sec. 2.1, one can write the kinetic terms by using the Maurer-Cartan form, as

$$\mathcal{L} \supset \sum_{\mathbf{r}\in\mathbf{r}_\Pi} \frac{f_{\mathbf{r}}^2}{2} d_\mu^{\hat{a}_{\mathbf{r}}} d^{\mu,\hat{a}_{\mathbf{r}}} \ , \tag{3.11}$$

where the main difference with Eq. (2.10) is the inclusion of independent decay constants $f_{\mathbf{r}}$ for each irreducible representation. However, as all decay constants are naively expected to be of the same size, for the sake of simplicity we will take the same numerical value for them, calling it f. These kinetic terms also contain the SM gauge fields, as the Maurer-Cartan form involves a covariant derivative. If we assume a vacuum for the pNGB fields that preserves U(1) electromagnetic symmetry, this implies evaluating fields H and H_4 in their VEVs: v and v_4. By doing this, Eq. (3.11) generates a mass term for the Z and Ws, where we get the following matching:

$$v_{\rm SM}^2 = (246\text{GeV})^2 = \frac{f^2}{6}\left[9\sin^2\left(\frac{3v_4}{\sqrt{2}f}\right) + 2\sin^2\left(\frac{v}{f}+\frac{v_4}{\sqrt{2}f}\right) + \sin^2\left(\frac{2v}{f}-\frac{v_4}{\sqrt{2}f}\right)\right] . \tag{3.12}$$

This equation can be compared with the MCHM case, Eq. (2.13). Eq. (3.12) is invariant under the following combined transformation: $v \to -v$ and $v_4 \to -v_4$. Less obvious, but straightforward to check, it is also invariant under the combined transformation: $v \to v + 2\pi f/3$ and $v_4 \to v_4 + \sqrt{2}\pi f/3$. Besides, it has period πf and $\sqrt{2}\pi f$ in the variables v and v_4. We show $v_{\rm SM}/f$ as function of v/f and v_4/f in the right-panel of Fig. 3.1.

3.2.1. Sector of fermions

We are now in a position to write an invariant Lagrangian including the interactions between NGBs and fermion fields. This procedure has been outlined in Chapter 2, specifically in Sec. 2.1.2. This makes it possible to write G-invariant terms containing the usual Higgs Yukawa and leptoquark interactions, as well as an infinite series of terms with higher powers of the NGBs. For quark bilinears, since all the quarks have been embedded in the representation **286**, one has to sum over all the irreducible representations of H contained in **286**: $\sum_{\mathbf{r}\subset\mathbf{286}} \left[\widetilde{\bar{\Psi}}_q^{\mathbf{r}}(c_{\mathbf{r}}^u \widetilde{\Psi}_u^{\mathbf{r}} + c_{\mathbf{r}}^d \widetilde{\Psi}_d^{\mathbf{r}})\right]_{\mathbf{1}}$. In this expression $c_{\mathbf{r}}^u$ and $c_{\mathbf{r}}^d$ are coefficients independent of the fields. Expanding to first order in the

NGBs and putting to zero the non-dynamical fermions, it is straightforward to obtain the usual Yukawa interactions of the up- and down-type quarks. The same results apply for the leptons, now embedded in the representation **78** of G: $\sum_{\mathbf{r}\subset\mathbf{78}} c^e_{\mathbf{r}}(\widetilde{\bar{\Psi}}^{\mathbf{r}}_l \widetilde{\Psi}^{\mathbf{r}}_e)_{\mathbf{1}}$. One can also write invariants with quarks and leptons, that will lead to leptoquark interactions. The common H-representations in the decomposition of **286** and **78** can be read in Eq. (B.3) of Ap. A.1: $\mathbf{r} \sim (\mathbf{1},\mathbf{3},\mathbf{2},\mathbf{2}), (\mathbf{6},\mathbf{3},\mathbf{1},\mathbf{1})$, thus leptoquark interactions can be obtained from invariants as: $\sum_{\mathbf{r}} c^{ql}_{\mathbf{r}}(\widetilde{\bar{\Psi}}^{\mathbf{r}}_{q^c} \widetilde{\Psi}^{\mathbf{r}}_l)_{\mathbf{1}}$, where the sum is over the common $\mathbf{r}$'s. It is straightforward to check that, to first order in the NGBs, only the usual Yukawa interactions with the Higgs, as well as interactions with S_3, are generated, no more interactions are present to this order. In Sec. 3.4 we will show explicitly the leading terms in an expansion in powers of the NGBs.

By dressing the fermions with U, one can write all quadratic combinations as is shown in Eq. (2.24), where a sum over generations is understood. We are taking $f, f' = q, u, d, l, e$, where we are not including the neutrino sector as it depends on the nature of the neutrino, and as such is more model dependent.

The inclusion of the charge conjugate fermions stems from the fact that the interaction with a state S_3, being an $\mathrm{SU}(2)_L$ triplet, allows for invariants to be formed involving two doublets q_L and l_L, one of which needs to be conjugated.

Explicit expressions for these form factors can be obtained by working with a model of resonances, as outlined in Sec. 2.4.

We can evaluate the NGBs on their EM-invariant VEVs, *i.e.* v and v_4, and keep only the dynamical elementary fermions. This allows for a simpler expression for the effective theory to be obtained, like that of Eq. (2.26), which however also includes the gauge sector. In this Chapter we wish to focus on the fermion sector, which alone can trigger EWSB in certain cases.

We will obtain correlators Π_f and M_f expressed in terms of functions $i^{\mathbf{r}}_{f,f'}$ and $j^{\mathbf{r}}_f$, as in Eq. (2.28), now functions of v and v_4. As the NGB matrix has a closed form in the case of this EM-preserving vacuum, these functions can be computed to all orders in v/f and v_4/f. Defining $s_z = \sin z$, $c_z = \cos z$, $x = v/f + v_4/(f\sqrt{2})$ and $y = v/f - \sqrt{2}v_4/f$, we show our results for the quarks in Table 3.1. For simplicity and due to the potential being top-dominated, we omit the results for leptons, which can be similarly obtained.

i	**(6,3,1,1)**	**(6,1,1,3)**	**(6,1,3,1)**	**(6,3,2,2)**
i_{q,u_L}	$\frac{1}{3}s^2_{x+y}$	$\frac{1}{6}(s_x - s_{x+y})^2$	$\frac{1}{6}(s_x + s_{x+y})^2$	$\frac{1}{6}(3 + c_{2x} + 2c_{2x+2y})$
i_{q,d_L}	$\frac{1}{6}s^2_{2x}$	$\frac{1}{12}(s_{2x} - s_y)^2$	$\frac{1}{12}(s_{2x} + s_y)^2$	$\frac{1}{12}(9 + 2c_{4x} + c_{2y})$
i_{u_R}	$\frac{1}{2}s^2_x s^2_y$	$c^2_x s^4_{y/2}$	$c^2_x c^4_{y/2}$	$\frac{1}{2}(1 - c_{2x}c^2_y)$
i_{d_R}	$\frac{1}{2}s^4_x$	$\frac{1}{16}(c_{2x} - 2c_y + 1)^2$	$\frac{1}{16}(c_{2x} + 2c_y + 1)^2$	$\frac{1}{8}(-c_{4x} - 2c_{2y} + 3)$
j_u	$\frac{1}{\sqrt{6}}(s_x s_y s_{x+y})$	$\sqrt{\frac{2}{3}}c_x s^3_{y/2} c_{x+y/2}$	$-\sqrt{\frac{2}{3}}c_x c^3_{y/2} s_{x+y/2}$	$\frac{1}{\sqrt{6}}(c_y s_{2x+y})$
j_d	$\frac{1}{\sqrt{3}}(c_x s^3_x)$	$\frac{1}{4\sqrt{3}}(c_y - c^2_x)(s_{2x} - s_y)$	$-\frac{1}{4\sqrt{3}}(c_y + c^2_x)(s_{2x} + s_y)$	$\frac{1}{4\sqrt{3}}(s_{4x} + s_{2y})$

Table 3.1: Invariants evaluating the NGBs in their VEVs, with $s_z = \sin z$, $c_z = \cos z$, $x = v/f + v_4/(f\sqrt{2})$ and $y = v/f - \sqrt{2}v_4/f$. The columns are associated to representations **r** present in the decomposition of **286** under H.

The fermionic spectrum can be obtained from the equations of motion, as described below Eq. (2.29).

3.3. Potential

The SM fields explicitly break the global symmetry of the SCFT. Keeping only the dynamical SM fields, and putting to zero the spurions that were introduced to obtain full representations of SO(13), a potential for the NGBs is generated. We follow Sec. 2.1.3 where we have outlined this procedure. From the effective Lagrangian, which is quadratic in the SM fields, one can define a matrix or kernel, whose determinant gives the 1-loop potential in the pNGBs. Here we focus on the fermionic contribution to the Coleman-Weinberg potential alone, we write

$$V = -\frac{1}{2}\int \frac{d^4p}{(2\pi)^4} \log \mathrm{Det}\left(\frac{\mathcal{K}_f}{\mathcal{K}_f^0}\right) , \tag{3.13}$$

where $\mathcal{K}$ is the "matrix" in the Lagrangian of Eq. (2.24), when it is written as: $\mathcal{L}_{\text{eff}} = \bar{F}\mathcal{K}_f(\Pi)F$, with $F^t = (f, f^c)$ and f the chiral fermions of the SM. $\mathcal{K}_f$ has the $\mathrm{SU}(3)_c$ and $\mathrm{SU}(2)_L$ indices of the fermions in f and it depends on the NGBs. Since in the anarchic approach q and u of the third generation have the largest interactions with the SCFT, they dominate the contributions to the potential, thus we will not consider the effect of the other fermions for the calculation of V. In this case $\mathcal{K}_f$ is a matrix of dimension nine. To shorten notation, in this section we will simply use q and u for the quarks of the third generation, without writing the generation index.

For simplicity we have not considered the contribution of the gauge fields to the potential, although it is straightforward to include it. Since the interactions of the third generation of fermions are usually stronger than the gauge ones, we expect the

gauge fields to give a subdominant correction to the potential. Moreover, the gauge contributions to the potential can be shown to be always aligned with the symmetric vacuum. That is, in absence of fermions, no EWSB is present. Thus the inclusion of fermions alone is enough to check if there is spontaneous symmetry breaking, as long as the effect of gauge field does not counter this and restore the symmetry. [6]

We have not been able to resum the matrix U when all the NGBs are present. One can perform an expansion of V in powers of the NGBs. In Sec. 2.1.3 we have described a method for this perturbative expansion. To fourth order in Π the potential can be written as:

$$V(\Pi) \simeq V_2 + V_3 + V_4 + \mathcal{O}(\Pi^5) \tag{3.14}$$

where V_n is of order n in the NGB,

$$V_2 = m_{S_3}^2 |S_3|^2 + m_{\tilde{R}_2}^2 |\tilde{R}|^2 + m_{\hat{R}_2}^2 |\hat{R}|^2 + m_H^2 |H|^2 + m_{H4}^2 |H_4|^2 \ , \tag{3.15}$$

$$V_3 = m_1 S_3 \tilde{R} H^\dagger + m_2 S_3 \hat{R} H + m_3 S_3 \tilde{R} H_4^\dagger + m_4 S_3 \hat{R} H_4 + \text{ h.c.} \ , \tag{3.16}$$

and

$$V_4 = V_4^H + V_4^{\rm LQ} + V_4^{H\rm LQ} = \sum_{j=1,\dots 49} c_j \ (\Pi_{a_j} \Pi_{b_j} \Pi_{d_j} \Pi_{e_j}) \ , \tag{3.17}$$

where the superindex in V_4 specifies the kind of NGBs, H for color singlets and LQ for leptoquarks, c_j is a quartic coupling and $(\Pi_{a_j} \Pi_{b_j} \Pi_{d_j} \Pi_{e_j})$ is a SM singlet of fourth order in the NGBs. Since there are forty-nine quartic terms, we list them in Ap. A.2. There are eight invariants in V_4^H, one involving only H, two with H_4 and five with H and H_4, twenty-one in $V_4^{\rm LQ}$ and twenty in $V_4^{H\rm LQ}$, involving two fields that are color singlets and two leptoquarks. For details see Ap. A.2. The coefficients of Eqs. (3.15)-(3.17) can be expressed as momentum integrals of the form factors of the effective theory. We show explicit expressions for the quadratic and cubic couplings in Ap. A.3, the quartic ones involve very long expressions, therefore we only show some of them in the limit of large Z_f.

For the analysis of EWSB of the next section, it will be useful to know explicitly V_4^H:

$$\begin{aligned} V_4^H =& c_1 (H_2^\dagger H_2)_1^2 + c_2 (H_4^2)_3 (H_4^{\dagger 2})_3 + c_3 (H_4^2)_7 (H_4^{\dagger 2})_7 + c_4 (H_2^\dagger H_2)_1 (H_4^\dagger H_4)_1 \\ &+ c_5 (H_2^\dagger H_2)_3 (H_4^\dagger H_4)_3 + c_6 H_2^{\dagger 2} H_2 H_4 + c_7 H_4^{\dagger 2} H_4 H_2 + c_8 (H_2^2)_3 (H_4^{\dagger 2})_3 + \text{h.c.}, \end{aligned} \tag{3.18}$$

where the h.c. is required for the last three terms. The subindex in the parenthesis shows the dimension of the $\mathrm{SU}(2)_L$ representation chosen from the product of fields.

[6] If $g_{\rm SM}/g_* \sim \epsilon_{q3,u3}$, the gauge contributions to the potential are expected to be of the same size as the contribution of the fermions, thus they must be included.

Other quartic invariants depending on these fields can be written in terms of the ones shown in Eq. (3.18).

It is also useful to study the potential expanding it in powers of the degree of compositeness of the fermions: ϵ_f. To $\mathcal{O}(\epsilon_f^4)$, it can be written as [84]

$$V \simeq \frac{m_*^4}{16\pi^2}\left[\epsilon_q^2 F_q^{(2)}(\Pi/f) + \epsilon_u^2 F_u^{(2)}(\Pi/f) + \epsilon_q^4 F_q^{(4)}(\Pi/f) + \epsilon_u^4 F_u^{(4)}(\Pi/f) + \epsilon_q^2\epsilon_u^2 F_{qu}^{(4)}(\Pi/f)\right] \tag{3.19}$$

where $F_f^{(n)}$ are functions of the NGBs arising from the invariants, thus depending on the representations of the fermions.

By using the expansion of Eq. (3.19) one can estimate the size of the coefficients of Eqs. (3.15)-(3.17). Up to accidental cancellations of leading terms, we obtain:

$$m_\Pi^2 \sim \epsilon_f^2 \frac{m_*^4}{16\pi^2 f^2}\ , \qquad m_n \sim \epsilon_f^2 \frac{m_*^4}{16\pi^2 f^3}\ , \qquad c_j \sim \epsilon_f^2 \frac{m_*^4}{16\pi^2 f^4}\ . \tag{3.20}$$

3.3.1. EWSB

Successful EWSB requires a non-trivial minimum, where a U(1) symmetry associated with electromagnetism is preserved. Relying on the fourth order expansion of the potential, we demand:

$$m_H^2 < 0\ , \qquad m_\Pi^2 > 0\ , \qquad \Pi = S_3,\ \tilde{R}_2,\ \hat{R}_2,\ H_4\ , \tag{3.21}$$

as well as positive quartic couplings stabilizing the minimum. The presence of the coupling c_6 induces a VEV of the neutral component of H_4 [130]:

$$v^2 \simeq -\frac{m_H^2}{c_1}\ , \qquad v_4 \simeq -c_6 v\left[\frac{v^2}{2m_4^2} + \mathcal{O}\left(\frac{c_i v^4}{m_4^4}\right)\right] \tag{3.22}$$

As usual in composite Higgs models, in the absence of tuning: $v \sim f$. However, as discussed in Sec. 3.1.3, EW precision observables require $\xi \ll 1$, in this case v_4 is suppressed by a factor ξ compared with v.

It is possible to obtain the one-loop potential of Eq. (3.13) to all orders in v and v_4. Similar to the MCHM, the one-loop potential is that given by Eq. (2.33). We write it here again, for the sake of clarity, where we only keep contributions coming from third generation quarks:

$$V(v_\Pi) = -2N_c \int \frac{d^4p}{(2\pi)^4}\Big\{\log\left[p^2(Z_q + \Pi_{u_L})(Z_u + \Pi_{u_R}) - |M_u|^2\right] + \log\left[p^2(Z_q + \Pi_{d_L})\right]\Big\} - V(v_\Pi = 0)\ , \tag{3.23}$$

where the first term is the contribution from the top, the second term is the contribution from the Left-handed bottom, and the correlators are defined in Eq. (2.28). We are ignoring contributions coming from gauge fields, and from leptons. The invariants in this case are those from Table 3.1. Due to the presence of the trigonometric functions in the invariants, the potential of Eq. (3.23) is invariant under the same transformations, and has the same periodicity with v_4, as Eq. (3.12). As a function of v, it has period $2\pi f$.

We can expand Eq. (3.23) in powers of $1/Z_f$, which is similar to an expansion in powers of ϵ_f. At the leading order, we get:

$$V(v_\Pi) \simeq -2N_c \int \frac{d^4p}{(2\pi)^4} \left\{ \frac{\Pi_{u_L} + \Pi_{d_L}}{Z_q} + \frac{\Pi_{u_R}}{Z_u} \right\} + \mathcal{O}\left(\frac{1}{Z_f^2}\right) , \tag{3.24}$$

where we see that only the diagonal correlators $\Pi_{f_{L/R}}$ play a role at the lowest order, and the Left-Right correlator M_u is subleading. We can evaluate this expression for the invariants in this model, for simplicity we take the case where only v is nonzero, and we get:

$$V(v) \simeq \alpha\ (\mathrm{c}_{v/f} - 1) + \beta\ \mathrm{s}_{v/f}^2 + \gamma\ \mathrm{s}_{v/f}^4 + \delta\ \mathrm{c}_{v/f}\ \mathrm{s}_{v/f}^2 + \mathcal{O}\left(\frac{1}{Z_f^2}\right) , \tag{3.25}$$

with the coefficients given by:

$$\begin{aligned}
\alpha &= -2N_c \int \frac{d^4p}{(2\pi)^4} \frac{\Pi_u^{(6,1,1,3)} - \Pi_u^{(6,1,3,1)}}{2Z_u} , \\
\beta &= -2N_c \int \frac{d^4p}{(2\pi)^4} \left[\frac{8\Pi_q^{(6,3,1,1)} + 5\Pi_q^{(6,1,1,3)} + 5\Pi_q^{(6,1,3,1)} - 18\Pi_q^{(6,3,2,2)}}{4Z_q} \right. \\
&\qquad \left. + \frac{3}{4Z_u} \left(2\Pi_u^{(6,3,2,2)} - \Pi_u^{(6,1,1,3)} - \Pi_u^{(6,1,3,1)}\right) \right] , \\
\gamma &= -2N_c \int \frac{d^4p}{(2\pi)^4} \left[\frac{1}{Z_q} \left(4\Pi_q^{(6,3,2,2)} - 2\Pi_q^{(6,3,1,1)} - \Pi_q^{(6,1,1,3)} - \Pi_q^{(6,1,3,1)}\right) \right. \\
&\qquad \left. + \frac{1}{4Z_u} \left(2\Pi_u^{(6,3,1,1)} + \Pi_u^{(6,1,1,3)} + \Pi_u^{(6,1,3,1)} - 4\Pi_u^{(6,3,2,2)}\right) \right] , \\
\delta &= -2N_c \int \frac{d^4p}{(2\pi)^4} \left[\frac{\Pi_q^{(6,1,3,1)} - \Pi_q^{(6,1,1,3)}}{Z_q} + \frac{\Pi_u^{(6,1,1,3)} - \Pi_u^{(6,1,3,1)}}{2Z_u} \right] .
\end{aligned} \tag{3.26}$$

If the coefficients of the potential (3.25) are of the same order, the minimum of the potential is at $v = 0$ or $v \sim f$. For $\mathrm{s}_{v/f} \ll 1$, the potential of Eq. (3.25) is minimized by:

$$\mathrm{s}_{v/f}^2 \simeq \frac{-2\alpha - 4(\beta + \delta)}{\alpha + 8\gamma - 4\delta} , \tag{3.27}$$

requiring tuning for a partial cancellation of the numerator. As usual the tuning is expected to be of order ξ^{-1}, see Sec. 3.3.3.

3.3.2. Numerical results

In this section we present the results obtained by computing the potential of Eq. (3.23). For numerical calculations, it is necessary to know the fermionic form-factors. An explicit realization can be obtained by working in a two-site model, with the elementary fields associated to the degrees of freedom of one site, and the first level of resonances of the SCFT associated to the degrees of freedom of the other site, as described in Sec. 2.4. We give a brief description of this, and show explicitly the form-factors obtained in Ap. A.4. As mentioned before, since in our approach the potential is dominated by the third generation of quarks, we only include massive resonances associated to the doublet q_L and the singlet u of the third generation, both in the representation $\mathbf{R} = \mathbf{286}$ of SO(13). The masses of these multiplets of resonances, before mixing with the elementary sector and EWSB, are denoted as M_q and M_u. Since both multiplets are in the same representation, an SO(13) invariant mass mixing term is allowed, whose coefficient we call M_y. By using the formalism of Sec. 3.2.1, it is also possible to write Yukawa interactions between these fermionic resonances and the NGBs, we call these couplings $y_{\mathbf{r}}$, they are of order g_*.

Below we describe a benchmark point of the parameter space, where the top and Higgs masses, as well as $v_{\rm SM}$, can be reproduced:

$$\begin{aligned}
&\epsilon_{q3} = 0.76\ , && \epsilon_{u3} = 0.97\ , && f = 1.63\ \text{TeV}\ ,\\
&y_{(\mathbf{6},\mathbf{3},\mathbf{1},\mathbf{1})} = -0.8\ , && y_{(\mathbf{6},\mathbf{1},\mathbf{3},\mathbf{1})} = -1.6\ , && y_{(\mathbf{6},\mathbf{1},\mathbf{1},\mathbf{3})} \sim -y_{(\mathbf{6},\mathbf{2},\mathbf{2},\mathbf{3})} \sim 1\ ,\\
&M_y = 4.6\ \text{TeV}\ , && M_q = 2.3\ \text{TeV}\ , && M_u = 1.7\ \text{TeV}\ .
\end{aligned} \tag{3.28}$$

The values of $y_{(\mathbf{6},\mathbf{1},\mathbf{1},\mathbf{3})}$ and $y_{(\mathbf{6},\mathbf{3},\mathbf{2},\mathbf{2})}$ are, either allowed to vary in an interval, or fixed to values of $\mathcal{O}(1)$, we specify their values for each analysis done below. The other Yukawa couplings do not play any role in the minimization of the potential, as long as Eq. (3.21) is satisfied. In the following sections they will be needed to determine, for example, the masses of the leptoquarks, we will give their values in those sections.

As an example of the form of the potential, in the left panel of Fig. 3.1 we show V as function of h/f and h_4/f for the benchmark point, with $y_{(\mathbf{6},\mathbf{1},\mathbf{1},\mathbf{3})} = 1.1$ and $y_{(\mathbf{6},\mathbf{3},\mathbf{2},\mathbf{2})} = -0.73$. The lines indicate the height of the potential, with lighter gray for the maxima and darker gray for the minima, located inside the closed-curves with label -0.2. The plot exhibits the symmetries of the potential.

Once the potential is minimized, fixing the value of v and v_4, on the right panel of Fig. 3.1 one can read the value of $v_{\rm SM}/f$.

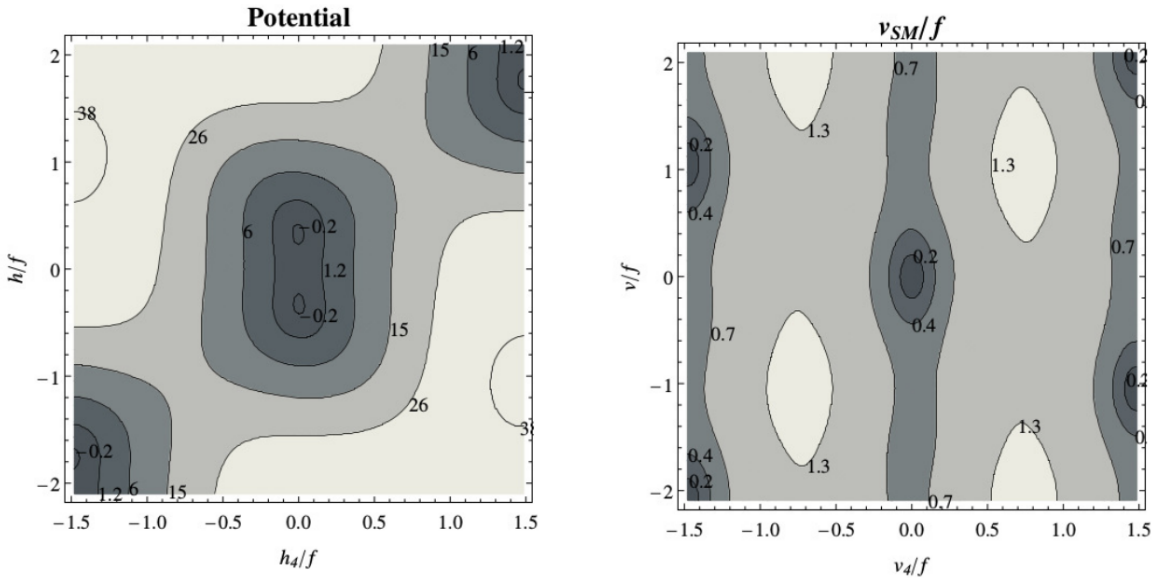

Figure 3.1: On the left we show a contour plot of the potential, lighter (darker) gray shows higher (lower) values of the potential, and the labels on the contours indicate the height of the potential. The small contours with label -0.2 contain the minima of the potential defining v and v_4. The parameters corresponding to this potential are defined by the benchmark point of Eq. (3.28) and $y_{(\mathbf{6},\mathbf{1},\mathbf{1},\mathbf{3})} = 1.1$ and $y_{(\mathbf{6},\mathbf{3},\mathbf{2},\mathbf{2})} = -0.73$. On the right we show contour lines of $v_{\rm SM}/f$ defined in Eq. (2.13).

In Fig. 3.2 we show several interesting predictions of the model for the benchmark point, with $y_{(\mathbf{6},\mathbf{1},\mathbf{1},\mathbf{3})} \in (0.2, 1.2)$ and $y_{(\mathbf{6},\mathbf{3},\mathbf{2},\mathbf{2})} \in (-0.95, -0.25)$. In the white region there is no EWSB, whereas in the gray area $v > 0$. The blue line shows the region where $v_{\rm SM}$ takes the value of the SM, whereas the orange and green lines correspond to the regions where the top and the Higgs have masses: $m_t \simeq 150$ GeV[7] and $m_h \simeq 125$ GeV. Around the region $y_{(\mathbf{6},\mathbf{1},\mathbf{1},\mathbf{3})} = 1$ and $y_{(\mathbf{6},\mathbf{3},\mathbf{2},\mathbf{2})} = 0.33$, $v_{\rm SM}$, m_t and m_h take simultaneously the values of the SM. The red lines show regions where m_{H_4}, defined in Eq. (3.15), has constant values. Up to effects of EWSB, these values give the mass of the components of H_4. The violet lines show constant regions for v_4/v, as can be seen it is $\mathcal{O}(10^{-3})$ in the region that looks like the SM, and it becomes $\mathcal{O}(10^{-2})$ below that region. As explained above, the masses of the leptoquarks are not shown in this plot, because they depend on a set of Yukawa couplings that have not been fixed yet, we discuss them in Sec. 3.4.

3.3.3. Tuning

As is well known, EW precision tests require a separation between v and f. Since generically the potential leads to no EWSB: $\xi = 0$, or maximal EWSB: $\xi \sim 1$, an amount of tuning of order ξ^{-1} is needed to obtain a separation between these scales.

[7] We are using $m_t \approx 150$ GeV as a reference value for the mass of the top quark at an energy scale $\mu \sim$ TeV [132, 133].

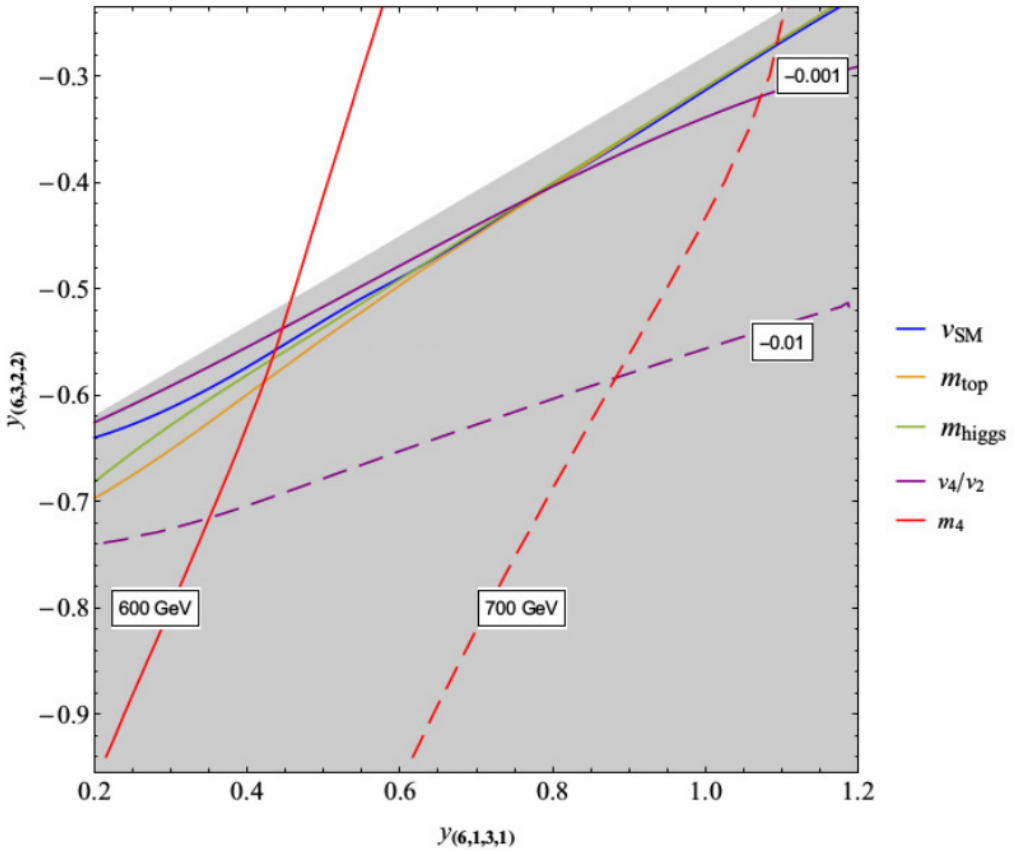

Figure 3.2: In gray and white we show the regions with and without EWSB in the plane $y_{(\mathbf{6},\mathbf{1},\mathbf{1},\mathbf{3})} - y_{(\mathbf{6},\mathbf{3},\mathbf{2},\mathbf{2})}$, with the other parameters fixed by the benchmark point described in Eq. (3.28). In the plot ξ increases from zero in the white region, to ~ 0.41 in the down-right corner, with $v_{\rm SM} = 246$ GeV along the blue line. In the orange and green lines $m_t \simeq 150$ GeV and $m_h \simeq 125$ GeV, respectively. The violet lines indicate constant values of v_4/v, whereas the red ones show constant values of m_{H4}.

In composite Higgs models with custodial symmetry, EW precision tests require $\xi \lesssim 0.1 - 0.3$, the bound being mainly dominated by the S parameter and $Zb_L\bar{b}_L$. In our model, as discussed in Sec. 3.1.3, v_4 breaks the custodial symmetry, and the fermion embedding chosen does not protect the $Zb_L\bar{b}_L$ coupling, therefore we expect more tuning, compared with composite Higgs models with custodial protection of g_{b_L}, to pass the EWPT.

We use the sensitivity parameter defined in Refs. [84, 134, 135], as an estimate of the fine tuning of the model. We study the dependence of the potential on the parameters of the theory: the masses of the fermionic resonances, the composite Yukawa couplings, the mass mixing the fermionic resonances and the decay constant of the NGBs, as well as the degree of compositeness of the light fermions: ϵ_f.

For the benchmark of Eq. (3.28) the estimated tuning is $\sim \xi^{-1} \simeq 40$. Calculating the tuning over the curve with $v_{SM} = 246$ GeV of Fig. 3.2, we find the tuning to vary between 40 and 90, diminishing as $y_{(\mathbf{6},\mathbf{3},\mathbf{1},\mathbf{3})}$ increases. If we explore higher values of this Yukawa, we find that the tuning can get as low as 25, when $y_{(\mathbf{6},\mathbf{3},\mathbf{1},\mathbf{3})} \sim 1.7$, and after

this increasing up to 200 as $y_{(\mathbf{6},\mathbf{3},\mathbf{1},\mathbf{3})} \sim 5$. It is dominated by ϵ_q and ϵ_u.

3.4. Phenomenology

In this section we compute the corrections to $Zb_L\bar{b}_L$ induced at tree level by the presence of the fermionic resonances, showing that they saturate the bounds for the benchmark region of the parameter space. We also discuss some properties of the pNGBs interesting for their phenomenology, as their masses and couplings. Finally, we analyze the effect of the leptoquarks on flavor physics, as the B-anomalies, $B \to K^{(*)\nu\bar{\nu}}$ and lepton flavor universality violation, and we briefly comment on constraints from colliders.

3.4.1. Corrections to Z couplings

As discussed in Sec. 3.1.3, the composite fermions mixing with the elementary b_L are not in the proper representation of the custodial symmetry to protect g_{b_L}. Describing the composite fermionic resonances with the two-site model defined in Ap. A.4, we have computed δg_{b_L} at tree level by the following procedure. We have considered only the multiplets associated to q and u of the third generation, there are ten down-type fermions in representation **286**. With this content of fermionic resonances, we have computed the mass matrix of the down-sector, in the elementary-composite basis. We have performed a diagonalization of the mass matrix expanding in powers of ξ, in fact only the lightest eigenstate is needed for the calculation of δg_{b_L}. Expressing the interactions with the Z in terms of the mass basis states, we obtained:

$$\begin{aligned}\frac{\delta g_{b_L}}{g/c_W} \simeq & \xi\lambda_{q3}^2 f^4 \left(24\{M_q^2 M_u^2 + f^2\lambda_{q3}^2[M_u^2 + (M_y + f y_{(\mathbf{6},\mathbf{3},\mathbf{2},\mathbf{2})})^2]\}\right)^{-1} \\ & \left[8y_{(\mathbf{6},\mathbf{3},\mathbf{1},\mathbf{1})}^2 + y_{(\mathbf{6},\mathbf{1},\mathbf{3},\mathbf{1})}^2 - 16 y_{(\mathbf{6},\mathbf{3},\mathbf{1},\mathbf{1})} y_{(\mathbf{6},\mathbf{3},\mathbf{2},\mathbf{2})} - 2 y_{(\mathbf{6},\mathbf{1},\mathbf{3},\mathbf{1})} y_{(\mathbf{6},\mathbf{3},\mathbf{2},\mathbf{2})}\right. \\ & \left. + 9(y_{(\mathbf{6},\mathbf{1},\mathbf{1},\mathbf{3})}^2 - 2 y_{(\mathbf{6},\mathbf{1},\mathbf{1},\mathbf{3})} y_{(\mathbf{6},\mathbf{3},\mathbf{2},\mathbf{2})} + 2 y_{(\mathbf{6},\mathbf{3},\mathbf{2},\mathbf{2})}^2)\right] + \mathcal{O}(\xi^2) \ . \end{aligned} \tag{3.29}$$

The full mass matrix depends on a set of Yukawa couplings that have not been fixed in the benchmark point. For numerical results we have varied these couplings randomly, with $|y_{\mathbf{r}}| \in (0.3, \pi)$. By comparison with the results obtained doing the full numerical diagonalization, we have verified that, for the region of the parameter space of Fig. 3.2, the accuracy of Eq. (3.29) is of percent level. For the region of Fig. 3.2 where $v_{\rm SM}$ is around the SM value, $\delta g_{b_L} \simeq (0.2 - 0.4)\,\%$, with the smallest value for smaller $y_{(\mathbf{6},\mathbf{1},\mathbf{1},\mathbf{3})}$, and increasing smoothly with this Yukawa.

In Sec. 3.1.3 we estimated, up to factors of $\mathcal{O}(1)$ that depend on the representations $\mathbf{R}_q$ and $\mathbf{R}_u$, $\delta g_{b_L} \sim \xi\epsilon_q^2$. For the benchmark point this leads to $\delta g_{b_L} \sim 1\,\%$. Doing the

calculation, we obtain that the Clebsch-Gordan coefficients, as well as the moderate values of the composite Yukawa, lead to an extra factor of order $0.2 - 0.4$. Therefore, for the benchmark region of Fig. 3.2, δg_{b_L} is of the order of the bound from precision measurements.

As we will discuss in Sec. 3.4.4, it is also interesting to consider the possibility of large degree of compositeness of τ_L. Eq. (3.10) shows that the lepton doublets are embedded in a $(\mathbf{2},\mathbf{2})_0$ of $\mathrm{SU}(2)_L\times\mathrm{SU}(2)_R\times\mathrm{U}(1)_X$, thus the $Z\tau_L\bar{\tau}_L$ coupling is protected by P_{LR} symmetry, allowing large ϵ_{l3} [101]. This is not the case of W-interactions, as will be discussed in 3.4.4. Besides it is not possible to protect $Z\nu\bar{\nu}$ simultaneously with $Z\tau_L\bar{\tau}_L$, thus we expect corrections in the Z coupling to neutrinos of the third generation, that will have an effect in the invisible width of the Z.

3.4.2. Masses of the pNGBs

Let us now discuss the spectrum of the pNGBs. For the minimum of Eq. (3.21), the masses of the leptoquarks and H_4 are estimated by the equation on the left of (3.20), in terms of the mass of a usual resonance: $m_\Pi \sim m_*(\epsilon_f g_*/4\pi)$, with $\Pi \neq H$. For $m_* \sim 2-10$ TeV, $\epsilon \sim 1$ and moderate values of $g_* \sim 2-5$, we expect: $m_\Pi \sim 0.4-3$ TeV.

After EWSB, the pNGBs with the same electric charge are mixed. Labeling the mass matrices with an index that indicates the electric charge of the states, for the color neutral scalars we obtain:

$$M_0^2 = \begin{pmatrix} m_H^2 + v^2\, 3c_1 & -v^2\frac{3}{4}c_6 & 0 \\ \dots & m_{H_4}^2 + v^2\left(\frac{c_4}{2} - \frac{c_5}{4\sqrt{10}} - \frac{2c_8}{\sqrt{10}}\right) & 0 \\ \dots & \dots & m_{H_4}^2 + v^2\left(\frac{c_4}{2} - \frac{c_5}{4\sqrt{10}} + \frac{2c_8}{\sqrt{10}}\right) \end{pmatrix} ,$$

$$M_1^2 = \begin{pmatrix} m_{H_4}^2 + \frac{v^2}{4}\left(2c_4 + c_5\frac{1}{\sqrt{10}}\right) & v^2\sqrt{\frac{3}{10}}c_8 \\ \dots & m_{H_4}^2 + \frac{v^2}{4}\left(2c_4 - c_5\frac{3}{\sqrt{10}}\right) \end{pmatrix} , \tag{3.30}$$

$$M_2^2 = m_{H_4}^2 + v^2\left(\frac{1}{2}c_4 + c_5\frac{3}{4\sqrt{10}}\right) , \tag{3.31}$$

whereas the leptoquark mass matrices are given by:

$$M^2_{2/3} = \begin{pmatrix} m^2_{\tilde{R}_2} + v^2\frac{\sqrt{2}c_{30}+c_{31}}{4} & -v\frac{m_1}{\sqrt{3}} \\ \dots & m^2_{S_3} - v^2\frac{2\sqrt{3}c_{34}-3c_{35}}{12} \end{pmatrix},$$

$$M^2_{-1/3} = \begin{pmatrix} m^2_{\tilde{R}_2} + v^2\frac{\sqrt{2}c_{30}-c_{31}}{4} & v\frac{-m_1}{\sqrt{6}} & -\frac{v^2}{2}c_{47} \\ \dots & m^2_{S_3} - v^2\frac{c_{34}}{2\sqrt{3}} & v\frac{m_2}{2\sqrt{3}} \\ \dots & \dots & m^2_{\hat{R}_2} + v^2\frac{\sqrt{2}c_{32}+c_{33}}{4} \end{pmatrix},$$

$$M^2_{-4/3} = \begin{pmatrix} m^2_{S_3} + v^2\frac{2\sqrt{3}c_{34}+3c_{35}}{12} & v\frac{m_2}{\sqrt{6}} \\ \dots & m^2_{\hat{R}_2} + v^2\frac{\sqrt{2}c_{32}-c_{33}}{4} \end{pmatrix}. \tag{3.32}$$

Since the mass matrices are symmetric, we have not written the elements of the left-down block. We use a superindex to denote the electric charge of each component of the scalars. From the diagonal elements of the mass matrices it is straightforward to identify the basis, as an example, for leptoquarks $S^{-4/3}$, the basis is: $\{S_3^{-4/3}, \hat{R}_2^{-4/3}\}$, whereas for the colorless neutral states, the basis is: $\{H, \mathrm{Re}[H_4^{(0)}], \mathrm{Im}[H_4^{(0)}]\}$. The coefficients m_i are the cubic couplings of the potential, Eq. (3.16), whereas c_i are the quartic ones, Eq. (3.17), thus they can be written in terms of integrals of the correlators, as detailed in Ap. A.2. Besides their size they can be estimated using Eq. (3.20).

Let us consider first an analytical study of the spectrum of scalars, and after that we present some numerical results. For the analysis of the spectrum of the neutral states, we trade $m_H^2 \to -c_1 v^2$ in M_0^2, as required from the minimization of the potential, Eq. (3.22), and we diagonalize M_0^2. The lightest neutral state, to be identified with the physical Higgs, has a mass: $m_0^2 \simeq 2c_1 v^2$, with corrections suppressed by powers of ξ. This state is to leading order given by the neutral component of the doublet H. To next order it mixes with the neutral states in H_4, with mixing angle $\frac{3c_6 v^2}{4m^2_{H_4}} \sim \xi$. The other neutral states receive corrections from the Higgs VEV: $m^2_{1,2} \simeq m^2_{H_4} + v^2\left(c_4\frac{1}{2} - c_5\frac{1}{4\sqrt{10}} \mp c_8\frac{2}{\sqrt{10}}\right)$, that induces a splitting between them. We have checked this approximation in the numeric analysis of the one-loop potential, performed to all orders in ξ.

The masses of the charged states also receive corrections from the Higgs VEV. The splitting of the states with charge $+1$ is of order $v^2\sqrt{\left(\frac{3}{16}c_5^2 + c_8^2\right)\frac{6}{5}}$.

The masses of the leptoquarks are corrected by the Higgs VEV as well, this induces splittings of order $\delta m^2_{LQ} \sim \mathcal{O}(c_j v^2)$. Since the non-diagonal terms of the mass matrices are of order v, instead of v^2 as for the colorless states, the mixing angles of the leptoquarks are $\mathcal{O}(\sqrt{\xi})$.

For a numerical study of the masses, we define two separate regions of the parameter space in terms of the benchmark region of Eq. (3.28) and the following Yukawa couplings:

Region	$y_{(\mathbf{6},\mathbf{3},\mathbf{2},\mathbf{2})}$	$y_{(\mathbf{15},\mathbf{3},\mathbf{1},\mathbf{1})}$	$y_{(\mathbf{15},\mathbf{1},\mathbf{2},\mathbf{2})}$	$y_{(\mathbf{1},\mathbf{1},\mathbf{2},\mathbf{2})}$	$y_{(\mathbf{1},\mathbf{3},\mathbf{2},\mathbf{2})}$	$y_{(\mathbf{1},\mathbf{3},\mathbf{3},\mathbf{1})}$	$y_{(\mathbf{1},\mathbf{3},\mathbf{1},\mathbf{3})}$
A	-1.51	-0.58	-1.08	-0.15	-1.36	-0.79	1.38
B	1.51	-0.63	-1.36	-0.72	-1.13	-1.23	-1.41

We show our results in Fig. 3.3, neglecting the effect of v. Region A on the left, and region B on the right, we do not take into account the effect of the Higgs VEV in those plots. For region A, the masses can vary quite abruptly, from order TeV to vanishing values. It is also possible to obtain negative squared masses, although in this case the quadratic coefficient is not the mass, and there can be breaking of $\mathrm{SU}(3)_c$. On the right we show a typical region where the masses acquire larger values, with positive squares.

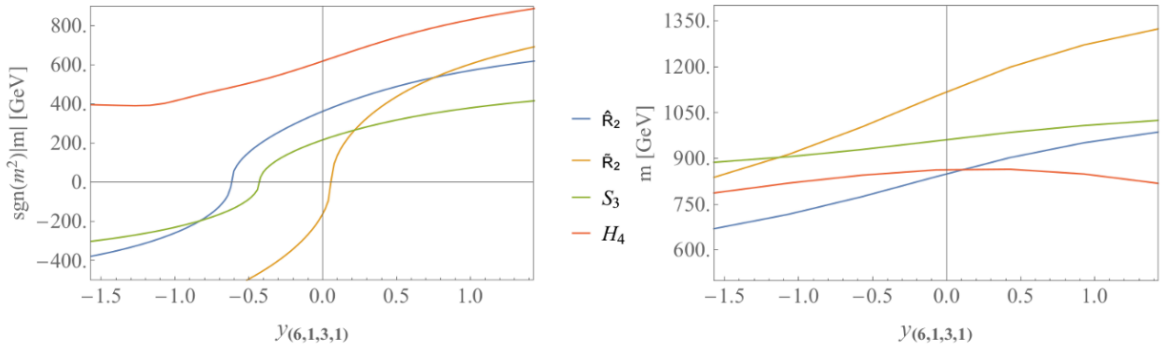

Figure 3.3: Plot of leptoquark masses along with m_4, for two different regimes. On the left frame, in a region where the masses squared become negative. We plot the absolute value of the mass, along with the sign of m^2. On the right frame we plot a region where leptoquark masses are all higher, reaching about a TeV.

We have also computed the effect of v. In region B there is no splitting since there is no EWSB, $v = 0$. In region A we calculated the splittings between components of each leptoquark multiplet. These splittings (with respect to the masses before EWSB) get as large as $\sim 20\,\%$ near $y_{(\mathbf{6},\mathbf{1},\mathbf{3},\mathbf{1})} \sim -1.5$, where the masses squared are negative. As this Yukawa increases and the masses become real, their splittings become lower. For S_3 they are lower than $1\,\%$, for $\tilde{R}_2$, around $2\,\%$, and for $\hat{R}_2$ around $3\,\%$.

By a random scan over all the Yukawa couplings in the interval $[-\pi/2, \pi/2]$, we find that the dominant Yukawas are $y_{(\mathbf{6},\mathbf{1},\mathbf{3},\mathbf{1})}$ and $y_{(\mathbf{6},\mathbf{3},\mathbf{2},\mathbf{2})}$.

3.4.3. Couplings of the leptoquarks

Other very important quantity for the phenomenology of the pNGBs, is their coupling with the SM fields. Expanding the effective Lagrangian for fermions, Eq. (2.24), in powers of the NGBs it is possible to obtain the Yukawa interactions with the fields H, H_4 and the leptoquarks. The flavor structure of the couplings is determined by the structure of the mixings ϵ_f, as well as by the anarchic structure of the SCFT. They

can be estimated similarly to Eq. (2.21) [90],

$$y_{ff'} \sim c_{ff'}\ g_*\ \epsilon_f\, \epsilon_{f'}\ , \tag{3.33}$$

where we are explicitly writing the dimensionless factors $c_{ff'} \sim \mathcal{O}(1)$.

Expanding the Lagrangian to first order in the leptoquarks and to second order in H, we obtain the following leptoquark interactions:

$$\begin{aligned}\mathcal{L}_{\rm int} \supset\ & y_3 S_3 \bar{q}_L^c l_L + \frac{1}{f} H (y_{3,1} S_3 \bar{q}_L e_R + y_{2,1} \tilde{R}_2 \bar{q}_L^c l_L + y_{3,2} S_3 \bar{d}_R l_L) \\ & + \frac{1}{f^2} H^2 (y_{3,3} S_3 \bar{q}_L^c l_L + y_{2,2} \tilde{R}_2 \bar{q}_L e_R + y_{3,4} S_3 \bar{d}_R^c e_R + y_{2,3} y \hat{R}_2 \bar{d}_R l_L) + \text{h.c.}\ , \end{aligned} \tag{3.34}$$

where flavor indices are understood. Due to the structure of the unbroken group H and the embedding of the quarks and leptons, only S_3 interacts with operators of dimension four. Interactions with $\hat{R}_2$ and $\tilde{R}_2$ are only present at the level of higher dimensional operators involving the Higgs. For this reason their effect in the phenomenology is suppressed compared with S_3, in particular the impact of $\tilde{R}_2$ in $R_K^{(*)}$ can be neglected.

The couplings of Eq. (3.34) can be expressed in terms of the fermionic correlators. A good approximation can be obtained by evaluating the correlators at zero momentum. We get:

$$y_3 = \frac{\Pi_{q,l}^{(1,3,2,2)}(0)}{\sqrt{Z_l + \Pi_{l,l}^{(1,3,2,2)}(0)}\sqrt{Z_q + \Pi_{q,q}^{(6,3,2,2)}(0)}} \tag{3.35}$$

The fact that y_3 depends on $\Pi_{q,l}^{(1,3,2,2)}$ only, can be understood from the following simple argument. The only way of contracting the dressed fields, when evaluating Eq. (2.24) at first order in the NGB fields, is by choosing either $\mathbf{r}_l = (\mathbf{1},\mathbf{3},\mathbf{2},\mathbf{2})$, or $\mathbf{r}_q = (\mathbf{6},\mathbf{3},\mathbf{2},\mathbf{2})$. However, only $\mathbf{r}_l$ is among the common H-representations in the decomposition of **78** and **286**. The denominator of Eq. (3.35) arises after canonical normalization of the fermion fields.

The couplings of Eq. (3.34) are not expected to be aligned in flavor space. This happens because different correlators depend on different combinations of composite Yukawa couplings that, having uncorrelated flavor structures, lead to couplings with the SM fields that are not aligned. A full numerical calculation of them would require the introduction of three generations of composite resonances, as well as elementary fermions. We have chosen not to do that calculation in the present work, which would have increased the number of parameters required for the numerical computations, choosing instead to use the estimates of Eq. (3.33) in the following.

3.4.4. Analysis of flavor physics

As it has been discussed in Sec. 2.2.1, in partial compositeness the flavor violating processes mediated by composite resonances are suppressed by the same small mixings that generate the hierarchical spectrum of SM fermions and mixing angles. In the present section we will not make a detailed analysis of those bounds. Instead we will focus on some of the most important effects of the leptoquarks on flavor transitions and lepton flavor universality violation, discussing their effect in the B-anomalies, as well as the largest constraints. Since the interactions with $\tilde{R}_2$ and and $\hat{R}_2$ are suppressed by positive powers of ξ, we only consider the effects from S_3. In the following we will make extensive use of the bounds presented in Ref. [60], as well as what was presented in Sec. 2.3.

At low energies the leptoquarks can be integrated out at tree-level, leading to the following effective Lagrangian

$$\mathcal{L}_{\text{eff}} \supset \frac{C}{v^2}[(\bar{q}_L\gamma^\mu\sigma^a q_L)(\bar{l}_L\gamma_\mu\sigma^a l_L) + 3(\bar{q}_L\gamma^\mu q_L)(\bar{l}_L\gamma_\mu l_L)] \ , \tag{3.36}$$

where generation indices are understood. The dimensionless coefficient C is given by [8]

$$C^{ijmn} = y_{3,in}y^*_{3,jm}\frac{v^2}{4m^2_{S_3}} \sim c_{in}c^*_{jm}\epsilon_{qi}\epsilon_{qj}\epsilon_{lm}\epsilon_{ln}\frac{g^2_* v^2}{4m^2_{S_3}} \ . \tag{3.37}$$

The effective Lagrangian in Eq. (3.36) gives contributions to coefficients g_{V_L} in Eq. (2.103), as well as $\Delta C^9 = -\Delta C^{10}$ of operators in Eq. (2.107). It is necessary to analyze the size of these couplings and whether they can accommodate the anomalies in $R_{K^{(*)}}$ and $R_{D^{(*)}}$ in our present model.

B-anomalies

It is well known that for suitable values of the leptoquark Yukawa couplings, an S_3 at the TeV scale can explain the deviations in R_K and R_{K^*}. Following Ref. [60], a global fit of $b \to s\mu\mu$ (neglecting effects in ee) gives:[9]

$$\Delta C^\mu_9 = -\Delta C^\mu_{10} = \frac{4\pi}{\alpha_{\text{em}}V_{tb}V^*_{ts}}C^{2322} = -0.61 \pm 0.12 \ . \tag{3.38}$$

By making use of the structure of APC, Eqs. (2.63-2.65), along with Eqs. (3.36) and (3.38), in our model we obtain:

$$g_*^{3/2} f \sim 4 \text{ TeV} \ , \tag{3.39}$$

[8] For comparison with the literature: $C_T = -C^{3333}$ and $C_S = -3C^{3333}$, minus the coefficients of the current-triplet and -singlet when all the fermions are in the third generation.

[9] Note this is a fit using older data than that presented in Sec. 2.3. The analysis, however, does not change considerably when using a more recent bound.

up to factors of $\mathcal{O}(1)$. This equation fits nicely with $f \sim$ TeV and moderate values of g_*.

We can now briefly comment on the anomalies on $R_{D^{(*)}} \equiv R^{\tau\ell}_{b\to c}$. The Lagrangian of Eq. (3.36) gives a symmetric contribution to both R_D and R_{D^*}:

$$R_{D^{(*)}} \simeq 1 + 2\sum_j C^{3j33}\frac{V_{cj}}{V_{cb}} \tag{3.40}$$

and we can use the average value from Eq. (2.102).

Again, we are making use of Eqs. (2.63-2.65), (3.36) and (3.40), but this time we keep the dependence on ϵ_{l3}. Eq. (3.40) and Eq. (2.102) require

$$\frac{g_* f}{\epsilon_{l3}} \sim 7.5 \text{ TeV} , \tag{3.41}$$

From Eqs. (3.39) and (3.41), we obtain that, in order to simultaneously explain $R_{K^{(*)}}$ and $R_{D^{(*)}}$: $\sqrt{g_*}\epsilon_{l3} \sim 0.5$. One must compare this result with the estimate for the τ-Higgs Yukawa coupling in the case of $\epsilon_{li} = \epsilon_{ei}$, Eq. (2.66), that gives $\sqrt{g_*}\epsilon_{l3} \sim 0.08$. Thus, in order to explain $R_{D^{(*)}}$, one has to abandon the assumption of similar degree of compositeness of both chiralities of the τ, and consider instead the case $\epsilon_{e3}/\epsilon_{l3} \sim 0.04$. In this case, although $Z\tau_L\bar{\tau}_L$ is protected, large ϵ_{l3} induces corrections in the W couplings with the τ lepton [60]. In the next section we will show that the bounds from precision measurement of this coupling do not allow to fit $R_{D^{(*)}}$.

Constraints from τ decays and $B \to K^{(*)}\nu\bar{\nu}$

In the present scenario the tightest bounds in flavor physics arise from flavor universality violation in τ decays. $B \to K^{(*)}\nu\bar{\nu}$ is also a good process to look for effects of the leptoquarks, since neutrinos of third generation can potentially give large contributions. We will not perform a full analysis of flavor observables, instead we will analyze these two processes in the presence of the low energy effective interactions of Eq. (3.36).

One-loop corrections to the W coupling in the presence of leptoquarks give:[60, 136]

$$\left|\frac{g_{W\tau}}{g_{W\ell}}\right| = 1 - \frac{6y_t^2}{(4\pi)^2}C^{3333}\log\frac{\Lambda}{m_t} \simeq 1 - 0.084C^{3333} , \tag{3.42}$$

where Λ has been fixed to 2 TeV. Departures of this coupling from lepton flavor universality cannot be larger than per mil level. Making use of Eqs. (2.64), (2.65), (3.36) and (3.42), and leaving the dependence on ϵ_{l3}, we obtain:

$$\frac{g_* f}{\epsilon_{l3}} \gtrsim 28 \text{ TeV} . \tag{3.43}$$

Using Eq. (3.39) in (3.43), we obtain: $\sqrt{g_*}\epsilon_{l3} \lesssim 0.15$, that can be easily satisfied for $\epsilon_{l3} \simeq \epsilon_{e3}$, but is smaller than the value needed to fit $R_{D^{(*)}}$.

The 95 %CL bound on $B \to K^{(*)}\nu\bar{\nu}$ [60, 137] in our model can be approximated by:

$$B_{K^{(*)}\nu\bar{\nu}} \simeq \frac{1}{3}\left[2 + \left|1 + \frac{2\pi}{\alpha_{\rm em}}\frac{C^{3233}}{C_\nu^{\rm SM} V_{ts}^* V_{tb}}\right|^2\right] < 5.2 \ , \tag{3.44}$$

where $B_{K^{(*)}\nu\bar{\nu}} \equiv {\rm Br}(B \to K^{(*)}\nu\bar{\nu})_{\rm exp}/{\rm Br}(B \to K^{(*)}\nu\bar{\nu})_{\rm SM}$ and $C_\nu^{\rm SM} = -6.4$. Making use of Eqs. (2.64), (2.65), (3.36) and (3.44), and keeping ϵ_{l3}, we obtain:

$$\frac{g_* f}{\epsilon_{l3}} \gtrsim 17 - 22 \text{ TeV} \ , \tag{3.45}$$

depending on the complex phase of the correction. Using Eq. (3.39) in (3.45), we obtain: $\sqrt{g_*}\epsilon_{l3} \lesssim 0.2 - 0.25$, again compatible with $\epsilon_{l3} \simeq \epsilon_{e3}$, but smaller than the value needed to fit $R_{D^{(*)}}$.

3.4.5. Collider physics

We discuss very briefly constraints of our model at colliders, and we mention some interesting signals.

Direct searches of new physics also give constraints, the most important ones from leptoquark pair production by QCD interactions at LHC. Different analyses of the collected data give bounds on scalar leptoquark masses that are roughly of order 1 TeV [62, 138–140], to be compared with the predictions for these masses in the present model, that are $\sim 0.4 - 1.2$ TeV, for $f \sim 1.6$ TeV.

Other production processes are: single production, that has been studied, for example, in Refs. [60, 138], and non-resonant production, that can be found in [141]. Single and non-resonant leptoquark production at LHC are more model dependent, since they depend on the leptoquark Yukawa couplings with the SM fermions, that are not fixed. The framework of partial compositeness gives an estimate of the size of these couplings. These processes, with couplings compatible with partial compositeness, become competitive for leptoquarks masses larger than $1 - 1.5$ TeV.

In the present case, with larger couplings to quarks and leptons of the third generation, one can expect interesting phenomena associated with top and bottom quark production, as well as tau leptons. Final states with muon leptons are also interesting, due to the cleaner final state. In all cases, the promising channels are those with multi-leptons in the final state. We refer the reader to the references of the previous paragraphs of this section, and references therein, for detailed analysis of the collider phenomenology.

Another very interesting signal at colliders is the creation of fermionic resonan-

ces. As usual in models with extended global symmetries and partial compositeness, there are custodians with masses that can be lighter than m_*. In our model, for the benchmark region of the parameter space, we find colored states with exotic charges ($Q = 5/3, -4/3$) and masses of order 1 TeV. There are also color octets and sextets, as can be seen in Ap. A.1, that can be created in pairs by QCD interactions. A study of their phenomenology is beyond the scope of this work.

3.5. Summary and discussion

The B-anomalies are one of the most exciting phenomena reported by experiments in the last years. Leptoquarks at the TeV scale could be responsible for them. In the present Chapter we have given an effective description of a new strongly interacting sector at the TeV scale, that contains leptoquarks and Higgses as NGBs. The global symmetry group was chosen as the minimal simple group containing the SM plus the custodial symmetry, and able to deliver the Higgs and a leptoquark S_3 as NGBs. Given the pattern of global symmetry breaking, the content of leptoquarks and Higgses was fixed, in our case, besides the Higgs, a colorless $\mathrm{SU}(2)_L$-fourplet and three leptoquarks were present: an $S_3 \sim (\bar{\mathbf{3}}, \mathbf{3})_{1/3}$, as well as two EW doublets transforming as $(\bar{\mathbf{3}}, \mathbf{2})_{1/6}$ and $(\bar{\mathbf{3}}, \mathbf{2})_{-5/6}$. The assumption of anarchic partial compositeness of the SM fermions, as well as the choice of the representations of the fermionic resonances under the global symmetry, determined the structure of Yukawa couplings and the structure of the potential. We have shown that the interactions with the SM fermions can trigger EWSB successfully, and generate leptoquarks masses of order TeV. By modeling the resonances of the SCFT with a two-site theory, we have computed the one-loop potential and the spectrum of pNGBs. We have found a benchmark region of the parameter space where the masses of the SM states, the Ws, the top and Higgs, are around their experimental values, and the pNGBs have masses of order $0.4 - 1.3$ TeV, with a NGB decay constant $f = 1.6$ TeV.

Some amount of tuning is needed to obtain a separation between the EW scale and the NGB decay constant, that characterizes the scale of the SCFT. We found that, for the benchmark region analyzed, the tuning is dominated by the degree of compositeness of the quarks of the third generation, varying between 40 and 90 for $v_{\mathrm{SM}} \simeq 246$ GeV. Those values are compatible with the estimate given by $\xi^{-1} \simeq 40$.

We have analyzed several constraints, as the corrections to the ρ parameter due to the VEV of the colorless fourplet, and the Z-couplings. We have shown that the VEV of H_4 is suppressed by ξ, in agreement with the results of Ref. [130]. For the benchmark region of the parameter space where $v_{\mathrm{SM}} \simeq 246$ GeV we obtained: $v_4/v \sim \mathcal{O}(10^{-3})$, allowing to pass constraints from the ρ parameter. For the Z-couplings, since the resonances that mix with b_L were embedded in a representation of the custodial symmetry

that does not allow to protect $Zb_L\bar{b}_L$, there could be large corrections. For the benchmark region of the parameter space we obtained $\delta g_{b_L}/g \simeq 0.2 - 0.4\,\%$, saturating the bound from precision measurements. Tighter bounds would require, either a larger tuning, or a larger representation of the fermionic resonances, allowing custodial protection of g_{b_L}, as in the case of the SO(13) representation $\mathcal{R}_q = \overline{\mathbf{715}}$. Thus within the present model, and for $f \sim 1.3 - 2$ TeV, deviations of order few per mil can be expected.

As discussed in Refs. [60, 61, 72], the presence of an additional leptoquark in the representation $(\bar{\mathbf{3}}, \mathbf{1})_{1/3}$, with a mass similar to that of S_3 and couplings with the same flavor structure, would allow to explain simultaneously $R_{K^{(*)}}$ and $R_{D^{(*)}}$, without too large corrections to flavor processes (as violation of lepton flavor universality in W coupling to τ, or in flavor changing neutral current decays as $B \to K\nu\bar{\nu}$). Also a new leptoquark in $(\bar{\mathbf{3}}, \mathbf{2})_{7/6}$ could be a possibility. [142] It is straightforward to include states with these charges in the present model, but not as NGBs, instead they would be ordinary resonances, with larger masses. In this case, it is not possible in general to satisfy bounds from flavor physics (fine tuning would be needed to ensure, for example, a partial cancellation of the Wilson coefficients of dangerous operators). An interesting possibility would be to find a simple group able to generate these states also as NGBs, as well as embeddings of the SM fermions leading to the right Yukawa couplings.

In the next Chapter we will study a model with a vector LQ from a composite model, capable of simultaneously addressing both B-anomalies, as Table. 1.2 suggests. A model involving leptoquark S_1 along with S_3 as pNGBs will be instead considered in Chapter 5.

Chapter 4

A model with vector leptoquark U_1

In this Chapter we will look at a different approach for explaining the hints of lepton flavor universality violation in B-meson decays. Just as in Ch. 3, we are interested in a composite Higgs model which has the ability to solve the hierarchy problem present in the SM, and which also involves leptoquarks at the TeV scale. However, instead of including a scalar leptoquark as in the case of S_3, we are interested in having a spin-1 LQ, which is known in the literature as U_1, and transforms as $(\mathbf{3},\mathbf{1})_{2/3}$ under the SM gauge group. This leptoquark, when coupled preferentially to fermions of the third generation, can offer a combined explanation of both neutral and charged current B-decays. The preferred solutions involve mainly Left-handed couplings to the SM quarks, with suppressed Right-handed couplings, and a mass of order few TeV. As $R_{D^{(*)}}$ requires a large mixing for τ_L, the resulting Right-handed mixings are suppressed by the ratio of charged lepton mass over the Higgs vacuum expectation value, giving very small Right handed couplings with U_1. Thus anarchic partial compositeness gives, as a very good approximation, interactions of U_1 with Left-handed currents and negligible interactions with Right handed currents, without any additional hypotheses

We are once again interested in a Composite Grand Unified Theory which is able to deliver this vector LQ in its spectrum, along with the Higgs as a pseudo Nambu Goldstone Boson. However, we are not interested in precise gauge coupling unification, being guided by the low energy phenomenology instead.

An effective weakly coupled description of the above dynamics can be obtained by working with a theory of resonances. We will consider a three-site theory, with the first site describing the elementary sector and the other two sites describing resonances of the SCFT. In this case the one-loop potential of the NGBs is finite and can be calculated explicitly, as well as the spectrum of new states and their couplings, leading to well defined predictions. We will show that composite GUTs can simultaneously explain the B-anomalies and stabilize the Higgs potential. Besides, due to the large degree of compositeness required for τ_L, the third generation of Left-handed leptons

plays an important role in the potential. This situation was considered in Ref. [143], although in a different context.

This Chapter is organized as follows: in Sec. 4.1 we show a composite GUT containing the usual ingredients of composite Higgs models, as well as a vector leptoquark for the B-anomalies. We describe the coset structure of the SCFT, the content of NGBs, the fermionic representations and flavor structure, as well as some important bounds and estimates associated to B-physics, as $R_{D^{(*)}}$ and $R_{K^{(*)}}$. In the same section we present the effective low energy physics obtained after integration of the massive resonances of the SCFT, whose structure depends only on the pattern of symmetries, and the one-loop potential of the NGBs. In Sec. 4.2 we present an effective description of the resonances of the SCFT in terms of a three-site model. In Sec. 4.3 we describe the phenomenology of the theory, we scan the parameter space finding regions with EWSB and we compute the spectrum of new particles. We also calculate the corrections to several observables, comparing them with the present bounds, as well as the corrections to flavor quantities as $R_{D^{(*)}}$. We comment very briefly on the phenomenology of the new pseudo Nambu Goldstone boson (pNGB) states. Finally, we end with a summary of the results and some discussion in Sec. 4.4.

4.1. A Composite GUT for the B-anomalies

We follow the basic idea of Sec. 2.1 and as described in the model of Ch. 3. We consider a theory with two different sectors: an SCFT or composite sector and another sector called elementary that is weakly coupled with the SCFT. The SCFT is assumed to have a simple global symmetry group G, spontaneously broken by the strong dynamics to a subgroup H. This breaking generates a set of NGBs associated to the broken generators of the coset G/H. Some of these NGBs will be identified as a composite Higgs. The conserved Noether currents of the SCFT can create resonances of spin one, transforming with the adjoint representation of G. Besides, we also assume that there are fermionic operators $\mathcal{O}^{\rm SCFT}$ that can create spin 1/2 resonances, transforming with linear irreducible representations of G. These representations are not fixed a priori, leading to some freedom for model building. The masses of the first level of resonances, collectively denoted as m_*, are taken of order few TeV, whereas the interactions between them are characterized by a single coupling g_*, taken as: $g_{\rm SM} \ll g_* \ll 4\pi$, thus for simplicity we assume that all the couplings between resonances are of the same order. The NGB decay constant is $f = m_*/g_*$, of order TeV.

The main difference with the model studied in Ch. 3 is the scale of the composite sector: as the U_1 LQ is now a vector resonance of mass m_*, which in order to properly explain deviations in $R_{K^{(*)}}$ and $R_{D^{(*)}}$ needs to be of order TeV, there is no longer a mass gap with respect to the other resonances of the theory. This in turn will be in

tension with certain constraints, as shown in Sec. 2.2.1, that push the mass scale m_* to $\mathcal{O}(10)$ TeV.

4.1.1. Coset structure

Let us briefly discuss the reasoning behind the choice of symmetry groups in the model. We have found that SO(11)/SO(10) is the minimal coset of simple groups with the following properties: it contains the SM gauge symmetry group as well as custodial symmetry, it delivers a Higgs as a pNGB and, after proper identification of hypercharge, it contains a composite spin one state that has the proper quantum numbers to be identified with the U_1 leptoquark. [1] However, since in this case U_1 is associated to a broken generator, it is heavier than, for example, W' and Z' resonances, resulting in a suppressed effect in $R_{K^{(*)}}$ and $R_{D^{(*)}}$, that are proportional to $m_{U_1}^{-2}$, and thus cannot be accommodated. For this reason, we will consider instead a larger coset: SO(12)/SO(11), such that U_1 can be associated with an unbroken generator. Let us discuss the coset structure in some detail.

We start by describing some features of the unbroken group. SO(11) contains SO(10) that, as is well known from the study of GUTs, can accommodate a Left-Right symmetric extension of the SM gauge group. A possible pattern of subgroups that allows to see this property is:

$$\mathrm{SO}(11) \to \mathrm{SO}(10) \to \mathrm{SO}(6)\times\mathrm{SO}(4) \to \mathrm{SU}(3)_c \times \mathrm{SU}(2)_L \times \mathrm{SU}(2)_R \times \mathrm{U}(1)_X \equiv \mathrm{H}_{\mathrm{min}} \ , \tag{4.1}$$

with SO(6)$\sim$SU(4)$\supset SU(3)\times$U(1) and SO(4)$\sim$SU(2)$\times$SU(2). Besides, we identify hypercharge with the following combination:

$$Y \equiv T^{3R} + \frac{4}{\sqrt{6}} T^X \ . \tag{4.2}$$

The set of broken generators in the coset SO(12)/SO(11) transform, under SO(11), with the representation **11**. Under SO(10) and $\mathrm{H}_{\mathrm{min}}$ the representation **11** decomposes as:

$$\mathbf{11} \sim \mathbf{1} \oplus \mathbf{10} \sim (\mathbf{1},\mathbf{1},\mathbf{1})_{\mathbf{0}} \oplus (\mathbf{1},\mathbf{2},\mathbf{2})_{\mathbf{0}} \oplus (\bar{\mathbf{3}},\mathbf{1},\mathbf{1})_{-\mathbf{1}/\sqrt{\mathbf{6}}} \oplus \text{c.c.} \ , \tag{4.3}$$

where $\oplus$ c.c. means that, for the complex representations as the color triplet, one has to add the charge conjugate one. Eq. (4.3) shows the transformation properties of the NGBs, those associated to the colorless generators lead to two multiplets: a SM singlet that we call φ and the Higgs field H, whereas the ones associated to the color triplet lead to a leptoquark usually called $\bar{S}_1$ in the literature.

[1] The first two properties were already shown in Ref. [144], the last one, as far as we know, has not been considered before.

The currents of the SCFT associated to the global symmetry SO(12) can create spin one states that transform with the adjoint representation **66**, that under SO(11) decomposes as: $\mathbf{66} \sim \mathbf{55} \oplus \mathbf{11}$. We have shown in Eq. (4.3) the decomposition of **11**, the representation **55** decomposes under SO(10) and $\mathrm{H}_{\mathrm{min}}$ as:

$$\begin{aligned}\mathbf{55} \sim & \mathbf{45} \oplus \mathbf{10} \\ \sim & (\mathbf{8},\mathbf{1},\mathbf{1})_0 \oplus (\mathbf{1},\mathbf{3},\mathbf{1})_0 \oplus (\mathbf{1},\mathbf{1},\mathbf{3})_0 \oplus (\mathbf{1},\mathbf{1},\mathbf{1})_0 \oplus (\mathbf{3},\mathbf{1},\mathbf{1})_{-2/\sqrt{6}} \oplus (\mathbf{3},\mathbf{2},\mathbf{2})_{1/\sqrt{6}} \\ & \oplus (\mathbf{1},\mathbf{2},\mathbf{2})_0 \oplus (\mathbf{3},\mathbf{1},\mathbf{1})_{1/\sqrt{6}} \oplus \text{c.c.} \ . \end{aligned} \tag{4.4}$$

where the first line contains the decomposition of the **45**, and the second one of the **10**. With the identification of hypercharge of Eq. (4.2), the multiplets $(\mathbf{3},\mathbf{1},\mathbf{1})_{1/\sqrt{6}} \oplus \text{c.c.}$ contained in the **10** of **55** and **11** can be identified with U_1 leptoquarks. The leptoquark in **55** is associated to an unbroken generator, whereas the leptoquark in **11** is associated to a broken one, thus the former results lighter than the latter.

Besides U_1, there is another spin one leptoquark: $\tilde{V}_2 \sim (\mathbf{3},\mathbf{2})_{1/6}$, as well as two new states transforming as: $(\mathbf{3},\mathbf{2})_{7/6}$ and $(\mathbf{3},\mathbf{1})_{-4/3}$. In generic leptoquark models $\tilde{V}_2$ can induce baryon decay, however, as we will show in Sec. 4.1.4, the present model has a global $\mathrm{U}(1)_B$ that forbids proton decay. The other two states do not have dimension-four operators with SM fermions.

It is also possible to choose other identifications of hypercharge, as $Y \equiv T^{3R} - 2T^X/\sqrt{6}$, that allow to embed U_1 in $(\mathbf{3},\mathbf{1},\mathbf{1})_{-2/\sqrt{6}} \oplus \text{c.c.}$. However in this case the NGB leptoquark is an S_1, giving contributions to B-physics that can destabilize the U_1 solution.

We will add a discrete Z_2-symmetry, that corresponds to a parity and enlarges SO(12) to O(12). We are interested in the transformation under which broken and unbroken generators are, respectively, odd and even under this parity, leading to odd NGBs. In the basis defined in Ap. B.1, for the representation **12** this parity can be written in terms of a 12×12 matrix as: $P_{ij} = \delta_{ij} - 2\delta_{i12}\delta_{j12}$. As we will show, the presence of P will lead to several simplifications as well as a candidate for dark matter.

4.1.2. Fermions

The operators $\mathcal{O}^{\mathrm{SCFT}}$ that interact linearly with the SM fermions can be decomposed under G_{SM} as sums of irreducible representations. To avoid explicit breaking of G_{SM}, these decompositions must contain the representations of the SM fermions. Given Eq. (4.2), partners of the SM fermions can be found in the following representations of SO(10):

$$u, l \subset \mathbf{10} \ , \qquad q, e \subset \mathbf{45} \ , \qquad q, d, l \subset \mathbf{120} \ . \tag{4.5}$$

A Right-handed neutrino can be embedded in a singlet or in the adjoint representation of SO(10). Larger representations are also possible. The representations of Eq. (4.5) can be embedded in representations of SO(12), we are interested in the following:

$$\begin{aligned} \mathbf{66} &\sim \mathbf{55} \oplus \mathbf{11} \sim (\mathbf{45} \oplus \mathbf{10'}) \oplus (\mathbf{10} \oplus \mathbf{1}) \ , \\ \mathbf{220} &\sim \mathbf{165} \oplus \mathbf{55} \sim (\mathbf{120} \oplus \mathbf{45'}) \oplus (\mathbf{45} \oplus \mathbf{10'}) \end{aligned} \tag{4.6}$$

where we have shown the decompositions under SO(11) and SO(10). We have used the marks to distinguish SO(10) representations that arise from the decomposition of different representations of SO(11).

In order to obtain interactions between all the SM fermions and the SCFT, we will consider that the following operators are present: $\mathcal{O}^{\rm SCFT}_{\mathbf{66}}$ and $\mathcal{O}^{\rm SCFT}_{\mathbf{220}}$. Each elementary fermion can interact with more than one SCFT operator, for example q can interact with $\mathcal{O}^{\rm SCFT}_{\mathbf{66}}$ and $\mathcal{O}^{\rm SCFT}_{\mathbf{220}}$, however we will assume that the SCFT operators have different anomalous dimensions, such that one of the interactions dominates over the other (see Sec. 4.1.3), and as a simplification of this situation we will consider that each elementary fermion interacts just with one $\mathcal{O}^{\rm SCFT}$. In particular, as shown in Table 4.1, we assume that q, u and l interact with $\mathcal{O}^{\rm SCFT}_{\mathbf{66}}$ only, whereas d and e interact with $\mathcal{O}^{\rm SCFT}_{\mathbf{220}}$. Besides, from Eqs. (4.5) and (4.6) one can see that the elementary fermions u and l can interact with several components of $\mathcal{O}^{\rm SCFT}_{\mathbf{66}}$: either with the $\mathbf{10} \subset \mathbf{11}$ or with the $\mathbf{10'} \subset \mathbf{55}$. The parity P can distinguish between both **10**s inside **66**: $\mathbf{10'}$ is even and **10** is odd, thus if we assign a well defined parity to the elementary fermions, P is conserved and the elementary fermions u and l interact only with one multiplet of SO(11) in $\mathcal{O}^{\rm SCFT}_{\mathbf{66}}$. In the following we will assign the parities of Table 4.1 to the elementary fermions, and we will mix them with the components of the SCFT operators shown in that table.

Field	P	SO(12)	SO(11)	SO(10)	$\mathrm{H}_{\rm min}$
q	+	**66**	**55**	**45**	$(\mathbf{3},\mathbf{2},\mathbf{2})_{1/\sqrt{6}}$
l	+	**66**	**55**	**45**	$(\mathbf{1},\mathbf{2},\mathbf{2})_{0}$
u	-	**66**	**11**	**10**	$(\mathbf{3},\mathbf{1},\mathbf{1})_{1/\sqrt{6}}$
d	-	**220**	**165**	**120**	$(\mathbf{3},\mathbf{1},\mathbf{3})_{1/\sqrt{6}}$
e	-	**220**	**165**	**45'**	$(\mathbf{1},\mathbf{1},\mathbf{3})_{0}$
H	-	×	**11**	**10**	$(\mathbf{1},\mathbf{2},\mathbf{2})_{0}$
$\bar{S}_1$	-	×	**11**	**10**	$(\bar{\mathbf{3}},\mathbf{1},\mathbf{1})_{-1/\sqrt{6}}$
φ	-	×	**11**	**1**	$(\mathbf{1},\mathbf{1},\mathbf{1})_{0}$

Table 4.1: Embedding of the composite partners of the elementary fermions, from SO(12) down to $\mathrm{H}_{\rm min}$. In the last three lines of the table we show the NGBs that transform with the fundamental representation of SO(11).

It is also interesting to consider the scenario without P, we will briefly comment on the consequences of this assumption in Sec. 4.3.5.

Let us now describe the interactions between the elementary fermions and the Higgs. As described in Sec. 2.1.1, since bilinear interactions with the Higgs have been assumed to be suppressed, the interactions with the Higgs are mediated by the linear interactions of Eq. (2.15). The resonances of the SCFT interact with the composite Higgs and Eq. (2.15) leads to Yukawa interactions of the elementary fermions. The SCFT has a global unbroken symmetry SO(11), thus in order to obtain the proper Yukawa interactions of the SM, the interactions between the resonances containing the partners of the SM fermions and the Higgs must be SO(11)-invariant. For the up-type quarks, from the embeddings of Table 4.1: $\mathbf{55} \times \mathbf{11} \sim \mathbf{11} \oplus \mathbf{165} \oplus \mathbf{429}$, whereas for the down-type quarks and the charged leptons: $\mathbf{55} \times \mathbf{165} \sim \mathbf{11} \oplus \ldots$, thus our choice is compatible with the Higgs embedded in an $\mathbf{11}$, and P-symmetry is respected by Yukawa interactions.

Usually the SM fermions are embedded in the representation $\mathbf{32}$ of SO(11), however in order to do that one has to take a different identification of hypercharge [144]. It is also possible to take other representations, as $\mathbf{12}$, that contains l and u, both P-odd, but for simplicity we will not consider them.

4.1.3. Partial compositeness and flavor structure

The flavor structure of the model is given by the prescription given in Sec. 2.2. Quark masses and mixings are reproduced by the pattern given by Eqs. (2.63), and (2.64), whereas in the case of leptons only the product of Left- and Right-handed compositeness are fixed, as in Eq. (2.65) and the remaining freedom can only be fixed after a choice of the specific nature and realization of the neutrino masses. As we will show in Sec. 4.1.5, in the present scenario the B-anomalies can be fitted with a hierarchical mixing of the Left-handed leptons: $\epsilon_{l1} \ll \epsilon_{l2} \ll \epsilon_{l3}$. We will also show in that section that, for the given values of ϵ_{li}, the mixings of the Right-handed charged leptons are also hierarchical: $\epsilon_{e1} \ll \epsilon_{e2} \ll \epsilon_{e3}$, and besides, at least for the second and third generations, they are smaller than the corresponding Left-handed ones: $\epsilon_{e2} \ll \epsilon_{l2}$ and $\epsilon_{e3} \ll \epsilon_{l3}$. This is a departure from Eq. (2.66) regarding a Left-Right symmetric scheme for the leptons, as was also the case in Ch. 3. As these hierarchical mixings give small mixing angles for the matrices diagonalizing the charged mass matrix, the large angles in the PMNS must be generated in the neutrino sector. We assume this to be the case and do not elaborate further.

Let us now look at the interactions with the spin one resonances. They have a flavor structure which is similar to the Higgs Yukawa couplings, except that in this case the factor g_* is universal, due to the global symmetry of the SCFT, thus generically they

are misaligned with the Yukawa couplings. The interactions with U_1 leptoquarks are of special interest for our analysis:

$$\mathcal{L} \supset g^{(n)}_{Ljk}\bar{q}^j_L\gamma^\mu U^{(n)}_{1\mu} l^k_L \; + g^{(n)}_{Rjk}\bar{d}^j_R\gamma^\mu U^{(n)}_{1\mu} e^k_R \; , \tag{4.7}$$

where the index n numerates the U_1 states, a sum over n is understood. The couplings can be estimated as:

$$g^{(n)}_{Ljk} \sim \frac{c_{jk}}{\sqrt{2}}\epsilon_{qj} g_* \epsilon_{lk} \; , \qquad g^{(n)}_{Rjk} \sim \frac{c_{jk}}{\sqrt{2}}\epsilon_{dj} g_* \epsilon_{ek} \; , \tag{4.8}$$

where the factor $1/\sqrt{2}$ arises from the SO(11) generators, and the factor $c_{jk} \sim \mathcal{O}(1)$.

Using the APC estimates for ϵ_{dj}, Eqs. (2.63), (2.64), as well as the ones of Sec. 4.1.5 for ϵ_{ej}, the couplings $g^{(n)}_{Rjk}$ become very suppressed, and the Right-handed interactions of the second term of Eq. (4.7) can be safely ignored. See Ap. B.3 for their numerical estimates.

4.1.4. Baryon and lepton number conservation

Leptoquarks can mediate baryon decay making the theory phenomenologically unacceptable, unless they have very large masses, typically of order $\sim 10^{16}$ GeV. [2] In the present model there are, for example, vector leptoquarks $\tilde{V}_2$, with masses of order few TeV, that in principle could couple to diquarks inducing baryon decay. However the SO(11) subgroup contains a generator that can be identified with an operator of baryon number: $B = \sqrt{2/3}T^X$, with T^X the generator of the $\mathrm{U}(1)_X$ defined in Eq. (4.1). This symmetry assigns the expected baryon number to the resonances, and acts in the usual way on the elementary states, forbidding the coupling of leptoquarks to diquarks and ensuring baryon number conservation. Thus in the present model $Y = T^{3R} + 2B$.

As discussed in Ref. [144], the Weinberg dimension five operator can be induced, with a Wilson coefficient that can be generically estimated to be of order ϵ_l^2/m_*, resulting in a too large contribution to neutrino masses. To avoid these contributions one can add a $\mathrm{U}(1)_L$ global symmetry to the composite sector, assigning the usual numbers to the operators mixing with the elementary fields, for example: $L\mathcal{O}_l^{SCFT} = \mathcal{O}_l^{SCFT}$ and $L\mathcal{O}_q^{SCFT} = 0$.

4.1.5. B-anomalies

As discussed in Sec. 2.3, in order to study the B-physics it is convenient to work with the effective theory resulting from the tree-level integration of the resonances. Except

[2] In fact this scale depends on the nature of the leptoquark, as well as on the size of its couplings to the SM fermions.

where explicitly stated, we will closely follow the analysis of Ref. [60]. As discussed in Sec. 4.1.3, only the effect of the U_1 leptoquarks on Left-handed currents is important in our model. These currents give contributions to the following effective Lagrangian

$$\mathcal{L}_{\text{eff}} \supset \frac{C^{ijrs}}{v_{\text{SM}}^2}[(\bar{q}_L^i\gamma^\mu\sigma^a q_L^j)(\bar{l}_L^r\gamma_\mu\sigma^a l_L^s) + (\bar{q}_L^i\gamma^\mu q_L^j)(\bar{l}_L^r\gamma_\mu l_L^s)] \ , \tag{4.9}$$

with i,j,r,s being generation indices. The dimensionless coefficient C^{ijrs} is given by:

$$C^{ijrs} = g_{Lis}^{(n)} g_{Ljr}^{(n)*} \frac{v_{\text{SM}}^2}{2m_{U_1}^{(n)2}} \sim c_{is}c_{jr}^*\epsilon_{qi}\epsilon_{qj}\epsilon_{lr}\epsilon_{ls}\frac{v_{\text{SM}}^2}{f^2} \ , \tag{4.10}$$

where we have used that: $m_{U_1} \simeq g_* f/\sqrt{2}$, and we have assumed that the contribution from the lightest resonance dominates the sum, as we will show that happens in a three-site model. Below we estimate the contributions of our model to B-physics, and in Sec. 4.3.3 we show the numerical predictions in a three-site model.

In Sec. 2.3 we showed the averages for $R_{D^{(*)}}$ along with their SM predictions, in Eq. (2.101). In our model, Eq. (4.9) gives a contribution to $R_{D^{(*)}}$ that, to linear order in C, can be approximated by:

$$\frac{R_{D^{(*)}}}{R_{D^{(*)}}^{\text{SM}}} \simeq 1 + 2C^{3233}\left(1 - \frac{V_{tb}^*}{V_{ts}^*}\frac{g_{L23}}{g_{L33}}\right) \ . \tag{4.11}$$

Using the estimates for APC, for the quark degree of compositeness, a fit of $R_{D^{(*)}}$ requires $c_{23}g_{L33}/m_{U_1} \sim 1/\text{TeV}$, with $c_{23} \sim \mathcal{O}(1)$ arising from the dependence of the Wilson coefficient on the coupling g_{L23}. In our model this ratio can be estimated as: $\sim \epsilon_{q3}\epsilon_{l3}/f$, therefore we obtain: $\epsilon_{q3}\epsilon_{l3}/f \sim \mathcal{O}(1)/\text{TeV}$. This implies that, for $f \sim$TeV, the Left-handed τ must have a large degree of compositeness.

As we discussed in Sec. 2.3, the deviations in $R_{K^{(*)}}$ point to LFU violation in $b \to s\ell\ell$. For negligible coupling to electrons, the preferred contribution from Left-Handed new physics to the Wilson coefficients $\Delta C_9^{\ell\ell}$ and $\Delta C_{10}^{\ell\ell}$ is: [122, 123, 145]

$$\Delta C_9^{\mu\mu} = -\Delta C_{10}^{\mu\mu} = \frac{4\pi}{\alpha_{\text{em}}V_{tb}V_{ts}^*}C^{2322} = -0.40 \pm 0.12 \ . \tag{4.12}$$

Using Eq. (4.10) we obtain: $g_{L32}g_{L22}^*/m_{U_1}^2 \simeq 10^{-3}$ TeV^{-2}. Making use of the APC estimates, Eqs. (2.63) and (2.64), leads to $\epsilon_{q3}\epsilon_{l2}/f \sim 0.1/\text{TeV}$. This fixes the order of magnitude of ϵ_{l2}.

As long as $\epsilon_{l1} \ll \epsilon_{l2}$, the electron does not play any important role in the B-anomalies, thus ϵ_{l1} is not fixed by them if the latter limit is satisfied, as we will assume from now on.

Once the Left-handed mixings of μ and τ are fixed, the Right-handed ones can be

adjusted to obtain the proper masses. Using Eq. (2.65) one obtains: $\epsilon_{e3} \simeq 0.7 \times 10^{-2}/g_*$ and $\epsilon_{e2} \simeq 0.4 \times 10^{-3}/g_*$.

4.1.6. Bounds

One of the most stringent constraints on a U_1 leptoquark arises from LFU violation in τ decays. At one-loop U_1 modifies the W coupling of the τ, that is in agreement with the SM prediction at the per mil level. Following Ref. [146] the violation of LFU can be parametrized in the ratio:

$$\left|\frac{g_\tau^W}{g_\mu^W}\right| = 1.0000 \pm 0.0014 \ . \tag{4.13}$$

One-loop radiative corrections can be estimated as: [60, 136]

$$\left|\frac{g_\tau^W}{g_\mu^W}\right| = 1 - 0.08 C^{3333} \ . \tag{4.14}$$

From Eqs. (4.13) and (4.14), we obtain $g_{L33}/m_{U_1} \lesssim 0.8/\text{TeV}$. This bound can be compared with the value required to fit $R_{D^{(*)}}$: $c_{23} g_{L33}/m_{U_1} \sim 1/\text{TeV}$. Although this puzzle seems to introduce some tension, a factor $c_{23} \sim 2-3$ is enough to satisfy both requirements.

The large degree of compositeness of l_3 can induce large deviations in the couplings $Z\tau_L\bar{\tau}_L$ and $Z\nu\bar{\nu}$, that are in agreement with the SM at the per mil level also. In generic models with partial compositeness the correction to these couplings can be estimated as: $\delta g_l^Z/g_l^Z \sim \xi\epsilon_l^2$. However, in our model τ_L mixes with a resonance having $T^{3L} = T^{3R}$ and $(T^L)^2 = (T^R)^2$, realizing a discrete LR symmetry that protects $g_{\tau_L}^Z$ [101]. In this case the leading tree-level corrections are $\delta g_{\tau_L}^Z/g_{\tau_L}^Z \sim \xi\epsilon_{l3}^2 (g/g_*)^2 \sim$ few $\times\, 10^{-3}$ (see Ref. [147] for an explicit calculation in the case of the b-quark). Since it is not possible to protect g_ν^Z at the same time, this coupling gets a larger modification, requiring extra tuning of order $(g_*/g)^2$ to pass the constraints [148]. We will show the numerical results performing a tree-level calculation in Sec. 4.3.2.

A similar situation holds for $Zb_L\bar{b}_L$. Given our choice for the embedding of the resonance mixing with the elementary b_L, the discrete LR symmetry also protects $g_{b_L}^Z$, leading to corrections of order 10^{-3}. In Sec. 4.3.2 we will describe the numerical predictions in a three-site model.

As discussed in Sec. 2.2.1, in a model with anarchic partial compositeness from linear interactions, there are several quantities that push the compositeness scale to larger values. In Sec. 2.2.1 we named a few possible ways of addressing these problems, for instance considering flavor symmetries [89, 110], or the use of different scales for different flavors [113], or the inclusion of naturally tiny bilinear interactions[93]. The

proposal of Ref. [93], where the lepton doublet and singlet of the first generation are elementary, as well as the first generation Right-handed up- and down-quarks, can be implemented straightforwardly in the present model. In this case, the most dangerous contributions to the aforementioned processes are suppressed, though transitions from operators like $(\bar{s}_R d_L)^2$ and $(\bar{d}_L^i \gamma^\mu d_L^j)^2$ require $m_* \gtrsim 6-7$ TeV. An interesting alternative is proposed in Ref. [112], where the authors consider a composite sector with CP symmetry, as well as a flavor $\mathrm{U}(1)^3$ symmetry in the composite "leptonic" sector. Either if the elementary-composite interactions respect $\mathrm{U}(1)^3$, or if it is broken by the couplings λ_ψ, the constraints on m_* are relaxed to $\lesssim 10$ TeV. Concerning the B-anomalies, Ref. [112] analyzes two different cases: $\epsilon_{li} \sim \epsilon_{ei}$, and $\epsilon_{li} \sim \epsilon_{lj}$, showing that both scenarios can explain the anomalies. This proposal can be implemented straightforwardly in our model, by extending G to $\mathrm{G}\times\mathrm{U}(1)^3 \times$ CP. Although the composite fermion multiplets contain states with lepton and baryon number, the elementary fermions are not unified, in the sense that q^i and l^i interact with SCFT operators that have different charges under $\mathrm{U}(1)^3$, thus in this scenario ϵ_{qi} and ϵ_{li} are independent as required in our set-up (and similar for the Right-handed fermions).

As discussed in Ref. [149], bounds from $\bar{B} - B$ mixing combined with a solution to $R_{D^{(*)}}$ lead to $f \lesssim 0.7$ TeV. This condition introduces a tension with EW precision tests, that usually require, at least: $f \gtrsim 0.75$ TeV [150], slightly increasing the amount of tuning of the model.

4.1.7. Effective theory

We can construct an effective field theory, in the manner that was outlined in Sec. 2.1. This is the low energy theory obtained after integration of the resonances of the SCFT, and containing the elementary fermions and gauge fields as well as the NGBs, and it can be built based on symmetry principles alone. As the coset considered in this model, SO(12) /SO(11), transforms as an irreducible representation **11**, there is a single decay constant f. U, the NGB matrix, also has the property that in the fundamental and adjoint representations of SO(12) (**12** and **66**, respectively) it can be written in a closed form, as:

$$U = I + \frac{\sin(\rho/f)}{\rho}\Pi + \frac{\cos(\rho/f)-1}{\rho^2}\Pi^2 \ , \qquad \rho^2 = \sum_{\hat{a}} (\Pi^{\hat{a}})^2 \tag{4.15}$$

The kinetic term for these NGBs is given by Eq. (2.10), that, assuming that only H has a VEV, it generates a mass term for the EW gauge bosons. In the present coset the matching equation is identical to that of the MCHM, namely Eq. (2.13).

We are not considering VEVs for the other pNGB states for this matching, in the case of $\overline{S}_1$ because it is a colored state and would thus break the $\mathrm{SU}(3)_c$ gauge

symmetry, and in the case of the φ it does not couple via the covariant derivative to the gauge fields because it is a singlet. As usual in CHM we define: $\xi \equiv \frac{v_{\rm SM}^2}{f^2}$.

Fermions are embedded in representations of SO(12), following the discussions of Sec. 4.1.2. This is shown in Table 4.1.

As described in Sec. 2.1.2, with the CCWZ formalism one can build SO(12)-invariants by dressing the fields with $U^\dagger$. We project over each of the irreducible representations $\mathbf{r}$ of SO(11), and in this way we can write the effective Lagrangian as that of Eq. (2.24),

$$\begin{aligned}\mathcal{L}_{\rm eff} \supset & \sum_f Z_f \bar{\Psi}_f \not{p} \Psi_f + \sum_{f,f'} \sum_{\mathbf{r}} \Pi^{\mathbf{r}}_{ff'} (\bar{\Psi}_f U) \hat{P}_{\mathbf{r}} (U^\dagger \Psi_{f'}) \\ & f, f' = q, u, d, l, e \end{aligned} \tag{4.16}$$

in this case there is no need to include complex conjugate fermions f^c, as they do not add new interactions given the field content of the coset. In Sec. 4.2 we resort to a three site model as an explicit realization of the theory of resonances. This will allow us to compute the form factors, and with these the pNGB potential and the spectrum of states.

We also wish to consider the effect of the gauge fields in the symmetry breaking. For this, we embed the elementary gauge fields in the adjoint representation of SO(12), this is done by adding non-dynamical degrees of freedom. We then have an effective Lagrangian at quadratic order in the elementary gauge fields a_μ, as in Eq. (2.25), with their field normalization defined as $Z_g = 1/g_{0,a}^2$.

As described in Sec. 2.1.2, one can evaluate the effective theory in the Higgs VEV, this allows to express the interactions in terms of correlators as defined in Eq. (2.28). In the case of our coset SO(12) /SO(11) and our identification of $\rm G_{SM}$ inside SO(11), they are the same as can be found of certain fermion embeddings in the case of the MCHM, as those shown in Table 2.1. We repeat the table here, for the sake clarity, in Table 4.2. We are only presenting the invariants which involve fields with a large degree of compositeness, that play an important role in the potential that determines the VEV; the other invariants are straightforward to compute once the corresponding representations are built.

SO(12)	SO(11)	i_{u_L}	i_{d_L}	i_{u_R}	i_{ν_L}	i_{e_L}	j_u	i_g	i_w
66	**55**	$1 - s_v^2/2$	1	s_v^2	$1 - s_v^2/2$	1	$ic_v s_v/\sqrt{2}$	1	$1 - s_v^2/2$
	11	$s_v^2/2$	0	c_v^2	$s_v^2/2$	0	$-ic_v s_v/\sqrt{2}$	0	$s_v^2/2$

Table 4.2: Invariants $i_f^{\mathbf{r}}$ and $j_f^{\mathbf{r}}$ of the kinetic and mass terms, in the background of the Higgs VEV, with no VEV for $\bar{S}_1$. We have used $s_v = \sin v/f$ and $c_v = \cos v/f$. We only show the invariants of the fields that have a non-negligible degree of compositeness.

Finally, for obtaining the spectrum of fermions, the procedure is the same as has been outlined in Chs. 2 and 3, below Eq. (2.29).

4.1.8. Potential

The interaction with the elementary sector, explicitly breaks the SCFT symmetry and generates a potential for the NGBs. In the present model, that role is mainly played by q_L, u_R and l_L of the third generation, and we also consider the effect of the gluons g^k and the weak fields w^i on $V(\Pi)$, the effect of the other fields is subleading and it will not be taken into account. Here we take much of Sec. 2.1.3. The potential is given by Eq. (2.30), with the matrices involved defined in Eq. (2.31). In the present, for $\mathcal{K}_f$ we are including only the fermions of the third generation giving the largest contribution to V, and for $\mathcal{K}_a$ we are considering the elementary gauge fields of $\mathrm{SU}(3)_c$: g^k, with $k = 1,\dots 8$, and the ones of $\mathrm{SU}(2)_L$: w^i, with $i = 1,2,3$, *i.e.*: $f^t = (u_L, d_L, \nu_L, e_L, u_R)$, $a^t = (g^k, w^i)$. Notice that, since the quarks have color indices, for our approximation $\mathcal{K}_f$ is a matrix of dimension eleven. The matrices $\mathcal{K}$ can be calculated by making use of Eqs. (4.15) and (4.16). The specific form of the fermionic contribution depends on the embedding of the elementary fermions into SO(12), leaving freedom for model building. Since $\bar{S}_1$ is a singlet of $\mathrm{SU}(2)_L$ and H is a color singlet, at one-loop level the gluons contribute only to the potential of $\bar{S}_1$ and the ws only to the potential of the Higgs.

Since the dependence on the pNGBs is contained in the matrix U, V is a complicated function of φ, H and $\bar{S}_1$, with an infinite series of terms. In order to analyze the stability of the potential, we find it useful to perform an expansion of V in powers of φ, H and $\bar{S}_1$ to fourth order, obtaining:

$$V \simeq \sum_{\Pi=H,\bar{S}_1,\varphi} [m_\Pi^2 |\Pi|^2 + \lambda_\Pi (|\Pi|^2)^2] + \lambda_{H\bar{S}_1} |H|^2 |\bar{S}_1|^2 + \lambda_{H\varphi} |H|^2 \varphi^2 + \lambda_{\varphi\bar{S}_1} \varphi^2 |\bar{S}_1|^2 + \dots \ , \tag{4.17}$$

where the dots stand for higher order terms. The quadratic and quartic coefficients of Eq. (4.17) can be expressed as momentum integrals of combinations of the fermionic and bosonic form factors $\Pi^{\mathbf{r}}_{ff'}$ and $\Pi^{\mathbf{r}}_G$. Generically, these quadratic and quartic coefficients can be estimated to be of order: $m_\Pi^2 \sim \epsilon_f^2 m_*^4/(16\pi^2 f^2)$ and $\lambda_\Pi \sim \epsilon_f^2 m_*^4/(16\pi^2 f^4)$. The absence of terms with an odd number of fields is guaranteed by the P-symmetry. Notice that in the absence of this symmetry, a term linear in φ can be present, triggering a VEV for φ.

For $m_H^2 < 0$, $m_{\bar{S}_1}^2, m_\varphi^2 > 0$ and suitable quartic couplings, V is minimized by a non-trivial Higgs VEV: $v^2 = -m_H^2/\lambda_H$ and zero leptoquark and singlet VEV. Using the estimates of the previous paragraph in the solution for the Higgs VEV, for generic regions of the parameter space one obtains: $v \sim f$. As is well known, EWPT demands a separation between v and f, leading to a tuning of order ξ, as usual in composite

Higgs models.

For the embedding of Table 4.1, the quadratic coefficients are:

$$
\begin{aligned}
m_H^2 = &-\int \frac{d^4p}{(2\pi)^4}\left(2\frac{\Pi_l^{\mathbf{55}}-\Pi_l^{\mathbf{11}}}{Z_l+\Pi_l^{\mathbf{55}}}+2N_c\frac{\Pi_q^{\mathbf{55}}-\Pi_q^{\mathbf{11}}}{Z_q+\Pi_q^{\mathbf{55}}}+4N_c\frac{\Pi_u^{\mathbf{11}}-\Pi_u^{\mathbf{55}}}{Z_u+\Pi_u^{\mathbf{11}}}\right.\\
&\left.+2N_c\frac{|M_u^{\mathbf{55}}-M_u^{\mathbf{11}}|^2}{(Z_q+\Pi_q^{\mathbf{55}})(Z_u+\Pi_u^{\mathbf{11}})}-\frac{9}{4}\frac{\Pi_G^{\mathbf{11}}-\Pi_G^{\mathbf{55}}}{-Z_w p^2+\Pi_G^{\mathbf{55}}}\right)\,,\\
m_{\bar{S}_1}^2 = &-\int \frac{d^4p}{(2\pi)^4}\left(4\frac{\Pi_q^{\mathbf{55}}-\Pi_q^{\mathbf{11}}}{Z_q+\Pi_q^{\mathbf{55}}}+10\frac{\Pi_u^{\mathbf{11}}-\Pi_u^{\mathbf{55}}}{Z_u+\Pi_u^{\mathbf{11}}}-\frac{16}{3}\frac{\Pi_G^{\mathbf{10}}-\Pi_G^{\mathbf{45}}}{-Z_g p^2+\Pi_G^{\mathbf{45}}}\right)\,,\\
m_\varphi^2 = &-\int \frac{d^4p}{(2\pi)^4}4N_c\frac{\Pi_u^{\mathbf{11}}-\Pi_u^{\mathbf{55}}}{Z_u+\Pi_u^{\mathbf{11}}}\,,
\end{aligned}
\tag{4.18}
$$

the last terms show the gauge contributions, that are independent of the fermion embedding. Having explicit expressions of the form factors it is possible to compute these coefficients.

We have also computed the quartic couplings, but we do not show them because they lead to too long expressions.

Finally, we can now consider the potential that determines the Higgs VEV, in the case of neither VEV of $\bar{S}_1$, nor of φ. The potential is given by Eq. (2.33), with the form factors obtained by making use of the Eqs. (2.28) and (2.27), as well as Table 4.2.

In the next section we will show a three-site description of the resonances of the SCFT that allows to model the form factors. In Sec. 4.3.1 we will show numerical results for regions of the parameter space where the one-loop potential breaks the EW symmetry, preserving $\mathrm{SU}(3)_c\times\mathrm{U}(1)_{\mathrm{em}}$. We will also show the predictions for the masses of the pNGBs.

4.2. A three-site model

In this section we wish to model the sector of resonances in such a way that allows to calculate the form factors of Sec. 4.1.7, and in that way to be able to calculate the potential and spectrum of states. We consider a theory of three sites, which we have outlined in Sec. 2.4, and in the present model we identify $\mathrm{G}_1 = \mathrm{G}_2 = \mathrm{SO}(12)$, and $\mathrm{H}_2 = \mathrm{SO}(11)$.

As described in Secs. 2.1.2 and 2.4, it is useful to add non-dynamical elementary degrees of freedom that allow to embed the elementary fields in full multiplets of SO(12). We will call A_μ to the embedding of the gauge fields into SO(12), and Ψ_f to the embeddings of the elementary fermions, with $f = q, u, d, l, e$, these latter embeddings being defined in Table 4.1. The Lagrangian for the bosonic sector is the one given in Eq (2.110). In the present construction, the two σ-model fields provide 132 NGBs, which in the unitary gauge 121 NGBs become the longitudinal degrees of freedom

of the 66 spin one resonances at site-1 and the 55 resonances at site-2, that become massive. 11 NGBs remain in the spectrum, they correspond to H, $\bar{S}_1$ and φ. Their decay constant is given by the matching Eq. (2.111) after going to the unitary gauge.

The Lagrangian of the fermionic sector is given by Eq. (2.112). It consists of kinetic terms for fermions on each site, mass terms on sites 1 and 2, with the property that on site-2 these mass terms can be split for each particular representation $\mathbf{r}$ of SO(11) contained in the SO(12) fermion representations $\mathbf{R}$. Finally, we have the interactions between sites, mediated by the σ-models $\Omega_{1,2}$. The couplings between site-0 and site-1 correspond to the elementary-composite mixings, and they can span a hierarchy of values, as has been discussed in Sec. 2.1.1 for example.

Following the discussion of Sec. 4.1.2, one would have to include two massive Dirac fermions per generation in each composite site, one in the representation **66** and one in **220**. The elementary fermions q, l and u mix with $\Psi_1^{\mathbf{66}}$, whereas d and e mix with $\Psi_1^{\mathbf{220}}$. From the structure of fermion mixings under APC (Eqs. (2.63), (2.64) and (2.65)) and the discussions of Sec. 4.1.5, we obtained that q, u and l of the third generation have a large degree of compositeness, whereas the mixing λ_d and λ_e must be suppressed to reproduce the bottom and tau masses. Given that the mixings with $\Psi_1^{\mathbf{220}}$ are very suppressed, to simplify our analysis of the potential, as well as the analysis of q and l couplings with leptoquarks, from now on we will consider that there is just one resonance in each site: $\Psi_j^{\mathbf{66}}$, and we will neglect the effects of $\Psi_j^{\mathbf{220}}$. [3] Thus, for the calculation of the potential, we can rewrite the Lagrangian for the fermionic sector as:

$$\begin{aligned}\mathcal{L}_{\rm f} =& \bar{\Psi}_1^{\mathbf{66}}(i\not{D} - m_1)\Psi_1^{\mathbf{66}} + i\bar{\Psi}_2^{\mathbf{66}}\not{D}\Psi_2^{\mathbf{66}} + \sum_{\mathbf{r}=\mathbf{55},\mathbf{11}} m_{2,\mathbf{r}}\bar{\Psi}_{2,\mathbf{r}}^{\mathbf{66}}\Psi_{2,\mathbf{r}}^{\mathbf{66}} + \lambda_{1,2}f_2\ \bar{\Psi}_1^{\mathbf{66}}\Omega_2\Psi_2^{\mathbf{66}} \\ &+ f_1\sum_{f=q,l,u}\lambda_f(\bar{\Psi}_f\Omega_1\Psi_1^{\mathbf{66}} + i\bar{\Psi}_f\not{D}\Psi_f) + \text{h.c.}\ . \end{aligned} \tag{4.19}$$

The mass matrices obtained from bosonic and fermonic sectors (Eqs. (2.110) and (4.19)) are shown in Ap. B.2.

The states at sites 2 and 3 give an effective description of the lightest level of resonances of the SCFT. To gain some insight into the dynamics of the SCFT, it is useful to study first the spectrum neglecting the mixing with the elementary fields as well as the contributions from the Higgs VEV. As described in Sec. 2.4, one can perform a diagonalization of the mass matrix to study the spectrum. In the case of spin one states, taking $g_0 \to 0$, we find one multiplet in the representation **11** of SO(11), located on site-1, with mass $g_1\sqrt{(f_1^2+f_2^2)/2}$, that does not mix with any other state in this limit. Plus, there are two multiplets in the representation **55** of SO(11), that are mixed

[3] Even if $\lambda_d = \lambda_e = 0$, $\Psi_2^{\mathbf{220}}$ can mix with $\Psi_2^{\mathbf{66}}$ through a mass term that is SO(11)-invariant: $\hat{m}_2\bar{\Psi}_{2L,\mathbf{55}}^{\mathbf{66}}\Psi_{2R,\mathbf{55}}^{\mathbf{220}} + \hat{m}_2'\bar{\Psi}_{2R,\mathbf{55}}^{\mathbf{66}}\Psi_{2L,\mathbf{55}}^{\mathbf{220}}$, distorting the spectrum of fermions. We are neglecting these effects also.

by f_2 as shown in Eq. (2.110), after diagonalization of this mixing, for $f_1 = f_2$ and $g_1 = g_2$ the mass eigenstates have masses: $\simeq g_1 f_1/2$ and $\simeq g_1 f_1$. When considering the effect of nonzero g_0, this mixes elementary and composite states. By diagonalizing this mixing, and before EWSB, one obtains a set of massless and partially composite fields that are in one to one correspondence with the gauge bosons of the SM. One can define a degree of compositeness of the massless states: ϵ_g, as shown previously in Eq. (2.113).

$$\epsilon_g^2 = 1 - \frac{g_1^2 g_2^2}{g_0^2 g_1^2 + g_0^2 g_2^2 + g_1^2 g_2^2} \simeq g_0^2 \left(\frac{1}{g_1^2} + \frac{1}{g_2^2}\right) + \mathcal{O}\left(\frac{g_0}{g_i}\right)^4 , \tag{4.20}$$

For the fermions we can proceed in an analogous way. Taking the limit of $\lambda_f = 0$, the masses of the fermionic resonances depend on the masses at each site, as well as on the mixings between sites: $\lambda_{1,2}$. There are two multiplets in the **55** that get split in two levels, as well as two multiplets in the **11** that also split in two levels, with masses:

$$m_{\mathbf{r}}^{(\pm)} = \frac{1}{2}\{m_1 + m_{2,\mathbf{r}} \pm [(m_1 - m_{2,\mathbf{r}})^2 + 4\lambda_{1,2}^2 f_2^2]\} , \qquad \mathbf{r} = \mathbf{55}, \mathbf{11} . \tag{4.21}$$

Since we will take $\lambda_{1,2} \sim g_1 \sim g_2$, and all the fermionic mass parameters of order $g_j f_j$, the masses of the fermionic resonances, before mixing with the elementary states, are of the same size as the masses of the spin one resonances.

One can also perform a biunitary diagonalization of the fermionic mass matrices before EWSB. Considering just one generation, this allows us to define the degree of compositeness as:

$$\begin{aligned} \epsilon_q^2 &= \lambda_q^2 \frac{\lambda_{1,2}^2 f_2^2 + m_{2,\mathbf{55}}^2}{(m_1 m_{2,\mathbf{55}} - \lambda_{1,2}^2 f_2^2)^2 + \lambda_q^2 (m_{2,\mathbf{55}}^2 + \lambda_{1,2}^2 f_2^2)^2} , \\ \epsilon_u^2 &= \epsilon_q^2(\lambda_q \to \lambda_u, m_{2,\mathbf{55}} \to m_{2,\mathbf{11}}) , \\ \epsilon_l^2 &= \epsilon_q^2(\lambda_q \to \lambda_l) . \end{aligned} \tag{4.22}$$

The mixing with the elementary states also shifts the masses of the resonances, leading to what is usually known as light custodians when the mixing is large.

In the next sections we will show numerical predictions for the spectrum and couplings. We will take into account all the mixings for these predictions, including those induced by the Higgs VEV.

Finally, by integrating the resonances at sites 2 and 3, it is possible to obtain explicit expressions for the form factors of the low energy effective theory of Sec. 4.1.7. For the fermions we obtain:

$$\begin{aligned} \Pi_{qq}^{\mathbf{r}} &= S(\lambda_q, m_{2,\mathbf{r}}) , \qquad \Pi_{uu}^{\mathbf{r}} = S(\lambda_u, m_{2,\mathbf{r}}) , \\ \Pi_{ll}^{\mathbf{r}} &= S(\lambda_l, m_{2,\mathbf{r}}) , \qquad \Pi_{qu}^{\mathbf{r}} = M(\lambda_q, \lambda_u, m_{2,\mathbf{r}}) , \end{aligned} \tag{4.23}$$

with S and M defined as:

$$\begin{aligned}
&S(\lambda, m_{2,\mathbf{r}}) = \lambda^2 f_1^2 (p^2 - \lambda_{1,2}^2 f_2^2 - m_{2,\mathbf{r}}^2)/d \ , \\
&M(\lambda, \lambda', m_{2,\mathbf{r}}) = \lambda\lambda' f_1^2 [(-p^2 + m_{2,\mathbf{r}}^2) m_1 - \lambda_{1,2}^2 f_2^2 m_{2,\mathbf{r}}]/d \ , \\
&d = [\lambda_{1,2}^2 f_2^2 + (m_1 - p)(p - m_{2,\mathbf{r}})][-\lambda_{1,2}^2 f_2^2 + (m_1 + p)(p + m_{2,\mathbf{r}})] \ .
\end{aligned} \tag{4.24}$$

Whereas, for the gauge fields we get:

$$\begin{aligned}
\Pi_G^{\mathbf{55}} &= \frac{p^2 f_1^2 [2p^2 - f_2^2 (g_1^2 + g_2^2)]}{4p^4 - 2p^2 g_1^2 (f_1^2 + f_2^2) + g_2^2 f_2^2 (-2p^2 + g_1^2 f_1^2)} \ , \\
\Pi_G^{\mathbf{11}} &= \frac{f_1^2 (2p^2 - f_2^2 g_1^2)}{4p^2 - 2g_1^2 (f_1^2 + f_2^2)} \ .
\end{aligned} \tag{4.25}$$

4.3. Phenomenology

In this section we study the phenomenology of the composite GUT, with the lowest level of resonances effectively described by the three-site model of the previous section. We compute first the spectrum of pNGBs, looking for regions of the parameter space where the SM states have the proper masses, and showing the predictions for the masses of φ, $\bar{S}_1$ and the spin one states U_1, as well as the lightest Z'. After that we study the corrections to the Z couplings of τ_L, b_L and ν_L at tree level, showing that, thanks to the P_{LR}-symmetry, the corrections are of order $\sim$ few $\times$ 0.1 % for $\xi \sim 0.1$. After that, we study the corrections to $R_{D^{(*)}}$ and show that, for large degree of compositeness of τ_L, it is possible to be within 1σ of the experimental average value. In this case the correction to $W\tau$ coupling saturates the bounds. Finally, we discuss the phenomenology of the pNGBs.

4.3.1. EW symmetry breaking and spectrum of resonances

We have performed a scan of the parameter space of the three-site model, calculating the pNGB potential and the Higgs VEV. For this, we let most of the parameters to vary randomly, with a number of constrains. As we wish to maintain perturbativity, at each site dimensionful couplings should not exceed $4\pi f_n$. At sites 1 and 2, gauge couplings were chosen in the interval [2.1,3.6], and the couplings at the elementary site where adjusted to match the value of the SM couplings, as discussed in Eq. (2.110). The scan was also optimized to select the elementary-composite couplings such as to have the fermionic degrees of compositeness of fermions $\{q_{L,3},\ u_{R,3},\ l_{L,3}\}$ larger than 0.5, as the points consistent with phenomenology would be at larger mixings. For each point we calculated the one-loop potential at all orders in the Higgs VEV, obtaining the value of v in the cases with EWSB. We discarded all the points with maximal breaking, as

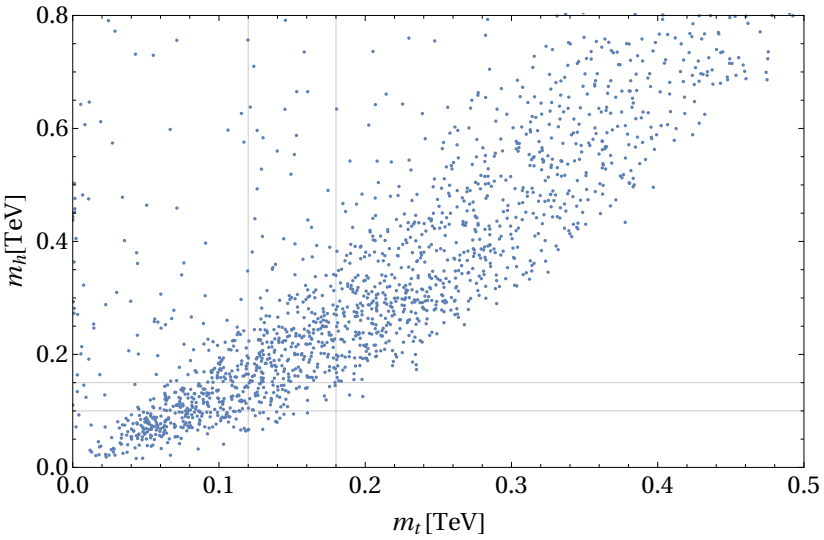

Figure 4.1: Scatter plot for top mass versus Higgs mass. Only points with $f \geq 0.7$ TeV were selected for this plot. In gray we highlight the limits for the benchmark window, defined by $m_t \in [0.12, 0.18]$TeV and $m_h \in [0.1, 0.15]$ TeV.

well as those without breaking. For each point kept, we obtained the Higgs mass by calculating the curvature around the minimum. The top mass is calculated as well, by biunitary diagonalization of the up quark mass matrix in presence of VEV. Last, by rescaling all the dimensionful parameters, we fixed: $\sqrt{\xi} f = 246$ GeV, as indicated in the matching of Eq. (2.13).

We defined a benchmark window, selecting phenomenologically viable points, as $f \geq 0.7$ TeV, $m_t \in [120, 180]$ GeV and $m_h \in [100, 150]$ GeV, a smaller window requires more time of CPU running, with almost no impact in the phenomenology that we want to study. The W mass was fixed to its experimental value by the rescaling described in the previous paragraph, whereas the Z mass is related with the W one by custodial symmetry. In Fig. 4.1 we show a scatter plot of m_t versus m_h obtained with the random scan, selecting points with $f > 700$ GeV. The random points contain the phenomenologically interesting region of the SM, although the model prefers a ratio m_h/m_t slightly larger than the experimental value.

We have also calculated the masses of the other scalar states by taking into account both: the gauge and the fermion contribution to the potential, as shown in Eq. (4.18). The gauge contribution is always positive, whereas the fermionic one can be either positive or negative. In Fig. 4.2 we show both masses plotted one against the other, along with the line $m_\varphi = m_{\bar{S}_1}$, we only show the results with both masses positive. Red triangles correspond to points within the benchmark region, whereas blue circles are for points that lie outside that region. Just by counting red triangles we obtain that there are more points with $m_{\bar{S}_1} > m_\varphi$, than the other way around. For masses larger than 1 TeV it seems that there are more red triangles with $m_{\bar{S}_1} > m_\varphi$, however, since the blue circles do not show that pattern, we cannot be sure if this a fluctuation due

to the somewhat small number of points lying in the benchmark region, or if it is a reliable tendency. The masses of these states are in the range 0.1-2.5 TeV, with a larger density of points in the interval 100-700 GeV.

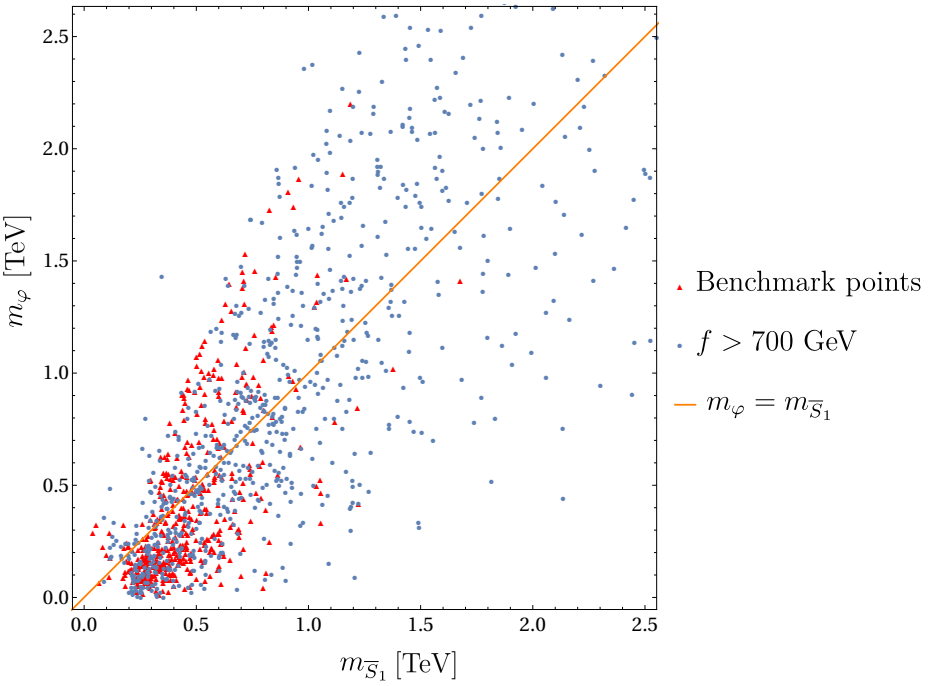

Figure 4.2: Scatter plot of the φ particle mass as a function of the mass of the scalar LQ. Plotted in blue are points with f > 700 GeV and in red the ones inside the benchmark window. Also included is the line $m_\varphi = m_{\bar{S}_1}$.

For the vector leptoquark U_1 we calculated its mass and its coupling to b_L and τ_L. This was also done by diagonalizing the fermion and boson mass matrices, and by writing the Lagrangian in terms of physical degrees of freedom. As there are three U_1 states, we obtained three masses and three different couplings. For the fermion embeddings that we have chosen, the parity P implies that one of these states does not couple to the physical fermions, and as such it does not contribute to $R_{D^{(*)}}$. In Fig. 4.3 we present the mass of the lightest U_1 state, as a function of the decay constant of the pNGBs, for the benchmark region. The dependence with f can be understood from the discussion of the spectrum above Eq. (4.21). We obtain that, for the benchmark region, $m_{U_1} \sim 1 - 4$ TeV, with a larger density of points near $1 - 2$ TeV. In the next section we will show the ratio $g_{U_1^{(n)}}/m_{U_1^{(n)}}$.

By calculating the eigenvalues of the mass matrix of the spin one neutral states, we find the spectrum of neutral vector resonances. Besides the SM Z boson, the next 5 states are of two kinds. The lightest 4 are actually degenerate in mass, and do not mix with the elementary Z, while the 5th one is around 5 % heavier, and does mix with the elementary Z. As the first generation of quarks and leptons have a very low degree of compositeness, in the approximation in which they are fully elementary, their couplings to these fully composite Z' is zero. As such, their generation in pp collisions is highly

suppressed, as the parton distribution functions of the 2nd and 3rd generations in the proton are suppressed. A process that can put bounds on these Z' with couplings mostly to the third generation is four tops, which constrains the size of 4 quark operators that can be generated as a Z' exchange [151]. However, all points in the benchmark window pass these constraints, as they are not too restrictive. In that case, points were only accepted or rejected according to the lightest Z' that does couple to first generation, following experimental bounds on these heavy vector bosons into either leptons, light jets, bottom and top quarks [152–157]. In Fig. 4.3 we present m'_Z as a function of ξ, for points inside the phenomenological window. Using that $m_{Z'}$ scales with f, as well as Eq. (2.13), one can understand the dependence of $m_{Z'}$ with ξ. We see that $m_{Z'} \gtrsim 2$ TeV for values of $\xi \lesssim 0.1$. The distinction between points that are ruled out by Z' detection and those that pass the experimental constraints can be seen by the marker, where red triangles are points that pass, and blue circles are those that do not.

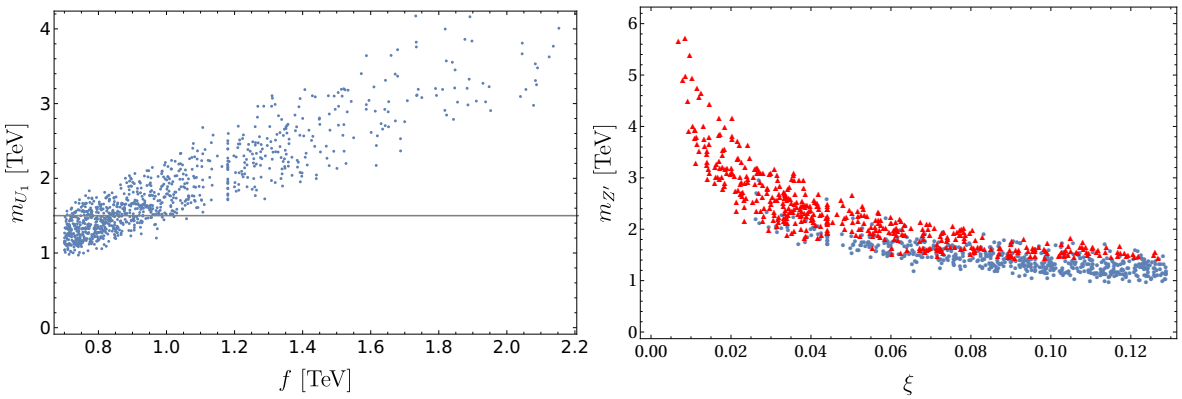

Figure 4.3: On the left panel we show a scatter plot of mass of the vector leptoquark U_1, as a function of the Higgs decay constant f, for the benchmark region. We observe the predicted linear dependence with f. Also pictured is the line at 1.5 TeV, often cited as a bound for its mass in direct searches [1]. On the right panel we show a scatter plot of mass for the first Z' resonance, as a function of $\xi = v_{\rm SM}^2/f^2$, for points on the benchmark window. Red triangles pass the experimental constraints, whereas blue circles do not.

4.3.2. Bounds

We have computed the coupling of Z to τ_L, ν and b_L in our three-site model. By rewriting the three-site interaction Lagrangian in terms of the physical states, one finds the value of the couplings g_τ^Z, g_ν^Z and g_b^Z.

The coupling g_τ^Z has been measured with an accuracy of order few per mil [148]. In the right panel of Fig. 4.4 we present the relative difference of $g_{\tau_L}^Z$ coupling, as a function of ξ. As expected from the estimates of Sec. 4.1.6, it scales linearly with ξ, the dispersion arising from the dependence of the coupling on ϵ_l and ϵ_g. We find that the relative corrections to the coupling can reach values below 2-5 per mil from $\xi \lesssim 0.1$ onwards. The coupling g_ν^Z has also been measured at the per mil level [148], but in

this case, since there is no symmetry protection, the corrections are a factor $1/\epsilon_g^2$ larger than for the charged lepton. As can be seen in the left panel of Fig. 4.4, the bounds require $\xi \lesssim 0.02$, increasing the amount of tuning.

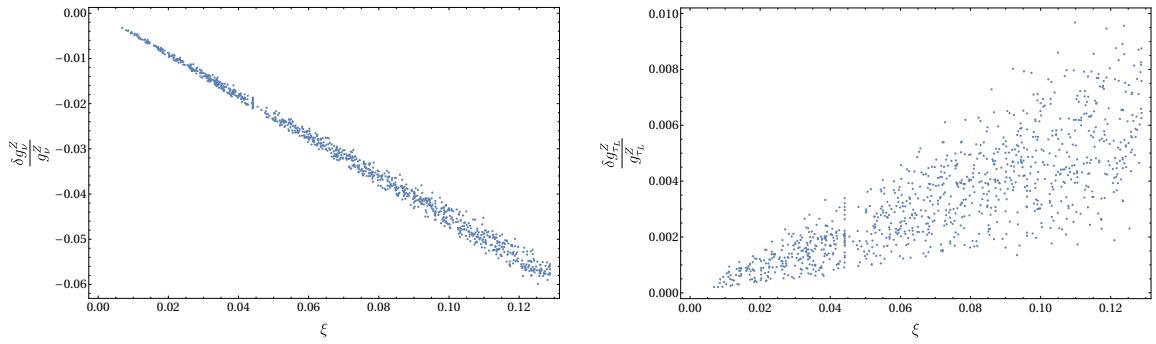

Figure 4.4: Relative correction of the couplings $Z\nu\bar{\nu}$ on the left panel, and $Z\tau_L\bar{\tau}_L$ on the right panel, as a function of ξ, for points in the benchmark region.

We omit the same graph for the coupling of Z to bottom quarks, since the values and distribution of this coupling are similar.

As described in Sec. 4.1.6, LFU violation in W couplings give constraints on C^{3333}. We have computed this Wilson coefficient for the benchmark points. In the next section we will distinguish the points that pass these constraints form those that do not, showing that a large portion of the former can also explain $R_{D^{(*)}}$.

4.3.3. Predictions for $R_{D^{(*)}}$

The contribution of the U_1 leptoquarks to $R_{D^{(*)}}$ is given in Eq. (4.11). Making use of the flavor structure arising from partial compositeness, C^{3233} can be estimated as:

$$C^{3233}\left(1-\frac{V_{tb}^*\,g_{L23}}{V_{ts}^*\,g_{L33}}\right)\sim C^{3333}\lambda_C^2\frac{c_{23}}{c_{33}}\left(1+\frac{c_{23}}{c_{33}}\right)\,, \tag{4.26}$$

with

$$C^{3333}=\sum_n C_U^{(n)}\,,\qquad C_U^{(n)}\equiv\frac{1}{2}\left(\frac{v g_{L33}^{(n)}}{m_{U_1}^{(n)}}\right)^2\,. \tag{4.27}$$

Thus, up to a factor of $\mathcal{O}(1)$, arising from the last two factors of the r.h.s. of Eq. (4.26), we can obtain C^{3233} by knowing $g_{L33}^{(n)}/m_{U_1^{(n)}}$. In Fig. 4.5 we present the coefficients $C_U^{(n)}$ of both U_1 states having nonzero couplings to b and τ, as a function of the bottom quark mixing ϵ_q. We find that the coefficient of the lightest state is approximately an order of magnitude higher than the coefficient of the heaviest state, the suppression mainly due to the difference in masses between both states. Thus the sum of Eq. (4.27) is dominated by the lightest state. As expected, larger ϵ_q leads to larger $C_U^{(n)}$, whereas the dispersion of points is generated by the random variation of the other parameters of the model. A similar dependence is found for ϵ_l.

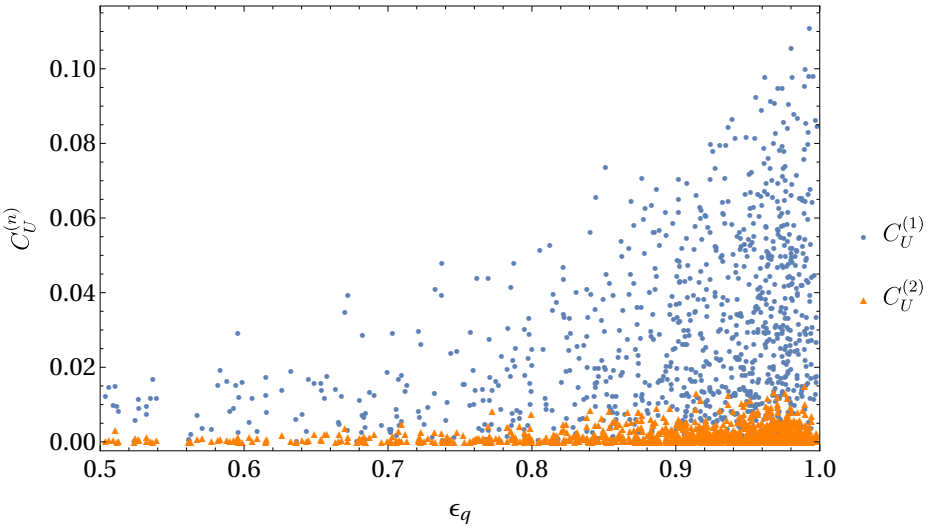

Figure 4.5: Scatter plot of $C_U^{(n)} = 1/2(vg_{L33}^{(n)}/m_{U_1}^{(n)})^2$ for points inside the benchmark window, as a function of the degree of compositeness of the quark doublet of the third generation: ϵ_q.

To obtain the coefficient of $R_{D^{(*)}}$ we sum both contributions, and multiply by a random factor c to account for the factors $c_{32}/c_{33}(1 - V_{tb}^* g_{L23}/V_{ts}^* g_{L33})$ on Eq. (4.26), that is: $c(C_{U_1}^{(1)} + C_{U_1}^{(2)})$, with $|c| < 3$. In Fig. 4.6 we present a plot of R_{D^*} vs. R_D. In it, we show the SM prediction, the world average for experimental values, along with confidence ellipses for 1, 2 and 3 σ. We present our prediction in two groups, one such that $\sum_n C_U^{(n)} \leq 0.02$, to be consistent with LFU in τ decays, and the rest of the points up to $\sum_n C_U^{(n)} = 0.06$. As can be seen in Fig. 4.5, this coefficient can actually reach values of order 0.1, we do not show points with $\sum_n C_U^{(n)} \in [0.06, 0.1]$. One can see that many points lie in the 1σ region without violating the bounds from g_τ^W. On the other hand, the bound on ξ from g_ν^Z is very stringent, we have checked that only 6 % of the points satisfy this bound, almost reaching the border of the 1 σ ellipse from below.

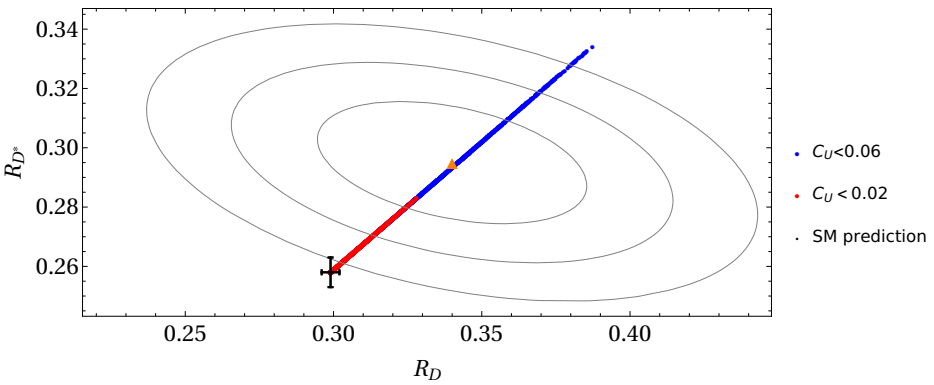

Figure 4.6: Theoretical predictions for R_D and R_{D^*} for our model. In red are plotted those points that agree with $\sum_n C_U^{(n)} \leq 0.02$, consistent with current bounds on LFU violation in tau decays. In blue, we plot the rest of points, up to $\sum_n C_U^{(n)} = 0.06$. Also plotted is the experimental point along with the confidence ellipses for coverage probabilities of 68.27 %, 95.45 % and 99.73 % (1 to 3 σ)

4.3.4. Phenomenology of the pNGB scalars

Let us start with the pNGB Higgs. Since the invariants of Table 4.2 are the same as for the MCHM with fermions embedded in the fundamental representation of SO(5), the Higgs phenomenology is similar to that case. We will not describe it here, as it has been extensively discussed in the literature, see for instance Refs. [83, 86, 143], and references therein.

The presence of the P-symmetry has important consequences for the phenomenology of $\bar{S}_1$ and φ. Let us consider two different cases: first the situation with no elementary ν_R, and second the case with an elementary ν_R with even parity (+1). In the first case, it is not possible to write a gauge invariant operator, P-even , with SM fields and just one power of either $\bar{S}_1$ or φ. The lowest dimensional operators with these fields have dimension six and contain both fields, φ and $\bar{S}_1$, they are: $\mathcal{O}_{ql} = \partial_\mu \varphi \bar{q}_L \bar{S}_1^* \gamma^\mu l_L$ and $\mathcal{O}_{qe} = \varphi \bar{q}_L \bar{S}_1^* H e_R$. Depending on the relation between m_φ and $m_{\bar{S}_1}$, they can mediate either the decay $\varphi \to \bar{S}_1^* \bar{q} l$, or the decay $\bar{S}_1 \to \varphi \bar{q} l$. The first case leads to a stable particle with electric charge and color: $\bar{S}_1$, and is not phenomenologically viable. The second case is much more interesting because φ is stable and can be a good dark matter candidate (see also Ref. [158] for another scenario solving $R_{K^{(*)}}$ and with a dark matter candidate). In Fig. 4.2 we have shown the spectrum of these states, showing that both situations are possible in the model.

Adding an elementary ν_R even under P allows to include a dimension four operator: $\mathcal{O}_{u\nu} = \bar{u}_R \bar{S}_1^* \nu_R$ that can mediate $\bar{S}_1$ decay: $\bar{S}_1^* \to t\nu$. In this case φ decays also, mediated by its interactions with $\bar{S}_1$: $\varphi \to \bar{S}_1^* \bar{q} l \to t\nu \bar{q} l$, with $\bar{S}_1$ off-shell for $m_\varphi < m_{\bar{S}_1}$. This ν_R cannot have Yukawa interactions with l, since the operator $\bar{l}_L H \nu_R$ is odd under P.

Let us discuss briefly the creation of $\bar{S}_1$ and φ at LHC. $\bar{S}_1$, being a color triplet, can be created in pairs by QCD interactions: $gg \to \bar{S}_1 \bar{S}_1^*$. This is the main creation channel at LHC. As discussed in the previous paragraphs, the final state is model dependent. In the interesting case of a stable φ, one could get a final state with a pair of quarks and leptons of the third generation as well as two scalar singlets: $q\bar{q}l\bar{l}\varphi\varphi$, with the singlets giving missing energy. φ could be created in pairs through a dimension six operator as $G_{\mu\nu}G^{\mu\nu}\varphi^2$, or in association with $\bar{S}_1$, for example in $qZ^* \to \bar{S}_1^* \varphi l \to q\varphi\varphi l\bar{l}$, with the virtual Z^* emitted from the initial proton. A detailed study of these processes is beyond the scope of this work.

Direct searches of $\bar{S}_1$ at LHC give bounds on $m_{\bar{S}_1}$ of order ~ 1 TeV, however these bounds depend on which are the dominant decay channels. Since in the present model the decay channels are model dependent, a dedicated analysis must be done for the different cases.

4.3.5. Case without P-symmetry

Another possible scenario is the case where P-symmetry is violated by the interactions with the elementary sector. There are several possibilities for this violation, we have studied the case where the elementary fermions u_R and l_L interact simultaneously with **10** and **10**', respectively contained in **11** and **55** of **66**, as shown in Eq. (4.6). Since **11** is odd and **55** is even under P, it is not possible to assign a well defined parity to the elementary fermions such that the elementary-composite interactions are invariant under P. It is also possible to break this symmetry with the other elementary fermions, but since their mixing with the SCFT is much smaller than the mixing of u_R and l_L of the third generation, we have not studied them.

In this case there are many new operators, as for example dimension one and dimension three operators: φ, $\varphi|H|^2$ and $\varphi|\bar{S}_1|^2$, and the dimension five operators: $\varphi\bar{\psi}\not{p}\psi$ (with ψ being any elementary fermion), $\bar{q}_L\bar{S}_1^*\not{p}l_L$ and $\bar{u}_R\bar{S}_1^*H^\dagger l_L$. The presence of the operators of dimension one and three change drastically the potential, since a VEV for φ is generated, that can be estimated to be of order f. We have computed the one-loop potential to all orders in φ and H in the cases without P-symmetry, confirming that, in the absence of tuning $\langle\varphi\rangle \sim f$. This VEV has a number of new effects, as: it gives large contributions to the EW scale, it induces mixing between φ and h, it opens new decay channels for φ and $\bar{S}_1$.

The amount of P violation can be controlled by the mixing of u_R with **10**', as well as the mixing of l_L with **10**, that we will call $\hat{\lambda}_u$ and $\hat{\lambda}_l$ respectively (λ_u and λ_l are for the mixings used in the previous sections of this Chapter: **10** for u and **10**' for l_L). In the limit $\hat{\lambda}_u = \hat{\lambda}_l = 0$ the symmetry is recovered, while taking these mixings small the violation of P is suppressed, and one can obtain $\langle\varphi\rangle \ll f$. As discussed below in Sec. 2.1.1, under some suitable conditions the size of λ_ψ is determined by the anomalous dimension of the corresponding SCFT operator $\mathcal{O}_\psi^{\rm SCFT}$. At the UV scale where the composite operators are defined, $\mathcal{O}_\psi^{\rm SCFT}$ transforms linearly with a representation of SO(12), thus $\lambda_u = \hat{\lambda}_u$ and $\lambda_l = \hat{\lambda}_l$ at the UV scale. At low IR scales SO(12) is spontaneously broken, allowing a different evolution of λ_ψ and $\hat{\lambda}_\psi$, however, since in our scenario the EW scale is taken only one order of magnitude smaller than the infrared (IR) scale, the window for running is rather small and it is not natural to expect a large hierarchy between λ_ψ and $\hat{\lambda}_\psi$ at the EW scale. Therefore the scenario with small violation of P requires some extra tuning.

We will not elaborate more on this interesting case, and leave it for future work.

4.4. Summary and discussion

We have considered a strongly coupled field theory with a unified global symmetry group SO(12) spontaneously broken to SO(11) by the strong dynamics. The breaking SO(12)→SO(11) has the following properties: it contains the SM gauge symmetry and the custodial symmetry, it develops a set of NGBs that include the Higgs, an $\bar{S}_1$ leptoquark and a SM singlet φ, and it contains massive spin one states that can be identified with U_1 leptoquarks addressing the B-anomalies. We have shown that an anarchic flavor structure of the SCFT, together with partial compositeness from linear mixing, can reproduce the SM spectrum and CKM, simultaneously leading to a suitable flavor pattern of couplings of U_1. In particular, we have shown that to reproduce the shift in $R_{D^{(*)}}$ a large degree of compositeness of l_L and q_L of the third generation is required. This configuration could induce large corrections to Z couplings of τ_L and b_L, that are in agreement with the SM at the per mil level, however we have shown that it is possible to protect those couplings with a well known LR symmetry, by properly choosing the representations of the fermionic operators under the global symmetry of the SCFT. We have shown that q_L, l_L and u_R can be embedded in the adjoint representation of SO(12), the **66**, whereas d_R and e_R can be embedded in the representation **220**. The elementary-composite interactions, dominated by the third generation, generate a potential for the NGBs at one-loop level, that can trigger EWSB and give masses to the extra NGBs. To obtain the suppression in the masses of the bottom quark and tau, the mixing of b_R and τ_R must be small, leading to a suppression in the coupling of U_1 with the Right handed currents, and realizing the scenario in which only Left handed currents interact with U_1.

We have shown an explicit realization of the SCFT dynamics in terms of a weakly coupled theory of resonances. For that we have built an effective low energy theory containing the lowest level of resonances by making use of a three-site theory. This description allows to compute the spectrum and couplings of the resonances, as well as the one-loop potential that is finite. Choosing a large degree of compositeness for q_L, l_L and u_R of the third generation, we have scanned the parameter space of the three-site theory within a natural region, obtaining a large set of points with EWSB, as well as the right spectrum of SM states. We obtained masses of $\bar{S}_1$ and φ of order $0.2-2$ TeV, and a lightest U_1 with mass of order $1-3$ TeV. We computed the couplings of U_1 and showed that it is possible to obtain the proper correction to $R_{D^{(*)}}$, without conflict with other observables as the W coupling to τ_L. The anomalies in $R_{K^{(*)}}$ can be solved by properly choosing a small mixing for q_L and l_L of the second generation, estimates of the couplings with U_1 are given in Ap. B.3. We have also shown that the corrections to $Zb_L\bar{b}_L$ and $Z\tau_L\bar{\tau}_L$ are of order 0.1 % for $\xi \lesssim 0.1$. On the other hand, since there is no protection for g^Z_ν, bounds from this coupling require $\xi \lesssim 0.02$, increasing the amount

of tuning and introducing some tension with $R_{D^{(*)}}$. In fact the points with $\xi \lesssim 0.02$ do not enter into the 1σ region, such that: an improvement of the precision of $R_{D^{(*)}}$, with the same central value, could not be explained in the present model. For the points of the parameter space that induce the proper shift on $R_{D^{(*)}}$, the corrections to g_τ^W almost saturate the bounds, thus in the present model one can expect to measure deviations in g_τ^W if measurements of this coupling increase their precision.

We have discussed very briefly the phenomenology of the new scalar states at LHC, finding a very rich set of signals. Since the phenomenology depends on whether the P-symmetry, as well as a light elementary Right-handed neutrino with parity $+1$, are present or not, a detailed study of the production and detection of $\bar{S}_1$ and φ at LHC could allow to distinguish the different realizations of the model. Besides, the size and flavor structure of the couplings are fixed, giving a rather predictive scenario. Although such study is beyond the scope of this work, a careful analysis of direct signals of new physics that could be related with the B-anomalies must be done, particularly at LHC. We find this avenue very interesting and leave its study for future work.

Finally, we stress that the coset SO(11)/SO(10) is big enough to contain the SM and the custodial symmetry, develop H as a NGB and generate a U_1 leptoquark. However, since in this case U_1 is associated to broken generators, its mass results heavier than the lightest resonances associated to Z and W. EWPT give lower bounds on the latter of order 2-3 TeV, thus $m_{U_1} \gtrsim 4-6$ TeV. These values of m_{U_1} give an extra suppression to the contribution to $R_{D^{(*)}}$, that results approximately a factor 4 smaller than what is needed to fit the anomalies. It could be interesting to study the possibility of finding a group smaller than SO(12) that could do the job.

Chapter 5

A Singlet-Triplet model

Back in Chap. 3 we explored a composite Higgs model involving one scalar leptoquark triplet S_3 in the spectrum, and we looked at its ability to explain the deviations in the ratio $R_{K^{(*)}}$. However, we saw how the inclusion of this leptoquark alone is incapable of simultaneously dealing with the anomalies present in charged currents, measured in $R_{D^{(*)}}$. In Chap. 4, we explored a different possibility, that of a vector leptoquark U_1, which as a leptoquark solution for B-anomalies is one of the most economical, as its Left-handed couplings to quarks and leptons of second and third generation can provide a simultaneous explanation of both ratios $R_{K^{(*)}}$ and $R_{D^{(*)}}$. However, the inclusion of this vector resonance coming from the dynamics of the strong sector is not without some tension, as the preferred scale for the leptoquark mass in order to explain the B-meson anomalies is of order TeV, whereas bounds coming from APC push the scale of all resonances of the theory, m_*, to values of $5 - 10$ TeV and higher in some cases. This problem is alleviated when studying scalar leptoquarks coming from the NGB sector, as their masses present a loop factor suppression with respect to the scale of the remaining resonances m_*. In the present Chapter we are interested in a model which can provide now two scalar leptoquark states, a singlet S_1 and a triplet S_3, as pseudo Nambu Goldstone bosons from a composite Higgs theory. Several phenomenological analyses have shown the structure of couplings required for these states, most of them assuming interactions with Left-handed fermions only [44, 60, 61], but there are also some references that have included interactions with the Right-handed ones [41, 42, 49, 53, 159]. When considering models with anarchic couplings in the composite sector (APC), we have shown in Chs. 3 and 4 how this naturally couples the leptoquarks to Left-handed fermions with increased strength over the Right-handed ones, which in certain cases are negligible. There have been a few attempts to obtain the scalar LQs from ultraviolet complete theories in the literature [72, 142]. In this Chapter, we will consider that there is a new strongly coupled sector that generates resonances at a scale of order few tens of TeV, with the LQs S_1 and S_3 as well as the Higgs

emerging as NGBs, after spontaneous symmetry breaking by the strong dynamics. As usual in our previous models, instead of a fundamental description, we consider the effective weakly coupled theory of resonances, showing a coset that generates only these states as NGBs. The SM gauge bosons will gauge a subgroup of the global symmetry of the new sector and the SM fermions will be assumed to interact linearly with it. Assuming flavor anarchy of the new sector, we study if it is possible to explain the B-anomalies, while simultaneously passing flavor and EW bounds.

This Chapter is organized as follows: in Sec. 5.1 we will describe the effective theory of resonances, the one loop potential of the scalars and the low energy theory, necessary to compute the contributions to flavor physics. In Sec. 5.2 we will show the predictions of the model for the set of observables that receive the largest contributions, compared with the present bounds, and in Sec. 5.3 we will show the numerical predictions. In Sec. 5.4 we will describe the spectrum of fermion and vector resonances, and we end with some discussion. We leave some technical details in Appendices C.

5.1. A model with composite LQs and Higgs

We are interested in the formulation of a model able to deliver the Higgs and the LQs S_1 and S_3 as pseudo-NGB resonances, generated by the spontaneous breaking of the global symmetry of an strongly coupled field theory (SCFT). We construct a model with the characteristics outlined in Sec. 2.1, as well as in Chs. 3 and 4. The strongly coupled field theory is characterized by global symmetry group G and its spontaneous symmetry breaking into a subgroup H. We proceed to discuss the choice of these symmetry groups in order to obtain the right field content in the coset.

5.1.1. Global symmetries of the composite sector

We consider the following coset G/H of the SCFT:

$$[\mathrm{SO}(10)\times\mathrm{SO}(5)]/[\mathrm{SO}(6)\times\mathrm{SU}(2)_A\times\mathrm{SU}(2)_B\times\mathrm{SO}(4)] \tag{5.1}$$

that can deliver exactly S_1, S_3 and H as pNGBs. Below we describe it in detail. As usual, we use upper case letters for representations of G, and lower case letters for those of H.

The adjoint representation of a group G decomposes in representations of a subgroup H as $\mathbf{Adj}(\mathrm{G}) \to \mathbf{Adj}(\mathrm{H}) \oplus \mathbf{r}_\Pi$, with $\mathbf{r}_\Pi$ the representation of the NGBs, that can be reducible. Considering that $\mathrm{SO}(4) \sim \mathrm{SU}(2)_C\times\mathrm{SU}(2)_R$, where the subindices are used to distinguish the different SU(2) subgroups in Eq. (5.1), the SO(5) /SO(4) factor delivers a set of fields that transform as a singlet of $\mathrm{SO}(6)\times\mathrm{SU}(2)_A\times\mathrm{SU}(2)_B$ and as a

bidoublet of SO(4), and can be identified with the Higgs as in the MCHM.

Regarding the other factor: $\mathrm{SO}(10)/\mathrm{SO}(6)\times\mathrm{SU}(2)_A\times\mathrm{SU}(2)_B$, the adjoint representation of SO(10) decomposes as

$$\mathbf{45} \sim (\mathbf{15},\mathbf{1},\mathbf{1}) \oplus (\mathbf{1},\mathbf{3},\mathbf{1}) \oplus (\mathbf{1},\mathbf{1},\mathbf{3}) \oplus (\mathbf{6},\mathbf{2},\mathbf{2}) \ , \tag{5.2}$$

where the first 3 representations correspond to the adjoint of the unbroken subgroup, and the last one to the broken generators. Joining the two factors we then have that the coset transforms as

$$\mathbf{r}_\Pi = (\mathbf{6},\mathbf{2},\mathbf{2},\mathbf{1},\mathbf{1}) \oplus (\mathbf{1},\mathbf{1},\mathbf{1},\mathbf{2},\mathbf{2}) \equiv \mathbf{r}_S + \mathbf{r}_H \ . \tag{5.3}$$

Now we discuss the embedding of the SM gauge symmetry, $\mathrm{G_{SM}}$, inside the subgroup H. The factor $\mathrm{SO}(6) \sim \mathrm{SU}(4)$ contains a subgroup $\mathrm{SU}(3)_c\times\mathrm{U}(1)_X$, where we have identified the first factor with the color of $\mathrm{G_{SM}}$. Using that a **6** of SU(4) decomposes under $\mathrm{SU}(3)_c\times\mathrm{U}(1)_X$ as

$$\mathbf{6} \sim \mathbf{3}_2 \oplus \bar{\mathbf{3}}_{-2} \ , \tag{5.4}$$

and that for SU(2) doublets: $\mathbf{2}\otimes\mathbf{2} \sim \mathbf{3}\oplus\mathbf{1}$, the singlet and triplet LQs, as well as the Higgs, can be obtained by identifying $\mathrm{SU}(2)_L \equiv \mathrm{SU}(2)_{A+B+C}$ and $Y = T^{3R} - X/6$. Notice that the embedding of $\mathrm{SU}(2)_L$ is different from the usual one in SO(10) grand unification, since in that case $\mathrm{SU}(2)_R$ is a subgroup of SO(10).

Under the unbroken global symmetry of the SCFT, both LQs are indistinguishable, as they are contained into a single irreducible representation. Since under $\mathrm{SU}(2)_L$ they split in a triplet and a singlet, the weak interactions of the SM distinguish them.

5.1.2. Representations of fermions

The elementary fermions interact with the pNGBs after mixing with the fermionic resonances of the SCFT, as described in Sec. 2.1.1. For simplicity we assume that each elementary fermion mixes with just one operator, except in the case of leptons, where we explicitly consider two mixings: $\mathcal{L} \supset \bar{l}(\omega_{l_a}\mathcal{O}^{l_a} + \omega_{l_b}\mathcal{O}^{l_b}) + \bar{e}(\omega_{e_a}\mathcal{O}^{e_a} + \omega_{e_b}\mathcal{O}^{e_b})$. We choose the same set of representations for all the generations.

There is another requirement that guide us in the choice of the representations of the fermions of the SCFT: we demand Yukawa interactions with the pNGBs to reproduce the standard Higgs interactions, as well as interactions with the LQs needed for the phenomenology of the B-mesons.

We will consider the following SO(10) representations, and their decompositions

under SO(6)×SU(2)$_A$×SU(2)$_B$:

$$\begin{aligned}\mathbf{16} &\sim (\mathbf{4},\mathbf{2},\mathbf{1}) \oplus (\bar{\mathbf{4}},\mathbf{1},\mathbf{2}) \ , \\ \overline{\mathbf{144}} &\sim (\bar{\mathbf{4}},\mathbf{2},\mathbf{1}) \oplus (\mathbf{4},\mathbf{1},\mathbf{2}) \oplus (\mathbf{4},\mathbf{3},\mathbf{2}) \oplus (\bar{\mathbf{4}},\mathbf{2},\mathbf{3}) \oplus (\overline{\mathbf{20}},\mathbf{2},\mathbf{1}) \oplus (\mathbf{20},\mathbf{1},\mathbf{2}) \ ,\end{aligned} \tag{5.5}$$

as well as the fundamental representation of SO(5) and its decomposition under SO(4):

$$\mathbf{5} \sim (\mathbf{2},\mathbf{2}) \oplus (\mathbf{1},\mathbf{1}) \ . \tag{5.6}$$

To follow the color charges of the fermions, it is also useful to know the following branching rules of SO(6) to SU(3)$_c$×U(1)$_X$:

$$\mathbf{4} \sim \mathbf{3}_{-1} + \mathbf{1}_3 \ , \qquad \mathbf{15} \sim \mathbf{8_0} + \bar{\mathbf{3}}_{\mathbf{4}} + \bar{\mathbf{3}}_{-\mathbf{4}} + \mathbf{1_0} \ , \qquad \mathbf{20} \sim \mathbf{3}_{-1} + \bar{\mathbf{3}}_{-5} + \bar{\mathbf{6}}_{-1} + \mathbf{8}_3 \ . \tag{5.7}$$

In Table 5.1 we define the representations of the fermionic operators of the SCFT and the resonances created by them. Each row is associated with an elementary fermion and the corresponding resonance mixing with it, as indicated by the subindices. On the first column we show the representations of the resonances under the full global symmetry G, in the second column we show the component under H containing the degrees of freedom with the same quantum numbers as the elementary fermions, while in the third and fourth columns we show the X and T^{3R} charges of the components mixing with the elementary fermions.

Field	SO(10)×SO(5)	SO(6)×SU(2)^4	X	T^{3R}
q	$\mathbf{R}_q = (\mathbf{16},\mathbf{5})$	$\mathbf{r}_q$=(**4**,**2**,**1**,**1**,**1**)	-1	0
u, d	$\mathbf{R}_{u,d} = (\mathbf{16},\mathbf{5})$	$\mathbf{r}_{u,d}$=(**4**,**2**,**1**,**2**,**2**)	-1	$\pm 1/2$
l_a	$\mathbf{R}_{l_a} = (\overline{\mathbf{16}},\mathbf{5})$	$\mathbf{r}_{l_a}$=(**4**,**1**,**2**,**1**,**1**)	3	0
e_a	$\mathbf{R}_{e_a} = (\overline{\mathbf{16}},\mathbf{5})$	$\mathbf{r}_{e_a}$=(**4**,**1**,**2**,**2**,**2**)	3	-1/2
l_b	$\mathbf{R}_{l_b} = (\overline{\mathbf{144}},\mathbf{5})$	$\mathbf{r}_{l_b}$=(**4**,**3**,**2**,**1**,**1**)	3	0
e_b	$\mathbf{R}_{e_b} = (\overline{\mathbf{144}},\mathbf{5})$	$\mathbf{r}_{e_b}$=(**4**,**3**,**2**,**2**,**2**)	3	-1/2

Table 5.1: In the different columns we show the embeddings of the states with the same quantum numbers as the SM fermions, the rows indicate which elementary fermion mixes with them. We also show the charges X and T^{3R} of those components.

By making use of Eqs. (5.5-5.7) and the algebra of SU(2) it is straightforward to show that these massive resonances contain components with the same quantum numbers as the SM fermions. For $\mathbf{r}_{u,d}$ and $\mathbf{r}_{e_a}$ one must select the singlet contained in $\mathbf{2}_A \otimes \mathbf{2}_C$ and $\mathbf{2}_B \otimes \mathbf{2}_C$, respectively, whereas for $\mathbf{r}_{l_b}$ and $\mathbf{r}_{e_b}$ one chooses the doublet in $\mathbf{3}_A \otimes \mathbf{2}_B$ and the singlet in $\mathbf{3}_A \otimes \mathbf{2}_B \otimes \mathbf{2}_C$, respectively, with the subindex labeling the corresponding SU(2) factors.

Let us comment on several aspects of the chosen embedding. First, with respect to the SO(10) factor, it is possible to embed all the SM fermions either in **16** or **144** and one of their conjugates. Second, for the representation $(\overline{\mathbf{144}}, \mathbf{5})$, besides the component $(\mathbf{4},\mathbf{3},\mathbf{2},\mathbf{1},\mathbf{1})$, it is also possible to embed l_L in the component $(\mathbf{4},\mathbf{1},\mathbf{2},\mathbf{1},\mathbf{1})$, as in the case of $(\overline{\mathbf{16}}, \mathbf{5})$. We will assume that the mixing with the components shown on the second column of Table 5.1 dominates over the others, and for simplicity we will consider only those interactions. Third, the symmetry $\mathrm{SU}(2)_A \times \mathrm{SU}(2)_B$ does not allow diquark interactions of type $qqS_{1,3}$ and duS_1, we will elaborate more on this topic in the end of this section.

The unbroken global symmetry allows the following interactions between resonances:

$$\mathcal{L}_* \supset y_{E*}\bar{L}HE + y_{U*}\bar{Q}\tilde{H}U + y_{D*}\bar{Q}HD + y_{3*}\bar{Q}^c\epsilon\sigma^a S_3^a L + y_{1*}\bar{Q}^c\epsilon S_1 L + y_{U*}\bar{U}^c S_1 E + \text{h.c.}\,, \tag{5.8}$$

where $y_* \sim g_*$ denote the couplings with the pNGBs, and $\epsilon = i\sigma_2$. Here we have used capital letters for the components of the multiplets of resonances that have the same quantum numbers as the elementary fermions, for example: if Φ_Q transforms as $\mathbf{R}_q$, thus $\Phi_Q = Q + \ldots$, where Q is the component that mixes with the elementary fermion q_L, meaning that it transforms as $(\mathbf{3},\mathbf{2})_{1/6}$ under $\mathrm{G_{SM}}$. A similar notation is assumed for the other states.

The embedding of the fermions can lead to relations between the couplings of the LQs. Embedding L into $\overline{\mathbf{16}}$ of SO(10) leads to: $y_{1*} = y_{3*}$, whereas embedding it into $\overline{\mathbf{144}}$ gives: $y_{1*} = -3y_{3*}$, this is shown explicitly in Ap. C.2. The first case leads to a cancellation of the contributions to $R_{D^{(*)}}$ to leading order, instead one can consider either both embeddings, mixing l_L with two resonances and obtaining independent linear combinations of couplings with the scalar LQs, or just the second one.

5.1.3. Flavor structure: anarchic partial compositeness

We consider an anarchic SCFT, meaning that there is no flavor structure, and all flavor transitions are of the same order. We follow the logic outlined in Sec. 2.2. APC is able to provide a natural way of explaining spectrum and mixings of quarks as well as that of leptons, Eqs. (2.63, 2.64), and (2.65).

Regarding the lepton sector, in the present model there are two mixings per elementary multiplet, labeled by subindices a, b in Table 5.1. We will assume that $\epsilon_{\psi_a} \simeq \epsilon_{\psi_b}$, although it is also possible to consider the situation with $\epsilon_{\psi_a} \ll \epsilon_{\psi_b}$, and in the following we will not write this subindex anymore. Reproducing the masses of the charged leptons fixes the product of Right and Left compositeness fractions, thus requiring the relations of Eq. (2.65). As explained in Sec. 2.2, mixings depend on the precise

nature and realization of neutrino masses, thus the relation between ϵ_{li} is model dependent. Guided by the B-anomalies we will consider hierarchical Left-handed mixing: $\epsilon_{l1} \ll \epsilon_{l2} \ll \epsilon_{l3}$, as well as $\epsilon_{ei} \ll \epsilon_{li}$. We will consider these as free parameters, and in Sec. 5.3 we will show the numerical values which are favored by flavor observables.

Regarding the interaction of elementary fermions with scalar leptoquarks, after integration of the composite fermionic resonances, at zero momentum, one obtains an effective Lagrangian

$$\mathcal{L}'_{\text{eff}} \supset x_3 \bar{q}^c_L \epsilon \sigma^a S^a_3 l_L + x_1 \bar{q}^c_L \epsilon S_1 l_L + x_u \bar{u}^c_R S_1 e_R + \text{h.c.} \tag{5.9}$$

where we only show the terms involving the LQs, although similar interactions with the Higgs are present. If ν_R is included, there are new interactions containing this state. Flavor indices have been omitted.

Anarchic partial compositeness also generates a hierarchy of flavor in these LQ couplings, that is related with the hierarchy of the fermion masses:

$$x_{3,i\alpha} \sim g_* \ \epsilon_{qi} \ c_{3,i\alpha} \ \epsilon_{l\alpha} \ , \qquad x_{1,i\alpha} \sim g_* \ \epsilon_{qi} \ c_{1,i\alpha} \ \epsilon_{l\alpha} \ , \qquad x_{u,i\alpha} \sim c_{u,i\alpha} \frac{m_{u_i} m_{\ell_\alpha}}{\epsilon_{qi} \epsilon_{l\alpha} v^2_{\text{SM}} g_*} \ , \tag{5.10}$$

where we have written $y_{n*} = g_* c_n$, for $n = 1, 3, u$, with $c_{n,ij} = \mathcal{O}(1)$. It is this hierarchy which suggests a natural way to combine leptoquarks into a composite Higgs model, in a manner that can provide an explanation to B-anomalies without involving an ad-hoc structure of couplings or extremely tuned regions of parameter space. We showed estimates of this in Sec. 2.3.

5.1.4. Constraints

We consider now some general constraints, as proton stability and EW precision tests.

Grand unified theories usually lead to proton decay by exchange of LQs that also interact with diquarks, demanding a huge mass scale for these states. In the present model the LQs have masses $\lesssim \mathcal{O}(30)$ TeV, depending on whether they are pNGB as S_1 and S_3, or spin-1 resonances. However it is straightforward to show that, given the embeddings chosen for the fermions, at tree level there are no interactions of type qqLQ. In fact there is a discrete symmetry that forbids those interactions, and makes the proton stable, a parity under which the quark resonances and $S_{1,3}$ are odd, whereas the leptonic resonances are even, allowing qlS and forbidding qqS. One possibility to build such a transformation is by considering a 2π rotation with $\text{SU}(2)_A$, under which objects with half-integer spin, as quarks and S, are even, whereas objects with integer spin, as leptons, are singlets, as shown in Eq. (5.3) and Table 5.1. By demanding

the elementary quarks (leptons) to be odd (even), this symmetry is preserved by the fermionic mixings.

The previous symmetry does not forbid $n - \bar{n}$ oscillations, that can be mediated by dimension nine operators containing six fermionic resonances that mix with the quarks of the first generation [131]. However Ref. [71] has shown that in anarchic partial compositeness, with resonances in the TeV scale and couplings $g_* \sim 4\pi$, the bounds on the WCs of these operators can be satisfied. Below we discuss briefly the corrections to $Zb\bar{b}$ coupling and flavor observables arising from the presence of heavy massive resonances, the effect of the lighter pNGB LQs is considered in detail in the next section.

As mentioned in Sec. 2.2.1, the $Zb_L\bar{b}_L$ coupling has been measured in agreement with the SM at the level of $\sim 0.25\,\%$. Corrections in composite Higgs models characterized by one scale and one coupling can be estimated as $\delta g_{b_L}/g_{b_L} \sim \epsilon_{q3}^2 v_{\rm SM}^2/f^2$. As we estimate in Sec. 5.1.5, $v_{\rm SM}^2/f^2 \sim 0.05$ for our benchmark region of parameters, thus for $\epsilon_{q3} \sim 1$ the bound is saturated. Although it is possible to protect this coupling with symmetries, the fermion embedding that we have chosen does not protect it, thus for the largest values of $\epsilon_{q3}^2 v_{\rm SM}^2/f^2$ considered in this work some extra tuning should be present, whereas for the smallest values the estimate is an order of magnitude below the bound.

As we described in Sec. 2.2.1, meson phenomenology, as mixing and decays, put very strong limits on partial compositeness with flavor anarchy, demanding $m_* \gtrsim 10 - 30$ TeV [88, 110]. We take this scale for the resonances, at the price of increasing the amount of tuning demanded by the EW scale. Besides the mesons, the corrections to the neutron and electron dipole moments, as well as $\mu \to e\gamma$, demand even larger scales. There are different proposals to satisfy or alleviate these bounds [88, 110, 113], most of them require departures from anarchy. However some interesting solutions for the lepton sector involving U(1) and CP symmetries have been discussed, for example, in Ref. [112], whereas Ref. [93] has considered vanishing Right-handed mixing for the first generation: $\epsilon_{u1,d1,e1} \simeq 0$ and tiny bilinear interactions.

5.1.5. Potential

In order to estimate the masses of the LQs and analyze EWSB, we make use of the effective theory containing only the elementary fields and NGBs, which we obtain after the usual algorithm described in Secs. 2.1 and 2.1.2. As the effective theory is determined by the symmetries alone, we are able to obtain generic estimates without specifying more details of the dynamics of the underlying theory. We only consider fermions of the third generation that, having the largest degree of compositeness, give the dominant contribution to the potential. Given that in our set-up the degree of compositeness of b_R and τ_R are much smaller than the compositeness of the other

fermions, we do not include them in this section.

As usual, in order to build the effective theory we promote the elementary fields to complete multiplets of the global symmetry of the SCFT: G=SO(10)×SO(5). This is done by including spurions in their multiplets, which are set to zero at the end of calculations. According to Table 5.1, we embed q and u in $\psi_{q,u} \sim (\mathbf{16}, \mathbf{5})$, whereas for l we consider two embeddings: $\psi_{l_a} \sim (\overline{\mathbf{16}}, \mathbf{5})$ and $\psi_{l_b} \sim (\overline{\mathbf{144}}, \mathbf{5})$. Only one linear combination of the components of ψ_{l_a} and ψ_{l_b}, transforming as $(1,2)_{-1/2}$ of $\mathrm{G_{SM}}$, is dynamical.

Using the NGB matrix $U = e^{i\Pi/f}$, one can write their kinetic terms, as in Eq. (2.10), and the interaction with the elementary fermions, Eq. (2.24). We focus on the fermionic interactions and their contribution to the potential, ignoring the gauge one which is however straightforward to obtain. We can calculate the potential, following the prescription of Sec. 2.1.3, where we only consider the fermionic contribution to Eq. (2.30).

Masses of the LQs

Following the algorithm described in Sec. 2.1.3, we make an expansion of the potential in powers of the NGBs Π, this way obtaining the masses of the LQs as momentum integrals of combinations of the correlators $\Pi^{\mathbf{r}_H}_{ff'}(p)$. We get, for the singlet and triplet:

$$M_1^2 = \tilde{M}^2 + \Delta M_1^2 \ , \qquad M_3^2 = \tilde{M}^2 + \Delta M_3^2 \ , \tag{5.11}$$

with $\tilde{M}^2$ and $\Delta M^2_{1,3}$ defined in Eq. (C.9) of Ap. C.3.

We find that the splitting between the LQs is driven by Ψ_{l_b}, which as previously seen and detailed in Ap. C.2, is the lepton embedding that couples differently to singlet and triplet leptoquarks. For positive values of M_1^2 and M_3^2 there is no color breaking and Eq. (5.11) gives the LQ masses to $\mathcal{O}(v^0)$. By noticing that $\Pi^{\mathbf{r}_H}_{ff} \sim \mathcal{O}(\epsilon_f^2)$, the order of these masses can be estimated as:

$$M^2_{1,3} \sim \frac{g_*^2}{16\pi^2} m_*^2 \epsilon_f^2 = (3\ \mathrm{TeV})^2 \left(\frac{m_*}{20\ \mathrm{TeV}} \ \frac{g_*}{4} \ \frac{\epsilon_f}{1/2} \right)^2 \ . \tag{5.12}$$

Breaking of the EW symmetry

We start this analysis with some simple considerations about the gauge contributions to the Higgs potential. Since the Higgs arises as a NGB from the spontaneous breaking of the SO(5) factor, its interactions with the EW gauge bosons are as in the MCHM, the SO(10) factor does not play any role at one loop. The gauge contributions to the potential can be found, for example, in Refs. [65, 86]. The matching with the SM Higgs VEV is given by the usual in MCHM, Eq. (2.13), For $m_* \simeq 20$ TeV and $g_* \simeq 4$ one gets: $s_v \simeq 0.05$, requiring a larger tuning than in the case of $f \sim 0.5 - 1$ TeV. The

fermionic contributions alone can induce EWSB. Following Sec. 2.1.2, one can evaluate the effective Lagrangian in the Higgs VEV, getting the fermionic terms in Eq. (2.26). By matching with the full effective Lagrangian one obtains expressions for the correlators $\Pi_f(p)$ and $M_f(p)$ in terms of the form factors $\Pi_{ff'}$ and of functions $i_f^{\mathbf{r}}(v)$ and $j_f^{\mathbf{r}}(v)$, as in Eq. (2.28). The only addition in the present model is that there are two lepton embeddings, giving two independent contributions to the leptonic correlators:

$$\Pi_{f_L} = \sum_{\mathbf{r}_H} \left(i_{fa}^{\mathbf{r}_H} \; \Pi_{l_a l_a}^{\mathbf{r}_H} + i_{fb}^{\mathbf{r}_H} \; \Pi_{l_b l_b}^{\mathbf{r}_H} \right) \; , \qquad f = \nu, \ell \; . \tag{5.13}$$

These functions $i_f^{\mathbf{r}_H}(v)$ and $j_f^{\mathbf{r}_H}(v)$ encode the dependence with the Higgs VEV, they are given in Table 5.2, with $c_v \equiv \cos(v/f)$, $s_v \equiv \sin(v/f)$.

H	i_{u_L}	i_{d_L}	i_{u_R}	$i_{\nu_L a}$	$i_{\ell_L a}$	$i_{\nu_L b}$	$i_{\ell_L b}$	j_u
$\mathbf{r}_q$	c_v^2	c_v^2	$\frac{1}{4}s_v^2$	0	0	0	0	$-\frac{is_{2v}}{4}$
$\mathbf{r}_{u,d}$	s_v^2	s_v^2	$\frac{7+c_{2v}}{8}$	0	0	0	0	$\frac{is_{2v}}{4}$
$\mathbf{r}_{l_a}$	0	0	0	c_v^2	c_v^2	0	0	0
$\mathbf{r}_{e_a}$	0	0	0	s_v^2	s_v^2	0	0	0
$\mathbf{r}_{l_b}$	0	0	0	0	0	c_v^2	c_v^2	0
$\mathbf{r}_{e_b}$	0	0	0	0	0	s_v^2	s_v^2	0

Table 5.2: Fermionic invariants evaluated in the Higgs VEV. The first column indicates the representation under SO(6)×SU(2)^4, as defined in the third column of Table 5.1

Let us make a brief comment on the relation with the MCHM. The fermionic invariants are determined by the embedding of the elementary fermions in the larger symmetry of the SCFT. Given the identification of $\mathrm{SU}(2)_L$, the SM doublets/singlets are embedded into singlets/doublets of $\mathrm{SU}(2)_C$, as shown in Table 5.1. Thus, taking into account this subtlety and up to possible normalization factors, the v-dependence of the fermionic invariants can be obtained from the invariants of the MCHM with fermions in the fundamental representation.

Having expressions for the correlators, the Coleman-Weinberg potential can be computed, which determines v at one loop. An expansion in s_v can be done, as in Eq. (2.34). We show the quadratic and quartic coefficients as integrals of the correlators in Ap. C.3. Expressions for the Higgs VEV, and mass, can be approximated, by expressions given in Eqs. (2.36) and (2.37).

As we mentioned in Ch. 2, both the Higgs VEV and mass require a certain amount of tuning. Regarding the VEV, if one demands $v_{\mathrm{SM}} \ll f$, there is a tuning of order $1/s_v^2$ from the estimates of α and β alone. The different scaling of α and β with ϵ_f has

been considered in Ref. [84], and is typical of fermionic embeddings in the fundamental and adjoint representations of SO(5). Regarding the Higgs mass, there is also some tension with the observed value of $m_h \approx 125$ GeV when using the estimates for α and β. However, by looking at the explicit expressions for these parameters in Eq. (C.10), we notice that there are some $\mathcal{O}(1)$ factors inherited from Clebsch-Gordan coefficients, whose contributions to α are a factor 2-8 larger than in β, that can alleviate this tension.

In the case of lighter fermionic states, a similar argument than that which was applied to the Higgs mass can be utilized in the estimates for the scalar LQ masses, Eq. (5.12). In this case the masses are also rescaled by k_ψ^2, such that for $k_\psi \simeq 0.5$ one can expect masses of $\mathcal{O}(1$ TeV).

5.1.6. Low energy effective theory

We consider now the effective theory at scales lower than the masses of S_1 and S_3. Given the large value of $m_* \gg M_{1,3}$, we do not consider in our analysis the effect of the heavy spin-1 resonances on the low energy observables. At low energies, integrating-out the LQs and Fierzing, leads to:

$$\mathcal{L}_{\text{eff}}^{\Lambda} \supset \sum \frac{C^i}{\Lambda^2}\mathcal{O}^i + \text{h.c.} \ , \tag{5.14}$$

with $\mathcal{O}^i$ given by:

$$\begin{aligned} \mathcal{O}^T_{\beta\alpha ij} &= (\bar{q}^i_L\gamma_\mu\sigma^a q^j_L)(\bar{l}^\alpha_L\gamma^\mu\sigma^a l^\beta_L) \ , \qquad \mathcal{O}^1_{\beta\alpha ij} = (\bar{u}^i_R q^j_L)\epsilon(\bar{e}^\beta_R l^\alpha_L) \ , \\ \mathcal{O}^S_{\beta\alpha ij} &= (\bar{q}^i_L\gamma_\mu q^j_L)(\bar{l}^\alpha_L\gamma^\mu l^\beta_L) \ , \end{aligned} \tag{5.15}$$

and

$$\begin{aligned} \frac{C^T_{\beta\alpha ij}}{\Lambda^2} &= -\frac{x_{1,i\beta}x^*_{1,j\alpha}}{4M_1^2} + \frac{x_{3,i\beta}x^*_{3,j\alpha}}{4M_3^2} \ , \qquad \frac{C^1_{\beta\alpha ij}}{\Lambda^2} = \frac{x_{1,i\beta}x^*_{u,j\alpha}}{4M_1^2} \ , \\ \frac{C^S_{\beta\alpha ij}}{\Lambda^2} &= \frac{x_{1,i\beta}x^*_{1,j\alpha}}{4M_1^2} + 3\frac{x_{3,i\beta}x^*_{3,j\alpha}}{4M_3^2} \ , \end{aligned} \tag{5.16}$$

where i, j and α, β stand for generation indices of quarks and leptons, respectively. [1]

Below the EW scale we rotate the fermions to the mass basis, replacing: $\psi^i_X \to V^\psi_{X,ij}\psi^j_X$ for $\psi = u, d, \ell, \nu$ and $X = L, R$. For simplicity we choose the basis where $V^d_L = V^\ell_L = \mathbb{1}_3$, the identity matrix in three dimensions. It is straightforward to write the WCs of Eq. (5.16) in the new basis.

Other related operators that we are interested in, now written in the mass basis,

[1] Notice that $C^{S,T}$ are normalized differently from Ref. [60].

are:

$$\mathcal{O}^{9(10)}_{\ell_h\ell_i d_j d_k} = \frac{\alpha_{\rm em}}{4\pi}\left[\bar{d}_j\gamma^\mu P_L d_k\right]\left[\bar{\ell}_h\gamma_\mu\left(\gamma_5\right)\ell_i\right] \ , \tag{5.17}$$

$$\mathcal{O}^{7}_{d_j d_k} = \frac{e}{16\pi^2} m_k \left[\bar{d}_j\sigma^{\mu\nu} P_R d_k\right] F_{\mu\nu} \ , \tag{5.18}$$

$$\mathcal{O}^{\rm VL(AL)}_{\ell_h\nu_i u_j u_k} = \left[\bar{u}_j\gamma^\mu(\gamma_5)d_k\right]\left[\bar{\ell}_h\gamma_\mu P_L\nu_i\right] \ , \tag{5.19}$$

$$\mathcal{O}^{L(R)}_{\ell_h\ell_i} = \frac{e}{16\pi^2}\left[\bar{\ell}_h\sigma^{\mu\nu}P_{L(R)}\ell_i\right] F_{\mu\nu} \ , \tag{5.20}$$

$$\mathcal{O}^{SL(R)}_{\ell_h\nu_i u_j u_k} = \left[\bar{u}_j P_{L(R)} d_k\right]\left[\bar{\ell}_h P_L\nu_i\right] \ , \tag{5.21}$$

$$\mathcal{O}^{dd}_{1,ij} = (\bar{d}^i_L\gamma_\mu d^j_L)^2 \ . \tag{5.22}$$

In what follows we will denote by a capital letter C, with indices denoting the effective operator name, the NP contributions to the Wilson Coefficients. Otherwise, the SM contribution to these WC will be explicitly stated.

For our estimations it is enough knowing that the masses of the LQs are of the same order, as discussed in the previous section, thus for simplicity we will take $M_1 = M_3 = M$. We find it useful to define:

$$\delta \equiv \frac{g_*^2 v_{\rm SM}^2}{4M^2} \ . \tag{5.23}$$

Looking at the definition of δ above, and taking into account the estimate for the LQ masses in Eq. (5.12), we expect δ to be approximately in the range $[0.02, 0.3]$.

5.2. Observables

In this section we analyze the impact of the new physics on low energy observables. We start with the so called B-anomalies: $R_{D^{(*)}}$ and $R_{K^{(*)}}$, and after them we consider constraints from other observables. We write the contributions in terms of the LQ couplings and then, making extensive use of partial compositeness, we show their dependence on the mixings, δ and M, as well as on the combinations of c parameters defined in Eq. (5.10), that are taken of $\mathcal{O}(1)$. In the next section we will use these results for a combined numerical analysis of all the observables.

In this section we mostly follow the calculations of Refs. [60] and [159].

In what follows, expressions for $R_{D^{(*)}}$ and $R^{\mu/e}_{b\to c}$ actually refer to the ratio of its value with respect to the SM value, thus being equal to 1 in absence of NP contributions.

5.2.1. $R_{D^{(*)}}$

Being a $b \to c\tau\nu$ process, this observable involves the operator $\mathcal{O}^{VL} - \mathcal{O}^{AL}$, that is generated at tree level by the LQ states. Following Ref. [60], we obtain:

$$\begin{aligned} R^{\tau\ell}_{D^{(*)}} &\simeq 1 + 2C^T_{3333} + 2\frac{V^*_{tb}}{V^*_{ts}} C^T_{3323} \\ &\simeq 1 + \frac{v^2_{\rm SM}}{2}\left(\frac{|x_{1,33}|^2}{M_1^2} - \frac{|x_{3,33}|^2}{M_3^2}\right) + \frac{V_{cs} v^2_{\rm SM}}{2V_{cb}}\left(\frac{x_{1,23}x^*_{1,33}}{M_1^2} - \frac{x_{3,23}x^*_{3,33}}{M_3^2}\right) \\ &\sim 1 + 2\delta\left\{\epsilon^2_{q3}\epsilon^2_{l3}\left(|c_{1,33}|^2 - |c_{3,33}|^2\right) + \frac{V_{cs}}{V_{cb}}\epsilon^2_{l3}\epsilon_{q_2}\epsilon_{q3}(c_{1,23}c^*_{1,33} - c_{3,23}c^*_{3,33})\right\} \ . \end{aligned} \tag{5.24}$$

For the last estimate, that is valid up to coefficients of $\mathcal{O}(1)$, we have used partial compositeness. The coefficients $c_{i,jk}$ are of $\mathcal{O}(1)$, as discussed in Sec. 5.1.3 they are assumed to be anarchic. Notice that all the corrections are of the same order given our flavor scheme. As reference value, we use the one of Eq. (2.102) for the ratio of the experimental to the SM value, averaged between R_D and R_{D^*}, due to the NP contribution being a symmetric one.

5.2.2. $R_{K^{(*)}}$

This process requires a transition $b \to s\mu\mu$, involving the operator $\mathcal{O}^9 - \mathcal{O}^{10}$. These operators can be written in terms of $\mathcal{O}^T$ and $\mathcal{O}^S$, that in turn are expressed as a function of the LQ couplings as: [60]

$$\begin{aligned} C^9_{2223} = -C^{10}_{2223} &= \frac{-\pi}{\alpha_{\rm em} V_{tb}V^*_{ts}}\left(C^T_{2223} + C^S_{2223}\right) \\ &= \frac{4\pi}{\alpha_{\rm em} V_{tb}V^*_{ts}}\frac{v^2_{\rm SM}}{4M_3^2} x_{3,22}x^*_{3,32} \\ &\sim \frac{4\pi}{\alpha_{\rm em} V_{tb}V^*_{ts}}\ \delta\ \epsilon^2_{l2}\epsilon_{q_2}\epsilon_{q3}\ c_{3,22}c^*_{3,32} \ . \end{aligned} \tag{5.25}$$

The estimate of the third line is a consequence of the assumed flavor structure, and we show the dependence on the $\mathcal{O}(1)$ coefficients $c_{i,jk}$.

The fitted value consistent with experiment is [124]: $C^{9,\rm exp}_{2223} = -0.61 \pm 0.12$.

5.2.3. $R^{\mu/e}_{b\to c}$

This observable is related to $R_{D^{(*)}}$, and is also generated at tree level by the LQs. The main contribution is [60]:

$$\begin{aligned} R^{\mu/e}_{b\to c} - 1 &= 2C^T_{2233} - 2\frac{V^*_{tb}}{V^*_{ts}}C^T_{2223} \\ &= \frac{v^2_{\rm SM}}{2}\left(\frac{|x_{1,32}|^2}{M_1^2} - \frac{|x_{3,32}|^2}{M_3^2}\right) + \frac{V_{cs}v^2_{\rm SM}}{2V_{cb}}\left(\frac{x_{1,22}x^*_{1,32}}{M_1^2} - \frac{x_{3,22}x^*_{3,32}}{M_3^2}\right) \\ &\sim 2\delta\left\{\epsilon^2_{q3}\epsilon^2_{l2}\left(|c_{1,32}|^2 - |c_{3,32}|^2\right) + \frac{V_{cs}}{V_{cb}}\epsilon^2_{l2}\epsilon_{q_2}\epsilon_{q3}(c_{1,22}c^*_{1,32} - c_{3,22}c^*_{3,32})\right\} \end{aligned} \tag{5.26}$$

The experimental value is [17]: $R^{\mu/e}_{b\to c,\rm exp} - 1 = 0.00 \pm 0.02$.

5.2.4. $B_{K^{(*)}\nu\bar{\nu}}$

This observable also receives contributions at tree level in our model. The branching ratio of $B \to K^{(*)}\nu\bar{\nu}$, normalized to the SM, is [60]:

$$\begin{aligned} B_{K^{(*)}\nu\bar{\nu}} &= 1 + \frac{2}{3}\frac{\pi}{\alpha_{\rm em}V_{tb}V^*_{ts}C^{\rm SM}_\nu}\left(C^T_{3323} - C^S_{3323} + C^T_{2223} - C^S_{2223}\right) \\ &= 1 + \frac{2}{3}\frac{\pi}{\alpha_{\rm em}V_{tb}V^*_{ts}C^{\rm SM}_\nu}\frac{v^2_{\rm SM}}{2}\left(\frac{x_{1,23}x^*_{1,33}}{M_1^2} + \frac{x_{3,23}x^*_{3,33}}{M_3^2} + \frac{x_{1,22}x^*_{1,32}}{M_1^2} + \frac{x_{3,22}x^*_{3,32}}{M_3^2}\right) \\ &\sim 1 + \frac{4}{3}\frac{\pi}{\alpha_{\rm em}V_{tb}V^*_{ts}C^{\rm SM}_\nu}\delta\epsilon^2_{l3}\epsilon_{q_2}\epsilon_{q3}(c_{1,23}c^*_{1,33} + c_{3,23}c^*_{3,33}) + (l3 \to l2)\ , \end{aligned} \tag{5.27}$$

where $C^{\rm SM}_\nu = -6.4$.

The experimental constraint is $B_{K^{(*)}\nu\bar{\nu},\rm exp} < 2.6$ [160], at 90 %CL.

By using the estimated values for δ above, we can check how relevant this bound is. For $\delta \sim 0.02$, we have $B_{K^{(*)}} - 1 \sim 0.11\,(2\epsilon)^4$, which does not greatly restrict the degree of compositeness of the third generation fermions. For larger values of δ this observable becomes more restrictive, but its importance still remains below that of other observables.

5.2.5. $B \to K\tau\mu$ and $B_s \to \tau\mu$

The scalar LQs induce $b \to s\tau\mu$ transitions that contribute to the decays $B \to K\tau\mu$ and $B_s \to \tau\mu$ with the operators of Eq. (5.17).

We start with $B \to K\tau\mu$, in terms of their WCs [159, 161]:

$$\text{Br}\left[B \to K\tau^\pm\mu^\pm\right] = 10^{-9}\left\{9.6\left(|C^9_{2323}|^2 + |C^9_{3223}|^2\right) + 10\left(|C^{10}_{2323}|^2 + |C^{10}_{3223}|^2\right)\right\}\ . \tag{5.28}$$

With the contribution of S_3 to these WCs we have $C^9 = -C^{10}$, with:

$$C^9_{2323} = \frac{v^2_{\rm SM}\pi}{V_{tb}V_{ts}\alpha M^2} x_{3,32}x^*_{3,23} \ . \tag{5.29}$$

Using the estimates of anarchic partial compositeness for the couplings we get:

$$\text{Br}\left[B \to K\tau^\pm\mu^\pm\right] \sim 0.06\,\delta^2\epsilon^4_{q3}\epsilon^2_{l2}\epsilon^2_{l3}\left(|c_{3,33}|^2|c_{3,22}|^2 + |c_{3,32}|^2|c_{3,23}|^2\right) \ , \tag{5.30}$$

the experimental bound being 4.8×10^{-5}, at 90 %CL. This observable is not expected to be too relevant under partial compositeness, as the combination above, for $\delta \sim 0.2$, $\epsilon_{q3}, \epsilon_{l3} \sim 0.5$, $\epsilon_{l2} \sim 0.2$ gives 1.5×10^{-6}, which is well below the bound.

For $B_s \to \tau\mu$, using again $C^9 = -C^{10}$, one obtains [159]:

$$\text{Br}\left(B_s \to \tau\mu\right) = \frac{\alpha^2}{128v^4\pi^3}|V_{tb}V_{ts}|^2 f^2_{B_s}\tau_{B_s}\left(m_\tau + m_\mu\right)^2\eta(\frac{m_\tau}{m_{B_s}}, \frac{m_\mu}{m_{B_s}})|C^9_{3223}|^2 F(m_\tau, m_\mu) \ , \tag{5.31}$$

with $\eta(x,y) = \sqrt{1-2(x+y)+(x-y)^2}$, and

$$F = 1 - \left(\frac{m_\tau - m_\mu}{m_{B_s}}\right)^2 + \left(\frac{m_\tau - m_\mu}{m_\tau + m_\mu}\right)^2\left(1 - \left(\frac{m_\tau + m_\mu}{m_{B_s}}\right)^2\right) \ . \tag{5.32}$$

Using $f_{B_s} = 0.225$ GeV, $\tau_{B_s} = 1.47 \times 10^{-12}\,s$, $m_{B_s} = 5.36$ GeV we get

$$\begin{aligned}\text{Br}\left(B_s \to \tau\mu\right) &\simeq 5.3 \times 10^{-3} V^2_{ts}\left(\frac{g_*\text{TeV}}{M}\right)^4 \epsilon^4_{q3}\epsilon^2_{l2}\epsilon^2_{l3}|c_{3,33}|^2|c_{3,22}|^2 \\ &\sim 0.037\,\delta^2\,\epsilon^4_{q3}\epsilon^2_{l2}\epsilon^2_{l3}\,|c_{3,33}|^2|c_{3,22}|^2 \ .\end{aligned} \tag{5.33}$$

The experimental bound is: $\text{Br}\left(B_s \to \tau\mu\right)_{\rm exp} \leq 4.2 \times 10^{-5}$, at 95 %CL. Same as above, we estimate the contribution to this observable to be 9.2×10^{-7}, which is also safely below the bound.

5.2.6. $B_s \to \tau\tau$

For this decay we have the branching ratio [159]

$$\frac{\text{Br}(B_s \to \tau\tau)}{\text{Br}(B_s \to \tau\tau)_{\rm SM}} = \left|1 + \frac{C^{10}_{3323}}{C^{10,\rm SM}_{3323}}\right|^2 \lesssim 8 \times 10^3 \qquad (95\,\%\text{CL}). \tag{5.34}$$

The prediction for the ratio of coefficients is:

$$\frac{C^{10}_{3323}}{C^{10,\rm SM}_{3323}} \simeq -\frac{v^2_{\rm SM}}{V_{ts}V_{tb}\alpha M^2_3} x_{3,33}x^*_{3,23} \sim 1700\,\delta\,\epsilon^2_{q3}\epsilon^2_{l3}\,c_{3,33}\,c^*_{3,23} \ . \tag{5.35}$$

In this case, for the range of values of δ, ϵ_{q3} and ϵ_{l3} of Sec. 3.1, we estimate the ratio of the Wilson Coefficients to be of order $\sim \mathcal{O}(20)$, which gives a contribution to the branching ratio that in general is one order of magnitude below the bound, although in some cases it can reach the bound.

5.2.7. $\tau \to \phi\mu$

A contribution to this process is generated by $dd\ell\ell$ operators. The branching ratio can be expressed in terms of Left-handed couplings of S_3 as [52]:

$$\mathrm{Br}\left(\tau \to \phi\mu\right) = \frac{f_\phi^2 m_\tau^3 \tau_\tau}{128\pi} \frac{\left(x_{3,22} x_{3,23}^*\right)^2}{M_3^4} \left(1 - \frac{m_\phi^2}{m_\tau^2}\right)\left(1 + 2\frac{m_\phi^2}{m_\tau^2}\right) \ . \tag{5.36}$$

We use $f_\phi = 0.225$ GeV, $m_\phi = 1.02$ GeV and we get

$$\mathrm{Br}\left(\tau \to \phi\mu\right) \sim 4 \times 10^{-6} \delta^2 \, \epsilon_{q3}^4 \epsilon_{l2}^2 \epsilon_{l3}^2 \, c_{22}^2 \left(c_{23}^*\right)^2 \ . \tag{5.37}$$

The experimental bound is 8.4×10^{-8}, at 90 %CL. Typical values for the parameters give a contribution of $\sim \mathcal{O}(10^{-10})$.

5.2.8. $B_c \to \tau\nu$

The branching ratio of $B_c \to \tau\nu$ can be expressed in terms of WCs as [162, 163]:

$$\mathrm{Br}\left(B_c \to \tau\nu\right) = 0.02 \left(\frac{f_{B_c}}{430\mathrm{GeV}}\right)^2 \left|1 + C_{\tau\tau bc}^{VL} + 4.3(C_{\tau\tau bc}^{SR} - C_{\tau\tau bc}^{SL})\right|^2 \ . \tag{5.38}$$

Both LQs contribute to C^{VL}, whereas only S_1 contributes to C^{SL}, as:

$$\begin{aligned} C_{\tau\tau cb}^{VL} &= \frac{-v_{\mathrm{SM}}^2}{4V_{cb}} \sum_k \left(-\frac{V_{ck} x_{1,k3}^* x_{1,33}}{M_1^2} + \frac{V_{ck} x_{3,k3}^* x_{3,33}}{M_3^2}\right) \\ &\simeq \frac{-v_{\mathrm{SM}}^2}{4V_{cb}} \left(-\frac{V_{cs} x_{1,23}^* x_{1,33} + V_{cb}|x_{1,33}|^2}{M_1^2} + \frac{V_{cs} x_{3,23}^* x_{3,33} + V_{cb}|x_{3,33}|^2}{M_3^2}\right) \ , \end{aligned} \tag{5.39}$$

$$C_{\tau\tau cb}^{SL} = \frac{-v_{\mathrm{SM}}^2}{4V_{cb}} \frac{x_{1,33} x_{u,23}^*}{M_1^2} \ , \tag{5.40}$$

while for Right-handed coefficients, without including ν_R: $C^{SR} = 0$. Besides, RGE running down, from the $M \sim$TeV, induces mixing between different WCs, such that the value of C^{SL} gets corrected by an additional factor of 2.9, whereas the C^{VL} coefficient has no correction [164].

The estimates in our model are given by:

$$C^{VL}_{\tau\tau bc} \sim 1.5\times 10^{-2}\left(\frac{g_*\text{TeV}}{M}\right)^2 \epsilon^2_{q3}\epsilon^2_{l3}(c_{3,33}c^*_{3,23}+|c_{3,33}|^2-c_{1,33\tau}c^*_{1,23}-|c_{1,33}|^2)\ , \quad (5.41)$$

$$C^{SL}_{\tau\tau bc} = \frac{-v^2_{\text{SM}}}{4V_{cb}}\frac{x_{1,33}x^*_{u,23}}{M^2} \sim -\frac{m_c m_\tau}{4V_{ts}V_{cb}M^2}c_{1,33}\widetilde{c}^*_{1,23}\ . \quad (5.42)$$

Combining both estimates we get:

$$\text{Br}\,(B_c\to\tau\nu) \simeq 0.02\Big|1{+}0.99\,\delta\,\epsilon^2_{q3}\epsilon^2_{l3}\,(c_{3,33}c^*_{3,23}+|c_{3,33}|^2-c_{1,33}c^*_{1,23}-|c_{1,33}|^2)\ , \\ +4.2\times 10^{-3}\left(\frac{\text{TeV}}{M}\right)^2 c_{1,33}\widetilde{c}^*_{1,23}\Big|^2\ . \quad (5.43)$$

This result has to be compared with an experimental bound $\text{Br}\,(B_c\to\tau\nu)_{\text{exp}}<0.1$, at 90 %CL. We do not expect this observable to play a significant role, as for the Left-handed contribution we estimate the branching ratio to be of ~ 0.02, while its Right-handed contribution gives also ~ 0.02 for $M\in[1,3]$ TeV.

5.2.9. Δm_{B_s}

The contribution to this observable comes from the four-quark operator $\mathcal{O}^{dd}_1$ of Eq. (5.22), whose WC is generated at loop level by the scalar LQs, through a box diagram. For the $B_s-\bar{B}_s$ system we have the following ratio:

$$\frac{\Delta m_{B_s}}{\Delta m^{\text{SM}}_{B_s}} = \left|1+\frac{C^1_{sb}}{C^{1,\text{SM}}_{sb}}\right| \quad (5.44)$$

with the coefficients being [165]

$$C^{1,\text{SM}}_{sb} = 2.35\frac{(V_{tb}V_{ts})^2}{8\pi^2}\left(\frac{m_W}{v^2_{\text{SM}}}\right)^2 \quad (5.45)$$

and [159]

$$C^1_{sb} = \frac{1}{128\pi^2M^2}\left(\left(x^*_{1,23}\right)^2x^2_{1,33}+5\left(x^*_{3,23}\right)^2x^2_{3,33}+2x^*_{1,23}x^*_{3,23}x_{1,33}x_{3,33}\right) \quad (5.46)$$

Among these three terms, when using anarchic partial compositeness, the one with the factor 5 will dominate the sum. We get

$$\frac{C^1_{sb}}{C^{1,\text{SM}}_{sb}} \sim 300\left(\frac{\text{TeV}}{M}\right)^2 \delta^2\epsilon^4_{q3}\epsilon^4_{l3}\left(c^*_{3,23}c_{3,33}\right)^2 \quad (5.47)$$

The most stringent bound is on the imaginary part of the WC [94]. We assume

maximally violating phases of the LQ couplings, such that their effects on Δm_{B_s} are restricted to be at most 20 % (95 %CL). We expect this observable to play a role, as the value of the WC ratio for $\delta \sim 0.2$, $\epsilon_{q3}, \epsilon_{l3} \sim 0.5$ and $M \sim 2$ TeV, is ~ 0.18, which is close to the experimental limit.

5.2.10. Leptonic interactions of the Z

We consider the flavor diagonal and flavor violating interactions of the Z with charged leptons and neutrinos, that receive corrections at loop order, in particular we will be interested in the processes: $Z \to \tau_L \tau_L$, $Z \to \nu_L \nu_L$, $Z \to \tau\mu$, $Z \to \mu\mu$. We follow the results of Ref. [159], see Ref. [166] for the inclusion of subleading effects.

We consider the interaction terms at zero momentum transfer:

$$\mathcal{L}^Z_{\text{int}} = \frac{g}{c_W}\left[\left(\bar{\ell}_f \Gamma_{L,\ell_f\ell_i}(0)\gamma^\mu P_L \ell_i\right) + \{L \to R\} + \Gamma_{\nu_f\nu_i}(0)(\bar{\nu}_f\gamma^\mu P_L \nu_i)\right] Z_\mu \ , \tag{5.48}$$

with g the weak coupling and c_W being the cosine of the Weinberg angle. At one loop level the dominant corrections from the LQs are dominated by the contribution containing the top:

$$\Gamma_{L,\ell_f\ell_i} = \Gamma^{\text{SM}}_{L,\ell_i}\delta_{fi} + \frac{N_c m_t^2}{32\pi^2}\left[\frac{V_{3k}x^*_{1,kf}V^*_{3l}x_{1,li}}{M_1^2}\left(1+\log\left(\frac{m_t^2}{M_1^2}\right)\right) + \{S_1 \to S_3, x_{1,i\alpha} \to x_{3,i\alpha}\}\right] \ , \tag{5.49}$$

$$\Gamma_{R,\ell_f\ell_i} = \Gamma^{\text{SM}}_{R,\ell_i}\delta_{fi} - \frac{N_c m_t^2}{32\pi^2}\frac{x^*_{u,3f}x_{u,3i}}{M_1^2}\left(1+\log\left(\frac{m_t^2}{M_1^2}\right)\right) \ , \tag{5.50}$$

$$\Gamma_{\nu_f\nu_i} = \Gamma^{\text{SM}}_{\nu_i}\delta_{fi} + \frac{N_c m_t^2}{16\pi^2}\frac{V_{3k}x^*_{3,kf}V^*_{3l}x_{3,li}}{M_3^2}\left(1+\log\left(\frac{m_t^2}{M_3^2}\right)\right) \ . \tag{5.51}$$

Writing these flavor diagonal couplings in terms of the parameters of the model, we have:

$$\Gamma_{L,\tau\tau} - \Gamma^{\text{SM}}_{L,\tau} \sim -0.04(|c_{1,33}|^2 + |c_{3,33}|^2)\,\delta\,\epsilon^2_{q3}\,\epsilon^2_{l3} \ , \tag{5.52}$$

$$\Gamma_{R,\tau\tau} - \Gamma^{\text{SM}}_{R,\tau} \sim -2\times 10^{-8}\left(\frac{\text{TeV}}{M}\right)^2 \frac{|\tilde{c}_{33}|^2}{\epsilon^2_{q3}\epsilon^2_{l3}} \ , \tag{5.53}$$

$$\Gamma_{L,\mu\mu} - \Gamma^{\text{SM}}_{L,\mu} \sim -0.04(|c_{1,32}|^2 + |c_{3,32}|^2)\,\delta\,\epsilon^2_{q3}\,\epsilon^2_{l2} \ , \tag{5.54}$$

$$\Gamma_{R,\mu\mu} - \Gamma^{\text{SM}}_{R,\mu} \sim -6\times 10^{-11}\left(\frac{\text{TeV}}{M}\right)^2 \frac{|\tilde{c}_{32}|^2}{\epsilon^2_{q3}\epsilon^2_{l2}} \ . \tag{5.55}$$

The Right-handed contributions to the couplings are heavily suppressed, the Left-handed contribution to the muon coupling is suppressed too, due to the small value for ϵ_{l2} compared with ϵ_{l3}. The SM predictions and the corresponding measurements can be found in Ref. [148].

Regarding the $\delta\Gamma_\nu$ bound, there is a recent paper which gives an updated bound $N_\nu = 2.9963 \pm 0.0074$ [167]. By using the relation $N_\nu = 3 + 4\,\delta\Gamma_\nu$, we get the bound

$$\delta\Gamma_\nu = -0.000925 \pm 0.00185\ . \tag{5.56}$$

The expression in terms of the parameters of the model is:

$$\delta\Gamma_\nu \sim -0.09\ |c_{3,33}|^2\,\delta\,\epsilon_{q3}^2\,\epsilon_{l3}^2 \tag{5.57}$$

For the $Z \to \tau\mu$ transition we have

$$\mathrm{Br}\,(Z \to \tau\mu) = \frac{K}{\Gamma_Z}\left(|\Gamma_{L,\tau\mu}|^2 + |\Gamma_{R,\tau\mu}|^2\right)\ , \tag{5.58}$$

with $\Gamma_Z = 2.5$ GeV the total Z width, and $K = 0.67$ GeV. Replacing with the usual anarchic partial compositeness relations we have

$$\Gamma_{L,\mu\tau} \sim -6.9\times10^{-4}\left(\frac{g_*\mathrm{TeV}}{M}\right)^2 \epsilon_{q3}^2\epsilon_{l2}\epsilon_{l3}\left(c_{1,33}c_{1,32}^* + c_{3,33}c_{3,32}^*\right) \tag{5.59}$$

and

$$\Gamma_{R,\mu\tau} \sim \frac{1.2\times10^{-9}\tilde{c}_{1,33}\tilde{c}_{1,32}^*\left(\frac{\mathrm{TeV}}{M}\right)^2}{\epsilon_{q3}^2\epsilon_{l2}\epsilon_{l3}}\ . \tag{5.60}$$

Joining everything we obtain

$$\mathrm{Br}\,(Z \to \tau\mu) \sim 2.8{\times}10^{-19}\,\frac{\left(\tilde{c}_{1,33}\tilde{c}_{1,32}^*\right)^2}{\left(\frac{M}{\mathrm{TeV}}\right)^4\epsilon_{q3}^4\epsilon_{l2}^2\epsilon_{l3}^2} + 8.46{\times}10^{-6}\,\left(c_{1,33}c_{1,32}^* + c_{3,33}c_{3,32}^*\right)^2\,\delta^2\epsilon_{q3}^4\epsilon_{l2}^2\epsilon_{l3}^2\ , \tag{5.61}$$

to be compared against an experimental value of 1.2×10^{-5}, at 95 %CL. Looking at its expression, we see that for values of order $\epsilon_{l3} \sim 0.5$, $\epsilon_{q3} \sim 0.5$, $\epsilon_{l2} \sim 0.1$, $M \sim$ TeV, the Right-handed contribution to this branching ratio is heavily suppressed with respect to the Left-handed one.

5.2.11. $\ell_i \to \ell_f\gamma$

These flavor violating decays are produced by operators $\mathcal{O}_{\ell_h\ell_i}^{L,R}$ of Eq. (5.20). Following Ref. [159], the LQs give a contribution to the WCs of these operators at one loop level that can be written as:

$$C_{\ell_f\ell_i}^L = -\frac{m_{\ell_f}x_{1,3f}^*x_{1,3i} + m_{\ell_i}x_{u,3f}^*x_{u,3i}}{8M_1^2} + \frac{m_t x_{u,3f}^*V_{3k}^*x_{1,ki}}{4M_1^2}\left(7 + 4\log\left(\frac{m_t^2}{M_1^2}\right)\right) + \frac{3m_{\ell_f}x_{3,3f}^*x_{3,3i}}{8M_3^2} \tag{5.62}$$

with $C^R = C^{L\dagger}$, due to hermiticity. The branching ratio for the transition is written as

$$\mathrm{Br}(\ell_i \to \ell_f \gamma) = \frac{\alpha_{\mathrm{em}} m_{\ell_i}^3 \tau_{\ell_i}}{256\pi^4} \left(|C^L_{\ell_f \ell_i}|^2 + |C^R_{\ell_f \ell_i}|^2 \right) \tag{5.63}$$

We want to estimate the size of the transition $\tau \to \mu\gamma$, and $\mu \to e\gamma$ For the first one, supposing only Left-handed S_3 couplings dominate, we get

$$\mathrm{Br}(\tau \to \mu\gamma) \sim 1.4 \times 10^{-3}\ \delta^2\, \epsilon_{q3}^4 \epsilon_{l2}^2 \epsilon_{l3}^2 |c_{3,33}|^2 |c_{3,32}|^2\ , \tag{5.64}$$

whereas if Right-handed couplings dominate, we get

$$\mathrm{Br}(\tau \to \mu\gamma) \sim 1.7 \times 10^{-6} \left(\frac{\mathrm{TeV}}{M}\right)^4 \frac{\epsilon_{l2}^2}{\epsilon_{l3}^2} \left(\widetilde{c}_{33}^2 c_{1,32}^2 + \left(\frac{m_\mu}{m_\tau}\right)^2 \left(\frac{\epsilon_{l3}}{\epsilon_{l2}}\right)^4 \widetilde{c}_{32}^2 c_{1,33}^2 \right)\ . \tag{5.65}$$

For this contribution to the branching ratio, we note first that it has an explicit dependence on M that goes like M^{-4}, thus, the contribution grows for smaller values of the LQ masses. Also, we recognize two regimes that contribute to this quantity. For $\epsilon_{l2} \gtrsim \epsilon_{l3}$, the second term is suppressed by the ratio of muon to tau mass. For $\epsilon_{l3} \gtrsim \sqrt{\frac{m_\tau}{m_\mu}}\epsilon_{l2}$, the second term starts to dominate.

The experimental bound from Ref. [168] is: $\mathrm{Br}(\tau \to \mu\gamma)_{\mathrm{exp}} < 4.4 \times 10^{-8}$, at 90 %CL.

In the case of $\mu \to e\gamma$, we use the expressions above, changing the lepton flavors and $m_e \sim 511$ keV, $\tau_\mu \sim 2\ \mu s$. For the Left-handed contribution, we get an expression similar to Eq. (5.64),

$$\mathrm{Br}(\mu \to e\gamma) \sim 7 \times 10^{-3}\ \delta^2\, \epsilon_{q3}^4 \epsilon_{l1}^2 \epsilon_{l2}^2 |c_{3,32}|^2 |c_{3,31}|^2\ , \tag{5.66}$$

Whereas for Right-handed couplings the contribution is

$$\mathrm{Br}(\mu \to e\gamma) \sim 8 \times 10^{-6} \left(\frac{\mathrm{TeV}}{M}\right)^4 \frac{\epsilon_{l1}^2}{\epsilon_{l2}^2} \left(\widetilde{c}_{32}^2 c_{1,31}^2 + \left(\frac{m_e}{m_\mu}\right)^2 \left(\frac{\epsilon_{l2}}{\epsilon_{l1}}\right)^4 \widetilde{c}_{31}^2 c_{1,32}^2 \right)\ . \tag{5.67}$$

The experimental bound is $\mathrm{Br}(\mu \to e\gamma) < 4.2 \times 10^{-13}$ [169], at 90 %CL. The Left-handed contribution, taking as an example similar degree of compositeness of both chiralities of the electron, $\epsilon_{l1} \sim \epsilon_{e1} \sim 7 \times 10^{-4}$, and other typical values for the parameters, is of order 3.6×10^{-15}. The Right-handed contribution, however, is a bit more compromised. Eq. (5.67) has a minimum for $\epsilon_{l1}/\epsilon_{l2} \sim 0.07$, leading to $\mathrm{Br}(\mu \to e\gamma) \sim 4 \times 10^{-8} (\mathrm{TeV}/M)^4$. In this setup, for $M = 1$ TeV a cancellation of order 10^{-5} is required, otherwise $M \gtrsim 20$ TeV in the absence of cancellations. Another possibility is to decouple the electron mass from partial compositeness, assuming that its degree of compositeness is much smaller than the previous estimates and that its mass is generated by anarchic tiny bilinear interactions of the elementary fermions with the

Higgs [93] (see also [113, 170] for other related approaches). In the following we will assume this to be the case.

5.2.12. $\ell_i \to 3\ell_f$

We consider here observables $\tau \to 3\mu$ and $\mu \to 3e$, which have loop level contributions, induced by the flavor violating $Z\mu\tau$ and $Ze\mu$ couplings, and four-lepton operators [60, 171]:

$$\begin{aligned}\mathrm{Br}\left(\ell_i \to 3\ell_f\right) &= 2.5\times 10^{-4}\left(C^T_{if33} - C^S_{if33}\right)^2 \\ &= 6.25\times 10^{-5}\left(\frac{v^2_{\rm SM}x_{1,3i}x^*_{1,3f}}{M_1^2} + \frac{v^2_{\rm SM}x_{3,3i}x^*_{3,3f}}{M_3^2}\right)^2 \\ &\sim 0.001\,\delta^2\epsilon^4_{q3}\epsilon^2_{lf}\epsilon^2_{li}\left(c^*_{1,3f}c_{1,3i} + c^*_{3,3f}c_{3,3i}\right)^2 \ . \end{aligned} \tag{5.68}$$

For $\tau \to 3\mu$ decay, we have $i \to 3$, $f \to 2$ in the expression above. The experimental bound is $\mathrm{Br}\left(\tau \to 3\mu\right)_{\rm exp} < 1.2\times 10^{-8}$, at 90 % CL. This value, along with the $\tau \to \mu\gamma$ are expected to increase in sensitivity by an order of magnitude in Belle II [172].

For the $\mu \to 3e$ decay, we set $i \to 2$, $f \to 1$. The experimental limit is, at 90 % CL is $\mathrm{Br}\left(\mu \to 3e\right)_{\rm exp} < 1.0\times 10^{-12}$ [173]. The expected size of this observable now depends on the size of the mixing to first generation leptons, ϵ_{l1}. For $\epsilon_{l1} \sim \epsilon_{e1}$, $\delta \sim 0.02 - 0.2$, $\epsilon_{q3} \sim 0.5$ and $\epsilon_{l2} \sim 0.2$, the size of this branching ratio is at least two orders of magnitude below the experimental limit. For non-symmetric mixing ϵ_{l1} can be taken of order 0.003 or 0.03 if $\delta \sim 0.2$ or 0.02, respectively. In the case of negligible linear mixing this process does give interesting constraints.

5.2.13. LFU in W couplings

The LQs generate contributions to W couplings at one loop that violate lepton universality. In the present model the relevant modifications are for the leptons of the third generation [60, 171]:

$$\begin{aligned}\left|\frac{g^W_\tau}{g^W_\ell}\right| &= 1 - 0.084\,C^T_{3333} = 1 - 0.084\left(\frac{v^2_{\rm SM}}{4M_1^2}|x_{1,33}|^2 - \frac{v^2_{\rm SM}}{4M_3^2}|x_{3,33}|^2\right) \\ &\sim 1 - 0.084\,\delta\,\epsilon^2_{q3}\epsilon^2_{l3}\left(|c_{1,33}|^2 - |c_{3,33}|^2\right)\end{aligned} \tag{5.69}$$

The ratio $|g^W_\tau/g^W_\ell|$ is measured to be 1.0000 ± 0.0014 [174], at 95 %CL.

5.3. Numerical results for flavor physics

We wish to test if the B-anomalies and the flavor constraints detailed above can be made compatible with an anarchic partial compositeness scenario. For this purpose we will explore if $R_{K^{(*)}}$ and $R_{D^{(*)}}$ can be fitted simultaneously to within 1σ of their experimental values, with the bounds being satisfied at the confidence levels specified in the previous section.

The observables depend on different combinations of the parameters $c_{1,i\alpha}, c_{3,i\alpha}$ and $\tilde{c}_{1,i\alpha}$, we will refer to those combinations as $\Delta_O^{(i)}$, with O the observable, and i an index labeling the number of independent combinations of that O. For example, for $R_{D^{(*)}}$ we have the combinations:

$$\Delta^{(1)}_{R_{D^{(*)}}} \equiv |c_{1,33}|^2 - |c_{3,33}|^2 \ , \qquad \Delta^{(2)}_{R_{D^{(*)}}} \equiv c_{1,23}c^*_{1,33} - c_{3,23}c^*_{3,33} \ . \tag{5.70}$$

For each observable that has a different combination of the parameters $c_{1,i\alpha}, c_{3,i\alpha}$ or $\tilde{c}_{1,i\alpha}$, as we are working under the assumption of flavor anarchy, we will take all these coefficients as independent and of the same order. For particular values of these coefficients, the model can pass all flavor constraints and simultaneously explain the B-anomalies, however, we will explore whether this happens for generic $\mathcal{O}(1)$ coefficients. Whenever some Δ_O is required to deviate from $\mathcal{O}(1)$, the assumption of anarchic partial compositeness is in tension with that observable. Typically, the bounds from flavor observables are expected to favor $\Delta_O < \mathcal{O}(1)$, showing the need of some alignment or tuning, since in the limit of vanishing Δ_O the new physics contributions vanish. On the other hand, an explanation of the B-anomalies requires sizeable $\Delta_{R_{D^{(*)}}}$ and $\Delta_{R_{K^{(*)}}}$, and for some regions of the parameter space they can be required to be: $\Delta_O > \mathcal{O}(1)$, deviating from the assumption of flavor anarchy.

Besides Δ_O, the observables depend on δ, defined in Eq. (5.23), on the LQ mass M, as well as on the Left-handed mixings of the top and the leptons, since we have used Eqs. (2.63), (2.64) and (2.65) to fix the size of the other mixings.

To estimate the amount of tuning one expects in the $\mathcal{O}(1)$ coefficients contributing to the B-anomalies, we proceed in the following way: for a given point of the parameter space, we compute which are the values of $\Delta_{\mathcal{O}}$ that cause the observables to fall within the 1σ experimental value and the corresponding CL intervals. In those cases where there is more than one Δ_O, as in $R_{D^{(*)}}$ or $\tau \to \mu\gamma$, we consider either the largest contribution, if they are of different order, or consider them separately, if their ordering depends on the particular region of the parameter space. Then we select the points that can reproduce all the flavor bounds with Δ_O of order 1, allowing for a certain threshold. To do this, we perform a random scan over the free parameters, we take: $\epsilon_{q3}, \epsilon_{l3} \in [0.5, 1]$, $\epsilon_{l2} \in [0.08, 0.25]$, $\delta \in [0.02, 0.2]$, and $M \in [1, 3]$ TeV. Scanning over

$200k$ initial points, we select the ones that have $\min(\Delta_O) \geq 0.95$, obtaining $\sim 10k$ points. There are 4 observables that have the smallest Δ_O, and can thus be identified as the most sensitive, these are: Δm_{B_s} on 35 % of the points, followed by g_τ^W on 28 % of the points, followed by $\tau \to \mu\gamma_{(\mathrm{R})}$ on 23 % of the points and by $\tau \to 3\mu$ with the remaining 14 %. These are the observables that impose the most stringent bounds on the parameter space. Then, to estimate the amount of tuning required to explain the B-anomalies, we plot the required values for $\Delta_{R_{D^{(*)}}}$ and $\Delta_{R_{K^{(*)}}}$ on these points. We show our results in the distribution of Fig. 5.1, where we have truncated the upper limits of the graph to have a better focus on its densest region, as the tails of the distribution go to higher values but with a very small density. In this figure we see that explaining $R_{D^{(*)}}$ at 1σ level requires some tuning, since the peak of $\Delta_{R_{D^{(*)}}}$ is in the range $3-6$, whereas $R_{K^{(*)}}$ can be explained with $\Delta_{R_{K^{(*)}}} \sim 0.25 - 1$. This result shows that the former observable is in tension with the flavor constraints. Similarly, by allowing for higher tuning in the flavor constraints, that is: allowing their $\Delta_O \sim 0.05 - 0.3$, one can take $\Delta_{R_{D^{(*)}}} \simeq 1$. Besides we find that the distribution of M is peaked around 1.8 TeV.

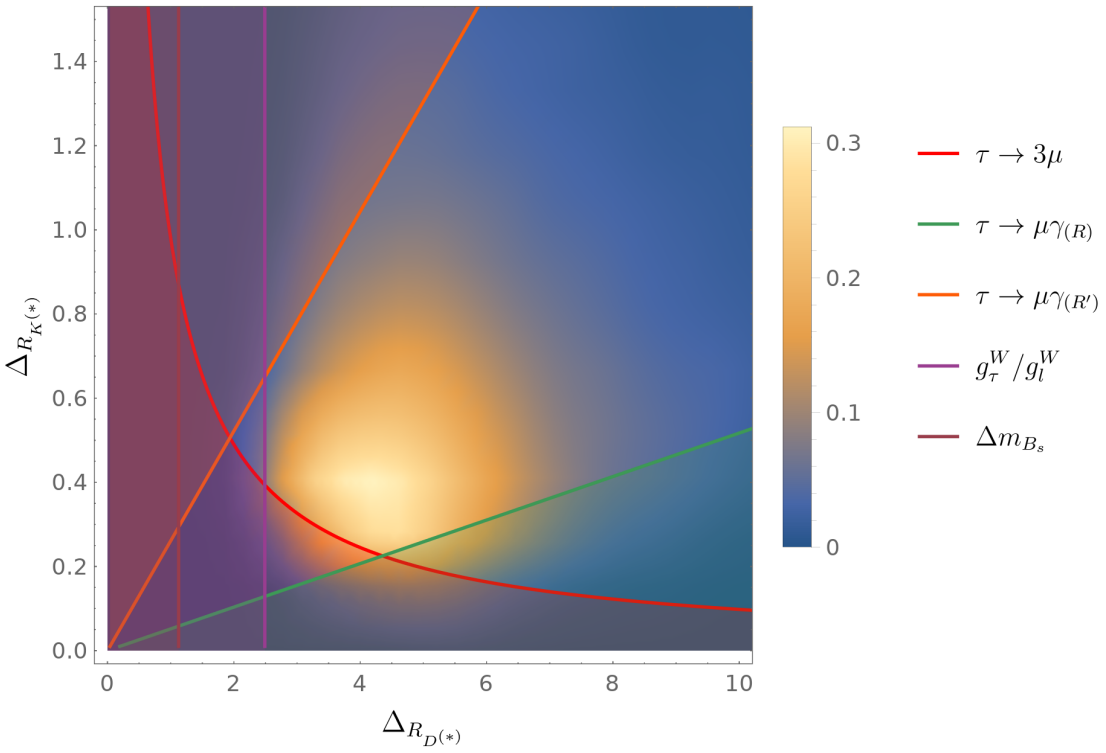

Figure 5.1: Distribution of required values for $\Delta_{R_{D^{(*)}}}$ and $\Delta_{R_{K^{(*)}}}$, for points passing all flavor observables with the other $\Delta_O \simeq 1$. The colored curves show the estimates of the bounds coming from Eq. (5.71) and below, for $M = 1.5$ TeV. The regions excluded following those approximations have been shaded.

We can explain the shape of the lower limit of this region by looking at what flavor constraint those points correspond to. Let us consider $\tau \to 3\mu$, we have to check this

observable's expression along with those of $R_{K^{(*)}}$ and $R_{D^{(*)}}$. We see that $\tau \to 3\mu$ depends on 4 of the 5 parameters in the random scans. Furthermore, we can multiply the expressions for $R_{K^{(*)}}$ and $R_{D^{(*)}}$, taking into account the lower 1σ limits for the observables. In this product, we then replace the combination of parameters $\delta^2\epsilon_{q3}^4\epsilon_{l2}^2\epsilon_{l3}^2$ that saturates the bound in $\tau \to 3\mu$, getting:

$$\Delta_{R_{K^{(*)}}}\Delta_{R_{D^{(*)}}} \simeq \frac{0.49 \times 0.083\, V_{tb}\, \alpha_{\rm em}\Delta_{\tau 3\mu}}{1.2 \times 10^{-5}\, 8\pi} \simeq \Delta_{\tau 3\mu}\ , \tag{5.71}$$

which partially explains the shape of the lower limit seen in Fig. 5.1 above. Making a similar analysis with g_τ^W we obtain: $\Delta_{R_{D^{(*)}}} \gtrsim 2.5\Delta_{g_\tau^W}$. The other observables depend also on M, from Δm_{B_s} we obtain: $\Delta_{R_{D^{(*)}}} \gtrsim 1.6M\Delta^{1/2}_{\Delta m_{B_s}}$, and from $\tau \to \mu\gamma$ we obtain a lower limit $\Delta_{R_{D^{(*)}}} \gtrsim 18(\text{TeV}/M)^4\Delta_{R_{K^{(*)}}}\Delta^{(R')}_{\tau\to\mu\gamma}$ and a lower limit $\Delta_{R_{D^{(*)}}} \lesssim 3.5(M/\text{TeV})^4\Delta_{R_{K^{(*)}}}/\Delta^{(R)}_{\tau\to\mu\gamma}$, where the superindices indicate the different combinations of coefficients present in the Right-handed contribution to this process. For $M \lesssim 1.3$ TeV the bounds from $\tau \to \mu\gamma$ are not compatible with $\Delta \simeq 1$, whereas g_τ^W and Δm_{B_s} give a lower bound $\Delta_{R_{D^{(*)}}} \gtrsim 2.5$.

The previous results show that there is a minimum amount of tuning, since $\Delta_{R_{D^{(*)}}}$, expected to be $\mathcal{O}(1)$, must be of $\mathcal{O}(2.5-7)$ when the other $\Delta_{\mathcal{O}}$ are of $\mathcal{O}(1)$, requiring some alignment or tuning. We will consider a scenario referred as minimal tuning, in which $\Delta_{R_{K^{(*)}}}, \Delta_{R_{D^{(*)}}} \leq 5$, whereas $\Delta_{\mathcal{O}} \geq 0.3$. In the case of the B-anomalies, we plot a contour line for those points that require $\Delta_{R_{D^{(*)}}} = 5$ and/or $\Delta_{R_{K^{(*)}}} = 5$ in order to explain $R_{D^{(*)},\text{exp}}$ or $R_{K^{(*)},\text{exp}}$, and we show in green the region where any of those Δ_O are required to be larger than 5. For the other observables, this is done by plotting a contour line with $\Delta_O = 0.3$, while in red we show the region with $\Delta_O < 0.3$. In the white region the observables can be reproduced with minimal flavor tuning.

In Fig. 5.2 we fix $\delta = 0.1$ and $M = 2$ TeV, that are values expected according to the estimates of Sec. 3.1. We also fix in each case one of the compositeness fractions ϵ_f, and scan along the other two. We include all three of those sections for a better picturing of this dependence. Looking at the first section of Fig. 5.2, in the plane $\epsilon_{l3} - \epsilon_{q3}$, we see that the allowed region is limited by $\tau \to 3\mu$, Δm_{B_s} and $R_{D^{(*)}}$. As can be seen from Eqs. (5.68), (5.47) and (5.24), the window moves with δ and powers of ϵ_f. As $\tau \to 3\mu$ depends quadratically on δ, this limit moves faster with increasing δ than the others. As the dependence is on positive powers of these ϵ_f, an increase in δ will translate into a decrease of the allowed values of these coefficients, thus lowering the location of the window. The remaining fixed parameters in this figure are ϵ_{l2} and M. Although not all the quantities depend explicitly on the LQ mass M, there are those that do in different ways. For example, Eq. (5.47) shows that Δm_{B_s} depends quadratically on M, whereas $\tau \to \mu\gamma$(R) has an M^{-4} dependence shown in Eq. (5.65). This means that the same figure, with a smaller value for M, will have a less stringent bound imposed by Δm_{B_s},

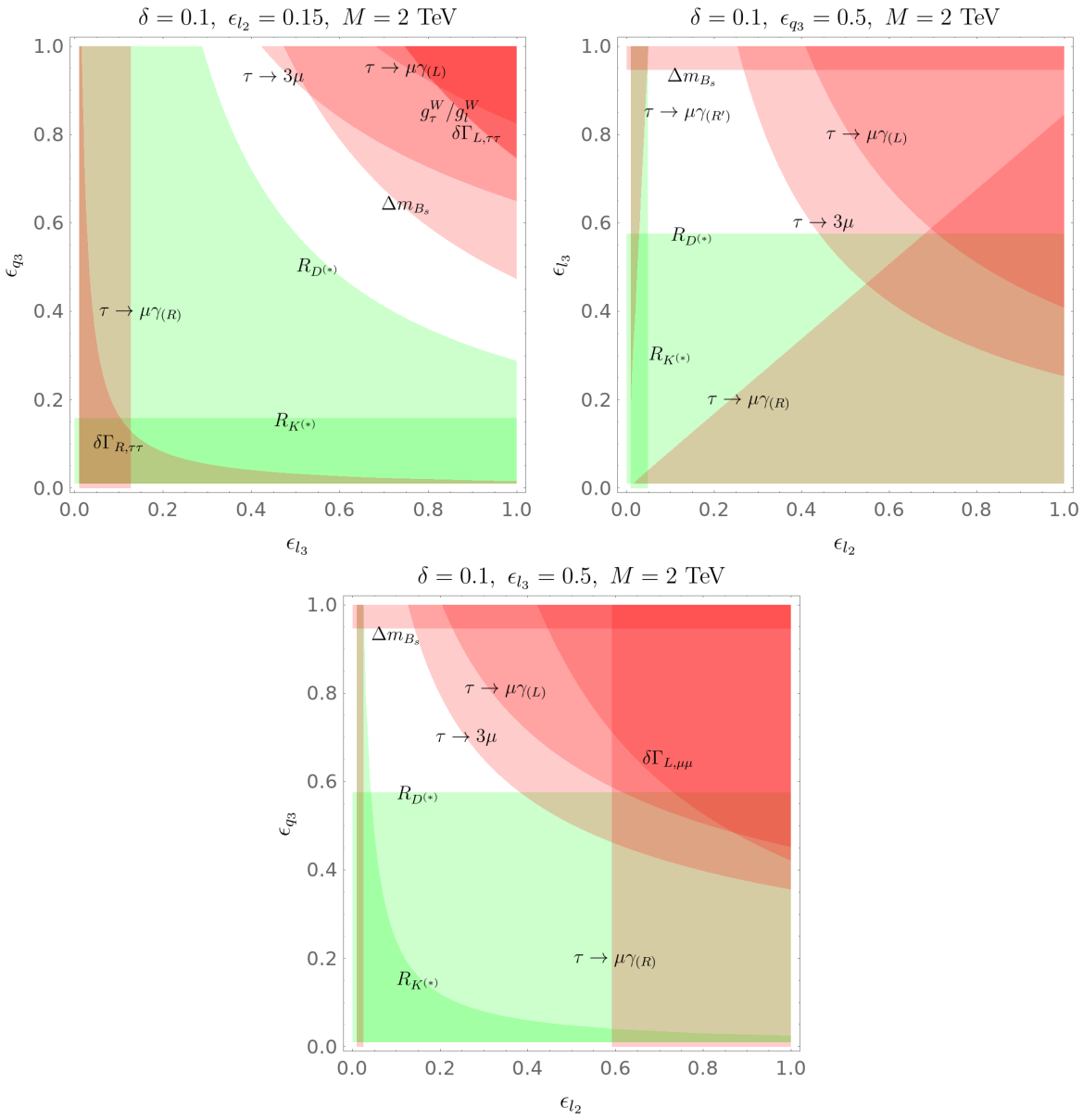

Figure 5.2: Scans in each pair of compositeness fraction ϵ_f, for fixed values of δ.

but a much more restrictive bound imposed by $\tau \to \mu\gamma$(R). The dependence on ϵ_{l2} can be seen by looking at the other sections in Fig. 5.2, or by looking at the expressions above. For example, as $R_{K^{(*)}}$ depends on ϵ_{l2}, we see how a lower value of ϵ_{l2} will make the bound imposed by R_K on the minimum ϵ_{q3} to increase, eventually becoming one of the bounds on the allowed window. The same reasoning can be applied to the other sections on the figure. In the plane $\epsilon_{l2} - \epsilon_{l3}$ we can see the two limits imposed by the two contributions to $\tau \to \mu\gamma$(R), where one dominates for $\epsilon_{l2} \gtrsim \epsilon_{l3}$, and the other in the limit $\epsilon_{l3} \gg \epsilon_{l2}$. These bounds are not as relevant for $M = 2$ TeV, however, but decreasing the value of the LQ mass to 1 TeV makes them become two of the most important bounds for the allowed window, surpassing the limits imposed by $R_{K^{(*)}}$ and by $\tau \to 3\mu$.

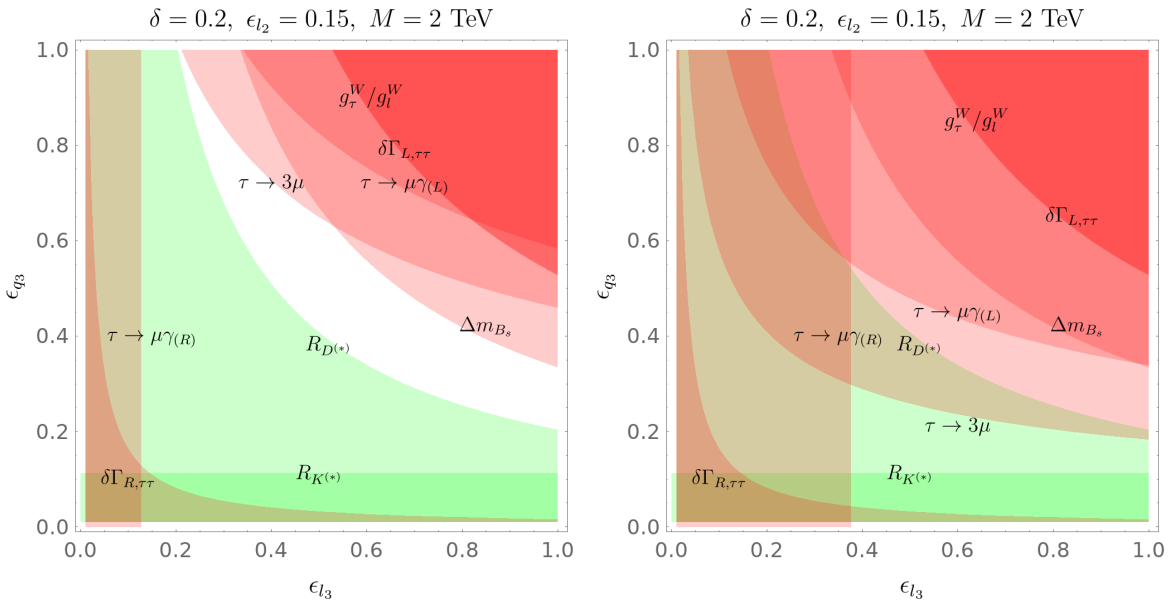

Figure 5.3: Left panel: Current bounds, Right panel: expected increase in sensitivity for LFV in τ decays

The bounds will change in the future, as the precision of experiments improves, particularly interesting is $\tau \to 3\mu$. For instance, in Belle II the expected sensitivity for the branching ratios in LFV searches in τ decays improves by either one or two orders of magnitude [172]. If no departure from the SM is observed, we expect:

$$\begin{aligned} \text{Br}(\tau \to \mu\gamma) &= 4.4 \times 10^{-8} \to 5 \times 10^{-9} \quad (90\,\%\text{CL}), \\ \text{Br}(\tau \to 3\mu) &= 1.2 \times 10^{-8} \to 3 \times 10^{-10} \quad (90\,\%\text{CL}). \end{aligned} \tag{5.72}$$

We can then check how the new bounds look on our 2d scans in ϵ_f space. For example, for $\epsilon_{l2} = 0.15$, we show the current and the expected bounds, side by side in Fig. 5.3. There we use a different value for one of the parameters, compared with Fig. 5.2: $\delta = 0.2$. In the left we show how some of the curves get modified by the enlargement of δ, whereas on the right we show the expected increase in sensitivity. The limit imposed by $\tau \to 3\mu$ rules out the selected window, meaning that either a higher tuning would be needed to pass the constraints, or that some violation of this quantity would have to be observed. We can tune some parameters to recover the window, for instance by lowering $\epsilon_{l2} = 0.08$ and increasing $M = 3$ TeV, we get a small window for $\epsilon_{l3} \simeq 1$. In this case the window is small and is located around $\epsilon_{q3} \simeq 0.3$, a somewhat low degree of compositeness compared with the usual scenarios of composite Higgs models.

5.4. Spectrum of resonances

In this section we describe the phenomenology of the composite model, focusing on the spectrum of resonances, both spin 1 and 1/2. The scale of the masses of these resonances is $m_* \simeq g_* f \sim 10-30$ TeV. The quantum numbers of the resonances are set by the group theory alone in the case of the spin-1 resonances, or by the embeddings of the SM fermions in irreducible representations of the global symmetry group of the SCFT.

Before describing those resonances we analyze very briefly the LHC phenomenology of the spin 0 states. Pair production of S_1 and S_3 by QCD interactions depend only on the LQ masses to leading order, whereas single production is more model dependent, being subleading for masses below $\sim 1.1-1.5$ TeV [60]. Given the flavor structure of the couplings to SM fermions, the LQs decay predominantly to fermions of the third generation, moreover, the charge $-1/3$ states decay to $b\nu$ and $t\tau$ with similar branching fractions [140]. ATLAS [175, 176] and CMS [177] have searched for these LQs in different final states, CMS taking into account contributions from double and single production, in the last case with couplings of order $1.5-2.5$, that are of similar size as the couplings expected in the present model. Those analyses exclude masses below $\sim 1.1-1.2$ TeV, leading to the most stringent bounds today from direct searches. Although in our model some bounds from flavor physics require masses above the limits from LHC: $m_{\rm LQ} \gtrsim 1.5$ TeV, there are two LQs with charge $-1/3$ that could add up and give a larger cross section than in the case of just one state, perhaps strengthening the bounds. This interesting situation deserves a careful analysis that is beyond the scope of this work.

5.4.1. Spin-1 resonances

To obtain the quantum numbers of the spin-1 resonances we use that $\mathbf{Adj}[\mathrm{SO}(10)\times \mathrm{SO}(5)] = (\mathbf{Adj}[\mathrm{SO}(10)], \mathbf{1}) \oplus (\mathbf{1}, \mathbf{Adj}[\mathrm{SO}(5)])$, and we decompose these adjoint representations under the SM symmetry group. Regarding the SO(5) adjoint representation, it is as in the MCHM, leading to resonances transforming under $\mathrm{G_{SM}}$ as:

$$(\mathbf{1},\mathbf{3})_0 + (\mathbf{1},\mathbf{1})_{\{+1,0,-1\}} + (\mathbf{1},\mathbf{2})_{\pm\frac{1}{2}} \tag{5.73}$$

Thus before EWSB there are multiplets that transform as the Ws and B of the SM, along with new states transforming as charged weak doublet and singlet. After EWSB, we get states with charges ± 1 and 0, similar to heavy resonances of W and Z bosons.

When looking at the SO(10) adjoint representation, using Eqs. (5.2), (5.4) and (5.7),

we get the following representations under G_{SM} for the remaining vectorial resonances:

$$(\mathbf{1},\mathbf{3})_0 + (\mathbf{3},\mathbf{1})_{-\frac{1}{3}} + (\mathbf{3},\mathbf{3})_{-\frac{1}{3}} + (\mathbf{1},\mathbf{1})_0 + (\mathbf{3},\mathbf{1})_{\frac{2}{3}} + (\mathbf{8},\mathbf{1})_0 + \text{h.c.} \ . \tag{5.74}$$

Here we recognize W-like, Z-like and gluon-like resonances, along with three representations transforming as color triplets and charged. If we look at their quantum numbers, we can identify them with LQs as:

$$\begin{aligned}
&(\mathbf{3},\mathbf{1})_{-\frac{1}{3}} \to \bar{U}_1 \ , \\
&(\mathbf{3},\mathbf{1})_{\frac{2}{3}} \to U_1 \ , \\
&(\mathbf{3},\mathbf{3})_{-\frac{1}{3}} \to X \ .
\end{aligned} \tag{5.75}$$

The state transforming as $(\mathbf{3},\mathbf{3})_{-1/3}$ which we call X, does not couple to the SM fermions through $d = 4$ operators, and hence all possible interactions will be suppressed by powers of a higher scale. At the same order the LQ $\bar{U}_1$ only has interactions involving Right-handed neutrinos ν_R, whereas U_1 has coupling with the doublets q_L and l_L. However, if we look at the $\mathrm{SU}(2)_A \times \mathrm{SU}(2)_B$ structure of the representations, we see there is no way to couple U_1 to both q_L and l_L at tree level, without further insertions of fields. This is because, under $\mathrm{SU}(2)_A \times \mathrm{SU}(2)_B$, $U_1 \sim (\mathbf{1},\mathbf{1})$, whereas $q_L \sim (\mathbf{2},\mathbf{1})$ and $l_L \sim (\mathbf{1},\mathbf{2})$, hence there is no singlet combination when multiplying these three fields.

We consider now the decay of these LQs. They are embedded in two different representations of SO(6): U_1 is in $\mathbf{15}$, whereas $\bar{U}_1$ and X are in the $\mathbf{6}$. The lowest dimensional operator respecting the H symmetry that allow the decay of U_1 require one insertion of a scalar LQ. Using that for SO(6): $\mathbf{4}\times\mathbf{4}\times\mathbf{15}\times\mathbf{6} \supset \mathbf{1}$, the following operators can be considered:

$$\mathcal{O}_U^6 = (\bar{q}_L^c \sigma_{\mu\nu} l_L)\ S_1\, \partial^{[\mu} U_1^{\nu]} \ , \qquad \tilde{\mathcal{O}}_U^6 = (\bar{q}_L^c \sigma_{\mu\nu} \sigma^a l_L)\ S_3^a\, \partial^{[\mu} U_1^{\nu]} \ . \tag{5.76}$$

The decay into SM particles proceeds then through a scalar LQ, with a final state containing 4 SM fermions: $U_1 \to \bar{q}\bar{\ell} S_{1,3}^\dagger \to \bar{q}\bar{q}'\bar{\ell}\bar{\ell}'$.

Regarding the LQs present in representation $(\mathbf{6},\mathbf{2},\mathbf{2})$, we can write dimension 5 operators:

$$\mathcal{O}_{\bar{U}}^5 = (\bar{q}_L^c \sigma_{\mu\nu} l_L)\ \partial^{[\mu} \bar{U}_1^{\nu]*} \ , \qquad \mathcal{O}_X^5 = (\bar{q}_L^c \sigma_{\mu\nu} \sigma^a l_L)\ \partial^{[\mu} X_a^{\nu]*} \ . \tag{5.77}$$

These two other states decay into a quark and a lepton, without a scalar LQ insertion.

The WCs of these operators are expected to be generated at loop level, requiring also insertions of the mixing factors $\epsilon_q\, \epsilon_l$, that are dominated by those of the third generation, thus the final fermions are preferentially of the third generation.

We can investigate the effect of these operators on the phenomenology by integrating-out the spin-1 states and estimating the size of their contributions to other WCs. Starting from the Lagrangian for a massive $\bar{U}_1$ and the interactions given by $c_{\bar{U}}\mathcal{O}^5_{\bar{U}}$, at low energies we get the effective dimension 8 interaction

$$\mathcal{L}_{qlql} = -\frac{3}{2}\frac{c^2_{\bar{U}}}{M^2_{\bar{U}_1}}\partial_\mu(\bar{q}^c_L\sigma^{\mu\nu}l_L)\partial^\rho(\bar{q}^c_L\sigma_{\rho\nu}l_L) \tag{5.78}$$

that is expected to be suppressed compared with the effect of dimension 6 operators. To estimate its effect on meson physics one has to make use of Fierz identities, to transform the Lorentz structure into the more familiar $(\bar{q}_L M q_L)(\bar{l}_L M l_L)$, with M generically representing some matrix with Lorentz indices. This is a somewhat involved process, as the matrix structure is not the usual $\sigma_{\mu\nu}\sigma^{\mu\nu}$ one, this one having two free Lorentz indices that are contracted with derivatives. Although the analysis of dimension 8 operators is beyond the scope of this work, one can make an estimate of the size of their WCs assuming that the energies are of order GeV, obtaining a coefficient: $(\partial)^2 c^2_{\bar{U}_1}/M^2_* \sim (\text{GeV})^2 c^2_{\bar{U}_1}/M^2_*$. This WC can be compared with those generated by the scalar LQs for dimension 6 operators at tree level, that are of order $\sim x^2/M^2_{1,3}$. Assuming that $c_{\bar{U}}$ is generated at loop level: $c_{\bar{U}} \sim (g_*/4\pi)^2 g_* \epsilon_q \epsilon_l / M_*$, one can estimate the ratio to be

$$\left(\frac{g_*}{4\pi}\right)^4 \left(\frac{\text{GeV}}{M_*}\right)^2 \left(\frac{M_{1,3}}{M_*}\right)^2 \sim 1.06\times 10^{-12}\left(\frac{g_*}{4}\right)^4 \left(\frac{M_{1,3}}{\text{TeV}}\right)^2 \left(\frac{10\text{ TeV}}{M_*}\right)^4 \tag{5.79}$$

If the operator $\mathcal{O}^5_{\bar{U}}$ were generated at tree-level, then this ratio would be enhanced by a factor $(4\pi/g_*)^4$, giving a ratio of $\sim 10^{-10}$. We therefore can expect the effect of the vector LQs on the meson phenomenology to be suppressed, since their interactions with the SM fermions arise from operators of dimension 5 or 6.

5.4.2. Fermionic resonances

In the case of fermion fields one can proceed in a similar way to study their quantum numbers, decomposing their representations under G_{SM}.

For $(\mathbf{16},\mathbf{5})$ we obtain:

$$(\mathbf{16},\mathbf{5}) \supset (\mathbf{3},\mathbf{2})_{\frac{1}{6}} + (\mathbf{1},\mathbf{2})_{-\frac{1}{2}} + (\mathbf{3},\mathbf{1})_{\{\frac{2}{3},-\frac{1}{3}\}} + (\mathbf{3},\mathbf{3})_{\{\frac{2}{3},-\frac{1}{3}\}} + (\mathbf{1},\mathbf{1})_{\{0,-1\}} + (\mathbf{1},\mathbf{3})_{\{0,-1\}} + \text{h.c.} \tag{5.80}$$

leading to massive resonances with the same quantum numbers as the SM fields: q_L, l_L, u_R, d_R, ℓ_R, as well as a singlet. Besides these states, we find fields similar to u_R, d_R, ℓ_R and ν_R, with the exception that they transform as triplets under $\text{SU}(2)_L$, instead of

singlets. This gives rise, after EWSB, to states with exotic charges, the color triplets with $Q = 5/3, -4/3$, and the color singlet with $Q = -2$.

When decomposing $(\overline{\mathbf{144}}, \mathbf{5})$ under the SM group we find a set of fields having, under $\mathrm{G_{SM}}$, the same properties appearing in $(\overline{\mathbf{16}}, \mathbf{5})$. Besides them, with the appearance of representations $(\mathbf{4}, \mathbf{3}, \mathbf{2})$ and $(\bar{\mathbf{4}}, \mathbf{2}, \mathbf{3})$, we get similar states but forming different multiplets under $\mathrm{SU}(2)_L$. For example, we get a quark-like state with quantum numbers $(\mathbf{3}, \mathbf{4})_{1/6}$, along with other states that transform as singlets, triplets and quintuplets under the weak group. Finally, when observing the representations that come from the decomposition of the **20** of SO(6), we get:

$$\begin{aligned}&(\mathbf{3},\mathbf{1})_{\{\frac{2}{3},-\frac{1}{3}\}} + (\mathbf{3},\mathbf{2})_{\frac{1}{6}} + (\mathbf{3},\mathbf{3})_{\{\frac{2}{3},-\frac{1}{3}\}} + (\bar{\mathbf{3}},\mathbf{1})_{\{\frac{4}{3},\frac{1}{3}\}} + (\bar{\mathbf{3}},\mathbf{2})_{\frac{5}{6}} + (\bar{\mathbf{3}},\mathbf{3})_{\{\frac{4}{3},\frac{1}{3}\}} \\ &+ (\bar{\mathbf{6}},\mathbf{1})_{\{\frac{2}{3},-\frac{1}{3}\}} + (\bar{\mathbf{6}},\mathbf{2})_{\frac{1}{6}} + (\bar{\mathbf{6}},\mathbf{3})_{\{\frac{2}{3},-\frac{1}{3}\}} + (\mathbf{8},\mathbf{1})_{\{0,-1\}} + (\mathbf{8},\mathbf{2})_{-\frac{1}{2}} + (\mathbf{8},\mathbf{3})_{\{0,-1\}} \end{aligned} \tag{5.81}$$

The $\overline{\mathbf{20}}$ contains the conjugate representations, that, besides the aforementioned states, leads to a new exotic color triplet with $Q = -7/3$. This state decays into another exotic-charged state of $Q = -4/3$, which then decays into SM states. In addition we find other states that transform as a sextet of $\mathrm{SU}(3)_c$. Given the algebra of SU(3): $\bar{\mathbf{3}} \times \bar{\mathbf{3}} = \mathbf{3} + \bar{\mathbf{6}}$, a $\bar{\mathbf{6}}_{2/3}$ decays into two color anti-triplets: a scalar LQ and a SM quark, leading to a final state with two quarks and one lepton after the decay of the scalar LQ. Notice that these interactions are allowed by the $\mathrm{SO}(6) \times \mathrm{SU}(2)_A \times \mathrm{SU}(2)_B$ subgroup of SO(10), since $\mathbf{20} \times \mathbf{6} \times \bar{\mathbf{4}} \supset \mathbf{1}$, thus an invariant can be formed with a resonance in a sextet, one LQ and one SM antiquark. The treatment for the octet is similar, it decays through an intermediate scalar LQ. The octet with $Q = -2$ decays through a LQ of charge $-4/3$ and an anti-top.

5.5. Summary and Discussion

We have proposed a model to explain the B-anomalies, investigating its capability to simultaneously pass the bounds from other flavor observables. We have considered a strongly coupled theory based on a global symmetry group $\mathrm{SO}(10) \times \mathrm{SO}(5)$, spontaneously broken to $\mathrm{SO}(6) \times \mathrm{SU}(2)_A \times \mathrm{SU}(2)_B \times \mathrm{SO}(4)$ by the strong dynamics. This pattern of symmetries have several properties: it contains the SM gauge symmetry group, it develops only the LQs S_1 and S_3, and the Higgs, as NGBs, it contains a custodial symmetry. We have determined the embeddings of the SM fermions into the larger symmetry group, selecting by phenomenological reasons (**16,5**) and $(\overline{\mathbf{144}}, \mathbf{5})$, as well as their conjugates. We have shown that the embedding of all the fermions in (**16,5**) and its conjugate results in Left-handed LQ interactions that are equal for S_1 and S_3, thus they cannot accommodate simultaneously the flavor constraints and the B-anomalies. We have shown that mixing the lepton doublet with a $\overline{\mathbf{144}} \times \mathbf{5}$ can solve

this problem. Moreover, mixing it with resonances in both representations allows for couplings with S_1 and S_3 that are independent. We have considered an anarchic flavor structure of the SCFT that, along with partial compositeness, give a rationale for the SM fermion spectrum and mixings, and contains a GIM-like mechanism suppressing flavor transitions. As is well known, this flavor framework does not pass some bounds from meson mixing, thus we have assumed a scale of resonances of order $10 - 30$ TeV, increasing the amount of tuning required for the EW scale, that is estimated to be at least of order $0.1 - 1\,\%$.

We have considered an effective description of the dynamics where only the NGBs and the SM fields are kept, armed with it we have shown how to compute the one loop potential, estimating the masses of the leptoquarks in the range of few TeV. We have also computed the Higgs potential, that is similar to the MCHM based on SO(5)/SO(4). Besides, we have estimated the corrections of the heavy resonances to the $Zb_L\bar{b}_L$ coupling, which, due to the large degree of compositeness of the third generation quarks, gets corrections that are near the saturation of the bound. This signals that certain amount of tuning could be required for this observable. We have also discussed briefly the proton decay, that is forbidden by a discrete symmetry.

We have estimated the size of the contributions of the scalar LQs to the B-anomalies and to the flavor observables that pose the most stringent constraints, some of these contributions arise at tree level and others at loop level. For that analysis we have used the hypothesis of anarchic partial compositeness. We have performed scans in the degrees of compositeness of second and third generation of leptons, the third generation of quarks, the masses of the LQs and the strength of the coupling between composite resonances. We found that a tension arises between an explanation of $R_{D^{(*)}}$ and some flavor observables, mostly $\tau \to 3\mu$, but also $Z\nu\bar{\nu}$ and $\tau \to \mu\gamma$, that requires a tuning of order $10 - 25\,\%$. We have defined a window in parameter space with "minimal tuning", this window requires sizeable degrees of compositeness for third generation l_L and q_L, but the amount of compositeness is also bounded from above by some flavor constraints, particularly $\tau \to 3\mu$ and Δm_{B_s}. We have shown how some of these flavor constraints are expected to change in the future, introducing even more tension with $R_{D^{(*)}}$, and have shown the change in this window accordingly. We have also considered observables $\mu \to 3e$ and $\mu \to e\gamma$. We found that the former can be easily accommodated by our model, while the latter comes into conflict with the expected degree of compositeness for the electron. This can be solved with the introduction of small bilinear couplings, that for the first generation allow to decouple its mass from its degree of compositeness.

Several authors have considered the possibility to explain also the anomalous magnetic moment of the muon with the presence of scalar leptoquarks. In anarchic partial compositeness the estimate for the correction to this quantity is independent of the fermion degree of compositeness, depending only on the mass of the LQs. An explana-

tion of the experimental result would require a rather small LQ mass, $M \lesssim 250$ GeV, incompatible with direct search bounds, or a higher amount of tuning in the anarchic coefficients.

We have analyzed the spectrum of resonances, finding heavier copies of SM particles, as well as exotic states. Regarding vector resonances, we have found resonances of the W and Z bosons, as well as heavy gluons, plus three colored states that can be associated with leptoquarks. However, none of these leptoquarks can couple to SM fermions with $d = 4$ operators, either because of their quantum numbers, or because of the $\mathrm{SU}(2)_A \times \mathrm{SU}(2)_B$ symmetry. We have shown the smallest dimensional operators that allow these leptoquarks to decay into SM particles. Regarding the fermionic resonances, besides the states with the same charges as the SM ones, there are exotic states with charges $-7/3,\ -4/3,\ 5/3$, that are color triplets or sextets, as well as color octets and singlets with integer charges.

Finally let us comment on a few possible directions that could be investigated. We have estimated many quantities assuming generic properties of the theory of resonances, it would be interesting to compute them by considering specific realizations, as discrete composite models, or extra-dimensions. On a different direction, since some of the leading constraints are related with modifications of Z-couplings, it would be interesting to explore other representations of fermions that could protect them, and eventually relax the tension between the anomalies and some of the flavor constraints.

Chapter 6

A flavor model with partial compositeness and Froggatt-Nielsen mechanism

The discovery of the Higgs boson has definitely established the Standard Model as the best description nowadays of the elementary particles and interactions. Whereas most interactions in the SM involve the different gauge bosons, they are universal with respect to the three different generations of quarks and leptons present in the spectrum. However, these quarks and leptons show a particular pattern of masses and mixing angles. Focusing on the quark sector, their mass ratios can be parametrized at the TeV scale [132] in terms of the sine of the Cabibbo angle λ_C as:

$$\begin{aligned} &m_u : m_c : m_t \sim \lambda_C^8 : \lambda_C^4 : 1 \ , \\ &m_d : m_s : m_b \sim \lambda_C^5 : \lambda_C^3 : 1 \ , \\ &m_b : m_t \sim \lambda_C^3 : 1 \ , \\ &(V_{\rm CKM})_{12} \sim \lambda_C \ , \quad (V_{\rm CKM})_{13} \sim \lambda_C^3 \ , \quad (V_{\rm CKM})_{23} \sim \lambda_C^2 \ . \end{aligned} \tag{6.1}$$

In the SM this pattern of masses comes from the Higgs Yukawa interactions, which are not universal, and are given at high energies. However, if the SM is an effective theory valid up to a scale much larger than the TeV, the Higgs potential suffers from the hierarchy problem of the electroweak (EW) scale. We have seen that a possible solution to this problem is to consider the Higgs as a composite state of a new sector that is strongly coupled at the TeV scale. In this case the Yukawa couplings depend on the type of interactions between the SM fermions and the new sector, and the flavor structure must be generated at energies much smaller than the Planck scale [113]. Within the composite Higgs framework, as we have seen in Ch. 2, that partial compositeness presents an interesting paradigm for the generation of flavor, in which the SM fermions

are elementary fields that couple linearly with the operators of the strongly interacting sector, and where bilinear interactions are highly suppressed [178]. At low energies these linear interactions lead to mixing between elementary fermions and composite resonances, generating the Yukawa couplings with the composite Higgs that are controlled by this mixing. If the theory at high energies does not have any flavor symmetries, then the partial compositeness is anarchic (APC), as we have described in Sec. 2.2 and have made extensive use in Chs. 3 – 5. In APC, the hierarchy of linear mixings gives a rationale for the hierarchy of masses and mixing angles. As all flavor transitions are controlled by this mixing, APC contains a built-in GIM mechanism [90, 106, 179]. Still, as we have seen in Sec. 2.2.1, constraints coming from the K-meson system, as well as B-meson mixings and neutron dipole moments require the scale of compositeness to be one order of magnitude above the TeV, reintroducing in this way a small tension with the stability of the EW scale. The most stringent constraints come from the Left-Right operator in the Kaon system, $(\bar{d}_R s_L)(\bar{d}_L s_R)$, and from dipole operators of quarks of the first generation, as can be seen from Table 2.2 and from Eq. (2.99). These constraints put lower bounds on the resonance masses of order 10 TeV, and on the mass over coupling m_*/g_* of order 5 TeV, respectively. There are a few schemes involving flavor and CP symmetries that can alleviate these issues [89, 109, 110], but they are in tension with LHC tests of compositeness of the light quarks [180]. Another more promising proposal is that of dynamical flavor scales [113], as well as the addition of tiny bilinear interactions [93].

Another, quite different approach to the flavor puzzle of the SM is the Froggatt-Nielsen mechanism [181, 182]. This proposal introduces an abelian U(1) flavor symmetry in order to explain the occurrence of the large mass ratios of Eq. (6.1), and similarly for the lepton sector. The quarks and leptons of the SM are assigned certain charges under this symmetry, and the mechanism also involves a scalar with unit charge, ϕ, as well as many heavy fermions with various charges. As a product of a spontaneous symmetry breaking, the singly charged scalar acquires a VEV, where the scale of the breaking is given by the ratio of this VEV over the UV scale of the theory (or the scale of the heavy fermions) Λ. As the Higgs field is also neutral under this new symmetry, it is through insertions of powers of this field, along with heavy fermions, that higher dimensional operators can be formed which give a Yukawa interaction with the Higgs field. In the limit of an exact conservation of this new symmetry, as Left- and Right-handed quarks have different assigned charges, they are massless. As the symmetry is broken, one obtains mass matrices which have their entries parametrized by powers of the symmetry breaking scale:

$$M^u_{ij} \sim \left(\frac{\langle\phi\rangle}{\Lambda}\right)^{L^u_i - R^u_j} \tag{6.2}$$

where $L_i^u - R_j^u$ are the U(1) charge differences between Left- and Right-handed up-type quarks, and equivalent expressions hold for the down-sector, and for leptons. It is these charge differences which have to be accounted for by the corresponding insertions of ϕ, thus forcing the different fermion charges to differ in integer amounts. This theoretically simple mechanism is able to provide an origin for the hierarchical structure of the Yukawa matrices of the SM, where the large mass ratios are traded for some charge differences under this new U(1) symmetry which are all roughly of the same order. There remain several details of this scenario which depend on the dynamics of the new sector, such as the mechanism that triggers spontaneous breaking of the U(1) symmetry, the scale of this breaking and the phenomenology of the associated axion.

In this Chapter we propose a model which combines partial compositeness with FN, by imposing a U(1) flavor symmetry in the composite sector. This symmetry is spontaneously broken by the strong dynamics and is respected by the mixings with the elementary fermions. The flavor structure of the light fermions of the spectrum, that are identified with the SM ones, now depends on the size of the elementary-composite mixing as well as on the U(1) charges. In this way the model allows to interpolate between APC and FN. While the top quark mass requires a considerable degree of compositeness and dimension four Yukawa interactions, the masses of the light quarks can be suppressed by a small mixing, as well as by the Wilson coefficient of the higher dimensional Yukawa interaction, that is determined by the U(1) charges. The Left- and Right-handed mixing angles of the SM fermions also follow a well defined pattern determined by both mixings and charges. This interplay opens up new possibilities, in particular for dimension six flavor violating operators that mediate $\Delta F = 1$ and $\Delta F = 2$ transitions, as well as for the flavor diagonal and CP violating dipole operators. We will show that for some scenarios it is possible to suppress the Wilson coefficient of 4-fermion operators involving light Right-handed quarks, as well as those of dipole operators. In this Chapter we will focus only on the sector of quarks.

Related attempts in the lepton sector have been proposed in [183], whereas not fully realistic proposals in the quark sector were presented in Refs. [184–186]. At the level of effective field theories some interesting attempts have been proposed within two Higgs doublet models in [187, 188]. Ref. [189] has considered an interesting model with a U(1) horizontal symmetry in which the Higgs and the axion are pseudo Nambu-Goldstone composite states. A more related proposal was recently given in Ref. [190], although a general analysis of flavor constraints is missing.

The Chapter is organized as follows, in Sec. 6.1 we describe the basic idea and introduce a model with a content of composite resonances of the strong sector that can generate the flavor structure of the quarks. We show a set of charges which reproduce the quark masses and the CKM matrix, and study the interactions with the

composite resonances that can induce flavor violating processes. In Sec. 6.2 we show the predictions for flavor and CP violating operators, comparing them with APC. These results are summarized in the tables shown in this section. In Sec. 6.2.4 we discuss very briefly constraints from dijets, and in Sec. 6.3 we show some general features of the interactions of the axion of the theory. Finally, we raise some discussions in Sec. 6.4.

6.1. Outline of the model

The proposal is similar to anarchic partial compositeness (APC), as was discussed in Sec. 2.2, where the SM fermions are elementary states that at a high energy scale $\Lambda_{\rm UV}$ have linear interactions with the operators of a new strongly interacting sector: $\mathcal{L}_{\rm int} \supset \tilde{\lambda} \bar{f} \mathcal{O}_f$. The main difference, however, is that in the anarchic scenario there are no flavor symmetries in the new sector, such that all flavor transitions involving $\mathcal{O}_f$ are allowed and of the same order. In the present model we consider a modification of the anarchic paradigm introducing a horizontal global symmetry $\mathrm{U}(1)_F$ in the strong sector, under which the operators can be charged. We assume that $\mathrm{U}(1)_F$ is respected by the linear interactions, thus assigning to the elementary fermion f the same charge as that of $\mathcal{O}_f$. In this case the linear couplings $\tilde{\lambda}$ are block diagonal, with different blocks associated to sectors with different charges.

At a low energy scale $\Lambda_{\rm IR}$ of order few TeV, the dynamics of the strong sector generates a mass gap and massive resonances, with the masses of the lowest level of composite states being $m_* \sim \Lambda_{\rm IR}$. Assuming approximate scale invariance of the strong sector, the running of the couplings is given by the dimensions of the corresponding operator, this generates a hierarchy of mixings in the IR.

The model also features a spontaneous breaking of $\mathrm{U}(1)_F$ in the composite sector, via a charged complex scalar operator $\mathcal{O}_\phi$ which is a singlet under the SM gauge symmetry. We normalize the charge of $\mathcal{O}_\phi$ to 1, $P_F \mathcal{O}_\phi = \mathcal{O}_\phi$, and we use p_f for the charges of the fermions, that are assumed to be integer numbers.

As the Higgs is a composite state of the strong sector, two effects enter in the Yukawa interactions. First, if the fermionic operators are charged under $\mathrm{U}(1)_F$, the Yukawa interactions require insertions of $\mathcal{O}_\phi$, leading to operators with higher dimensions than those occurring in partial compositeness. Second, the interactions with the elementary fermions are mediated by the linear mixing, such that the quark masses now depend on the mixing of each chirality and on the number of insertions of $\mathcal{O}_\phi$.

It is useful to describe the low energy limit of the above dynamics in terms of a two-site theory, with the elementary fermions and gauge fields of the SM associated to one site, and the first level of resonances of the strong sector, including the Higgs, associated to the other site [128]. We use small letters for the elementary fields and capital letters for the composite resonances. As usual, the resonances will have masses

m_*, that we take of the same order, couplings g_* that are taken as: $1 < g_* \ll 4\pi$, and we define $f = m_*/g_*$. For simplicity we assume that there is only one fermionic resonance for each elementary fermion, and that they have the same quantum numbers under the SM gauge symmetry as the elementary ones. We also assume that there is a single complex scalar resonance excited by the operator $\mathcal{O}_\phi$.

In the present Chapter we are not concerned with the particular details regarding the Higgs as a resonance of the composite sector, as what will be investigated is independent of that particular point. For this reason, we do not parametrize it in terms of a coset G/H, as was done in the previous chapters. All that follows, however, is compatible with such a pNGB description of the Higgs.

The interactions between elementary and composite fermions are given by:

$$\mathcal{L}^{(\text{mix})} \supset -f(\lambda_{qj}\bar{q}_j Q_j + \lambda_{uj}\bar{u}_j U_j + \lambda_{dj}\bar{d}_j D_j) + \text{h.c.} \ , \tag{6.3}$$

where due to the $\text{U}(1)_F$ symmetry, the couplings λ_{fj} do not mix generations if $p_j \neq p_k$ for $j \neq k$.

We find it useful to parametrize these diagonal couplings λ_{fj} as:

$$\lambda_{fj} = g_* \epsilon_{fj} = g_* \lambda_C^{n_{fj}} \ , \qquad f = q, u, d \ , \tag{6.4}$$

with ϵ_{fj} being the degree of compositeness of the fermion f_j, and $\lambda_C \simeq 0.22$, such that we parametrize the mixing in powers of λ_C. Note that n_{fj} do not need to be integer numbers.

We consider now the main interactions needed for our analysis. The strong sector has a global symmetry that contains the SM gauge symmetry group, as well as $\text{U}(1)_F$ factor. There are spin 1 resonances created by the conserved currents associated to these symmetries, that interact with the fermion resonances. Calling F_μ the lightest spin 1 resonance of $\text{U}(1)_F$ and P_F its generator, the composite sector contains the interactions:

$$\mathcal{L}_F^{(\text{cp})} = g_{*F}\bar{Q}_j P_F \not{F} Q_j + g_{*F}\bar{U}_j P_F \not{F} U_j + g_{*F}\bar{D}_j P_F \not{F} D_j \ , \tag{6.5}$$

that are not flavor universal if P_F is not proportional to the identity. There are also interactions with the resonances associated to the SM gauge group that are flavor universal.

There are higher dimensional interactions with the Higgs, that require insertions of either Φ or $\Phi^\dagger$ to compensate the $\text{U}(1)_F$ charges of the fermions, with Φ being the

effective complex scalar field describing the lowest lying excitation of $\mathcal{O}_\phi$:

$$\mathcal{L}_y^{(\mathrm{cp})} = -X^u_{jk}\bar{Q}_j\tilde{H}\left(\frac{\Phi^{(\dagger)}}{\Lambda}\right)^{\beta^u_{jk}} U_k - X^d_{jk}\bar{Q}_j H\left(\frac{\Phi^{(\dagger)}}{\Lambda}\right)^{\beta^d_{jk}} D_k + \mathrm{h.c.} \tag{6.6}$$

with Λ the scale at which these operators are generated and:

$$\beta^u_{jk} = |p_{qj} - p_{uk}| \ , \qquad \beta^d_{jk} = |p_{qj} - p_{dk}| \ . \tag{6.7}$$

The use of either Φ or $\Phi^\dagger$ depends on the sign of $(p_{qj} - p_{uk})$ and $(p_{qj} - p_{dk})$. We will consider an anarchic scenario, in which all the coefficients of the coupling X_f are of the same order, $\mathcal{O}(g_*)$. The scale Λ is expected to be of order f, although it depends on the ultra-violet dynamics that generates these interactions.

There is a spontaneous breaking of $\mathrm{U}(1)_F$ as Φ acquires a vacuum expectation value: $\langle\Phi\rangle = \delta\Lambda$, with $\delta \lesssim 1$. When evaluating Φ in its VEV, Higgs Yukawa couplings with the composite fermions are then generated:

$$Y^u_{jk} = X^u_{jk}\delta^{\beta^u_{jk}} \ , \qquad Y^d_{jk} = X^d_{jk}\delta^{\beta^d_{jk}} \ , \tag{6.8}$$

with no sum over repeated indices. We take the order of magnitude of the VEV to be of the size of the Cabibbo angle in units of Λ: $\delta \sim \lambda_C$.

There can also be interactions with spin 0 composite states, similar to the Higgs interactions if the states are neutral under $\mathrm{U}(1)_F$, and with a global shift of β for charged states. The Yukawa couplings of these spin 0 states, called $\widetilde{X}^f$, are of $\mathcal{O}(g_*)$, and they are generally not aligned with X^f. We will consider the effect of these interactions in the next section.

6.1.1. Fermion masses and mixing

The mixing generates interactions between the elementary fermions and the Higgs. To leading order in (v/f) and mixing the mass matrices of the light fermions of the SM are:

$$M^f_{j_k} \simeq v(\epsilon_q Y^f \epsilon_f)_{jk} = v\lambda_C^{n_{qj}} X^f_{jk}\delta^{\beta^f_{jk}}\lambda_C^{n_{fj}} = vX^f_{jk}\lambda_C^{n_{qj}+\beta^f_{jk}+n_{fk}} \ , \qquad f = u, d \ , \tag{6.9}$$

where the last equality is obtained by taking $\delta \sim \lambda_C$. A diagonalization of this matrix will result in the spectrum of the physical states, along with the rotations between interaction eigenstates and mass eigenstates. For a given pattern of charges β^f and mixings ϵ_f, this system can be solved perturbatively in powers of λ_C. Moreover, the mass spectrum and rotation angles can be approximately found under suitable conditions. By considering a system with two generations, for $M_{11} \ll M_{12,21}$, the eigenvalues and

eigenvectors can be estimated as:

$$m_{fj} \sim g_* v \lambda_C^{n_{qj}+\beta^f_{jj}+n_{fj}} , \tag{6.10}$$

$$\theta^f_{L,jk} \sim \lambda_C^{n_{qj}-n_{qk}+\beta^f_{jk}-\beta^f_{kk}} , \quad j<k , \tag{6.11}$$

$$\theta^f_{R,jk} \sim \lambda_C^{n_{fj}-n_{fk}+\beta^f_{kj}-\beta^f_{kk}} , \quad j<k . \tag{6.12}$$

Although a proof of a similar formula for three generations is more involved, we have checked by performing a perturbative diagonalization in powers of λ_C, that for the cases considered in this Chapter these estimates work well when considering three generations. Thus we will make extensive use of these estimates. In some cases we find corrections to these estimates, that end up being of the same order in powers of λ_C, we find this to be the case for quarks of the second generation. This occurs when the Yukawa matrices have off-diagonal entries that contribute at the same order as the diagonal ones.

Solutions leading to the SM quark masses and mixing angles

We consider the case in which the rotations into physical states U^u_L and U^d_L are of order $V_{\rm CKM}$. Since the most stringent constraints from flavor transitions arise from the K-system, we have explored the possibility to obtain $\theta^d_{L,jk}$ smaller than the CKM angles, but we have not found viable solutions of that kind. To minimize the flavor transitions we look for charge textures able to generate suppressed $\theta^d_{R,jk}$ and $\theta^u_{R,jk}$.

Avoiding suppression of the top mass requires that we take $n_{q3} = n_{u3} = \beta^u_{33} = 0$, this in turn means equality of the third generation charges: $p_{q3} = p_{u3}$. For simplicity we pick: $p_{q3} = p_{u3} = 0$; a nonzero value results in a shift of all charges by that value. By making use of Eq. (6.11), to reproduce the CKM angles in the up sector we demand:

$$|p_{q1}| \simeq 3 - n_{q1} , \qquad |p_{q2}| \simeq 2 - n_{q2} , \tag{6.13}$$

$$n_{q1} - n_{q2} + |p_{q1} - p_{u2}| - |p_{q2} - p_{u2}| \simeq 1 , \tag{6.14}$$

where we have assumed $n_{q1} \leq 3$ and $n_{q2} \leq 2$. Since the same n_{qj} and p_{qj} enter in the down-sector, Eq. (6.13) leads to $\theta^d_{L,13} \sim \lambda^3_C$ and $\theta^d_{L,23} \sim \lambda^2_C$, *i.e.*: $(U^d_L)_{j3} \sim (V_{\rm CKM})_{j3}$. Notice that, although the charges of the fermions are integer numbers, the previous equations do not require the degree of compositeness parametrized by n_{fj} to be associated with an integer number, thus in the rest of the Chapter we will take n_{fj} to be continuous variables.

For the bottom we take $p_{d3} = 0$, therefore the ratio m_b/m_t is controlled by ϵ_{d3}, with $n_{d3} \sim 3$, see Eq. (6.1). We will write the hierarchy of Right-handed down couplings in terms of ϵ_{d3}, as $\epsilon_{d1,2} = \lambda_C^{n_{d1,2}} \epsilon_{d3}$, while remembering that this hierarchy is further

suppressed with respect to the hierarchy of the up sector by a factor of λ_C^3, in the rest of the Chapter we will make extensive use of this relation.

We can then write a solution, consisting of the following charges, and parametrized by the Right-handed hierarchies $n_{ui},\ n_{di}$:

$$\begin{aligned} &p_{q1} = -1\ , \quad p_{q2} = 0\ , \quad n_{q1} = n_{q2} = 2\ , \\ &p_{u1} \simeq -7 + n_{u1}, \quad p_{u2} \simeq 2 - n_{u2}, \quad n_{u1} \in [0,6], \quad n_{u2} \in [0,2]\ , \\ &p_{d1} \simeq -4 + n_{d1}, \quad p_{d2} \simeq 1 - n_{d2}, \quad n_{d1} \in [0,3], \quad n_{d2} \in [0,1]\ . \end{aligned} \tag{6.15}$$

The left charges are fixed once we pick $n_{q1} = n_{q2} = 2$. There is freedom in the overall signs of the charges, but not in the relative sign between them. That is, in order to reproduce $U_L^{u\dagger} \simeq V_{\rm CKM}$, we make the choice $p_{q1} \leq 0$, $p_{q2} \geq 0$. The choice of $n_{q1} = n_{q2} = 2$ can be explained by looking at the interaction of the Left-handed quarks with spin 1 resonances, as we describe in Sec. 6.1.2. Once the Left-charges have been fixed, using Eq. (6.10) allows to fix the Right-charges, as a function of n_{fi}. The allowed ranges for the parameters n_{fi} are thus limited by the same equation, such that larger n_{fi} with fixed n_{qi} and β_{ii} implies a higher suppression of the fermion masses.

For this set of solutions, the β matrices as a function of the parameters n_{fi} are:

$$\beta^u(n_{ui}) = \begin{pmatrix} 6-n_{u1} & 3-n_{u2} & 1 \\ 7-n_{u1} & 2-n_{u2} & 0 \\ 7-n_{u1} & 2-n_{u2} & 0 \end{pmatrix}, \qquad \beta^d(n_{di}) = \begin{pmatrix} 3-n_{d1} & 2-n_{d2} & 1 \\ 4-n_{d1} & 1-n_{d2} & 0 \\ 4-n_{d1} & 1-n_{d2} & 0 \end{pmatrix}\ . \tag{6.16}$$

Notice that when $n_{fi} = n_{fi}^{\rm max}$ (i.e.: their upper limits) the diagonal elements become zero and all the mass suppression comes from the coefficients ϵ_{fi}, both Left and Right.

For the given solutions, the mass matrices of Eq. (6.9) are independent of the parameters n_{fi}, thus the spectrum and the rotations matrices are independent of the values of these parameters. As already mentioned, a peculiarity of this solution with $n_{q1} = n_{q2} = 2$ is that the rotation of the Left-handed down sector is also of order $U_L^d \simeq V_{\rm CKM}$. The same is not true for solutions that have $n_{q2} = 1$, where we do find a suppression in the angle $\theta_{L,12}^d$, but those solutions have an enhancement of the non-diagonal Left-handed coupling of the up-sector with respect to APC, while not having a suppression in the non-diagonal Left-handed coupling of the down sector.

To lowest order in λ_C the rotation matrices U_R^f are given by:

$$U_R^u \sim \begin{pmatrix} 1 & \lambda_C^5 & \lambda_C^7 \\ -\lambda_C^5 & 1 & \lambda_C^2 \\ -\lambda_C^7 & -\lambda_C^2 & 1 \end{pmatrix}, \qquad U_R^d \sim \begin{pmatrix} 1 & \lambda_C^3 & \lambda_C^4 \\ -\lambda_C^3 & 1 & \lambda_C^1 \\ -\lambda_C^4 & -\lambda_C^1 & 1 \end{pmatrix} \tag{6.17}$$

where we are writing these matrices in the spirit of the Wolfenstein parametrization of

$V_{\rm CKM}$, and omitting coefficients of $\mathcal{O}(1)$ that can however be calculated in terms of the coefficients X^f_{ij} of the Yukawa mass matrices. These coefficients, as well as higher order corrections that make these matrices unitary up to a given non-trivial order in λ_C, can be obtained by perturbative diagonalization of $M^{u,d}$ and are taken into account in our calculations.

Finally we need to address the charge degeneracy in these solutions. As one can see in Eq. (6.15), the charges of second and third generations of the Left-handed quarks are equal, as well as those of Right-handed down or up quarks when either $n_{d2} = n^{\rm max}_{d2}$ or $n_{u2} = n^{\rm max}_{u2}$. When charges are degenerated among different generations the couplings λ_{fj} do not need to be diagonal in that subspace. One can choose a basis for the elementary fermions such that the coupling becomes triangular in the subspace [112, 113], that is, there is a basis in which the mixing can be written as:

$$\mathcal{L}^{(\rm mix)} \supset -(\lambda_q)_{jk} f \bar{q}_j Q_k - (\lambda_u)_{jk} f \bar{u}_j U_k - (\lambda_d)_{jk} f \bar{d}_j D_k + \text{h.c.}\ , \tag{6.18}$$

with the coupling matrix

$$\lambda_f = \begin{pmatrix} \lambda_{f1} & 0 & 0 \\ 0 & \lambda_{f2} & 0 \\ 0 & t^f_{32}\lambda_{f2} & \lambda_{f3} \end{pmatrix}\ , \tag{6.19}$$

with $t^f_{32} = \mathcal{O}(1)$, in the case of generations 2 and 3 having degenerate charges. If another pair were degenerated, then $t^f_{ij} \neq 0,\ i > j$. This can further be parametrized as $\lambda_f = t^f g_* \epsilon_f$, with t^f a lower-triangular matrix with its diagonal elements equal to 1. One benefit of this factorization is that the effect of the degeneracy can be tracked via the insertion of the matrices t^f, with $f = q,\ u,\ d$, depending on which fermions are degenerate. As we will see below, this degeneracy will not play a significant role in most of our analysis, as the leading order in λ_C is dominated by the diagonal contributions or, in some particular cases, for this set of solutions the corrections are of the same order as the diagonal ones. t^q does however play a role in the modified Left-handed coupling between Ztc, where the absence of this correction results in a higher suppression of the coupling for certain values of the parameters.

6.1.2. Interactions with resonances

In order to study the flavor constraints, we must first obtain the couplings between the elementary fermions and the resonances of the theory, that are responsible of mediating flavor transitions. We find it useful to distinguish between interactions with resonances of either spin 1 or 0. These interactions can be written in terms of the elementary-composite mixings, and the couplings between resonances. One must

also rotate the elementary fermions into the mass eigenstates. We have, for spin 1 interactions:

$$\begin{aligned} g^f_{L,ij} &\simeq g_*(U^{f\dagger}_L \epsilon_q c_q \epsilon_q U^f_L)_{ij} \ , \\ g^f_{R,ij} &\simeq g_*(U^{f\dagger}_R \epsilon_f c_f \epsilon_f U^f_R)_{ij} \ , \qquad f = u, d \ , \end{aligned} \tag{6.20}$$

where c_q and c_f are diagonal matrices with coefficients of $\mathcal{O}(1)$, that are not degenerate for the case of $\mathrm{U}(1)_F$.

In the case of small mixing angles, one can obtain an estimate for the different flavor transitions by approximating the rotations:

$$\begin{aligned} g^f_{L,12} &\sim g_*[\theta^f_{L,12}(\epsilon^2_{q1} - \epsilon^2_{q2}) - \theta^f_{L,13}\theta^f_{L,23}\epsilon^2_{q3}] \ , \\ g^f_{L,23} &\sim g_*[\theta^f_{L,23}(\epsilon^2_{q2} - \epsilon^2_{q3}) - \theta^f_{L,13}\theta^f_{L,12}\epsilon^2_{q1}] \ , \\ g^f_{L,13} &\sim g_*[\theta^f_{L,13}(\epsilon^2_{q1} - \epsilon^2_{q3}) - \theta^f_{L,12}\theta^f_{L,23}\epsilon^2_{q2}] \ , \end{aligned} \tag{6.21}$$

Equivalent expressions hold for the Right-handed couplings, by replacing $\epsilon_q \to \epsilon_f$, and $\theta^f_L \to \theta^f_R$.

For the interaction with a spin-0 resonance, we have the following structure:

$$y^f_{ij} = (U^{f\dagger}_L \epsilon_q \widetilde{Y}^f \epsilon_f U^f_R)_{ij} \ , \tag{6.22}$$

which involves the matrix $\widetilde{Y}^f$, which has the same structure as the Yukawa couplings with the Higgs, but is not necessarily aligned to it, and hence is not diagonalized by rotations $U^f_{L,R}$. That is, $\widetilde{Y}^f_{jk} = \widetilde{X}^f_{jk}\, \delta^{\beta^f_{jk}}$, with $\tilde{X}$ being $\mathcal{O}(g_*)$ coefficients.

Let us briefly discuss the structure of the flavor violating couplings. As can be seen from the interactions with spin-1 resonances in the small-angle approximation, Eq. (6.21), flavor transitions depend on an interplay between the degree of compositeness and the mixing angles. On one hand in our model the degree of compositeness of some chiral fermions can be larger than in APC (compare for example the first generation having $n_{q1} = 2$, with APC, $n_{q1} = 3$ from Eq. (2.63), which would tend to increase the amount of flavor violation. On the other hand the Right-handed mixing angles can be much smaller than in APC, with their size being determined by the Froggatt-Nielsen charge of the fermions. Below we show that, given our choice of charges, the Right-handed mixing angles are very suppressed and the product is smaller than in APC, whereas the Left-handed couplings are of the same size as in APC. A similar situation holds for the couplings with spin 0 states, although in this case analytical expressions are far longer and more complicated.

Let us evaluate these interactions in the case of the solution described above. We have seen how the parameters $n_{d1,d2}$ and $n_{u1,u2}$ are not fixed, but n_{qi} are, as are the

rotations into physical states. This means that out of the couplings above, we expect g_L^f and y^f to be independent of n_{fi}. For the spin 0 interactions this is a consequence of the shape of matrices β^f, as the combination $\epsilon_q \cdot \lambda_C^{\beta^f} \cdot \epsilon_f$ produces a matrix that is independent of the n_{fi}. When evaluating these interactions, we must take into account that there may be phases in the different terms, and as such we must avoid artificial cancellations.

For interactions with a spin 1 resonance, we look at Eq. (6.21) for the Left-handed coupling. Using that $n_{q1} = n_{q2} = 2$, and $U_L^d \sim U_L^u \sim V_{\rm CKM}$, we have as the leading order:

$$g_L^d \sim g_L^u \sim g_* \epsilon_{q3}^2 \begin{pmatrix} \lambda_C^4 & \lambda_C^5 & \lambda_C^3 \\ \dots & \lambda_C^4 & \lambda_C^2 \\ \dots & \dots & \lambda_C^0 \end{pmatrix} , \tag{6.23}$$

where the lower triangular block is not shown since the matrix is symmetric. Notice that these flavor violating couplings are of the same size as in APC (see for example Eq. (2.75) regarding element 12, where $g_L \sim \sqrt{C_1} \sim \lambda_C^5$).

The Right-handed couplings of the spin 1 resonances depend on the values of n_{fi}, as U_R^f are fixed all the dependence will be through the values of ϵ_f. We get:

$$g_R^d \sim g_* \epsilon_{u3}^2 \begin{pmatrix} \lambda_C^{6-12} & \lambda_C^{9-11} & \lambda_C^{10} \\ \dots & \lambda_C^{6-8} & \lambda_C^7 \\ \dots & \dots & \lambda_C^6 \end{pmatrix} , \qquad g_R^u \sim g_* \epsilon_{u3}^2 \begin{pmatrix} \lambda_C^{0-12} & \lambda_C^{5-9} & \lambda_C^7 \\ \dots & \lambda_C^{0-4} & \lambda_C^2 \\ \dots & \dots & \lambda_C^0 \end{pmatrix} , \tag{6.24}$$

where again the lower triangular block is equal to the upper one. The coefficients that do not involve the third generation depend on n_{fi} through some non-trivial functions, the range shown in the exponent of these coefficients correspond to the interval of those functions for the values of n_{fi} in Eq. (6.15). On the other hand the coefficients involving the third generation are dominated by the contributions depending on n_{u3} or n_{d3}, which are fixed in our solution. Approximate expressions for these functions can be obtained straightforwardly by using the small angle approximation. To visualize this dependence we take n_{fi} real, we evaluate the $\mathcal{O}(1)$ numerical coefficients taking care to avoid spurious cancellations and we obtain the contour plots for $\log_{\lambda_C}(g_{R,12}^f / g_{R,12}^{f,(\rm APC)})$ as shown in Fig. 6.1, namely the power of λ_C that suppresses the coupling compared with APC. For down and up sectors a larger suppression requires larger values of n_{fi}, as well as $n_{d1} > 0$ and $n_{u1} > 1$. [1]

[1] Taking n_{fi} to be integer, to have a suppression with respect to APC one has to choose $n_{u2} = n_{u2}^{\max}$ and $n_{d2} = n_{d2}^{\max}$. This causes the charges of the Right-handed second generation quarks to be degenerate with those of the third generation.

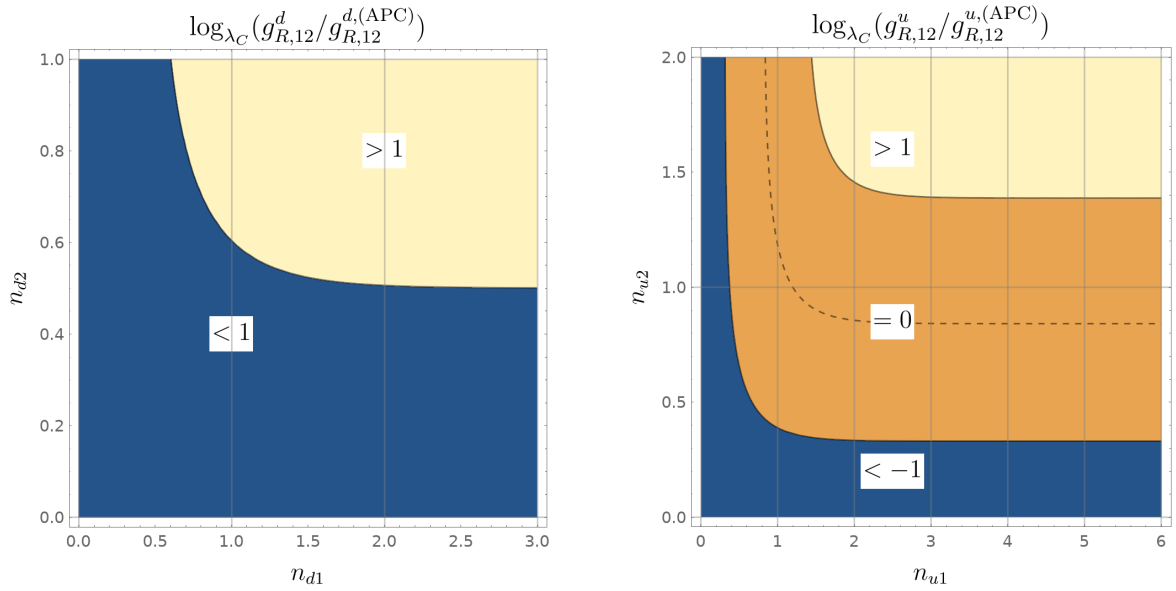

Figure 6.1: Flavor violating couplings of spin 1 resonances with light Right-handed quarks, compared with APC. On the left we show $\log_{\lambda_C}(g^f_{R,12}/g^{f,(\mathrm{APC})}_{R,12})$ for down-type quarks, and on the right for up-type quarks, as a function of the degree of compositeness of the quarks parametrized by the exponents n_{fi}. Darker color (left and down region) corresponds to smaller exponent, and lighter color (up and right region) to larger exponent. For down (up) quarks, the exponent in the upper-right corner is 2 (2), and in the lower-left corner is 0 (-2).

For the couplings with a spin 0 resonance we have to distinguish between up and down sectors. We get:

$$g^d_{LR} \sim g_* \epsilon_{q3} \epsilon_{u3} \begin{pmatrix} \lambda_C^8 & \lambda_C^7 & \lambda_C^6 \\ \lambda_C^9 & \lambda_C^6 & \lambda_C^5 \\ \lambda_C^7 & \lambda_C^4 & \lambda_C^3 \end{pmatrix}, \qquad g^u_{LR} \sim g_* \epsilon_{q3} \epsilon_{u3} \begin{pmatrix} \lambda_C^8 & \lambda_C^5 & \lambda_C^3 \\ \lambda_C^9 & \lambda_C^4 & \lambda_C^2 \\ \lambda_C^7 & \lambda_C^2 & \lambda_C^0 \end{pmatrix}. \tag{6.25}$$

Here we show only the dominant term in powers of the Cabibbo angle, and as stated above, these flavor transitions are all independent of the values of n_{fi}.

As mentioned above, in the presence of degenerate charges one must introduce couplings between elementary and composite sectors which are non-diagonal, but triangular, with nonzero elements connecting these generations. We considered the effect of these non-diagonal couplings, present in the left sector as $n_{q2} = 2$, and in the right sector only if $n_{d2} = n^{\max}_{d2}$ or $n_{u2} = n^{\max}_{u2}$. This is easily calculated by using the appropriate insertions of t^f in our calculations. We found that the leading order in powers of λ_C is unchanged in interactions with either scalar or vector resonances. This is a particular property of the solution that we are considering, in which the new contribution is of the same order as those arising from diagonal λ_f.

6.1.3. Coefficient of dipole operators

We find it useful to discuss in this section the general flavor structure of the Wilson coefficient of dipole operators, that are induced at one loop level by exchange of resonances. The dipole operators can be of different kinds, depending on which boson closes the loop. In Eq. (6.26) we show an estimate in terms of the relevant parameters, in which we add different contributions that include: $\mathrm{U}(1)_F$ resonance in the first three terms, neutral Higgs in the fourth term, and charged Higgs in the last term,

$$d^f_{ij} = g_*[U^{f\dagger}_L \epsilon_q (P_q^2 Y^f + P_q Y^f P_f + Y^f P_f^2 + Y^f Y^{f\dagger} Y^f + Y^{f'} Y^{f'\dagger} Y^f)\epsilon_f U^f_R]_{ij} \ . \quad (6.26)$$

where f is either u or d, and $f' \neq f$. There are also contributions with exchange of spin 1 resonances with the quantum numbers of the gluons, W's and Z that in general are suppressed [97], eventually we do not expect them to be larger than that of F.

Dipole operators can involve either $\bar{q}_{L,i}$ and $q_{R,j}$, or $\bar{q}_{R,i}$ and $q_{L,j}$, as usual in the case $i \neq j$ we call their Wilson coefficients C_{ij} and C'_{ij}, as in Sec. 2.2.1.

6.2. Constraints

In this section we study the main flavor constraints present in our model for the specific solution concerning the set of charges and elementary-composite mixings defined above. We also analyze constraints from dijets at LHC and from mixing of the real component of Φ with the Higgs field.

We make use of the couplings calculated in the previous section, at leading order in powers of λ_C. Having studied the constraints to the APC scenario in Sec. 2.2.1, here we do not concern ourselves with expressing these constraints as bounds for the scale of resonances of the model. Instead, we find it simpler to compare the size of the Wilson coefficients for the present model with respect to those of APC. Translating these ratios into bounds for m_* or f is straightforward. As was done in Ch. 2, we organize the flavor and CP violating processes of this section as: $\Delta F = 2$, $\Delta F = 1$ and $\Delta F = 0$.

6.2.1. Constraints from $\Delta F = 2$ transitions

For $\Delta F = 2$, we follow Sec. 2.2.1, where these processes are conveniently reduced into a basis of eight $d = 6$ operators involving 4-fermion interactions. See Eq. (2.72) for the operators in question.

As can be seen from Sec. 2.2.1, and particularly in Table 2.2, in APC the most stringent bounds for $\Delta F = 2$ processes arise from the Kaon system. Specifically from coefficients C_2^{sd}, $\tilde{C}_2^{sd}$ and $C_1^{d_i d_j}$, that require $m_* \gtrsim 5-8$ TeV, and from C_4^{sd} that requires

$m_* \gtrsim 10-20$ TeV, with some dependence on the details of the model. Less stringent but still sizeable are the bounds from $C^{bd}_{2,4}$, $C^{bs}_{2,4}$, $C^{cu}_{1,2,4}$, that require $m_* \gtrsim 0.5-3$ TeV. [18, 22]

There are contributions to these Wilson coefficients coming from exchange of either spin-1 or spin-0 resonances, which we can write in terms of the couplings as defined in the previous section. The spin-1 contributions are:

$$C_1^{ij} = \frac{(g^f_{L,ij})^2}{m_*^2} \,, \qquad \widetilde{C}_1^{ij} = \frac{(g^f_{R,ij})^2}{m_*^2} \,, \qquad C_4^{(1),ij} = \frac{g^f_{L,ij} g^f_{R,ij}}{m_*^2} \,. \tag{6.27}$$

Spin-0 resonances contribute to the following coefficients:

$$C_2^{ij} = \frac{(g^f_{LR,ij})^2}{m_*^2} \,, \qquad \widetilde{C}_2^{ij} = \frac{(g^f_{LR,ji})^2}{m_*^2} \,, \qquad C_4^{(0),ij} = \frac{g^f_{LR,ij} g^f_{LR,ji}}{m_*^2} \,. \tag{6.28}$$

We see that coefficients C_1 and $\widetilde{C}_1$ have contributions coming exclusively from vector resonances, whereas C_2 and $\widetilde{C}_2$ from scalar resonances, and C_4 from either of the two, which we indicate with an additional superindex.

To obtain a suppression of C_1^{sd} and C_1^{cu} in K and D systems as efficient as in APC requires $g_{f_L,12} \lesssim \lambda_C^5$. From the first term of Eq. (6.21), assuming $n_{q1} \geq n_{q2}$ and $\theta^f_{L,12} \sim \lambda_C$ gives: $n_{q2} \geq 2$, whilst the second term is saturated for $\theta^f_{L,23}\theta^f_{L,13} \sim \lambda_C^5$, *i.e.*: when $\theta^f_{L,23}$ and $\theta^f_{L,13}$ are of CKM order. This is the reason why we have not considered solutions with $n_{q2} < 2$. If $\theta_{23}^{\rm CKM}$ and $\theta_{13}^{\rm CKM}$ were generated one in the up- and the other in the down-sector, one could look for a solution with a suppressed second term in Eq. (6.21), but we have not found such a solution.

We show the prediction for the Wilson coefficients normalized in terms of what is obtained for APC, we express this ratio in powers of λ_C and focus on the exponent, such that larger exponent corresponds to larger suppression. This is shown in Table 6.1, where we write $\log_{\lambda_C}\left(C_X/C_X^{(\rm APC)}\right)$ for each meson.

$\Delta F = 2$	C_1	$\widetilde{C}_1$	$C_4^{(1)}$	C_2	$\widetilde{C}_2$	$C_4^{(0)}$
K	0	0 to 4	0 to 2	0	4	2
B_d	0	4	2	0	4	2
B_s	0	0	0	0	0	0
D	0	-4 to 4	-2 to 2	0	4	2

Table 6.1: Summary of model results for the Wilson coefficients of $\Delta F = 2$ operators. Each cell contains the value of $\log_{\lambda_C}\left(C_X/C_X^{(\rm APC)}\right)$, that shows the amount of suppression (or enhancement) with respect to APC, for each meson. For an explanation of the meaning of cells with a range of values read the text.

Several patterns emerge in Table 6.1. Columns corresponding to C_1 and C_2 are all zero, meaning that these coefficients are of the same size as in APC for the solution that we have chosen. The row corresponding to B_s is also zero, thus having no suppression with respect to APC for this meson. As we have previously shown, for our model the left handed couplings with a spin 1 resonance are all of the same order as those in APC, thus C_1 has this same behavior. C_2 is also of the same order as in APC, due to the fact that the couplings g^f_{LR}, Eq. (6.25), have the upper triangular block of the same order as APC. Regarding B_s, it also has couplings $g^d_{LR,32}$ and $g^d_{R,32}$ of the same size as APC, thus none of its Wilson Coefficients are suppressed. Regarding the dependence of these coefficients on $n_{u,d}$, as we discussed in the previous section, only those quantities that depend on g^f_R can have a dependence on n_f, then only coefficients $\widetilde{C}_1$ and $C_4^{(1)}$ have a dependence with these parameters. This dependence can be understood from the plots in Fig. 6.1, as those Wilson coefficients are proportional $(g^f_R)^2$ and g^f_R, respectively. In the table we show the range of values that are obtained for n_f varying in the corresponding intervals. For the K-meson a suppression is obtained as long as n_{d1} and n_{d2} are positive, with a suppression $\mathcal{O}(\lambda_C^2)$ in $\widetilde{C}_1$ and $\mathcal{O}(\lambda_C)$ in C_4 for $n_{d1} \gtrsim 1$ and $n_{d2} \gtrsim 0.5$, and a maximum suppression $\mathcal{O}(\lambda_C^4)$ in $\widetilde{C}_1$ and $\mathcal{O}(\lambda_C^2)$ in C_4 for the maximum values of $n_{d1,2}$. For the D-meson a suppression is obtained for $n_{u1}, n_{u2} \gtrsim 1$, with a suppression $\mathcal{O}(\lambda_C^2)$ in $\widetilde{C}_1$ and $\mathcal{O}(\lambda_C)$ in C_4 for $n_{u1}, n_{u2} \gtrsim 1.5$, and a maximum suppression $\mathcal{O}(\lambda_C^4)$ in $\widetilde{C}_1$ and $\mathcal{O}(\lambda_C^2)$ in C_4 for the maximum values of $n_{u1,2}$. [2]

Overall, we obtain that the most stringent constraints, those that involve Right-handed couplings, can be suppressed, whereas the Left-handed ones have the same size as in APC. This implies that a smaller Left-compositeness of the top quark ϵ_{q3} is required, trading it for larger Right-handed compositeness in order to accurately reproduce the top mass, as $\epsilon_{q3} = 1/g_*$ and $\epsilon_{u3} = 1$.

6.2.2. Constraints from $\Delta F = 1$ transitions

We described the main $\Delta F = 1$ flavor effects in Sec. 2.2.1, which can come from dipole operators, penguin operators modifying the Z couplings, and operators modifying the W couplings. The last two produce smaller effects and are model dependent, and can be protected via the introduction of symmetries [101]. The flavor violating effects coming from dipole operators are the ones that give the most stringent bounds of this subsection. Below we focus on these dipole operators, as well as on flavor violating Z couplings with the top.

[2] If only integers n_f are considered and the $\mathcal{O}(1)$ parameters of the theory are strictly fixed to unity, one gets only the extremes of the interval shown in the cells in the case of the K-meson, with the suppression corresponding to n_{d2} maximum and $n_{d1} > 0$. In the case of the D-meson, for integer n_f, there are three different values for these Wilson coefficients depending on the value of n_{ui}, for $\widetilde{C}_1$: $-4, 0, 4$ and for $\widetilde{C}_4^{(1)}$: $-2, 0, 2$.

Dipole operators

We follow Sec. 2.2.1, and we use the basis specified in Eq. (2.82) for the electro- and chromo-magnetic operators. As we saw in that section, specifically in Table 2.3, the dominant bounds in APC arise from the Wilson coefficients of: $C^{(\prime)}_{sdg}$, $C^{(\prime)}_{bsV}$ and $C^{(\prime)}_{cug}$, that require $f \gtrsim 1-2$ TeV [18, 91, 97].

The dipole operators can be of different kinds, depending on which boson closes the loop. In Eq. (6.26) we consider the different contributions, which include $\mathrm{U}(1)_F$ resonances, neutral Higgs and charged Higgs in the loop. We summarize our results in Table 6.2, where we show $\log_{\lambda_C}\left(d^f_{ij}/d^{f,(\mathrm{APC})}_{ij}\right)$ for the different flavor combinations involved.

$\Delta F = 1$	$\mathrm{U}(1)_F$	$(Y^f)^3$	$(Y^{f'})^2 Y^f$
$C_{bs\gamma}$	2	0	0
$C'_{bs\gamma}$	$\begin{cases} 0 & (n_{d2}=0) \\ 6 & (n_{d2}=1) \end{cases}$	0	0
C_{sdg}	0	0	0
C'_{sdg}	2	2	2
C_{cug}	0	0	0
C'_{cug}	2	2	2

Table 6.2: Summary of $\Delta F = 1$ coefficients of dipole operators. We show the value of $\log_{\lambda_C}(C/C^{(\mathrm{APC})})$, for the ratios of the Wilson coefficients normalized with respect to APC.

We obtain that in the case of $\Delta F = 1$, for most flavor transitions there is at least one contribution that is of the same size as in APC. This is not the case for one of the chiral structures of sdg and cug, where we obtain a suppression λ_C^2. For $C'_{bs\gamma}$ we obtain a range of values that depend on n_{d2}.

As a summary, adding all the contributions and chiral structures we do not obtain suppressions compared with APC.

Ztc and Zbs interactions

Experimental bounds on $\mathrm{Br}(t \to Zc)$ lead to $g^Z_{tc} \lesssim 0.01$ for Left- and Right-handed chiralities [191, 192]. Although these interactions are model dependent, since it is possible to protect one of the couplings with discrete symmetries [101], in general it is not possible to protect both chiral couplings at the same time. In partial compositeness one can estimate: $\delta g^Z_{tc} \sim (g/2)\epsilon_2\epsilon_3 c_{23} c_{33}(v/f)^2$, with c_{ij} numbers that depend on the flavor structure of the model, c_{23} connecting second and third generations in the composite

sector, ϵ_j being the Left-(Right-)handed degree of compositeness for $\delta g^Z_{L,tc}$ ($\delta g^Z_{R,tc}$).

In the present model the coefficients c_{ij} are given by $Y^u_{ij}/g_* \sim \lambda_C^{\beta^u_{ij}}$, Eq. (6.8), and the degree of compositeness is given by $\epsilon_{fj} \sim \lambda_C^{n_{fj}}$. For the solutions of Eq. (6.15) we find that the Right-handed coupling has a size $\delta g^Z_{R,tc} \sim \lambda_C^2 (v/f)^2$, that is of the same order as APC [193]. For $(v/f)^2 \sim 0.1$, $\delta g^Z_{R,tc} \sim 5 \times 10^{-3}$. The Left-handed coupling, however, has a dependence on parameters n_{di}. We find this coupling to be within the range $\lambda_C^2 (v/f)^2$ (for $n_{u2} = 2$) to $\lambda_C^4 (v/f)^2$ ($n_{u2} < 2$). We find that this coupling is affected by the matrix t^q which is present due to charge degeneracy between 2nd and 3rd generation Left-handed quarks. Without the effect of this matrix, however, coupling can be as small as $\lambda_C^6 (v/f)^2$ for $n_{u2} = 0,\ n_{u1} < 6$.

In the 14 TeV run of LHC, with 3000 fb^{-1}, it is expected to probe $\delta g^Z_{tc} \sim 3 - 6 \times 10^{-3}$ at 95 %CL, testing the Right handed coupling of the present model, as well as APC, for $(v/f)^2 \sim 0.1$.

For the Zbs interaction, we calculate the Left-handed coupling $\delta g^Z_{L,bs}$ to be within the range $\lambda_C^2 (v/f)^2$ (for $n_{d2} = 1$) to $\lambda_C^4 (v/f)^2$ (for $n_{d2} = 0$). The Right-handed coupling has a size $\delta g^Z_{R,bs} \sim \lambda_C^7 (v/f)^2$, that is of the same order as APC.

$B_s \to \mu\mu$ strongly constrains g^Z_{bs}. By making use of the experimental measurements [194–196], for a generic spectrum of resonances, a crude estimate leads to $\epsilon^2_{q3} (v/f)^2 \lambda_C^{2-4} \lesssim 10^{-5}$. This bound could be satisfied for $n^{\min}_{d2}$, $(v/f)^2 = 0.1$ and $\epsilon_{q3} \simeq 0.3$, but would require a tuning of order λ_C^{-2} for $n^{\max}_{d2}$. The presence of symmetries protecting down-type Z couplings can relax this tension.

6.2.3. Constraints from $\Delta F = 0$ processes

For $\Delta F = 0$ we also look at the dipole operators, that in APC are dominated by the down-quark, that requires $f \gtrsim 4 - 5$ TeV [18, 97], see also Eq. (2.99). We focus on d, u and c quarks. In order to get the leading contribution to these Wilson coefficients, we must analyze the misalignment taking place between the dipole operators and the mass matrix. This is of particular importance in the case of the $\mathrm{U}(1)_F$ vector closing the loop, because although the matrix combinations in the first three terms of Eq. (6.26) are proportional to the same Yukawa matrix, insertions of the fermion charges α_q and α_f break the alignment at higher orders, thus contributing to a phase. In Table 6.3 we show the power of the leading order contribution to these coefficients. We find a suppression of order λ_C^2 for the $\mathrm{U}(1)_F$ in the loop, in all three quarks d, u, and c. When looking at contributions from the Higgs in the loop, with a cubic dependence on the Yukawa, no such alignment is present. In those contributions we find, for both up and down sectors, a dependence on the parameters of our model $n_{u1,u2}$ or $n_{d1,d2}$.

$\Delta F = 0$	$\mathrm{U}(1)_F$	$(Y^f)^3$	$(Y^{f'})^2 Y^f$
ddV	2	$\begin{cases} 2-6\ (n_{d1}<3) \\ 0\ (n_{d1}=3) \end{cases}$	$\begin{cases} 2\ (n_{u1}<6) \\ 0\ (n_{u1}=6) \end{cases}$
uuV	2	$\begin{cases} 2-8\ (n_{u1}<6) \\ 0\ (n_{u1}=6) \end{cases}$	$\begin{cases} 2\ (n_{d1}<3) \\ 0\ (n_{d1}=3) \end{cases}$
ccV	2	$\begin{cases} 2-4\ (n_{u2}<2) \\ 0\ (n_{u2}=2) \end{cases}$	0

Table 6.3: Summary of $\Delta F = 0$ coefficients of dipole operators. We show the value of $\log_{\lambda_C}(C/C^{(\mathrm{APC})})$ for the ratios of the Wilson coefficients normalized with respect to APC. For the $\mathrm{U}(1)_F$ vector loop, as the coefficient can be aligned at zeroth order with the mass matrix, we show the first non-zero contribution.

To better understand the dependence of $\log_{\lambda_C}\left(d^f_{ii}/d^{f,(\mathrm{APC})}_{ii}\right)$ on the parameters of the theory we show in Fig. 6.2 the contribution from the neutral Higgs. We see that for ddV (left panel), no such suppression is found if $n_{d1} = n^{\max}_{d1} = 3$, however, for smaller values of n_{d1} the suppression can be of order λ_C^2 and larger. In the case of the up sector, we see a different dependence for the up quark (middle panel) or the charm quark (right panel). Whereas the contribution to the up quark is of order APC for $n_{u1} = n^{\max}_{u1} = 6$, and has larger suppressions for smaller values of n_{u1}, the contribution to the charm has a stronger dependence on n_{u2}, being of order APC when $n_{u2} = n^{\max}_{u2} = 2$ and smaller for $n_{u2} < n^{\max}_{u2}$. Here we see a small tension with $\Delta F = 2$ D-meson constraints that prefer larger $n_{u2} = n^{\max}_{u2}$ to suppress $\widetilde{C}_1$ and C_4, although there is a window where coefficients with Right-handed quarks are suppressed for both processes.

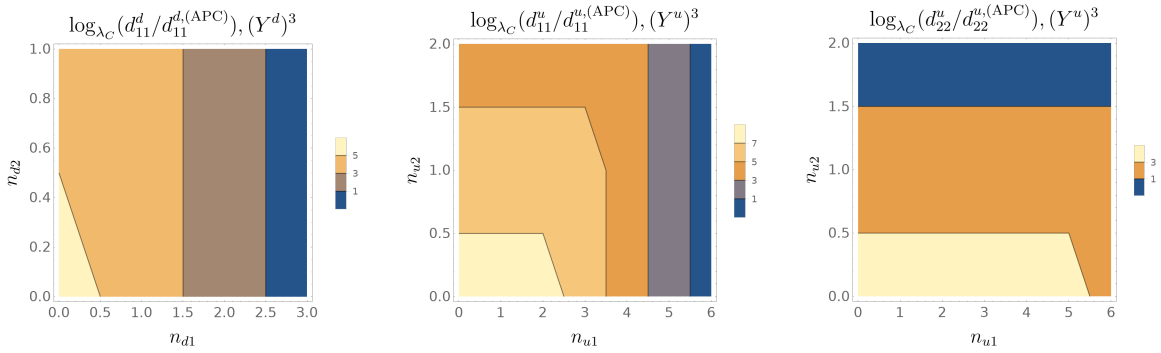

(a) ddV **(b)** uuV **(c)** ccV

Figure 6.2: Wilson coefficient of flavor diagonal dipole operators compared with APC: $\log_{\lambda_C}\left(d^f_{ii}/d^{f,(\mathrm{APC})}_{ii}\right)$ with neutral Higgs contributions, for down (left panel), up (middle panel) and charm (right panel) quarks, as function of n_{fi} parameters of the theory. A darker color corresponds to smaller exponent, and lighter color to a larger exponent. In all three cases, the exponent in blue regions is 0, thus leading to no suppression.

In the case of the charm dipoles, the contribution of a charged Higgs has the same

size as in APC, irrespective of values of $n_{ui,di}$. The fact that no suppression is observed in this WC is due to the fact that the contribution of the third generation quark inside the loop is dominant, as its degree of compositeness is the largest.

It is interesting to notice that the dependence on ϵ_f of the coefficients of dipole operators of Fig. 6.2 is opposite to the one of Right-handed couplings of spin 1 particles, Fig. 6.1. The behavior of the Right-handed couplings $g^f_{R,12}$ is determined by their quadratic dependence on ϵ_f, arising from the two insertions of elementary-composite mixing. The dependence of the dipole coefficients can be understood by considering a single generation: as the mass involves the combination $m \sim \epsilon_q Y \epsilon_f$, the dipole $d = \epsilon_1 Y^3 \epsilon_f$ scales with ϵ_f as $d \sim m^3 \epsilon_q^{-2} \epsilon_f^{-2}$. Considering the presence of three generations adds the rotations into physical states, which are however mostly dominated by their diagonal part.

6.2.4. Constraints from LHC

Dijets at LHC give bounds on the compositeness scale of the light quarks [197–203]. Following Ref. [204], see also [205], the most stringent constraints arise form the 13 TeV run, that gives bounds on the Wilson coefficients of 4-fermion operators with light quarks, roughly of order: $(g^f_{L/R,11} v/m_*)^2 \lesssim 10^{-3}$. For the present model one gets: $\lambda_C^{2n_{f1}} \lesssim f/(8\ \text{TeV})$, that if $f = 1$ TeV is saturated for $n_{f1} \simeq 0.7$. Thus one has to demand $n_{f1} \gtrsim 0.7$, discarding the region of the solutions with large degree of compositeness of the Right-handed quarks of the first generation.

The particles associated with the radial part of the field Φ, being electrically neutral and CP-even, can mix with the Higgs. As this field is a singlet, it has no effect on the oblique electroweak parameters, but it renormalizes the Higgs couplings to the SM fields. From Refs. [206, 207], a combination of ATLAS and CMS results for single Higgs production gives a bound on the mixing angle: $\cos\theta > 0.94$ at 95 % confidence level. By considering up to dimension four interactions compatible with the symmetries, the potential takes the form

$$V = -\mu_H^2 |H|^2 - \mu_\Phi^2 |\Phi|^2 + \lambda_H |H|^4 + \lambda_\Phi |\Phi|^4 + \lambda_{H\Phi} |\Phi|^2 |H|^2 \tag{6.29}$$

where the quartic coupling $\lambda_{H\Phi}$ is responsible for the mixing. Assuming vacuum expectation values for both fields, computing the mass matrix and performing the diagonalization one obtains for the mixing angle θ, in terms of the physical masses:

$$\sin 2\theta = \frac{4\, \lambda_{H\Phi}\, v_{\rm SM}\, v_\Phi}{M_\phi^2 - m_h^2} \tag{6.30}$$

In terms of the physical mass of the heavy state, this bound leads to $M_\phi/\lambda_{H\Phi} \gtrsim$

1.5 TeV, where for simplicity we are assuming $v_\Phi \sim M_\phi \gg m_h$.

6.3. The axion of composite Froggatt-Nielsen

There has been interest in composite axions in the last years [189, 208–210], see also Refs. [211, 212] for previous studies on the Froggatt-Nielsen axion. In the present model the axion is associated with the NGB of the complex SM singlet:

$$\Phi = f_a e^{ia/f_a} + \dots \tag{6.31}$$

with decay constant $f_a = \langle \Phi \rangle$. Usually f_a is expected to be of order m_*/g_*, although perhaps it could be possible to differentiate these scales, if for example they arise from different sectors or are generated at different energies.

In the absence of explicit breaking of $\mathrm{U}(1)_F$ in the elementary sector the axion remains massless, up to effects from anomalous breaking generated by QCD. In the presence of a composite sector with global $\mathrm{SU}(3)_c$ symmetry, gauged by QCD, there can be large contributions to the axion mass that dominate over the IR ones [213]. Besides, there can also be contributions from the elementary sector. These effects make the composite axion rather dependent on the details of the model. In the following we will only focus on the properties of the axion that are independent of those details, and leave a deeper analysis of its phenomenology for the future.

Since the SM fermions are charged under $\mathrm{U}(1)_F$, the axion is coupled to them, leading to a generalized DFSZ-type of model [214, 215]. By redefinition of the quarks: $f \to e^{i\gamma^5 P_F a/f_a} f$, the axion is removed from the Yukawa terms and axion-fermion interactions are generated in the kinetic term. In the mass basis we get:

$$\mathcal{L} \supset \frac{\partial_\mu a}{2f_a} \bar{f}_j \gamma^\mu (c^{Vf}_{jk} + c^{Af}_{jk}\gamma^5) f_k \ , \qquad f = u, d. \tag{6.32}$$

The vector and axial-vector couplings are:

$$c^{V,Af}_{jk} = (\pm U^\dagger_{f_L} P_F U_{f_L} + U^\dagger_{f_R} P_F U_{f_R})_{jk} \ . \tag{6.33}$$

For non-universal F-charges $c^{V,Af}$ are non-diagonal and induce flavor transitions. For small mixing angles, to leading order these couplings can be approximated by:

$$(U^\dagger_f P_F U_f)_{jk} = p_{fj}\delta_{jk} + (p_{fj} - p_{fk})\theta_{f,jk} + (p_{fj} + p_{fk} - 2p_{fl})\theta_{f,jl}\theta_{f,kl} \ , \qquad l \neq j,k \ . \tag{6.34}$$

By making use of Eqs. (6.11) and (6.12) in (6.33) it is straightforward to obtain the size of $C^{V,Af}$ in the model.

The flavor violating effects of the axion depend on the decay constant f_a and on

the axion mass, whose values we did not need to fix for the analysis of the previous sections. Since these quantities can take a wide range of values, particularly the mass can vary over many orders of magnitude depending on features that are not generic, we postpone their analysis for a future work.

6.4. Summary and discussions

We have built a model that realizes flavor in the quark sector by the interplay of two paradigms: partial compositeness of the fermions and the Froggatt-Nielsen mechanism, by including the FN field in the composite sector, as well as the Higgs field. FN gives a well defined pattern of Yukawa couplings in the composite sector, determined by the charges of the composite operators under the global $\mathrm{U}(1)_F$ symmetry. Partial compositeness is, as usual, realized by linear mixing of the elementary quarks with the composite sector, with the mixing controlling the interactions between both sectors. The two ingredients give rise to a rich pattern of flavor structures, that go beyond the usual scenario of APC. We have shown the basic rules for the determination of mixings and FN charges that lead to the masses and mixing angles of the quark sector of the SM.

We have chosen a set of solutions that lead to small mixing angles of Right-handed light quarks, and we have analyzed the predictions for the flavor and CP violating processes that have the most stringent constraints. We have compared them with APC that, for a scale of composite states of order few TeV, is known to pass many flavor tests, but gives too large contributions to $\Delta F = 2$ operators in the down sector and to diagonal dipole operators of light quarks, between others. We have found that Wilson coefficients of Left-handed $\Delta F = 2$ operators are of the same size as APC, as expected for Left angles of CKM size, but for operators involving Right-handed light quarks we have found solutions that are suppressed compared with APC. Particularly interesting is the case of Q_4^{sd}, that is one of the most constrained operators, for which we have found solutions with a Wilson coefficient suppressed by λ_C^2. Another interesting case are the flavor diagonal dipole operators, also with solutions suppressed by λ_C^2 compared with APC.

For the solution considered we explored a range of charges and degrees of compositeness of the Right-handed quarks of the first and second generations. Flavor constraints select a preferred set of charges and mixings, with the second generation of Right-handed quarks uncharged, whereas the first generation charges of Left- and Right-handed chiralities are of $\mathcal{O}(1)$, and there is a window for the degree of compositeness of the Right-handed quarks of the first generation: $\epsilon_{d1} \simeq \lambda_C^{4-5}$ and $\epsilon_{u1} \simeq \lambda_C^{2-5}$. The compositeness of the down quark is determined by the bounds from $\Delta F = 2$ processes in the K-system that prefer a larger ϵ_{d1}, and $\Delta F = 0$ dipole operators that prefer

a smaller ϵ_{d1}. A similar situation holds for the compositeness of the up quark, with constraints from D-system preferring a larger ϵ_{u1} and from uuV dipole preferring a smaller ϵ_{u1}. For the selected window of compositeness, dipole operators are suppressed at least by λ_C^2 and C_4 is suppressed at least by λ_C, relaxing $m_* \gtrsim 2.5 - 7.5$ TeV and f below the TeV. There are also regions where C_4 is suppressed by $\lambda_C^{3/2} \sim 10^{-1}$. The ccV dipole can only be suppressed if this quark is charged, being in tension with $\Delta F = 2$ constraints that prefer zero charge. Concerning flavor violating Z couplings, for a generic composite sector bounds from $B_s \to \mu\mu$ introduce tuning of order λ_C^2, that can be relaxed by the use of discrete symmetries protecting Left-handed down-type couplings.

Several questions were left open. At the level of bounds from flavor, we have not been able to find solutions that could lead to Left-handed mixing angles smaller than the CKM, either in the up- or in the down-sector, or a partial combination of them, while simultaneously passing bounds from $\Delta F = 2$ processes. We have neither been able to find solutions that could suppress the mixing in the B_s system, compared with APC. At a more theoretical level, it would be interesting to find a rationale for the values of the $\mathrm{U}(1)_F$ charges that, although being of order one, are arbitrary and have been chosen to be multiples of the charge of the FN scalar field. We have not explored the flavor of the leptons in the proposed scenario. It would also be interesting to build a more predictive model of the composite sector, as a realization in five dimensions. Last, we have not explored the different possibilities for the axion-like state of the model, that eventually could solve the strong CP problem and pass the axion flavor constraints.

Chapter 7

Conclusions

Finally we arrive at the closing chapter of this work. In the Introduction, Ch. 1, we outlined what the main motivations behind this work were. We were interested in the theoretical and experimental reasons for justifying new physics beyond the Standard Model. Namely, from the theoretical point of view we were encouraged by the Hierarchy Problem of the electroweak scale, where some of its solutions suggest the Higgs could be a composite object of a strongly interacting sector at higher energies. This is the main idea behind the so called Composite Higgs models. From the experimental point of view, we were interested in some particular deviations from theory featured in the so called B-anomalies. This is the name given to certain departures between theory and experiment found in observables exploring lepton flavor universality violation in semileptonic B-meson decays, particularly the ratios $R_{K^{(*)}}$ and $R_{D^{(*)}}$, involving neutral and charged currents, respectively. As with the Composite Higgs solutions to the Hierarchy Problem, accommodating these anomalies involves new physics at the TeV scale, therefore finding a common explanation for both poses an interesting challenge.

Another characteristic of the SM which remains unexplained is that of flavor: the theory possesses a three-fold multiplicity in the spectrum of fermions, without a specific underlying mechanism. Moreover, the only source of flavor violation is given by the Yukawa couplings with the Higgs, and more importantly, these couplings also show a hierarchy, which in the present theory remains unexplained. Additionally, current flavor constraints force any NP flavor structure to be particularly non-generic. Which is why new models must have a particular structure of couplings in flavor space, otherwise they may be both ruled out by experiment, and unable to provide a solution to the B-meson anomalies. Having a certain rationale for such couplings, as opposed to simply having *ad-hoc* values, is also preferable. This process accounts to building a theory of flavor, where the hierarchies no longer remain unexplained but are instead generated by some dynamics.

A way to equip a Composite Higgs theory with such a mechanism is that given

by partial compositeness, where linear couplings between the elementary fermions and the fermionic resonances of the strong sector have their low energy hierarchy generated by the renormalization group running over a large separation of scales. This allows for the creation of large hierarchies from small differences in operator dimensions of the same order. Particularly interesting is the hypothesis of anarchic partial compositeness, where the flavor structure of the strong sector is completely anarchic. This allows for the spectrum of masses and mixings of the SM fermions to be appropriately explained, while passing the different flavor constraints for moderate values of the scale of compositeness m_*. Some of these bounds can be further relaxed if the composite sector is equipped with certain flavor symmetries.

Among the new physics that can explain the deviations in the semileptonic ratios $R_{K^{(*)}}$ and $R_{D^{(*)}}$, we took special interest in those involving leptoquarks, which have interaction vertices with both quarks and leptons. In the present work we explored different models involving both Higgs and leptoquarks in the spectrum of composite resonances. The Higgs was always among the Nambu Goldstone bosons delivered by the strongly coupled field theory, whereas we considered different natures of leptoquarks. In one case, in Ch. 3, we studied a composite model which from a simple group delivered the $\mathrm{SU}(2)_L$ triplet leptoquark S_3. We showed how, when coupled with APC, this leptoquark can be responsible for the deviation in $R_{K^{(*)}}$, however not simultaneously in that of $R_{D^{(*)}}$. This leptoquark, being a scalar, was present in the NGB spectrum of the composite sector. We considered an effective theory description of the composite sector, this is adequate as we were interested in the low energy phenomenology, and not in the UV details of the underlying theory. The composite sector is then characterized by some global symmetry groups, G and its subgroup H, which after a spontaneous symmetry breaking delivers the massless scalars of the theory. In this case, we found that for the groups considered, this coset also included other scalar leptoquarks which however do not contribute to the B-anomalies, and a colorless $\mathrm{SU}(2)_L$ fourplet. This fourplet is interesting as its VEV can produce sizeable corrections to EW precision tests. The explicit breaking of the global symmetries of the composite sector, through its interactions with the elementary sector, produces a 1-loop potential for the pseudo NGB. We were able to study this potential in two approximate cases: an expansion in powers of the NGB, which allowed us to obtain estimates for the scalar masses, and the potential involving only the electromagnetic-neutral VEVs of H_2 and H_4. This study of the potential could only be done after modeling the sector of resonances, in this case we only modeled the first level of resonances in what is termed a 2-site theory. By performing numerical scans, we found sectors of parameter space which delivered the correct Higgs, top quark, and W-boson masses; and the remaining pNGB have masses of order $0.4 - 1.3$ TeV, roughly compatible with their absence in direct searches of new states so far. By including the S_3 leptoquark in the scalar sector, such that a 1-loop

factor suppresses its mass with respect to the composite scale m_* where the remainder of the composite states are expected, we could obtain a light enough leptoquark for the ratio $R_{K^{(*)}}$. At the same time, this scale separation pushes all other unobserved states to higher scales m_*. A certain tuning remains between the NGB decay constant f and the Higgs mass, typically measured by the parameter $\xi = v_{\rm SM}^2/f^2$. In our numerical study we found an amount of tuning compatible with typical estimates for $\xi \simeq 1/40$. In our study of the VEVs of the EM-neutral scalars, we found that the H_4 VEV is typically suppressed by ξ, this allowed the model to pass constraints on the parameter ρ coming from EWPT. We found other constraints, like modified Z couplings in $Zb_L\bar{b}_L$ to saturate the bounds. This can be improved by different choices of fermion representations for the global symmetry group G.

As the model with S_3 lacked the ability to explain the deviation in $R_{D^{(*)}}$, we considered two other composite models. One involved a single leptoquark explanation for both ratios, with the vector state U_1. The other involved a model which includes not only the triplet S_3 but also the singlet S_1 in its NGB spectrum.

Regarding the vector leptoquark model, we described it in Ch. 4. As a vector, and not a NGB from the coset, it lacks the 1-loop factor suppression in its mass. This means the scale of the resonance masses, m_*, needs to be pulled down to order $\sim$ TeV, therefore a certain tension with flavor constraints from APC is automatically present. This tension can be alleviated by the extension of the composite symmetry, with, for example a $\mathrm{U}(1)^3$ and CP symmetries. Besides this elementary difference in the nature of the main LQ responsible for the B-anomalies, there are many common elements with the previous model. A simple group is behind the symmetry of the composite sector, several scalar states originate from its spontaneous breaking. In this case, we found besides the Higgs doublet, a leptoquark $\mathrm{SU}(2)_L$ singlet $\bar{S}_1$ and a $\mathrm{G_{SM}}$ singlet φ. This latter state is interesting, as it can provide a dark matter candidate.

We also included APC as a main element for generating the appropriate flavor structure, both for Higgs Yukawas, as well as the correct structure of U_1 couplings leading to the right deviations in $R_{K^{(*)}}$ and $R_{D^{(*)}}$. That is, this vector mainly couples to Left-handed quarks and leptons of the third generation, with suppressed first generation, as well as Right-handed, interactions. We once again modeled the theory of resonances, in this case the first two levels, with a 3-site theory. While similar to the 2-site theory, in this case allowed for the resonances which are the counterparts to both Left- and Right-handed elementary fermions to be included in the same multiplet, something which is in principle not desirable in a 2-site model as it can lead to a divergent 1-loop potential. We performed a numerical study of the potential, which allowed us to identify regions of parameter space with viable phenomenological values for the SM states such as the top quark and the Higgs. The W and Z masses were simply fixed to the value of the Higgs SM VEV, as there was a custodial symmetry

and no other neutral states, such as the H_4 found in the previous model. We obtained masses for the other pNGBs $\bar{S}_1$ and φ of order $0.2 - 2$ TeV. The masses of U_1 vectors did not come from a 1-loop potential, but from diagonalization of spin-1 states in the three-site model. We found the masses for the lightest U_1 to be in the range $1 - 3$ TeV, a portion of which we showed are both compatible with a proper explanation of the B-anomalies, and constraints put by direct searches. We studied different constraints, especially we showed that those given by Z-coupling modifications can increase the amount of tuning, requiring smaller values of ξ, and reintroducing some tension with $R_{D^{(*)}}$. We also very briefly discussed the phenomenology of the new scalar states at LHC, where there is a very rich set of signals. The phenomenology depended on whether there was a particular parity present in the model, as well as the inclusion of a Right-handed neutrino with parity $+1$. Therefore, we note that a detailed study of the production and detection of $\bar{S}_1$ and φ at LHC could allow to distinguish the different realizations of the model. As the size and flavor structure of the couplings are fixed, this can offer a predictive scenario.

In Ch. 5, we constructed another composite model with leptoquarks for the B-anomalies. In this case, one involving both S_1 and S_3 in its spectrum of NGB, besides the Higgs. We found that the smallest coset delivering these scalar states alone is not one coming from a simple group: two group factors have to be considered instead. Also equipping the model with APC, we showed that for certain fermion representations the structure of couplings to S_1 and S_3 remain equal in strength, and such a symmetric case gives no contribution to $R_{D^{(*)}}$. This puts a restriction on the leptonic representations that could be used. We found that by considering two operators in different representations of G which mixed with the lepton doublet, the right pattern of couplings could be obtained. We did not concern ourselves with an explicit model of resonances, we simply calculated some expressions for the potential in terms of certain form factors, which allowed us to estimate the LQs and Higgs masses, and the size of the EWSB in general terms. We studied the effect of the leptoquark pair on a number of low-energy observables, both on the B-anomalies where their contribution is needed, and on those flavor constraints which provide the strongest bounds and have to be kept under control. Under the APC hypothesis, we performed scans over the compositeness of quarks and leptons of second and third generation, the LQ masses, and the strength of coupling between resonances. We found that certain observables are at odds with $R_{D^{(*)}}$, with some tension particularly between $\tau \to 3\mu$, $Z\nu\bar{\nu}$ and $\tau \to \mu\gamma$ which required a reasonable amount of tuning, of order $10 - 25\,\%$. We found a window in parameter space, one of "minimal tuning", which requires a sizeable amount of compositeness for third generation quark and lepton doublets. These compositeness fractions are in turn bounded from above by certain observables like $\tau \to 3\mu$ and Δm_{B_s}. We also showed how some of these windows are expected to change with improvements in precision over certain

observables in the nearby future. Moreover, observables involving the first generation, particularly $\mu \to e\gamma$ and $\mu \to 3e$ can be problematic in relation to the expected degree of compositeness of the electron. This can be alleviated by the introduction of small bilinear couplings alongside the linear ones central to APC. This allows for its mass to be slightly decoupled from its degree of compositeness.

We considered the explanation of the anomalous magnetic moment of the muon in the presence of scalar leptoquarks. In APC, its estimate becomes independent of the fermion degree of compositeness, being in turn only dependent on the LQ mass. However, this puts a rather small upper bound on the LQ masses, around 250 GeV, which comes in conflict with bounds on direct searches, or requires an extra amount of tuning from the $\mathcal{O}(1)$ anarchic coefficients.

We briefly reviewed the phenomenology of the vector and fermionic resonances of the theory. Regarding the remaining vector resonances, there were W, Z and gluon resonances, as well as three other LQs. These leptoquarks, however, do not couple with the SM particles with operators of $d = 4$. This was either due to symmetries of the theory, or simply due to their quantum numbers. We showed the smallest-dimensional operators with which they could be coupled to SM fermions, as well as estimates of the size of their contributions to WC of four-fermion operators, which are suppressed with respect to the dominant ones. Regarding fermion states, besides those with same charges as the SM ones, we found a number of exotic states in the spectrum.

A more specific realization of this model, with an explicit theory of resonances, for example in extra-dimensional or as a discrete composite model could be of interest. Just as in the previous 2-site and 3-site models, such a theory allows for the numerical calculation of many quantities. On a different note one could explore if other fermion representations can protect the Z couplings of the theory, this way relaxing the contributions of these to several of the flavor constraints and thus diminishing the tension between them and the B-anomalies.

In a different but related direction, in Ch. 6 we set aside the B-anomalies and composite leptoquarks, to focus fully on the flavor puzzle. We built a model which can achieve the flavor structure of the quark sector by uniting two existing paradigms: that of partial compositeness with the Froggatt-Nielsen (FN) mechanism. We included the FN field in the composite sector, as well as the Higgs. The regular Froggatt-Nielsen model includes a U(1) symmetry under which the fermions are charged. By the spontaneous breaking of this symmetry, a field with unit charge is able to generate the Yukawa interactions between Left- and Right-handed fermions via higher dimensional interactions. By including this scheme in conjunction to partial compositeness, it gives rise to a rich pattern of flavor structures, going beyond the usual APC scenario. We showed how the basic rules work for the determination of mixings and FN charges, which lead to the quark spectrum and CKM matrix.

We found a set of solutions, for which we obtain small mixing angles of light Right-handed quarks, and we analyzed the predictions for flavor and CP violating processes which give the strongest constraints. In APC, for a scale of compositeness m_* of a few TeV, many flavor tests are passed, however, certain $\Delta F = 2$ operators in the down sector, especially related to Kaon decays, as well as diagonal dipole operators of light quarks get too large contributions. We explored if our model, with FN-PC was able to ameliorate some of these bounds. We found certain suppression in Wilson coefficients of our model, with respect to those of APC, including some of the observables giving the most stringent constraints. Of particular interest, we can note that of operator Q_4^{sd}, where we found a suppression of order λ_C^2, as well as in flavor diagonal dipole operators, where we also found solutions with λ_C^2 suppression.

We explored a range of charges and degrees of compositeness for the Right-handed quarks of first and second generations. We found that passing the different flavor constraints selects a set of charges and mixings. The second generation Right-handed quarks remain uncharged, whereas a window remains for the degrees compositeness of the first generation. There is an interplay between $\Delta F = 2$ processes and $\Delta F = 0$ dipoles in the down sector, the former preferring a larger compositeness ϵ_{d1}, while the latter prefers a smaller one, and a similar picture holding for the up sector. For this selected window, the suppression is enough that the bound on the compositeness scale is relaxed $m_* \gtrsim 2.5 - 7.5$ TeV, and f below the TeV. Regarding the second generation, we found that the charm dipole ccV can only be suppressed if this quark is charged under the FN U(1), this fact being in tension with $\Delta F = 2$, which favor a scheme where they remain uncharged.

We also studied flavor violating Z couplings, where we found that for a generic composite sector, bounds from $B_s \to \mu\mu$ introduce a certain tuning of order λ_C^2. These bounds could be relaxed by the use of discrete symmetries in a specific model.

Several unanswered questions remained, for instance no solutions were found that allowed for suppressed Left-handed mixing angles with respect to the CKM matrix, in either up or down sectors, or a combination of both, while simultaneously being able to suppress $\Delta F = 2$ processes. Neither were solutions found able to suppress the mixing in the B_s-meson system with respect to APC. Moreover, from a theoretical point of view it would be interesting to find a rationale behind the values for the U(1) charges which, although of order one, have arbitrary values (as long as they are multiples of the charge of the scalar FN field). Nor did we explore the lepton sector in this combined FN-PC scenario. Another interesting question is that of an explicit realization of the composite model, for example in an extra-dimensional theory, which would endow it with more predictive power. As is the question of exploring the different possibilities surrounding the axion-like state present in the FN theory, product of the spontaneous breaking of the U(1). This axion could eventually solve the strong CP problem as well

as pass axion flavor constraints.

Appendix A

Appendices to Chapter 3

A.1. Representations of SO(13)

In this appendix we give a brief description of the algebra, as well as the lowest dimensional representations, of the group SO(3). A simple basis for the algebra of SO(13) in the fundamental representation is given by the set of generators $\{T_{\ell m}, \ell < m = 2, \dots 13\}$, with coefficients:

$$(\mathcal{T}_{\ell,m})_{jk} = i(\delta_{\ell j}\delta_{mk} - \delta_{mj}\delta_{\ell k}) \ , \qquad l < m \ . \tag{A.1}$$

An SO(7)×SO(6) subgroup can be defined by the transformations leaving invariant the block diagonal matrix:

$$A = \begin{pmatrix} aI_7 & 0 \\ 0 & bI_6 \end{pmatrix} \ , \tag{A.2}$$

with a and b different non-trivial numbers, I_n the identity matrix in n-dimensions and the action of the group being defined as:

$$A \to UAU^\dagger, \qquad U \in SO(13) \ . \tag{A.3}$$

An algebra of $\mathrm{SU}(2)_a \times \mathrm{SU}(2)_b \times \mathrm{SU}(2)_c$ inside SO(7) can be defined by:

$$\begin{aligned}
&T_1^a = -\frac{1}{2}(\mathcal{T}_{1,4} + \mathcal{T}_{2,3}) \ , && T_2^a = \frac{1}{2}(\mathcal{T}_{1,3} - \mathcal{T}_{2,4}) \ , && T_3^a = -\frac{1}{2}(\mathcal{T}_{1,2} + \mathcal{T}_{3,4}) \ , \\
&T_1^b = \frac{1}{2}(\mathcal{T}_{1,4} - \mathcal{T}_{2,3}) \ , && T_2^b = \frac{1}{2}(\mathcal{T}_{1,3} + \mathcal{T}_{2,4}) \ , && T_3^b = -\frac{1}{2}(\mathcal{T}_{1,2} - \mathcal{T}_{3,4}) \ , \\
&T_1^c = \mathcal{T}_{5,6} \ , && T_2^c = \mathcal{T}_{5,7} \ , && T_3^c = \mathcal{T}_{6,7} \ ,
\end{aligned} \tag{A.4}$$

An algebra of SU(3)×U(1) inside SO(6) can be defined by:

$$
\begin{aligned}
T_1^{\mathrm{SU(3)}} &= \frac{1}{2}(\mathcal{T}_{10,13} - \mathcal{T}_{11,12}) \ , & T_2^{\mathrm{SU(3)}} &= \frac{1}{2}(\mathcal{T}_{10,12} + \mathcal{T}_{11,13}) \ , \\
T_3^{\mathrm{SU(3)}} &= \frac{1}{2}(-\mathcal{T}_{10,11} + \mathcal{T}_{12,13}) \ , & T_4^{\mathrm{SU(3)}} &= \frac{1}{2}(\mathcal{T}_{8,13} - \mathcal{T}_{9,12}) \ , \\
T_5^{\mathrm{SU(3)}} &= \frac{1}{2}(\mathcal{T}_{8,12} + \mathcal{T}_{9,13}) \ , & T_6^{\mathrm{SU(3)}} &= \frac{1}{2}(\mathcal{T}_{8,11} - \mathcal{T}_{9,10}) \ , \\
T_7^{\mathrm{SU(3)}} &= \frac{1}{2}(\mathcal{T}_{8,10} + \mathcal{T}_{9,11}) \ , & T_8^{\mathrm{SU(3)}} &= \frac{1}{2\sqrt{3}}(-2\mathcal{T}_{8,9} + \mathcal{T}_{10,11} + \mathcal{T}_{12,13}) \ , \\
T^{\mathrm{U(1)}} &= -4(\mathcal{T}_{8,9} + \mathcal{T}_{10,11} + \mathcal{T}_{12,13}) \ ,
\end{aligned}
\tag{A.5}
$$

The parity $P = e^{iT_P\pi/2}$ can be obtained with $T_P = T^{\mathrm{U(1)}}$.

The adjoint representation (**78**), can be obtained by using the structure constants, or by using the algebra itself as a basis of the vector space of dimension 78.

The representation **286** can be obtained, for example, from the product $\mathbf{13} \otimes \mathbf{78} \sim \mathbf{13} \oplus \mathbf{286} \oplus \mathbf{715}$. Although we have built it explicitly for our calculations, we will not show the generators here because the matrices are too large.

The smallest representations of SO(13), and their decompositions under H are:

$$
\begin{aligned}
&\mathbf{13} \sim (\mathbf{6},\mathbf{1},\mathbf{1},\mathbf{1}) \oplus (\mathbf{1},\mathbf{1},\mathbf{2},\mathbf{2}) \oplus (\mathbf{1},\mathbf{3},\mathbf{1},\mathbf{1}) \ , \\
&\mathbf{64} \sim (\mathbf{4},\mathbf{1},\mathbf{2},\mathbf{2}) \oplus (\mathbf{4},\mathbf{2},\mathbf{1},\mathbf{2}) \oplus \text{c.c.} \ , \\
&\mathbf{78} \sim (\mathbf{15},\mathbf{1},\mathbf{1},\mathbf{1}) \oplus (\mathbf{1},\mathbf{3},\mathbf{1},\mathbf{1}) \oplus (\mathbf{1},\mathbf{1},\mathbf{3},\mathbf{1}) \oplus (\mathbf{1},\mathbf{1},\mathbf{1},\mathbf{3}) \oplus (\mathbf{1},\mathbf{3},\mathbf{2},\mathbf{2}) \oplus (\mathbf{6},\mathbf{3},\mathbf{1},\mathbf{1}) \\
&\qquad \oplus (\mathbf{6},\mathbf{1},\mathbf{2},\mathbf{2}) \ , \\
&\mathbf{286} \sim (\mathbf{15},\mathbf{3},\mathbf{1},\mathbf{1}) \oplus (\mathbf{15},\mathbf{1},\mathbf{2},\mathbf{2}) \oplus (\mathbf{1},\mathbf{1},\mathbf{1},\mathbf{1}) \oplus (\mathbf{1},\mathbf{1},\mathbf{2},\mathbf{2}) \oplus (\mathbf{1},\mathbf{3},\mathbf{2},\mathbf{2}) \oplus (\mathbf{1},\mathbf{3},\mathbf{1},\mathbf{3}) \\
&\quad \oplus (\mathbf{1},\mathbf{3},\mathbf{3},\mathbf{1}) \oplus (\mathbf{10},\mathbf{1},\mathbf{1},\mathbf{1}) \oplus (\mathbf{6},\mathbf{3},\mathbf{2},\mathbf{2}) \oplus (\mathbf{6},\mathbf{3},\mathbf{1},\mathbf{1}) \oplus (\mathbf{6},\mathbf{1},\mathbf{3},\mathbf{1}) \oplus (\mathbf{6},\mathbf{1},\mathbf{1},\mathbf{3}) \oplus \text{c.c.}
\end{aligned}
\tag{A.6}
$$

the complex conjugate representations must be added only when they are not equivalent to the original one.

These representations can be further decomposed under $\mathrm{H_{min}}$ to see which of them contain the SM fermions. Using the decompositions of Eq. (3.6) and the identification

$\mathrm{SU}(2)_L \equiv \mathrm{SU}(2)_{1+2}$, we obtain:

$$
\begin{aligned}
\mathbf{13} &\sim (\mathbf{3},\mathbf{1},\mathbf{1})_2 \oplus (\mathbf{1},\mathbf{2},\mathbf{2})_0 \oplus (\mathbf{1},\mathbf{3},\mathbf{1})_0 \oplus \text{c.c.}\ , \\
\mathbf{64} &\sim (\mathbf{3},\mathbf{2},\mathbf{2})_{-1} \oplus (\mathbf{3},\mathbf{1},\mathbf{1})_{-1} \oplus (\mathbf{3},\mathbf{3},\mathbf{1})_{-1} \oplus (\mathbf{1},\mathbf{2},\mathbf{2})_3 \oplus (\mathbf{1},\mathbf{3},\mathbf{1})_3 \oplus (\mathbf{1},\mathbf{1},\mathbf{1})_3 \oplus \text{c.c.}\ , \\
\mathbf{78} &\sim (\mathbf{8},\mathbf{1},\mathbf{1})_0 \oplus (\mathbf{3},\mathbf{1},\mathbf{1})_{-4} \oplus (\mathbf{3},\mathbf{3},\mathbf{1})_2 \oplus (\mathbf{3},\mathbf{2},\mathbf{2})_2 \\
&\quad \oplus (\mathbf{1},\mathbf{4},\mathbf{2})_0 \oplus (\mathbf{1},\mathbf{2},\mathbf{2})_0 \oplus (\mathbf{1},\mathbf{1},\mathbf{3})_0 \oplus 2(\mathbf{1},\mathbf{3},\mathbf{1})_0 \oplus (\mathbf{1},\mathbf{1},\mathbf{1})_0 \oplus \text{c.c.}\ , \\
\mathbf{286} &\sim (\mathbf{8},\mathbf{3},\mathbf{1})_0 \oplus (\mathbf{8},\mathbf{2},\mathbf{2})_0 \oplus (\mathbf{6},\mathbf{1},\mathbf{1})_{-2} \oplus (\mathbf{3},\mathbf{3},\mathbf{1})_{-4} \oplus 2(\mathbf{3},\mathbf{3},\mathbf{1})_2 \oplus (\mathbf{3},\mathbf{4},\mathbf{2})_2 \\
&\quad \oplus (\mathbf{3},\mathbf{2},\mathbf{2})_{-4} \oplus (\mathbf{3},\mathbf{2},\mathbf{2})_2 \oplus (\mathbf{3},\mathbf{1},\mathbf{3})_2 \oplus (\mathbf{3},\mathbf{1},\mathbf{1})_2 \oplus (\mathbf{1},\mathbf{3},\mathbf{3})_0 \oplus (\mathbf{1},\mathbf{4},\mathbf{2})_0 \\
&\quad \oplus (\mathbf{1},\mathbf{5},\mathbf{1})_0 \oplus 3(\mathbf{1},\mathbf{2},\mathbf{2})_0 \oplus 2(\mathbf{1},\mathbf{3},\mathbf{1})_0 \oplus (\mathbf{1},\mathbf{1},\mathbf{1})_6 \oplus 2(\mathbf{1},\mathbf{1},\mathbf{1})_0 \oplus \text{c.c.}\ . \qquad \text{(A.7)}
\end{aligned}
$$

From Eq. (A.7) it is straightforward to see that, besides the representations of Eq. (3.10), there are other embeddings containing the SM fermions, for example d_R could be embedded into $(\mathbf{6},\mathbf{1},\mathbf{1},\mathbf{1}) \subset \mathbf{13}$ and l_L into $(\mathbf{1},\mathbf{1},\mathbf{2},\mathbf{2}) \subset \mathbf{13}$. However, the H symmetry does not allow the proper dimension-four Yukawa couplings with H and S_3 for these embeddings.

A.2. Invariants of the quartic potential

In this appendix we show the quartic terms of the potential.

The quartic order contains 49 singlets, of which 8 are composed only of H and H_4, 20 only of leptoquarks, and the remaining 21 of H and leptoquarks. All these singlets were built using Clebsch-Gordan coefficients for SU(2), and for SU(3) the following product rules

$$
\begin{aligned}
\mathbf{3} \times \bar{\mathbf{3}} &\sim \mathbf{1} + \mathbf{8}\ , \\
\mathbf{3} \times \mathbf{3} &\sim \bar{\mathbf{3}}_A + \mathbf{6}_S\ ,
\end{aligned}
$$

where the A and S subscripts stand for anti-symmetric and symmetric products, respectively. For the **8** representation, we used the Gell-Mann matrices λ^a, $a \in \{1,..,8\}$. For instance, if ψ and ϕ are two fields transforming in the **3** of SU(3), if we form the products

$$
\sum_{ij} \lambda^a_{ij}\, \bar{\phi}_i\, \psi_j \equiv O^a\ , \qquad \text{(A.8)}
$$

then this object O^a transforms in the **8** (octet) representation.

We make a list of linear independent operators, using the following notation: when making the product of two representations, we will denote with a subindex in which representation of $\mathrm{SU}(3) \times \mathrm{SU}(2)$ it transforms, or when dealing only with color singlets,

just the SU(2) representation. Just with fields H_2 and H_4:

$$\begin{aligned}
&\mathcal{Q}_1 = \Big((H_2H_2^\dagger)_{(1)}\Big)^2, && \mathcal{Q}_2 = (H_4H_4)_{(3)}\cdot(H_4^\dagger H_4^\dagger)_{(3)},\\
&\mathcal{Q}_3 = (H_4H_4)_{(7)}\cdot(H_4^\dagger H_4^\dagger)_{(7)}, && \mathcal{Q}_4 = (H_2H_2^\dagger)_{(1)}\cdot(H_4H_4^\dagger)_{(1)},\\
&\mathcal{Q}_5 = (H_2H_2^\dagger)_{(3)}\cdot(H_4H_4^\dagger)_{(3)}, && \mathcal{Q}_6 = (H_2^\dagger H_2^\dagger)_{(3)}\cdot(H_2H_4)_{(3)} + \text{h.c.},\\
&\mathcal{Q}_7 = (H_4^\dagger H_4^\dagger)_{(3)}\cdot(H_2H_4)_{(3)} + \text{h.c.}, && \mathcal{Q}_8 = (H_2H_2)_{(3)}\cdot(H_4^\dagger H_4^\dagger)_{(3)} + \text{h.c.}.
\end{aligned} \tag{A.9}$$

Purely leptoquarks:

$$\begin{aligned}
&\mathcal{Q}_9 = (S_3S_3)_{(6,1)}\cdot(S_3^\dagger S_3^\dagger)_{(\bar6,1)}\ , && \mathcal{Q}_{10} = (S_3S_3)_{(6,5)}\cdot(S_3^\dagger S_3^\dagger)_{(\bar6,5)}\ ,\\
&\mathcal{Q}_{11} = (S_3S_3)_{(\bar3,3)}\cdot(S_3^\dagger S_3^\dagger)_{(3,3)}\ , && \mathcal{Q}_{12} = (\tilde R_2\tilde R_2)_{(\bar3,1)}\cdot(\tilde R_2^\dagger\tilde R_2^\dagger)_{(3,1)}\ ,\\
&\mathcal{Q}_{13} = (\tilde R_2\tilde R_2)_{(6,3)}\cdot(\tilde R_2^\dagger\tilde R_2^\dagger)_{(\bar6,3)}\ , && \mathcal{Q}_{14} = (\hat R_2\hat R_2)_{(\bar3,1)}\cdot(\hat R_2^\dagger\hat R_2^\dagger)_{(3,1)}\ ,\\
&\mathcal{Q}_{15} = (\hat R_2\hat R_2)_{(6,3)}\cdot(\hat R_2^\dagger\hat R_2^\dagger)_{(\bar6,3)}\ , && \mathcal{Q}_{16} = (\tilde R_2\tilde R_2^\dagger)_{(1,1)}\cdot(\hat R_2\hat R_2^\dagger)_{(1,1)}\ ,\\
&\mathcal{Q}_{17} = (\tilde R_2\tilde R_2^\dagger)_{(1,3)}\cdot(\hat R_2\hat R_2^\dagger)_{(1,3)}\ , && \mathcal{Q}_{18} = (\tilde R_2\tilde R_2^\dagger)_{(8,1)}\cdot(\hat R_2\hat R_2^\dagger)_{(8,1)}\ ,\\
&\mathcal{Q}_{19} = (\tilde R_2\tilde R_2^\dagger)_{(8,3)}\cdot(\hat R_2\hat R_2^\dagger)_{(8,3)}\ , && \mathcal{Q}_{20} = (\tilde R_2\tilde R_2^\dagger)_{(1,1)}\cdot(S_3S_3^\dagger)_{(1,1)}\ ,\\
&\mathcal{Q}_{21} = (\tilde R_2\tilde R_2^\dagger)_{(1,3)}\cdot(S_3S_3^\dagger)_{(1,3)}\ , && \mathcal{Q}_{22} = (\tilde R_2\tilde R_2^\dagger)_{(8,1)}\cdot(S_3S_3^\dagger)_{(8,1)}\ ,\\
&\mathcal{Q}_{23} = (\tilde R_2\tilde R_2^\dagger)_{(8,3)}\cdot(S_3S_3^\dagger)_{(8,3)}\ , && \mathcal{Q}_{24} = (\hat R_2\hat R_2^\dagger)_{(1,1)}\cdot(S_3S_3^\dagger)_{(1,1)}\ ,\\
&\mathcal{Q}_{25} = (\hat R_2\hat R_2^\dagger)_{(1,3)}\cdot(S_3S_3^\dagger)_{(1,3)}\ , && \mathcal{Q}_{26} = (\hat R_2\hat R_2^\dagger)_{(8,1)}\cdot(S_3S_3^\dagger)_{(8,1)}\ ,\\
&\mathcal{Q}_{27} = (\hat R_2\hat R_2^\dagger)_{(8,3)}\cdot(S_3S_3^\dagger)_{(8,3)}\ , && \mathcal{Q}_{28} = (S_3S_3)_{(3,3)}\cdot(\tilde R_2\hat R_2)_{(\bar3,3)} + \text{h.c.}\ ,\\
&\mathcal{Q}_{29} = (S_3S_3)_{(\bar6,1)}\cdot(\tilde R_2\hat R_2)_{(6,1)} + \text{h.c.}\ .
\end{aligned} \tag{A.10}$$

The operators with two leptoquarks and two color singlets are:

$$\begin{aligned}
&\mathcal{Q}_{30} = (H_2H_2^\dagger)_{(1)}(\tilde R_2\tilde R_2^\dagger)_{(1,1)}\ , && \mathcal{Q}_{31} = (H_2H_2^\dagger)_{(3)}\cdot(\tilde R_2\tilde R_2^\dagger)_{(1,3)}\ ,\\
&\mathcal{Q}_{32} = (H_2H_2^\dagger)_{(1)}(\hat R_2\hat R_2^\dagger)_{(1,1)}\ , && \mathcal{Q}_{33} = (H_2H_2^\dagger)_{(3)}\cdot(\hat R_2\hat R_2^\dagger)_{(1,3)}\ ,\\
&\mathcal{Q}_{34} = (H_2H_2^\dagger)_{(1)}(S_3S_3^\dagger)_{(1,1)}\ , && \mathcal{Q}_{35} = (H_2H_2^\dagger)_{(3)}\cdot(S_3S_3^\dagger)_{(1,3)}\ ,\\
&\mathcal{Q}_{36} = (H_4H_4^\dagger)_{(1)}(\tilde R_2\tilde R_2^\dagger)_{(1,1)}\ , && \mathcal{Q}_{37} = (H_4H_4^\dagger)_{(3)}\cdot(\tilde R_2\tilde R_2^\dagger)_{(1,3)}\ ,\\
&\mathcal{Q}_{38} = (H_4H_4^\dagger)_{(1)}(\hat R_2\hat R_2^\dagger)_{(1,1)}\ , && \mathcal{Q}_{39} = (H_4H_4^\dagger)_{(3)}\cdot(\hat R_2\hat R_2^\dagger)_{(1,3)}\ ,\\
&\mathcal{Q}_{40} = (H_4H_4^\dagger)_{(1)}(S_3S_3^\dagger)_{(1,1)}\ , && \mathcal{Q}_{41} = (H_4H_4^\dagger)_{(3)}\cdot(S_3S_3^\dagger)_{(1,3)}\ ,\\
&\mathcal{Q}_{42} = (H_4H_4^\dagger)_{(5)}\cdot(S_3S_3^\dagger)_{(1,5)}\ , && \mathcal{Q}_{43} = (H_2H_4^\dagger)_{(3)}\cdot(\tilde R_2\tilde R_2^\dagger)_{(1,3)} + \text{h.c.}\ ,\\
&\mathcal{Q}_{44} = (H_2H_4^\dagger)_{(3)}\cdot(\hat R_2\hat R_2^\dagger)_{(1,3)} + \text{h.c.}\ , && \mathcal{Q}_{45} = (H_2H_4^\dagger)_{(3)}\cdot(S_3S_3^\dagger)_{(1,3)} + \text{h.c.},\\
&\mathcal{Q}_{46} = (H_2H_4^\dagger)_{(5)}\cdot(S_3S_3^\dagger)_{(1,5)} + \text{h.c.}\ , && \mathcal{Q}_{47} = (H_2H_2)_{(3)}\cdot(\hat R_2\tilde R_2^\dagger)_{(1,3)} + \text{h.c.},\\
&\mathcal{Q}_{48} = (H_4H_4)_{(3)}\cdot(\hat R_2\tilde R_2^\dagger)_{(1,3)} + \text{h.c.}\ , && \mathcal{Q}_{49} = (H_2H_4)_{(3)}\cdot(\hat R_2\tilde R_2^\dagger)_{(1,3)} + \text{h.c.}
\end{aligned} \tag{A.11}$$

A.3. Matching couplings

In this appendix we give explicit expressions of the couplings of the effective theory in terms of the fermionic correlators and their momentum integrals. We include contributions coming from $\mathbf{r}_{q'}$.

The quadratic coefficients of the potential are:

$$
\begin{aligned}
m_H^2 =& -\int \frac{d^4p}{(2\pi)^4}\left[\frac{1}{4}\frac{24\Pi^{(6,3,1,1)}_{q,q}+3\Pi^{(6,1,1,3)}_{q,q}+27(\Pi^{(6,3,2,2)}_{q,q}-2\Pi^{(6,1,3,1)}_{q,q})}{Z_q+\Pi^{(6,3,2,2)}_{q,q}}\right.\\
&\left.+\frac{9}{2}\frac{\Pi^{(15,3,1,1)}_{q',q'}-\Pi^{(15,1,2,2)}_{q',q'}}{Z_{q'}+\Pi^{(15,1,2,2)}_{q',q'}}+\frac{9}{2}\frac{\Pi^{(6,3,2,2)}_{u,u}-\Pi^{(6,1,1,3)}_{u,u}}{Z_u+\Pi^{(6,1,1,3)}_{u,u}}-\frac{9}{2}\frac{\left(\Pi^{(6,3,2,2)}_{q,u}-\Pi^{(6,1,1,3)}_{q,u}\right)^2}{(Z_q+\Pi^{(6,3,2,2)}_{q,q})(Z_u+\Pi^{(6,1,1,3)}_{u,u})}\right]\\
m_{H_4}^2 =& -\int \frac{d^4p}{(2\pi)^4}\left[\frac{3}{2}\frac{\Pi^{(6,3,1,1)}_{q,q}+2\Pi^{(6,1,1,3)}_{q,q}-3\Pi^{(6,3,2,2)}_{q,q}}{Z_q+\Pi^{(6,3,2,2)}_{q,q}}+\right.\\
&\left.\frac{9}{2}\frac{\Pi^{(15,3,1,1)}_{q',q'}-\Pi^{(15,1,2,2)}_{q',q'}}{Z_{q'}+\Pi^{(15,1,2,2)}_{q',q'}}+\frac{9}{2}\frac{\Pi^{(6,3,2,2)}_{u,u}-\Pi^{(6,1,1,3)}_{u,u}}{Z_u+\Pi^{(6,1,1,3)}_{u,u}}\right]\\
m_{S_3}^2 =& -\int \frac{d^4p}{(2\pi)^4}\left[\frac{2\Pi^{(1,3,2,2)}_{q,q}-7\Pi^{(6,3,2,2)}_{q,q}+5\Pi^{(15,1,2,2)}_{q,q}}{Z_q+\Pi^{(6,3,2,2)}_{q,q}}+6\frac{\Pi^{(6,3,2,2)}_{q',q'}-\Pi^{(15,1,2,2)}_{q',q'}}{Z_{q'}+\Pi^{(15,1,2,2)}_{q',q'}}\right.\\
&\left.+\frac{3}{2}\frac{\Pi^{(1,1,3,3)}_{u,u}-\Pi^{(6,1,1,3)}_{u,u}}{Z_u+\Pi^{(6,1,1,3)}_{u,u}}-\frac{\left(\Pi^{(6,3,2,2)}_{q',q^C}-\Pi^{(15,1,2,2)}_{q',q^C}\right)^2}{(Z_q+\Pi^{(6,3,2,2)}_{q,q})(Z_{q'}+\Pi^{(15,1,2,2)}_{q',q'})}\right]
\end{aligned}
$$

$$
\begin{aligned}
m_{\tilde{R}_2}^2 =& -\int \frac{d^4p}{(2\pi)^4}\left[\frac{3}{4}\frac{3\Pi^{(1,3,1,3)}_{q,q}+\Pi^{(1,3,3,1)}_{q,q}-10\Pi^{(6,3,2,2)}_{q,q}+6\Pi^{(15,3,1,1)}_{q,q}}{Z_q+\Pi^{(6,3,2,2)}_{q,q}}\right.\\
&+\frac{3}{4}\frac{6\Pi^{(6,1,1,3)}_{q',q'}+2\Pi^{(6,1,3,1)}_{q',q'}+3\Pi^{(10,1,1,1)}_{q',q'}+3\Pi^{(\bar{10},1,1,1)}_{q',q'}-14\Pi^{(15,1,2,2)}_{q',q'}}{Z_{q'}+\Pi^{(15,1,2,2)}_{q',q'}}\\
&\left.+\frac{3}{2}\frac{\Pi^{(1,1,2,2)}_{u,u}-4\Pi^{(6,1,3,1)}_{u,u}+3\Pi^{(15,1,2,2)}_{u,u}}{Z_u+\Pi^{(6,1,1,3)}_{u,u}}\right]\\
m_{\hat{R}_2}^2 =& -\int \frac{d^4p}{(2\pi)^4}\left[\frac{3}{2}\frac{\Pi^{(1,3,3,1)}_{q,q}-3\Pi^{(6,3,2,2)}_{q,q}+2\Pi^{(15,3,1,1)}_{q,q}}{Z_q+\Pi^{(6,3,2,2)}_{q,q}}+3\frac{\Pi^{(15,1,2,2)}_{u,u}-\Pi^{(6,1,3,1)}_{u,u}}{Z_u+\Pi^{(6,1,1,3)}_{u,u}}\right.\\
&\left.+\frac{3}{4}\frac{4\Pi^{(6,1,3,1)}_{q',q'}+\Pi^{(10,1,1,1)}_{q',q'}+\Pi^{(\bar{10},1,1,1)}_{q',q'}-6\Pi^{(15,1,2,2)}_{q',q'}}{Z_{q'}+\Pi^{(15,1,2,2)}_{q',q'}}-\frac{3}{2}\frac{\left(\Pi^{(6,1,3,1)}_{q',u^C}-\Pi^{(15,1,2,2)}_{q',u^C}\right)^2}{(Z_u+\Pi^{(15,1,2,2)}_{u,u})(Z_{q'}+\Pi^{(15,1,2,2)}_{q',q'})}\right]
\end{aligned}
\tag{A.12}
$$

The coefficients m_1 and m_2 of Eq. (3.32) correspond to cubics involving H. We

have, at leading order in $1/Z_f$,

$$m_2 = -\int \frac{d^4p}{(2\pi)^4}\frac{3}{8\sqrt{6}} \left[\frac{8\Pi^{(1,3,2,2)}_{q,q} - 6\Pi^{(1,3,3,1)}_{q,q} - 3\Pi^{(6,1,1,3)}_{q,q} - 15\Pi^{(6,1,3,1)}_{q,q} + 8\Pi^{(6,3,1,1)}_{q,q} + 28\Pi^{(15,1,2,2)}_{q,q} - 20\Pi^{(15,3,1,1)}_{q,q}}{Z_q} + \frac{12\Pi^{(6,1,3,1)}_{q',q'} - 3\Pi^{(10,1,1,1)}_{q',q'} - 3\Pi^{(\bar{1}0,1,1,1)}_{q',q'} - 6\Pi^{(15,3,1,1)}_{q',q'}}{Z_{q'}} + \frac{6\Pi^{(1,3,3,1)}_{u,u} + 6\Pi^{(6,3,2,2)}_{u,u} - 12\Pi^{(15,1,2,2)}_{u,u}}{Z_u}\right] \tag{A.13}$$

with a similar structure for m_1

For the quartics, the most of the coefficients are much longer, even for a $1/Z_f$ expansion. We can present, for example, some of the shortest:

$$\begin{aligned} c_6 &= -\int \frac{d^4p}{(2\pi)^4}\frac{3}{4\sqrt{2}}\left[\frac{\Pi^{(6,1,1,3)}_{u,u} + \Pi^{(6,1,3,1)}_{u,u} + 2\Pi^{(6,3,1,1)}_{u,u} - 4\Pi^{(6,3,2,2)}_{u,u}}{Z_u}\right] \\ c_7 &= -\int \frac{d^4p}{(2\pi)^4}\sqrt{5}\left[\frac{1}{2}\frac{3\Pi^{(6,3,2,2)}_{q,q} - \Pi^{(6,1,1,3)}_{q,q} - 2\Pi^{(6,3,1,1)}_{q,q}}{Z_q} \right. \\ &\left. + \frac{3}{2}\frac{\Pi^{(15,3,1,1)}_{q',q'} - \Pi^{(15,1,2,2)}_{q',q'}}{Z_{q'}} + \frac{3}{4}\frac{\Pi^{(6,3,1,1)}_{u,u} - \Pi^{(6,1,1,3)}_{u,u}}{Z_u}\right] \end{aligned} \tag{A.14}$$

Whereas other coefficients can get as much as 20 terms at first order in $1/Z_f$.

A.4. Two-site theory

In this section we show the fermionic form factors that are obtained in a two-site theory. In this kind of theories the elementary sector is identified with one site, and the first level of resonances of the SCFT with another site. On the composite sector we include vector-like fermion resonances Ψ^Q and Ψ^U, with masses $M_{q,u} \sim g_* f/\sqrt{2}$, of order few TeV. As described in Sec. 3.1.1, these fermions are in the representation **286** of SO(13). To obtain a finite one-loop potential we only include NGB interactions with the chiral structure $y_{\mathbf{R}} f(\bar{\Psi}^Q_L U)_{\mathbf{R}}(U^\dagger \Psi^U_R)_{\mathbf{R}}$, as well as a term $M_y \bar{\Psi}^Q_L \Psi^U_R$, see Ref. [86]. Both sites interact through a σ-model field transforming bilinearly under the symmetries of both sites, with mixing λ_q and λ_u, Eq. (2.115). For a more detailed description we suggest the reading of Refs. [87, 128]. In the present case we follow the notation of Ref. [147].

The form factors are given by

$$\Pi^{\mathbf{r}}_{f,f}(p) = \lambda_f^2 f^2 \frac{M_{\hat{f}}^2 - p^2 + y_{\mathbf{r}}^2 f^2}{d_{\mathbf{r}}} \ , \qquad f = q, u \ , \qquad \hat{f} = u, q \ ,$$
$$\Pi^{\mathbf{r}}_{q,u}(p) = -\lambda_q \lambda_u f^2 \frac{M_q M_u y_{\mathbf{r}} f + M_y (p^2 - y_{\mathbf{r}}^2 f^2)}{d_{\mathbf{r}}} \ ,$$
$$d_{\mathbf{r}} = p^2 (M_u^2 + M_q^2) - M_q^2 M_u^2 + 2 M_q M_u M_y y_{\mathbf{r}} f + (M_y^2 - p^2)(p^2 - y_{\mathbf{r}}^2 f^2) \ . \quad \text{(A.15)}$$

Appendix B

Appendices to Chapter 4

B.1. Representations of SO(12)

In this appendix we give a brief description of the algebra, as well as the lowest dimensional representations, of the group SO(12). A simple basis for the algebra of SO(12) in the fundamental representation is given by the set of generators $\{T_{\ell m}, \ell < m = 2, \dots 12\}$, with coefficients:

$$(\mathcal{T}_{\ell,m})_{jk} = i(\delta_{\ell j}\delta_{mk} - \delta_{mj}\delta_{\ell k}) \ , \qquad l < m \ . \tag{B.1}$$

An SO(11) subgroup can be defined by choosing a vector $\hat{n}$ to point in a direction of the 12-dimensional space. For instance, selecting the twelfth coordinate, $\hat{n} = \hat{e}_{12}$, the algebra of SO(11) is defined by generators as in Eq. (B.1) with indices different from "12". Inside SO(11), we can define the subgroup SO(4)×SO(6), where we will embed $\mathrm{SU}(2)_L \times \mathrm{SU}(2)_R \times \mathrm{SU}(3)_C \times \mathrm{U}(1)_X$. The SO(4) algebra is defined by allowing indices to run from 1 to 4, while the SO(6) algebra by those indices between 6 and 11.

The algebra of $\mathrm{SU}(2)_L \times \mathrm{SU}(2)_R$ inside SO(4) can be defined by:

$$T_1^L = -\frac{1}{2}(\mathcal{T}_{1,4} + \mathcal{T}_{2,3}) \ , \qquad T_2^L = \frac{1}{2}(\mathcal{T}_{1,3} - \mathcal{T}_{2,4}) \ , \qquad T_3^L = -\frac{1}{2}(\mathcal{T}_{1,2} + \mathcal{T}_{3,4}) \ ,$$
$$T_1^R = \frac{1}{2}(\mathcal{T}_{1,4} - \mathcal{T}_{2,3}) \ , \qquad T_2^R = \frac{1}{2}(\mathcal{T}_{1,3} + \mathcal{T}_{2,4}) \ , \qquad T_3^R = -\frac{1}{2}(\mathcal{T}_{1,2} - \mathcal{T}_{3,4}) \ ,$$

An algebra of SU(3)×U(1) inside SO(6) can be defined by:

$$
\begin{aligned}
T_1^{\mathrm{SU}(3)} &= \frac{1}{2}(\mathcal{T}_{8,11} - \mathcal{T}_{9,10}) \ , & T_2^{\mathrm{SU}(3)} &= \frac{1}{2}(\mathcal{T}_{8,10} + \mathcal{T}_{9,11}) \ , \\
T_3^{\mathrm{SU}(3)} &= \frac{1}{2}(-\mathcal{T}_{8,9} + \mathcal{T}_{10,11}) \ , & T_4^{\mathrm{SU}(3)} &= \frac{1}{2}(\mathcal{T}_{6,11} - \mathcal{T}_{7,10}) \ , \\
T_5^{\mathrm{SU}(3)} &= \frac{1}{2}(\mathcal{T}_{6,10} + \mathcal{T}_{7,11}) \ , & T_6^{\mathrm{SU}(3)} &= \frac{1}{2}(\mathcal{T}_{6,9} - \mathcal{T}_{7,8}) \ , \\
T_7^{\mathrm{SU}(3)} &= \frac{1}{2}(\mathcal{T}_{6,8} + \mathcal{T}_{7,9}) \ , & T_8^{\mathrm{SU}(3)} &= \frac{1}{2\sqrt{3}}(-2\mathcal{T}_{6,7} + \mathcal{T}_{8,9} + \mathcal{T}_{10,11}) \ , \\
T^{\mathrm{U}(1)} &= -4(\mathcal{T}_{6,7} + \mathcal{T}_{8,9} + \mathcal{T}_{10,11}) \ ,
\end{aligned}
\tag{B.2}
$$

We construct the adjoint representation (**66**) by using the structure constants, or, by using the generators of the algebra as a basis of this vector space.

The smallest representations of SO(12), and their decompositions under SO(10):

$$
\begin{aligned}
\mathbf{12} &\sim \mathbf{1} \oplus \mathbf{11}, \\
\mathbf{66} &\sim \mathbf{11} \oplus \mathbf{55},
\end{aligned}
$$

Decomposing them further under $\mathrm{H}_{\mathrm{min}}$ to identify which representations contain SM fermions, we get:

$$
\begin{aligned}
\mathbf{1} &\sim (\mathbf{1},\mathbf{1},\mathbf{1})_0 \\
\mathbf{11} &\sim (\mathbf{3},\mathbf{1},\mathbf{1})_{1/\sqrt{6}} \oplus (\mathbf{1},\mathbf{2},\mathbf{2})_0 \oplus (\mathbf{1},\mathbf{1},\mathbf{1})_0 \oplus \text{c.c.} \ , \\
\mathbf{55} &\sim (\mathbf{3},\mathbf{2},\mathbf{2})_{1/\sqrt{6}} \oplus (\mathbf{3},\mathbf{1},\mathbf{1})_{1/\sqrt{6}} \oplus (\mathbf{3},\mathbf{1},\mathbf{1})_{-2/\sqrt{6}} \oplus (\mathbf{8},\mathbf{1},\mathbf{1})_0 \oplus (\mathbf{1},\mathbf{2},\mathbf{2})_0 \\
&\quad \oplus (\mathbf{1},\mathbf{3},\mathbf{1})_0 \oplus (\mathbf{1},\mathbf{1},\mathbf{3}) \oplus (\mathbf{1},\mathbf{1},\mathbf{1})_0 \oplus \text{c.c.} \ ,
\end{aligned}
\tag{B.3}
$$

the complex conjugate representations must be added only when they are not equivalent to the original one. As we need to consider a parity transformation in order to forbid odd terms in the pNGB potential, we will have to extend the group from SO(12) to O(12), as this transformation has a determinant equal to -1. We wish to make the pNGB states odd under this parity. One way to achieve this is to make this parity act over the fundamental representation **12** as:

$$
P\,\mathbf{11} = \mathbf{11} \tag{B.4}
$$

$$
P\,\mathbf{1} = -\mathbf{1} \tag{B.5}
$$

The way to represent this parity transformation in the basis here defined would be as a diagonal matrix with its first 11 entries +1, and the last entry -1. As the adjoint representation **66** can be built with the product of two **12** representations, we can find

how this parity acts on the adjoint by decomposing the product of representations:

$$P\,\mathbf{55} = \mathbf{55} \tag{B.6}$$

$$P\,\mathbf{11} = -\mathbf{11} \tag{B.7}$$

And the pNGB are inside this **11** representation within the adjoint, so they will be odd under this parity.

B.2. Mass matrices

In this appendix we show the mass matrices in the three-site model, for the fermions we consider just one generation and we do not include d_R, nor e_R partners, since their mixings are small.

For the up type quarks we get a nine-by-nine matrix, as there are four elements inside the adjoint representation with the same SM quantum numbers as this fermion. In the basis where we first put the elementary fermion, then the four representations of site 1, and then those of site 2, we get:

$$M_u = \begin{pmatrix} 0 & 0 & -i\lambda_u s_v/\sqrt{2} & i\lambda_u s_v/\sqrt{2} & \lambda_u c_v & 0 & 0 & 0 & 0 \\ 0 & m_1 & 0 & 0 & 0 & \lambda_{1,2} & 0 & 0 & 0 \\ \lambda_q s_{v/2}^2 & 0 & m_1 & 0 & 0 & 0 & \lambda_{1,2} & 0 & 0 \\ \lambda_q c_{v/2}^2 & 0 & 0 & m_1 & 0 & 0 & 0 & \lambda_{1,2} & 0 \\ -i\lambda_q s_v/\sqrt{2} & 0 & 0 & 0 & m_1 & 0 & 0 & 0 & \lambda_{1,2} \\ 0 & \lambda_{1,2} & 0 & 0 & 0 & m_{2,\mathbf{55}} & 0 & 0 & 0 \\ 0 & 0 & \lambda_{1,2} & 0 & 0 & 0 & m_{2,\mathbf{55}} & 0 & 0 \\ 0 & 0 & 0 & \lambda_{1,2} & 0 & 0 & 0 & m_{2,\mathbf{55}} & 0 \\ 0 & 0 & 0 & 0 & \lambda_{1,2} & 0 & 0 & 0 & m_{2,\mathbf{11}} \end{pmatrix} \tag{B.8}$$

For the down type quarks, the matrix is a smaller three-by-three matrix as there is only one representation inside **66** that contains the adequate quantum numbers. In the basis where we order the three elements as site 0, 1 and 2 respectively, we get:

$$M_d = \begin{pmatrix} 0 & 0 & 0 \\ \lambda_q & m_1 & \lambda_{1,2} \\ 0 & \lambda_{1,2} & m_{2,\mathbf{55}} \end{pmatrix} \tag{B.9}$$

There is a row of zeros because there are no mixing for d_R.

For the charged lepton we also get a nine-by-nine mass matrix:

$$M_e = \begin{pmatrix} 0 & 0 & 0 & 0 & 0 & 0 & 0 & 0 & 0 \\ -\lambda_l & m_1 & 0 & 0 & 0 & \lambda_{1,2} & 0 & 0 & 0 \\ 0 & 0 & m_1 & 0 & 0 & 0 & \lambda_{1,2} & 0 & 0 \\ 0 & 0 & 0 & m_1 & 0 & 0 & 0 & \lambda_{1,2} & 0 \\ 0 & 0 & 0 & 0 & m_1 & 0 & 0 & 0 & \lambda_{1,2} \\ 0 & \lambda_{1,2} & 0 & 0 & 0 & m_{2,\mathbf{55}} & 0 & 0 & 0 \\ 0 & 0 & \lambda_{1,2} & 0 & 0 & 0 & m_{2,\mathbf{55}} & 0 & 0 \\ 0 & 0 & 0 & \lambda_{1,2} & 0 & 0 & 0 & m_{2,\mathbf{55}} & 0 \\ 0 & 0 & 0 & 0 & \lambda_{1,2} & 0 & 0 & 0 & m_{2,\mathbf{11}} \end{pmatrix} \tag{B.10}$$

We do the same for the bosonic resonances. For the U_1 state, we get a three-by-three matrix, as there is, in site 1 both broken and unbroken generators identified with it, but in the site 2 only an unbroken one. We order the basis as the two unbroken generators in site 1 and 2, followed by the broken one in site 1. We get

$$M_{U_1} = \frac{1}{2}\begin{pmatrix} g1^2\left(f_1^2+f_2^2\right) & -f_2^2 g_1 g_2 & 0 \\ -f_2^2 g_1 g_2 & f_2^2 g_2^2 & 0 \\ 0 & 0 & g_1^2\left(f_1^2+f_2^2\right) \end{pmatrix} \tag{B.11}$$

For Z resonances we get a 14-by-14 matrix, as there are 8 elements in the algebra associated with the Z quantum numbers, but three of those belong to the unbroken generators, which are not present in site 2. Adding a source in the site 0, we get 14 degrees of freedom. We do not show the matrix because it is too large.

B.3. Numerical estimates of the Right-handed U_1 couplings

The couplings of the U_1 leptoquarks to elementary fermions were estimated in Eq. (4.8). Making use of Eqs. (2.63), (2.64) and (2.65), and assuming that all the couplings between the resonances are of the same order (this is known as the *one coupling* scenario), we obtain for the Right-handed couplings:

$$g_R^{(n)} \sim \epsilon_{u3}\begin{pmatrix} \frac{m_d m_e}{\lambda_C^3 v^2}\frac{1}{\epsilon_{l1}} & \frac{m_d m_\mu}{\lambda_C^3 v^2}\frac{1}{\epsilon_{l2}} & \frac{m_d m_\tau}{\lambda_C^3 v^2}\frac{1}{\epsilon_{l3}} \\ \frac{m_s m_e}{\lambda_C^2 v^2}\frac{1}{\epsilon_{l1}} & \frac{m_s m_\mu}{\lambda_C^2 v^2}\frac{1}{\epsilon_{l2}} & \frac{m_s m_\tau}{\lambda_C^2 v^2}\frac{1}{\epsilon_{l3}} \\ \frac{m_b m_e}{v^2}\frac{1}{\epsilon_{l1}} & \frac{m_b m_\mu}{v^2}\frac{1}{\epsilon_{l2}} & \frac{m_b m_\tau}{v^2}\frac{1}{\epsilon_{l3}} \end{pmatrix} \tag{B.12}$$

The experimental values of $R_{D^{(*)}}$ and $R_{K^{(*)}}$ can be reproduced by taking $\epsilon_{l3} \sim \epsilon_{u3} m_{U_1}/\text{ TeV}$ and $\epsilon_{l2}/\epsilon_{l3} \sim 0.2$. As discussed at the end of Sec. 4.1.5, ϵ_{l1} is not fixed

by the B-anomalies, as long as $\epsilon_{l1} \ll \epsilon_{l2}$. Taking for simplicity $\epsilon_{l1} \sim \epsilon_{e1} \sim (m_e/vg_*)^{1/2}$ and $\epsilon_{u3} \sim \epsilon_{q3} \sim 1/\sqrt{g_*}$, Eq. (B.12) takes the values:

$$g_R^{(n)} \sim \begin{pmatrix} 10^{-6} & 2\times 10^{-6}x & 5\times 10^{-6}x \\ 6\times 10^{-6} & 9\times 10^{-6}x & 3\times 10^{-5}x \\ 10^{-5} & 2\times 10^{-5}x & 6\times 10^{-5}x \end{pmatrix} , \qquad x = \frac{\text{TeV}}{m_{U_1}} . \tag{B.13}$$

The Right-handed couplings are much smaller than the Left-handed ones, thus with good accuracy one can neglect g_R and consider just the interactions with the Left-handed currents.

Appendix C

Appendices to Chapter 5

C.1. Group representations

In this appendix we briefly comment on the representations used in the calculations above, and on how to construct some of those representations. In this work we use a group consisting of the product of two groups, SO(10) and SO(5). Regarding SO(5), we concern ourselves with the fundamental and the adjoint representations, whereas, for the SO(10) factor we also have spinorial representations **16**, **144** and their conjugates. The generators of an SO(N) group in the fundamental representation can be parametrized in a simple fashion by a set of matrices $\{(\mathcal{T}_{lm})_{jk};\, l < m;\, m = 2, \ldots, N\}$

$$(\mathcal{T}_{lm})_{jk} = i\left(\delta_{lj}\delta_{mk} - \delta_{lk}\delta_{mj}\right) \ . \tag{C.1}$$

The adjoint representation can be constructed from the structure constants, or also by using the generators of the algebra as a basis for the vector space. As SO(N) has $N(N-1)/2$ generators, one defines a vector transforming in adjoint representation as a linear combination of said generators.

More interesting is how to build the spinorial representations **16** and $\overline{\mathbf{16}}$. This can be achieved by constructing a 32-dimensional Clifford algebra of matrices Γ^a, $a \in \{1 \ldots 10\}$. These Γ matrices can be built by tensor products of 5 Pauli matrices (also involving 2-by-2 identity matrices), thus producing $2^5 = 32$-dimensional matrices. They follow a simple structure, as

$$\begin{aligned}
\Gamma_1 &= \sigma_2 \otimes \sigma_3 \otimes \sigma_3 \otimes \sigma_3 \otimes \sigma_3 \ , & \Gamma_6 &= -\sigma_1 \otimes \sigma_3 \otimes \sigma_3 \otimes \sigma_3 \otimes \sigma_3 \ , \\
\Gamma_2 &= \mathbb{1} \otimes \sigma_2 \otimes \sigma_3 \otimes \sigma_3 \otimes \sigma_3 \ , & \Gamma_7 &= -\mathbb{1} \otimes \sigma_1 \otimes \sigma_3 \otimes \sigma_3 \otimes \sigma_3 \ , \\
&\ldots & &\ldots \\
\Gamma_5 &= \mathbb{1} \otimes \mathbb{1} \otimes \mathbb{1} \otimes \mathbb{1} \otimes \sigma_2 \ , & \Gamma_{10} &= -\mathbb{1} \otimes \mathbb{1} \otimes \mathbb{1} \otimes \mathbb{1} \otimes \sigma_1 \ .
\end{aligned} \tag{C.2}$$

One also needs to define $\Gamma_{11} \equiv (-i)^5 \prod_a \Gamma^a$, which anticommutes the other 10 matrices. With these matrices one can build the generators in the spinorial representation by use of the commutators

$$\Sigma_{ab} = \frac{i}{4}\left[\Gamma^a, \Gamma^b\right] \ . \tag{C.3}$$

Now this produces 45 32-by-32 matrices, corresponding to generators of SO(10), which we need to disentangle into representations **16** and $\overline{\mathbf{16}}$. We can do this by noting that Γ_{11} commutes with all generators, and its eigenvalues are ± 1. Thus, by diagonalizing Γ_{11}, we get block diagonal generators Σ_{ab} corresponding to both representations. [216]

Finally, in order to have different $q_L l_L S_{1,3}$ couplings, we need to consider representation $\overline{\mathbf{144}}$. One way to construct this representation is by the multiplication of smaller representations. We find the following product is the smallest that contains this representation

$$\mathbf{16} \times \mathbf{10} \to \overline{\mathbf{144}} + \overline{\mathbf{16}} \tag{C.4}$$

We start from these two representations, we have matrices $\{T_a^{(10)}\}$ and $\{T_a^{(16)}\}$. We construct the product representation of this algebra by taking the Kronecker product between these matrices and the identity matrix

$$T_a^{(160)} = T_a^{(10)} \otimes \mathbb{1}^{(16)} + \mathbb{1}^{(10)} \otimes T_a^{(16)} \tag{C.5}$$

These matrices generate the algebra in a reducible representation of dimension 160. We need to split them into two blocks corresponding to irreducible representations (irreps) $\overline{\mathbf{144}}$ and $\overline{\mathbf{16}}$. This amounts to finding the two orthogonal subspaces corresponding to these irreps. One way of finding these subspaces, is by using the quadratic Casimir. It so happens that the eigenvalues of the quadratic Casimir of these two representations are distinct. Thus, we write this Casimir element, and then diagonalize it

$$C_2 \equiv \sum_a \left(T_a^{(160)}\right)^2 \to U_c C_2 U_c^\dagger = C_2^{\text{diag}} \tag{C.6}$$

This unitary transformation is the one that defines the two orthogonal subspaces, and thus makes each of the generators split into the two blocks corresponding to each one of the irreps:

$$U_c T_a^{(160)} U_c^\dagger = T_a^{(\overline{144})} \oplus T_a^{(\overline{16})} \tag{C.7}$$

In this manner one can easily construct a 144-dimensional representation of SO(10), which we call $\overline{144}$.

C.2. Embeddings of l_L and LQ couplings

Putting q_L in $(\mathbf{4},\mathbf{2},\mathbf{1})$ and l_L in $(\mathbf{4},\mathbf{1},\mathbf{2})$ is problematic when constructing the interaction term for the LQs, because the Lagrangian couples S_1 and S_3 to $q_L l_L$ with equal strength. That is in equation 5.9, we get that $x_1 = x_3$. This alignment is insufficient when trying to explain the B-anomalies: for example, it gives no correction to $R_{D^{(*)}}$, as can be seen in Eq. (5.24).

To solve this problem we have to consider different fermion representations. First we have to understand why we get the same couplings for S_1 and S_3 when using the representations above. It is enough to look at the $\mathrm{SU}(2)_A \times \mathrm{SU}(2)_B$ representations, as the color contraction is straightforward between q and S, and regarding the SO(5) factor, they are all in trivial representations.

In the scheme previously defined, we have the LQ belonging in a bidoublet $S_{\alpha\beta} \sim (\mathbf{2},\mathbf{2})$, whereas quark and lepton are each embedded in a single doublet: $q_{\alpha'} \sim (\mathbf{2},\mathbf{1})$, $l_{a,\beta'} \sim (\mathbf{1},\mathbf{2})$. To write an invariant we start with the combination

$$S_{\alpha\beta}\, q_{\alpha'}\, l_{a,\beta'}\, G_{\alpha\beta\alpha'\beta'} \ .$$

We use the following Clebsch-Gordan (CG) coefficients for $\mathbf{2}\times\mathbf{2} \to \mathbf{1}+\mathbf{3}$,

$$\begin{aligned} C^0_{\alpha\alpha'} &= \frac{\delta_{\alpha\uparrow}\delta_{\alpha'\downarrow} - \delta_{\alpha\downarrow}\delta_{\alpha'\uparrow}}{\sqrt{2}} \ , \\ C^{1,k}_{\alpha\alpha'} &= \delta_{k,1}\delta_{\alpha\uparrow}\delta_{\alpha'\uparrow} + \delta_{k,0}\frac{\delta_{\alpha\uparrow}\delta_{\alpha'\downarrow} + \delta_{\alpha\downarrow}\delta_{\alpha'\uparrow}}{\sqrt{2}} + \delta_{k,-1}\delta_{\alpha\downarrow}\delta_{\alpha\downarrow} \ , \end{aligned}$$

(where we represent spin half with up and down arrows, and integer spin with the integer k). As we are combining doublets, the invariant combination we have $G_{\alpha\beta\alpha'\beta'} = C^0_{\alpha\alpha'} C^0_{\beta\beta'}$. Replacing in the above formula,

$$S_{\alpha\beta}\, q_{\alpha'}\, l_{a,\beta'}\, G_{\alpha\beta\alpha'\beta'} = \frac{1}{2}\left(S_{\uparrow\uparrow} l_{a,\downarrow} q_{\downarrow} + S_{\downarrow\downarrow} l_{a,\uparrow} q_{\uparrow} - S_{\uparrow\downarrow} l_{a,\uparrow} q_{\downarrow} - S_{\downarrow\uparrow} l_{a,\downarrow} q_{\uparrow}\right) \ .$$

We can rewrite these LQ states in terms of the triplet and the singlet:

$$\begin{aligned} S_{\uparrow\uparrow} &= S_3^1 \ , & S_{\downarrow\downarrow} &= S_3^{-1} \ , \\ S_{\uparrow\downarrow} &= \frac{S_3^0 + S_1}{\sqrt{2}} \ , & S_{\downarrow\uparrow} &= \frac{S_3^0 - S_1}{\sqrt{2}} \ . \end{aligned}$$

By doing this we get (omitting an overall factor of $\frac{1}{2}$)

$$S_3^1 l_{a,\downarrow} q_{\downarrow} + S_3^{-1} l_{a,\uparrow} q_{\uparrow} - S_3^0 \frac{l_{a,\uparrow} q_{\downarrow} + l_{a,\downarrow} q_{\uparrow}}{\sqrt{2}} - S_1 \frac{l_{a,\uparrow} q_{\downarrow} - l_{a,\downarrow} q_{\uparrow}}{\sqrt{2}} \ .$$

And here we see the same size of coupling for the SU(2) singlet and triplet.

Let us consider now a different embedding for the l_L that can differentiate between S_1 and S_3 couplings. We start by considering the representation $(\mathbf{3},\mathbf{2})$. We write $l_{b,k\beta'}$ for the degrees of freedom of a field transforming in that representation. If we take the full representation to be $(\mathbf{4},\mathbf{3},\mathbf{2},\mathbf{1},\mathbf{1})$, the dynamical degrees of freedom of this lepton doublet will be those of $\mathbf{2} \in \mathbf{3}\times\mathbf{2}$.

Once again we construct an invariant using q, l_b and S. We write

$$S_{\alpha\beta}\, q_{\alpha'}\, l_{b,k\beta'}\, \widetilde{G}_{\alpha\beta\alpha'\beta'k} \ .$$

The way to combine these fields into an invariant is now by the use of the CG: $\mathbf{2}\times\mathbf{2} \to \mathbf{3}$. We also have to make use of a matrix corresponding to a π rotation around the y axis (which corresponds to the CG for $\mathbf{3}\times\mathbf{3} \to \mathbf{1}$),

$$R_{kk'} = \begin{pmatrix} 0 & 0 & 1 \\ 0 & -1 & 0 \\ 1 & 0 & 0 \end{pmatrix}$$

in order to correctly contract two triplets. Now, we write the combination as

$$\widetilde{G}_{\alpha\beta\alpha'\beta'k} = R_{kk'}\, C^{1,k}_{\alpha\alpha'}\, C^{0}_{\beta\beta'} \ .$$

By replacing these matrices we get

$$\left(l_{b,1\beta'} S_{\downarrow\beta}\, q_{\downarrow} + l_{b,-1\beta'} S_{\uparrow\beta}\, q_{\uparrow} - l_{b,0\beta'} \frac{S_{\uparrow\beta}\, q_{\downarrow} + S_{\downarrow\beta}\, q_{\uparrow}}{\sqrt{2}} \right) C^{0}_{\beta\beta'} \ .$$

Again taking away an overall factor of $\frac{1}{2}$ we have

$$\begin{aligned} &S_{\uparrow\uparrow}\left(\sqrt{2} l_{b,-1\downarrow} q_{\uparrow} - l_{b,0\downarrow} q_{\downarrow}\right) + S_{\downarrow\downarrow}\left(l_{b,0\uparrow} q_{\uparrow} - \sqrt{2} l_{b,1\uparrow} q_{\downarrow}\right) + S_{\uparrow\downarrow}\left(l_{b,0\uparrow} q_{\downarrow} - \sqrt{2} l_{b,-1\uparrow} q_{\uparrow}\right) \\ &+ S_{\downarrow\uparrow}\left(\sqrt{2} l_{b,1\downarrow} q_{\downarrow} - l_{b,0\downarrow} q_{\uparrow}\right) \ . \end{aligned}$$

We can drop out the fields $l_{b,-1\downarrow}$ and $l_{b,1\uparrow}$ as they are the highest (and lowest) spin components of the fourplet of $\mathrm{SU}(2)_L$, of spin 3/2. Regarding the other components, one can use the CG to identify:

$$\begin{aligned} l_{b,1,\downarrow} &= \sqrt{\frac{2}{3}} l_{\uparrow} \ , & l_{b,0,\uparrow} &= -\frac{1}{\sqrt{3}} l_{\uparrow} \ , \\ l_{b,-1,\uparrow} &= -\sqrt{\frac{2}{3}} l_{\downarrow} \ , & l_{b,0,\downarrow} &= \frac{1}{\sqrt{3}} l_{\downarrow} \ , \end{aligned}$$

where we only turn on the dynamical d.o.f. belonging to the doublet of $\mathrm{SU}(2)_L$. Using

this and rewriting the LQ states in terms of $S_{1,3}$ we arrive to

$$\frac{1}{\sqrt{3}}\left(-S_3^1 l_\downarrow q_\downarrow - S_3^{-1} l_\uparrow q_\uparrow + S_3^0 \frac{l_\uparrow q_\downarrow + l_\downarrow q_\uparrow}{\sqrt{2}} - 3S_1 \frac{l_\uparrow q_\downarrow - l_\downarrow q_\uparrow}{\sqrt{2}}\right) .$$

Comparing to the previous formula we find both a relative sign difference and a different weight for the couplings of S_1 and S_3. This extra representation then allows us to have independent couplings for each of the LQs. If we name the couplings for l_a and l_b as x_{l_a} and x_{l_b}, we have:

$$x_3 \propto x_{l_a} - \frac{x_{l_b}}{\sqrt{3}} , \qquad x_1 \propto x_{l_a} + \sqrt{3}\, x_{l_b} . \tag{C.8}$$

Thus we see how two embeddings for the lepton doublet allow for independent couplings for S_1 and S_3 LQs.

C.3. Potential

In this appendix we include some additional calculations with respect to the NGB potential. In order to calculate the fermionic contribution to the 1-loop Coleman-Weinberg potential, we choose a basis for writing the matrix $\mathcal{K}$ and its expansion in powers of the NGB fields: $\{u_L^c, d_L^c, u_R^c, \ell_L, \nu_L\}$, with c being a color index, this way we get 11-by-11 matrices. We choose these degrees of freedom because they have the largest mixing angles and thus the largest contribution to the potential.

As usual, we replace $\Pi^{\mathbf{r}_H}_{ff'}(p) \to \not{p}\, \Pi^{\mathbf{r}_H}_{ff'}(p)$ for correlators involving elementary fermions with the same chirality.

For the masses of the LQs, defined according to Eq. (5.11), we get:

$$\tilde{M}^2 = \int \frac{d^4p}{(2\pi)^4}\left[\frac{\Pi^{\mathbf{r}_{l_a}}_{l_a l_a} - \Pi^{\bar{\mathbf{r}}_q}_{l_a l_a}}{Z_l + \Pi^{\mathbf{r}_{l_a}}_{l_a l_a} + \Pi^{\mathbf{r}_{l_b}}_{l_b l_b}} + 3\frac{\Pi^{\mathbf{r}_q}_{qq} - \Pi^{\bar{\mathbf{r}}_q}_{qq}}{Z_q + \Pi^{\mathbf{r}_q}_{qq}} + 3\frac{\Pi^{\mathbf{r}_u}_{uu} - \Pi^{\bar{\mathbf{r}}_{e_a}}_{uu}}{Z_u + \Pi^{\mathbf{r}_u}_{uu}} + \frac{(\Pi^{\mathbf{r}_{l_a}}_{q l_a} - \Pi^{\bar{\mathbf{r}}_q}_{q l_a})^2}{2(Z_l + \Pi^{\mathbf{r}_{l_a}}_{l_a l_a} + \Pi^{\mathbf{r}_{l_b}}_{l_b l_b})(Z_q + \Pi^{\mathbf{r}_q}_{qq})}\right]$$

$$\Delta M_1^2 = \int \frac{d^4p}{(2\pi)^4}\left[\frac{33\Pi^{\mathbf{r}_{e_b}}_{l_b l_b} + 10\Pi^{(\mathbf{20},\mathbf{1},\mathbf{2},\mathbf{2},\mathbf{2})}_{l_b l_b} + 5\Pi^{(\bar{\mathbf{4}},\mathbf{2},\mathbf{3},\mathbf{1},\mathbf{1})}_{l_b l_b} - 48\Pi^{\mathbf{r}_{l_b}}_{l_b l_b}}{9[Z_l + \Pi^{\mathbf{r}_{l_a}}_{l_a l_a} + \Pi^{\mathbf{r}_{l_b}}_{l_b l_b}]} + \frac{(45 - 36\sqrt{5})(\Pi^{\bar{\mathbf{r}}_q}_{q l_b})^2 + 36\sqrt{5}\Pi^{\bar{\mathbf{r}}_q}_{q l_b}\Pi^{\mathbf{r}_{l_a}}_{q l_a}}{72(Z_l + \Pi^{\mathbf{r}_{l_a}}_{l_a l_a} + \Pi^{\mathbf{r}_{l_b}}_{l_b l_b})(Z_q + \Pi^{\mathbf{r}_q}_{qq})}\right]$$

$$\Delta M_3^2 = \int \frac{d^4p}{(2\pi)^4}\left[\frac{\Pi^{\mathbf{r}_{e_b}}_{l_b l_b} + 10\Pi^{(\mathbf{20},\mathbf{1},\mathbf{2},\mathbf{2},\mathbf{2})}_{l_b l_b} + 5\Pi^{(\bar{\mathbf{4}},\mathbf{2},\mathbf{3},\mathbf{1},\mathbf{1})}_{l_b l_b} - 16\Pi^{\mathbf{r}_{l_b}}_{l_b l_b}}{Z_l + \Pi^{\mathbf{r}_{l_a}}_{l_a l_a} + \Pi^{\mathbf{r}_{l_b}}_{l_b l_b}} + \frac{(5+12\sqrt{5})(\Pi^{\bar{\mathbf{r}}_q}_{q l_b})^2 - 12\sqrt{5}\Pi^{\bar{\mathbf{r}}_q}_{q l_b}\Pi^{\mathbf{r}_{l_a}}_{q l_a}}{72(Z_l + \Pi^{\mathbf{r}_{l_a}}_{l_a l_a} + \Pi^{\mathbf{r}_{l_b}}_{l_b l_b})(Z_q + \Pi^{\mathbf{r}_q}_{qq})}\right] . \tag{C.9}$$

When calculating the potential for the Higgs component that acquires a VEV, the pNGB matrices can be calculated to all orders in this field. Hence, we can calculate the one loop potential to all orders in v. We can write the following quadratic and quartic coefficients defined in the expansion of Eq. (2.34), in the case of the model of Ch. 5 as integrals of the fermionic correlators:

$$\begin{aligned}
\alpha &= \int \frac{d^4p}{(2\pi)^4}\left\{\frac{4(\Pi^{\mathbf{r}_{e_a}}_{l_a} + \Pi^{\mathbf{r}_{e_b}}_{l_b} - \Pi^{\mathbf{r}_{l_a}}_{l_a} - \Pi^{\mathbf{r}_{l_b}}_{l_b})}{Z_\ell + \Pi^{\mathbf{r}_{l_a}}_{l_a} + \Pi^{\mathbf{r}_{l_b}}_{l_b}} - \frac{12(\Pi'_q - \Pi^{\mathbf{r}_u}_q)}{Z_q + \Pi'_q}\right. \\
&\left. - \frac{3}{2}\frac{(\Pi'_{qu} - \Pi^{\mathbf{r}_u}_{qu})^2}{(Z_q + \Pi'_q)(Z_u + \Pi^{\mathbf{r}_u}_u)} + \frac{3}{2}\frac{(\Pi'_u - \Pi^{\mathbf{r}_u}_u)}{(Z_u + \Pi^{\mathbf{r}_u}_u)}\right\} \\
\beta &= \int \frac{d^4p}{(2\pi)^4}\left\{\frac{2(\Pi^{\mathbf{r}_{e_a}}_{l_a} + \Pi^{\mathbf{r}_{e_b}}_{l_b} - \Pi^{\mathbf{r}_{l_a}}_{l_a} - \Pi^{\mathbf{r}_{l_b}}_{l_b})^2}{(Z_\ell + \Pi^{\mathbf{r}_{l_a}}_{l_a} + \Pi^{\mathbf{r}_{l_b}}_{l_b})^2} + \frac{6(\Pi'_q - \Pi^{\mathbf{r}_u}_q)^2}{\left(Z_q + \Pi'_q\right)^2}\right. \\
&+ \frac{3}{16}\frac{(\Pi'_u - \Pi^{\mathbf{r}_u}_u)^2}{(Z_u + \Pi^{\mathbf{r}_u}_u)^2} + \frac{3}{16}\frac{(\Pi'_{qu} - \Pi^{\mathbf{r}_u}_{qu})^4}{(Z_q + \Pi'_q)^2(Z_u + \Pi^{\mathbf{r}_u}_u)^2} \\
&\left. - \frac{3}{8}\frac{(\Pi'_{qu} - \Pi^{\mathbf{r}_u}_{qu})^2(\Pi'_u - \Pi^{\mathbf{r}_u}_u)}{(Z_q + \Pi'_q)(Z_u + \Pi^{\mathbf{r}_u}_u)^2} - \frac{2}{3}\frac{(\Pi'_{qu} - \Pi^{\mathbf{r}_u}_{qu})^2(\Pi^{\mathbf{r}_u}_q - \Pi'_q)}{(Z_q + \Pi'_q)^2(Z_u + \Pi^{\mathbf{r}_u}_u)}\right\} .
\end{aligned} \tag{C.10}$$

Bibliography

[1] A. Biswas, D. Kumar Ghosh, N. Ghosh, A. Shaw and A. K. Swain, *Collider signature of U_1 Leptoquark and constraints from $b \to c$ observables*, *J. Phys. G* **47** (2020) 045005, [1808.04169]. xii, 101

[2] A. Salam, *Weak and Electromagnetic Interactions*, *Conf. Proc. C* **680519** (1968) 367–377. 1

[3] S. L. Glashow, *The renormalizability of vector meson interactions*, *Nucl. Phys.* **10** (1959) 107–117.

[4] S. Weinberg, *A Model of Leptons*, *Phys. Rev. Lett.* **19** (1967) 1264–1266.

[5] P. W. Higgs, *Broken Symmetries and the Masses of Gauge Bosons*, *Phys. Rev. Lett.* **13** (1964) 508–509.

[6] S. Weinberg, *The Quantum Theory of Fields, Volume 1: Foundations*. Cambridge University Press, 2005.

[7] S. Weinberg, *The quantum theory of fields. Vol. 2: Modern applications*. 1996. 1, 8, 13

[8] *Approaches to Quantum Gravity: Toward a New Understanding of Space, Time and Matter*. Cambridge University Press, 2009, 10.1017/CBO9780511575549. 1

[9] G. Bertone, D. Hooper and J. Silk, *Particle dark matter: Evidence, candidates and constraints*, *Phys. Rept.* **405** (2005) 279–390, [hep-ph/0404175]. 1

[10] E. J. Copeland, M. Sami and S. Tsujikawa, *Dynamics of dark energy*, *Int. J. Mod. Phys. D* **15** (2006) 1753–1936, [hep-th/0603057]. 1

[11] Super-Kamiokande collaboration, Y. Fukuda et al., *Evidence for oscillation of atmospheric neutrinos*, *Phys. Rev. Lett.* **81** (1998) 1562–1567, [hep-ex/9807003]. 1

[12] R. Peccei and H. Quinn, *Cp conservation in the presence of pseudoparticles*, *Physical Review Letters - PHYS REV LETT* **38** (06, 1977) 1440–1443. 1

[13] S. Weinberg, *The cosmological constant problem*, *Rev. Mod. Phys.* **61** (Jan, 1989) 1–23. 2

[14] ATLAS collaboration, G. Aad et al., *Observation of a new particle in the search for the Standard Model Higgs boson with the ATLAS detector at the LHC*, *Phys. Lett. B* **716** (2012) 1–29, [1207.7214]. 2

[15] CMS collaboration, S. Chatrchyan et al., *Observation of a New Boson at a Mass of 125 GeV with the CMS Experiment at the LHC*, *Phys. Lett. B* **716** (2012) 30–61, [1207.7235]. 2

[16] W. A. Bardeen, *On naturalness in the standard model*, in *Ontake Summer Institute on Particle Physics*, 8, 1995. 2

[17] Particle Data Group collaboration, P. Zyla et al., *Review of Particle Physics*, *PTEP* **2020** (2020) 083C01. 3, 5, 121

[18] G. Panico and A. Wulzer, *The Composite Nambu-Goldstone Higgs*, vol. 913. Springer, 2016, 10.1007/978-3-319-22617-0. 3, 4, 13, 31, 34, 35, 38, 45, 61, 62, 154, 156, 157

[19] D. Bailin and A. Love, *Supersymmetric Gauge Field Theory and String Theory*. Graduate Student Series in Physics. CRC Press, 1994. 4

[20] M. Magg and C. Wetterich, *Neutrino Mass Problem and Gauge Hierarchy*, *Phys. Lett. B* **94** (1980) 61–64. 5

[21] S. King and N. Nimai Singh, *Inverted hierarchy models of neutrino masses*, *Nuclear Physics B* **596** (2001) 81–98. 5

[22] G. Isidori, Y. Nir and G. Perez, *Flavor Physics Constraints for Physics Beyond the Standard Model*, *Ann. Rev. Nucl. Part. Sci.* **60** (2010) 355, [1002.0900]. 5, 38, 154

[23] BaBar collaboration, J. Lees et al., *Measurement of an Excess of $\bar{B} \to D^{(*)}\tau^-\bar{\nu}_\tau$ Decays and Implications for Charged Higgs Bosons*, *Phys. Rev. D* **88** (2013) 072012, [1303.0571]. 7, 46

[24] Belle collaboration, S. Hirose et al., *Measurement of the τ lepton polarization and $R(D^*)$ in the decay $\bar{B} \to D^*\tau^-\bar{\nu}_\tau$*, *Phys. Rev. Lett.* **118** (2017) 211801, [1612.00529]. 46

[25] Belle collaboration, A. Abdesselam et al., *Measurement of $\mathcal{R}(D)$ and $\mathcal{R}(D^*)$ with a semileptonic tagging method*, 1904.08794. 46

[26] LHCb collaboration, R. Aaij et al., *Measurement of the ratio of branching fractions* $\mathcal{B}(\bar{B}^0 \to D^{*+}\tau^-\bar{\nu}_\tau)/\mathcal{B}(\bar{B}^0 \to D^{*+}\mu^-\bar{\nu}_\mu)$, *Phys. Rev. Lett.* **115** (2015) 111803, [1506.08614]. 46

[27] LHCb collaboration, R. Aaij et al., *Test of Lepton Flavor Universality by the measurement of the* $B^0 \to D^{*-}\tau^+\nu_\tau$ *branching fraction using three-prong* τ *decays*, *Phys. Rev. D* **97** (2018) 072013, [1711.02505]. 7, 46

[28] HFLAV, *Average for* $R(D)$ *and* $R(D^*)$ *for Spring 2019*. https://hflav-eos.web.cern.ch/hflav-eos/semi/spring19/html/RDsDsstar/RDRDs.html. 7, 46

[29] Belle collaboration, A. Abdesselam et al., *Test of lepton flavor universality in* $B \to K^*\ell^+\ell^-$ *decays at Belle*, 1904.02440. 7, 47

[30] LHCb collaboration, R. Aaij et al., *Test of lepton universality using* $B^+ \to K^+\ell^+\ell^-$ *decays*, *Phys. Rev. Lett.* **113** (2014) 151601, [1406.6482]. 47

[31] LHCb collaboration, R. Aaij et al., *Test of lepton universality with* $B^0 \to K^{*0}\ell^+\ell^-$ *decays*, *JHEP* **08** (2017) 055, [1705.05802]. 47

[32] LHCb collaboration, R. Aaij et al., *Search for lepton-universality violation in* $B^+ \to K^+\ell^+\ell^-$ *decays*, *Phys. Rev. Lett.* **122** (2019) 191801, [1903.09252]. 47

[33] LHCb collaboration, R. Aaij et al., *Test of lepton universality in beauty-quark decays*, *Nature Phys.* **18** (2022) 277–282, [2103.11769]. 7, 47

[34] A. Azatov, D. Bardhan, D. Ghosh, F. Sgarlata and E. Venturini, *Anatomy of* $b \to c\tau\nu$ *anomalies*, *JHEP* **11** (2018) 187, [1805.03209]. 7

[35] B. Bhattacharya, A. Datta, D. London and S. Shivashankara, *Simultaneous Explanation of the* R_K *and* $R(D^{(*)})$ *Puzzles*, *Phys. Lett. B* **742** (2015) 370–374, [1412.7164].

[36] R. Alonso, B. Grinstein and J. Martin Camalich, *Lepton universality violation and lepton flavor conservation in B-meson decays*, *JHEP* **10** (2015) 184, [1505.05164].

[37] A. Greljo, G. Isidori and D. Marzocca, *On the breaking of Lepton Flavor Universality in B decays*, *JHEP* **07** (2015) 142, [1506.01705].

[38] L. Calibbi, A. Crivellin and T. Ota, *Effective Field Theory Approach to* $b \to s\ell\ell^{(\prime)}$, $B \to K^{(*)}\nu\bar{\nu}$ *and* $B \to D^{(*)}\tau\nu$ *with Third Generation Couplings*, *Phys. Rev. Lett.* **115** (2015) 181801, [1506.02661].

[39] M. Bordone, G. Isidori and S. Trifinopoulos, *Semileptonic B-physics anomalies: A general EFT analysis within $U(2)^n$ flavor symmetry*, *Phys. Rev. D* **96** (2017) 015038, [1702.07238]. 7

[40] V. Gherardi, D. Marzocca and E. Venturini, *Matching scalar leptoquarks to the SMEFT at one loop*, *JHEP* **07** (2020) 225, [2003.12525].

[41] V. Gherardi, D. Marzocca and E. Venturini, *Low-energy phenomenology of scalar leptoquarks at one-loop accuracy*, 2008.09548. 109

[42] M. Bordone, O. Catà, T. Feldmann and R. Mandal, *Constraining flavour patterns of scalar leptoquarks in the effective field theory*, 2010.03297. 109

[43] M. Bordone, O. Catà and T. Feldmann, *Effective Theory Approach to New Physics with Flavour: General Framework and a Leptoquark Example*, *JHEP* **01** (2020) 067, [1910.02641].

[44] A. Angelescu, D. Bečirević, D. Faroughy and O. Sumensari, *Closing the window on single leptoquark solutions to the B-physics anomalies*, *JHEP* **10** (2018) 183, [1808.08179]. 7, 46, 56, 109

[45] D. Bečirević, S. Fajfer, N. Košnik and O. Sumensari, *Leptoquark model to explain the B-physics anomalies, R_K and R_D*, *Phys. Rev. D* **94** (2016) 115021, [1608.08501].

[46] D. Das, C. Hati, G. Kumar and N. Mahajan, *Towards a unified explanation of $R_{D^{(*)}}$, R_K and $(g-2)_\mu$ anomalies in a left-right model with leptoquarks*, *Phys. Rev. D* **94** (2016) 055034, [1605.06313].

[47] R. Barbieri, G. Isidori, A. Pattori and F. Senia, *Anomalies in B-decays and $U(2)$ flavour symmetry*, *Eur. Phys. J. C* **76** (2016) 67, [1512.01560].

[48] S. Fajfer and N. Košnik, *Vector leptoquark resolution of R_K and $R_{D^{(*)}}$ puzzles*, *Phys. Lett. B* **755** (2016) 270–274, [1511.06024].

[49] M. Bauer and M. Neubert, *Minimal Leptoquark Explanation for the $R_{D^{(*)}}$, R_K , and $(g-2)_g$ Anomalies*, *Phys. Rev. Lett.* **116** (2016) 141802, [1511.01900]. 109

[50] S. M. Boucenna, A. Celis, J. Fuentes-Martin, A. Vicente and J. Virto, *Phenomenology of an $SU(2) \times SU(2) \times U(1)$ model with lepton-flavour non-universality*, *JHEP* **12** (2016) 059, [1608.01349]. 7

[51] G. Hiller, D. Loose and K. Schönwald, *Leptoquark Flavor Patterns \& B Decay Anomalies*, *JHEP* **12** (2016) 027, [1609.08895].

[52] B. Bhattacharya, A. Datta, J.-P. Guévin, D. London and R. Watanabe, *Simultaneous Explanation of the R_K and $R_{D^{(*)}}$ Puzzles: a Model Analysis*, *JHEP* **01** (2017) 015, [1609.09078]. 123

[53] A. Crivellin, C. Greub, D. Müller and F. Saturnino, *Scalar Leptoquarks in Leptonic Processes*, 2010.06593. 109

[54] R. Barbieri, C. W. Murphy and F. Senia, *B-decay Anomalies in a Composite Leptoquark Model*, *Eur. Phys. J. C* **77** (2017) 8, [1611.04930].

[55] Y. Cai, J. Gargalionis, M. A. Schmidt and R. R. Volkas, *Reconsidering the One Leptoquark solution: flavor anomalies and neutrino mass*, *JHEP* **10** (2017) 047, [1704.05849].

[56] E. Megias, M. Quiros and L. Salas, *Lepton-flavor universality violation in R_K and $R_{D^{(*)}}$ from warped space*, *JHEP* **07** (2017) 102, [1703.06019].

[57] O. Popov, M. A. Schmidt and G. White, *R_2 as a single leptoquark solution to $R_{D^{(*)}}$ and $R_{K^{(*)}}$*, *Phys. Rev. D* **100** (2019) 035028, [1905.06339].

[58] C. Cornella, J. Fuentes-Martin and G. Isidori, *Revisiting the vector leptoquark explanation of the B-physics anomalies*, *JHEP* **07** (2019) 168, [1903.11517].

[59] J. Fuentes-Martin and P. Stangl, *Third-family quark-lepton unification with a fundamental composite Higgs*, *Phys. Lett. B* **811** (2020) 135953, [2004.11376]. 7

[60] D. Buttazzo, A. Greljo, G. Isidori and D. Marzocca, *B-physics anomalies: a guide to combined explanations*, *JHEP* **11** (2017) 044, [1706.07808]. 7, 46, 56, 78, 79, 80, 82, 90, 91, 109, 118, 119, 120, 121, 128, 134

[61] A. Crivellin, D. Müller and T. Ota, *Simultaneous explanation of $R(D^{(*)})$ and $b \to s\mu^+\mu^-$: the last scalar leptoquarks standing*, *JHEP* **09** (2017) 040, [1703.09226]. 7, 82, 109

[62] I. Doršner, S. Fajfer, A. Greljo, J. Kamenik and N. Košnik, *Physics of leptoquarks in precision experiments and at particle colliders*, *Phys. Rept.* **641** (2016) 1–68, [1603.04993]. 7, 59, 80

[63] D. B. Kaplan and H. Georgi, *SU(2) x U(1) Breaking by Vacuum Misalignment*, *Phys. Lett. B* **136** (1984) 183–186. 8

[64] H. Georgi and D. B. Kaplan, *Composite Higgs and custodial SU(2)*, *Physics Letters B* **145** (1984) 216–220.

[65] K. Agashe, R. Contino and A. Pomarol, *The Minimal composite Higgs model*, *Nucl. Phys. B* **719** (2005) 165–187, [hep-ph/0412089]. 8, 14, 17, 27, 116

[66] S. Pokorski, *Gauge Field Theories*. Cambridge Monographs on Mathematical Physics. Cambridge University Press, 2 ed., 2000, 10.1017/CBO9780511612343. 8

[67] L. Susskind, *Dynamics of Spontaneous Symmetry Breaking in the Weinberg-Salam Theory*, *Phys. Rev. D* **20** (1979) 2619–2625. 8

[68] S. Weinberg, *Implications of dynamical symmetry breaking*, *Phys. Rev. D* **13** (Feb, 1976) 974–996. 8

[69] R. Rattazzi, V. S. Rychkov, E. Tonni and A. Vichi, *Bounding scalar operator dimensions in 4D CFT*, *JHEP* **12** (2008) 031, [0807.0004]. 9

[70] B. Gripaios, *Composite Leptoquarks at the LHC*, *JHEP* **02** (2010) 045, [0910.1789]. 10

[71] B. Gripaios, M. Nardecchia and S. A. Renner, *Composite leptoquarks and anomalies in B-meson decays*, *JHEP* **05** (2015) 006, [1412.1791]. 61, 63, 115

[72] D. Marzocca, *Addressing the B-physics anomalies in a fundamental Composite Higgs Model*, *JHEP* **07** (2018) 121, [1803.10972]. 10, 82, 109

[73] Y. Nambu, *Quasiparticles and Gauge Invariance in the Theory of Superconductivity*, *Phys. Rev.* **117** (1960) 648–663. 13

[74] J. Goldstone, *Field Theories with Superconductor Solutions*, *Nuovo Cim.* **19** (1961) 154–164. 13

[75] J. Mrazek, A. Pomarol, R. Rattazzi, M. Redi, J. Serra and A. Wulzer, *The Other Natural Two Higgs Doublet Model*, *Nucl. Phys.* **B853** (2011) 1–48, [1105.5403]. 14, 17

[76] C. G. Callan, Jr., S. R. Coleman, J. Wess and B. Zumino, *Structure of phenomenological Lagrangians. 2.*, *Phys. Rev.* **177** (1969) 2247–2250. 15

[77] S. R. Coleman, J. Wess and B. Zumino, *Structure of phenomenological Lagrangians. 1.*, *Phys. Rev.* **177** (1969) 2239–2247. 15

[78] H. E. Logan, *TASI 2013 lectures on Higgs physics within and beyond the Standard Model*, 1406.1786. 16

[79] M. E. Peskin and T. Takeuchi, *Estimation of oblique electroweak corrections*, *Phys. Rev. D* **46** (Jul, 1992) 381–409. 16

[80] G. Altarelli, R. Barbieri and F. Caravaglios, *Electroweak precision tests: A Concise review*, *Int. J. Mod. Phys. A* **13** (1998) 1031–1058, [hep-ph/9712368].

[81] R. Barbieri, A. Pomarol, R. Rattazzi and A. Strumia, *Electroweak symmetry breaking after LEP-1 and LEP-2*, *Nucl. Phys. B* **703** (2004) 127–146, [hep-ph/0405040]. 16

[82] K. Agashe, R. Contino and R. Sundrum, *Top compositeness and precision unification*, *Phys. Rev. Lett.* **95** (Oct, 2005) 171804. 17

[83] R. Contino, L. Da Rold and A. Pomarol, *Light custodians in natural composite Higgs models*, *Phys. Rev. D* **75** (2007) 055014, [hep-ph/0612048]. 27, 104

[84] G. Panico, M. Redi, A. Tesi and A. Wulzer, *On the Tuning and the Mass of the Composite Higgs*, *JHEP* **03** (2013) 051, [1210.7114]. 27, 28, 68, 72, 118

[85] K. Kawarabayashi and M. Suzuki, *Partially conserved axial-vector current and the decays of vector mesons*, *Phys. Rev. Lett.* **16** (Feb, 1966) 255–257. 27

[86] M. Carena, L. Da Rold and E. Pontón, *Minimal Composite Higgs Models at the LHC*, *JHEP* **06** (2014) 159, [1402.2987]. 28, 53, 104, 116, 176

[87] S. De Curtis, M. Redi and A. Tesi, *The 4D Composite Higgs*, *JHEP* **04** (2012) 042, [1110.1613]. 28, 49, 53, 176

[88] C. Csaki, A. Falkowski and A. Weiler, *The Flavor of the Composite Pseudo-Goldstone Higgs*, *JHEP* **09** (2008) 008, [0804.1954]. 28, 34, 61, 115

[89] C. Csaki, A. Falkowski and A. Weiler, *A Simple Flavor Protection for RS*, *Phys. Rev. D* **80** (2009) 016001, [0806.3757]. 32, 45, 91, 142

[90] K. Agashe, G. Perez and A. Soni, *Flavor structure of warped extra dimension models*, *Phys. Rev. D* **71** (2005) 016002, [hep-ph/0408134]. 34, 45, 48, 77, 142

[91] K. Agashe, A. Azatov and L. Zhu, *Flavor Violation Tests of Warped/Composite SM in the Two-Site Approach*, *Phys. Rev. D* **79** (2009) 056006, [0810.1016]. 34, 156

[92] K. Agashe, T. Okui and R. Sundrum, *A Common Origin for Neutrino Anarchy and Charged Hierarchies*, *Phys. Rev. Lett.* **102** (2009) 101801, [0810.1277]. 35, 62

[93] L. Da Rold, *Anarchy with linear and bilinear interactions*, *JHEP* **10** (2017) 120, [1708.08515]. 35, 46, 62, 91, 92, 115, 128, 142

[94] G. Isidori, *Flavor physics and CP violation*, in *2012 European School of High-Energy Physics*, pp. 69–105, 2014. 1302.0661. DOI. 37, 124

[95] UTfit collaboration, M. Bona et al., *Model-independent constraints on $\Delta F = 2$ operators and the scale of new physics*, *JHEP* **03** (2008) 049, [0707.0636]. 37

[96] G. F. Giudice, C. Grojean, A. Pomarol and R. Rattazzi, *The Strongly-Interacting Light Higgs*, *JHEP* **06** (2007) 045, [hep-ph/0703164]. 39, 48

[97] M. König, M. Neubert and D. M. Straub, *Dipole operator constraints on composite Higgs models*, *Eur. Phys. J. C* **74** (2014) 2945, [1403.2756]. 40, 41, 45, 153, 156, 157

[98] W. Altmannshofer, P. Paradisi and D. M. Straub, *Model-Independent Constraints on New Physics in $b \to s$ Transitions*, *JHEP* **04** (2012) 008, [1111.1257]. 42

[99] W. Altmannshofer and D. M. Straub, *Cornering New Physics in $b \to s$ Transitions*, *JHEP* **08** (2012) 121, [1206.0273]. 42

[100] A. J. Buras, C. Grojean, S. Pokorski and R. Ziegler, *FCNC Effects in a Minimal Theory of Fermion Masses*, *JHEP* **08** (2011) 028, [1105.3725]. 43

[101] K. Agashe, R. Contino, L. Da Rold and A. Pomarol, *A Custodial symmetry for $Zb\bar{b}$*, *Phys. Lett. B* **641** (2006) 62–66, [hep-ph/0605341]. 43, 63, 74, 91, 155, 156

[102] R. Barbieri, D. Buttazzo, F. Sala, D. M. Straub and A. Tesi, *A 125 GeV composite Higgs boson versus flavour and electroweak precision tests*, *JHEP* **05** (2013) 069, [1211.5085]. 44, 45

[103] N. Vignaroli, *$\Delta F=1$ constraints on composite Higgs models with LR parity*, *Phys. Rev. D* **86** (2012) 115011, [1204.0478]. 44

[104] Y. Grossman and M. Neubert, *Neutrino masses and mixings in nonfactorizable geometry*, *Phys. Lett.* **B474** (2000) 361–371, [hep-ph/9912408]. 45

[105] S. J. Huber and Q. Shafi, *Fermion masses, mixings and proton decay in a Randall-Sundrum model*, *Phys. Lett.* **B498** (2001) 256–262, [hep-ph/0010195].

[106] T. Gherghetta and A. Pomarol, *Bulk fields and supersymmetry in a slice of AdS*, *Nucl. Phys.* **B586** (2000) 141–162, [hep-ph/0003129]. 142

[107] B. Keren-Zur, P. Lodone, M. Nardecchia, D. Pappadopulo, R. Rattazzi and L. Vecchi, *On Partial Compositeness and the CP asymmetry in charm decays*, *Nucl. Phys.* **B867** (2013) 394–428, [1205.5803]. 45

[108] G. Cacciapaglia, C. Csaki, J. Galloway, G. Marandella, J. Terning and A. Weiler, *A GIM Mechanism from Extra Dimensions*, *JHEP* **04** (2008) 006, [0709.1714]. 45

[109] J. Santiago, *Minimal Flavor Protection: A New Flavor Paradigm in Warped Models*, *JHEP* **12** (2008) 046, [0806.1230]. 142

[110] M. Redi and A. Weiler, *Flavor and CP Invariant Composite Higgs Models*, *JHEP* **11** (2011) 108, [1106.6357]. 91, 115, 142

[111] R. Barbieri, D. Buttazzo, F. Sala and D. M. Straub, *Flavour physics from an approximate $U(2)^3$ symmetry*, *JHEP* **07** (2012) 181, [1203.4218].

[112] M. Frigerio, M. Nardecchia, J. Serra and L. Vecchi, *The Bearable Compositeness of Leptons*, *JHEP* **10** (2018) 017, [1807.04279]. 45, 92, 115, 149

[113] G. Panico and A. Pomarol, *Flavor hierarchies from dynamical scales*, *JHEP* **07** (2016) 097, [1603.06609]. 46, 91, 115, 128, 141, 142, 149

[114] M. Bauer, R. Malm and M. Neubert, *A Solution to the Flavor Problem of Warped Extra-Dimension Models*, *Phys. Rev. Lett.* **108** (2012) 081603, [1110.0471]. 46

[115] L. Da Rold and I. A. Davidovich, *A symmetry for ϵ_K*, *JHEP* **10** (2017) 135, [1704.08704]. 46

[116] D. Bigi and P. Gambino, *Revisiting $B \to D\ell\nu$*, *Phys. Rev. D* **94** (2016) 094008, [1606.08030]. 46

[117] F. U. Bernlochner, Z. Ligeti, M. Papucci and D. J. Robinson, *Combined analysis of semileptonic B decays to D and D^*: $R(D^{(*)})$, $|V_{cb}|$, and new physics*, *Phys. Rev. D* **95** (2017) 115008, [1703.05330].

[118] S. Jaiswal, S. Nandi and S. K. Patra, *Extraction of $|V_{cb}|$ from $B \to D^{(*)}\ell\nu_\ell$ and the Standard Model predictions of $R(D^{(*)})$*, *JHEP* **12** (2017) 060, [1707.09977].

[119] D. Bigi, P. Gambino and S. Schacht, *$R(D^*)$, $|V_{cb}|$, and the Heavy Quark Symmetry relations between form factors*, *JHEP* **11** (2017) 061, [1707.09509]. 46

[120] G. Hiller and F. Kruger, *More model-independent analysis of $b \to s$ processes*, *Phys. Rev. D* **69** (2004) 074020, [hep-ph/0310219]. 47

[121] M. Bordone, G. Isidori and A. Pattori, *On the Standard Model predictions for R_K and R_{K^*}*, *Eur. Phys. J. C* **76** (2016) 440, [1605.07633]. 47

[122] J. Aebischer, W. Altmannshofer, D. Guadagnoli, M. Reboud, P. Stangl and D. M. Straub, *B-decay discrepancies after Moriond 2019*, *Eur. Phys. J. C* **80** (2020) 252, [1903.10434]. 48, 90

[123] A. K. Alok, A. Dighe, S. Gangal and D. Kumar, *Continuing search for new physics in $b \to s\mu\mu$ decays: two operators at a time*, *JHEP* **06** (2019) 089, [1903.09617]. 48, 90

[124] B. Capdevila, A. Crivellin, S. Descotes-Genon, J. Matias and J. Virto, *Patterns of New Physics in $b \to s\ell^+\ell^-$ transitions in the light of recent data*, *JHEP* **01** (2018) 093, [1704.05340]. 48, 120

[125] L. Randall and R. Sundrum, *A Large mass hierarchy from a small extra dimension*, *Phys. Rev. Lett.* **83** (1999) 3370–3373, [hep-ph/9905221]. 48

[126] N. Arkani-Hamed, A. G. Cohen and H. Georgi, *Electroweak symmetry breaking from dimensional deconstruction*, *Phys. Lett. B* **513** (2001) 232–240, [hep-ph/0105239]. 48

[127] N. Arkani-Hamed, A. G. Cohen, E. Katz and A. E. Nelson, *The Littlest Higgs*, *JHEP* **07** (2002) 034, [hep-ph/0206021].

[128] R. Contino, T. Kramer, M. Son and R. Sundrum, *Warped/composite phenomenology simplified*, *JHEP* **05** (2007) 074, [hep-ph/0612180]. 48, 144, 176

[129] G. Panico and A. Wulzer, *The Discrete Composite Higgs Model*, *JHEP* **09** (2011) 135, [1106.2719]. 49, 53

[130] K. S. Babu, S. Nandi and Z. Tavartkiladze, *New Mechanism for Neutrino Mass Generation and Triply Charged Higgs Bosons at the LHC*, *Phys. Rev.* **D80** (2009) 071702, [0905.2710]. 62, 68, 81

[131] D. G. Phillips, II et al., *Neutron-Antineutron Oscillations: Theoretical Status and Experimental Prospects*, *Phys. Rept.* **612** (2016) 1–45, [1410.1100]. 63, 115

[132] S. Antusch and V. Maurer, *Running quark and lepton parameters at various scales*, *JHEP* **11** (2013) 115, [1306.6879]. 71, 141

[133] CMS collaboration, A. M. Sirunyan et al., *Running of the top quark mass from proton-proton collisions at $\sqrt{s} = 13TeV$*, *Phys. Lett. B* **803** (2020) 135263, [1909.09193]. 71

[134] R. Barbieri and G. F. Giudice, *Upper Bounds on Supersymmetric Particle Masses*, *Nucl. Phys.* **B306** (1988) 63–76. 72

[135] G. W. Anderson and D. J. Castano, *Measures of fine tuning*, *Phys. Lett.* **B347** (1995) 300–308, [hep-ph/9409419]. 72

[136] F. Feruglio, P. Paradisi and A. Pattori, *Revisiting Lepton Flavor Universality in B Decays*, *Phys. Rev. Lett.* **118** (2017) 011801, [1606.00524]. 79, 91

[137] Particle Data Group collaboration, C. Patrignani et al., *Review of Particle Physics*, *Chin. Phys.* **C40** (2016) 100001. 80

[138] I. Doršner and A. Greljo, *Leptoquark toolbox for precision collider studies*, *JHEP* **05** (2018) 126, [1801.07641]. 80

[139] CMS collaboration, A. M. Sirunyan et al., *Search for third-generation scalar leptoquarks decaying to a top quark and a τ lepton at $\sqrt{s} = 13$ TeV*, *Eur. Phys. J.* **C78** (2018) 707, [1803.02864].

[140] E. Alvarez, L. Da Rold, A. Juste, M. Szewc and T. Vazquez Schroeder, *A composite pNGB leptoquark at the LHC*, 1808.02063. 80, 134

[141] E. Alvarez and M. Szewc, *Non-resonant Leptoquark with multigeneration couplings to $\mu\mu jj$ and $\mu\nu jj$ at LHC*, 1811.05944. 80

[142] D. Bečirević, I. Doršner, S. Fajfer, N. Košnik, D. A. Faroughy and O. Sumensari, *Scalar leptoquarks from grand unified theories to accommodate the B-physics anomalies*, *Phys. Rev.* **D98** (2018) 055003, [1806.05689]. 82, 109

[143] A. Carmona and F. Goertz, *Custodial Leptons and Higgs Decays*, *JHEP* **04** (2013) 163, [1301.5856]. 84, 104

[144] M. Frigerio, J. Serra and A. Varagnolo, *Composite GUTs: models and expectations at the LHC*, *JHEP* **06** (2011) 029, [1103.2997]. 85, 88, 89

[145] M. Algueró, B. Capdevila, A. Crivellin, S. Descotes-Genon, P. Masjuan, J. Matias et al., *Emerging patterns of New Physics with and without Lepton Flavour Universal contributions*, *Eur. Phys. J. C* **79** (2019) 714, [1903.09578]. 90

[146] HFLAV collaboration, Y. Amhis et al., *Averages of b-hadron, c-hadron, and τ-lepton properties as of summer 2016*, *Eur. Phys. J. C* **77** (2017) 895, [1612.07233]. 91

[147] E. C. Andrés, L. Da Rold and I. A. Davidovich, *Beautiful mirrors for a pNGB Higgs*, *JHEP* **03** (2016) 152, [1509.04726]. 91, 176

[148] ALEPH, DELPHI, L3, OPAL, SLD, LEP Electroweak Working Group, SLD Electroweak Group, SLD Heavy Flavour Group collaboration, S. Schael et al., *Precision electroweak measurements on the Z resonance*, *Phys. Rept.* **427** (2006) 257–454, [hep-ex/0509008]. 91, 101, 125

[149] A. Azatov, D. Barducci, D. Ghosh, D. Marzocca and L. Ubaldi, *Combined explanations of B-physics anomalies: the sterile neutrino solution*, *JHEP* **10** (2018) 092, [1807.10745]. 92

[150] C. Grojean, O. Matsedonskyi and G. Panico, *Light top partners and precision physics*, *JHEP* **10** (2013) 160, [1306.4655]. 92

[151] CMS collaboration, A. M. Sirunyan et al., *Search for the production of four top quarks in the single-lepton and opposite-sign dilepton final states in proton-proton collisions at* $\sqrt{s} = 13$ *TeV*, *JHEP* **11** (2019) 082, [1906.02805]. 101

[152] ATLAS collaboration, M. Aaboud et al., *Search for additional heavy neutral Higgs and gauge bosons in the ditau final state produced in 36 fb*$^{-1}$ *of pp collisions at* $\sqrt{s} = 13$ *TeV with the ATLAS detector*, *JHEP* **01** (2018) 055, [1709.07242]. 101

[153] ATLAS collaboration, M. Aaboud et al., *Search for WW/WZ resonance production in* $\ell\nu qq$ *final states in pp collisions at* $\sqrt{s} = 13$ *TeV with the ATLAS detector*, *JHEP* **03** (2018) 042, [1710.07235].

[154] ATLAS collaboration, M. Aaboud et al., *Search for resonances in the mass distribution of jet pairs with one or two jets identified as b-jets in proton-proton collisions at* $\sqrt{s} = 13$ *TeV with the ATLAS detector*, *Phys. Rev. D* **98** (2018) 032016, [1805.09299].

[155] CMS collaboration, A. M. Sirunyan et al., *Search for resonant* $\mathrm{t\bar{t}}$ *production in proton-proton collisions at* $\sqrt{s} = 13$ *TeV*, *JHEP* **04** (2019) 031, [1810.05905].

[156] CMS collaboration, A. M. Sirunyan et al., *Combination of CMS searches for heavy resonances decaying to pairs of bosons or leptons*, *Phys. Lett. B* **798** (2019) 134952, [1906.00057].

[157] CMS collaboration, *Search for a narrow resonance in high-mass dilepton final states in proton-proton collisions using 140* fb^{-1} *of data at* $\sqrt{s} = 13$ TeV, . 101

[158] J. M. Cline, *B decay anomalies and dark matter from vectorlike confinement*, *Phys. Rev. D* **97** (2018) 015013, [1710.02140]. 104

[159] A. Crivellin, D. Müller and F. Saturnino, *Flavor Phenomenology of the Leptoquark Singlet-Triplet Model*, *JHEP* **06** (2020) 020, [1912.04224]. 109, 119, 121, 122, 124, 125, 126

[160] Belle collaboration, J. Grygier et al., *Search for $B \to h\nu\bar{\nu}$ decays with semileptonic tagging at Belle*, *Phys. Rev. D* **96** (2017) 091101, [1702.03224]. 121

[161] A. Crivellin, L. Hofer, J. Matias, U. Nierste, S. Pokorski and J. Rosiek, *Lepton-flavour violating B decays in generic Z′ models*, *Phys. Rev. D* **92** (2015) 054013, [1504.07928]. 121

[162] M. Blanke, A. Crivellin, S. de Boer, T. Kitahara, M. Moscati, U. Nierste et al., *Impact of polarization observables and $B_c \to \tau\nu$ on new physics explanations of the $b \to c\tau\nu$ anomaly*, *Phys. Rev. D* **99** (2019) 075006, [1811.09603]. 123

[163] S. Iguro, T. Kitahara, Y. Omura, R. Watanabe and K. Yamamoto, *D^* polarization vs. $R_{D^{(*)}}$ anomalies in the leptoquark models*, *JHEP* **02** (2019) 194, [1811.08899]. 123

[164] M. González-Alonso, J. Martin Camalich and K. Mimouni, *Renormalization-group evolution of new physics contributions to (semi)leptonic meson decays*, *Phys. Lett. B* **772** (2017) 777–785, [1706.00410]. 123

[165] A. Lenz, U. Nierste, J. Charles, S. Descotes-Genon, A. Jantsch, C. Kaufhold et al., *Anatomy of New Physics in $B - \bar{B}$ mixing*, *Phys. Rev. D* **83** (2011) 036004, [1008.1593]. 124

[166] P. Arnan, D. Becirevic, F. Mescia and O. Sumensari, *Probing low energy scalar leptoquarks by the leptonic W and Z couplings*, *JHEP* **02** (2019) 109, [1901.06315]. 125

[167] P. Janot and S. Jadach, *Improved Bhabha cross section at LEP and the number of light neutrino species*, *Phys. Lett. B* **803** (2020) 135319, [1912.02067]. 126

[168] BaBar collaboration, B. Aubert et al., *Searches for Lepton Flavor Violation in the Decays tau+- —> e+- gamma and tau+- —> mu+- gamma*, *Phys. Rev. Lett.* **104** (2010) 021802, [0908.2381]. 127

[169] MEG collaboration, A. M. Baldini et al., *Search for the lepton flavour violating decay $\mu^+ \to e^+\gamma$ with the full dataset of the MEG experiment*, *Eur. Phys. J. C* **76** (2016) 434, [1605.05081]. 127

[170] O. Matsedonskyi, *On Flavour and Naturalness of Composite Higgs Models*, *JHEP* **02** (2015) 154, [1411.4638]. 128

[171] F. Feruglio, P. Paradisi and A. Pattori, *On the Importance of Electroweak Corrections for B Anomalies*, *JHEP* **09** (2017) 061, [1705.00929]. 128

[172] Belle-II collaboration, W. Altmannshofer et al., *The Belle II Physics Book*, *PTEP* **2019** (2019) 123C01, [1808.10567]. 128, 133

[173] U. Bellgardt, G. Otter, R. Eichler, L. Felawka, C. Niebuhr, H. Walter et al., *Search for the decay $\mu+ \to e + e + e-$*, *Nuclear Physics B* **299** (1988) 1–6. 128

[174] A. Pich, *Precision Tau Physics*, *Prog. Part. Nucl. Phys.* **75** (2014) 41–85, [1310.7922]. 128

[175] ATLAS collaboration, G. Aad et al., *Search for pair production of third-generation scalar leptoquarks decaying into a top quark and a τ-lepton in pp collisions at $\sqrt{s} = 13$ TeV with the ATLAS detector*, 2101.11582. 134

[176] ATLAS collaboration, G. Aad et al., *Search for new phenomena in final states with b-jets and missing transverse momentum in $\sqrt{s} = 13$ TeV pp collisions with the ATLAS detector*, 2101.12527. 134

[177] CMS collaboration, A. M. Sirunyan et al., *Search for singly and pair-produced leptoquarks coupling to third-generation fermions in proton-proton collisions at $\sqrt{s} = 13$ TeV*, *Phys. Lett. B* **819** (2021) 136446, [2012.04178]. 134

[178] D. B. Kaplan, *Flavor at SSC energies: A New mechanism for dynamically generated fermion masses*, *Nucl. Phys. B* **365** (1991) 259–278. 142

[179] S. J. Huber, *Flavor violation and warped geometry*, *Nucl. Phys. B* **666** (2003) 269–288, [hep-ph/0303183]. 142

[180] O. Domenech, A. Pomarol and J. Serra, *Probing the SM with Dijets at the LHC*, *Phys. Rev. D* **85** (2012) 074030, [1201.6510]. 142

[181] C. D. Froggatt and H. B. Nielsen, *Hierarchy of Quark Masses, Cabibbo Angles and CP Violation*, *Nucl. Phys. B* **147** (1979) 277–298. 142

[182] A. Davidson, M. Koca and K. C. Wali, *U(1) as the Minimal Horizontal Gauge Symmetry*, *Phys. Rev. Lett.* **43** (1979) 92. 142

[183] F. Bazzocchi, S. Bertolini, M. Fabbrichesi and M. Piai, *The Little flavons*, *Phys. Rev. D* **68** (2003) 096007, [hep-ph/0306184]. 143

[184] F. Bazzocchi, S. Bertolini, M. Fabbrichesi and M. Piai, *Fermion masses and mixings in the little flavon model*, *Phys. Rev. D* **69** (2004) 036002, [hep-ph/0309182]. 143

[185] F. Bazzocchi and M. Fabbrichesi, *A Heavy Higgs boson from flavor and electroweak symmetry breaking unification*, *Phys. Rev. D* **70** (2004) 115008, [hep-ph/0407358].

[186] F. Bazzocchi and M. Fabbrichesi, *Flavor and electroweak symmetry breaking at the TeV scale*, *Nucl. Phys. B* **715** (2005) 372–412, [hep-ph/0410107]. 143

[187] M. Bauer, M. Carena and K. Gemmler, *Flavor from the Electroweak Scale*, *JHEP* **11** (2015) 016, [1506.01719]. 143

[188] M. Bauer, M. Carena and K. Gemmler, *Creating the fermion mass hierarchies with multiple Higgs bosons*, *Phys. Rev. D* **94** (2016) 115030, [1512.03458]. 143

[189] T. Alanne, S. Blasi and F. Goertz, *Common source for scalars: Flavored axion-Higgs unification*, *Phys. Rev. D* **99** (2019) 015028, [1807.10156]. 143, 160

[190] Y. Chung, *Composite flavon-Higgs models*, *Phys. Rev. D* **104** (2021) 095011, [2104.11719]. 143

[191] CMS collaboration, A. M. Sirunyan et al., *Search for associated production of a Z boson with a single top quark and for tZ flavour-changing interactions in pp collisions at* $\sqrt{s} = 8$ *TeV*, *JHEP* **07** (2017) 003, [1702.01404]. 156

[192] ATLAS collaboration, M. Aaboud et al., *Search for flavour-changing neutral current top-quark decays* $t \to qZ$ *in proton-proton collisions at* $\sqrt{s} = 13$ *TeV with the ATLAS detector*, *JHEP* **07** (2018) 176, [1803.09923]. 156

[193] A. Azatov, G. Panico, G. Perez and Y. Soreq, *On the Flavor Structure of Natural Composite Higgs Models & Top Flavor Violation*, *JHEP* **12** (2014) 082, [1408.4525]. 157

[194] CMS collaboration, S. Chatrchyan et al., *Measurement of the* $B_s^0 \to \mu^+\mu^-$ *Branching Fraction and Search for* $B^0 \to \mu^+\mu^-$ *with the CMS Experiment*, *Phys. Rev. Lett.* **111** (2013) 101804, [1307.5025]. 157

[195] LHCb collaboration, R. Aaij et al., *Measurement of the* $B_s^0 \to \mu^+\mu^-$ *branching fraction and search for* $B^0 \to \mu^+\mu^-$ *decays at the LHCb experiment*, *Phys. Rev. Lett.* **111** (2013) 101805, [1307.5024].

[196] G. Buchalla, G. Hiller and G. Isidori, *Phenomenology of nonstandard Z couplings in exclusive semileptonic $b \to s$ transitions*, *Phys. Rev. D* **63** (2000) 014015, [hep-ph/0006136]. 157

[197] CMS collaboration, S. Chatrchyan et al., *Measurements of Differential Jet Cross Sections in Proton-Proton Collisions at $\sqrt{s} = 7$ TeV with the CMS Detector*, *Phys. Rev. D* **87** (2013) 112002, [1212.6660]. 159

[198] ATLAS collaboration, G. Aad et al., *Measurement of dijet cross sections in pp collisions at 7 TeV centre-of-mass energy using the ATLAS detector*, *JHEP* **05** (2014) 059, [1312.3524].

[199] ATLAS collaboration, G. Aad et al., *Measurement of the inclusive jet cross-section in proton-proton collisions at $\sqrt{s} = 7$ TeV using 4.5 fb^{-1} of data with the ATLAS detector*, *JHEP* **02** (2015) 153, [1410.8857].

[200] ATLAS collaboration, M. Aaboud et al., *Search for new phenomena in dijet events using 37 fb^{-1} of pp collision data collected at $\sqrt{s}$ =13 TeV with the ATLAS detector*, *Phys. Rev. D* **96** (2017) 052004, [1703.09127].

[201] CMS collaboration, A. M. Sirunyan et al., *Search for new physics with dijet angular distributions in proton-proton collisions at $\sqrt{s} = 13$ TeV*, *JHEP* **07** (2017) 013, [1703.09986].

[202] CMS collaboration, A. M. Sirunyan et al., *Search for narrow and broad dijet resonances in proton-proton collisions at $\sqrt{s} = 13$ TeV and constraints on dark matter mediators and other new particles*, *JHEP* **08** (2018) 130, [1806.00843].

[203] CMS collaboration, A. M. Sirunyan et al., *Search for high mass dijet resonances with a new background prediction method in proton-proton collisions at $\sqrt{s}$ = 13 TeV*, *JHEP* **05** (2020) 033, [1911.03947]. 159

[204] S. Alioli, M. Farina, D. Pappadopulo and J. T. Ruderman, *Precision Probes of QCD at High Energies*, *JHEP* **07** (2017) 097, [1706.03068]. 159

[205] B. Bellazzini, F. Riva, J. Serra and F. Sgarlata, *The other effective fermion compositeness*, *JHEP* **11** (2017) 020, [1706.03070]. 159

[206] ATLAS, CMS collaboration, G. Aad et al., *Measurements of the Higgs boson production and decay rates and constraints on its couplings from a combined ATLAS and CMS analysis of the LHC pp collision data at $\sqrt{s} = 7$ and 8 TeV*, *JHEP* **08** (2016) 045, [1606.02266]. 159

[207] S. Dawson and C. W. Murphy, *Standard Model EFT and Extended Scalar Sectors*, *Phys. Rev. D* **96** (2017) 015041, [1704.07851]. 159

[208] P. Cox, T. Gherghetta and M. D. Nguyen, *A Holographic Perspective on the Axion Quality Problem*, *JHEP* **01** (2020) 188, [1911.09385]. 160

[209] T. Gherghetta and M. D. Nguyen, *A Composite Higgs with a Heavy Composite Axion*, *JHEP* **12** (2020) 094, [2007.10875].

[210] Q. Bonnefoy, P. Cox, E. Dudas, T. Gherghetta and M. D. Nguyen, *Flavoured Warped Axion*, *JHEP* **04** (2021) 084, [2012.09728]. 160

[211] Y. Ema, K. Hamaguchi, T. Moroi and K. Nakayama, *Flaxion: a minimal extension to solve puzzles in the standard model*, *JHEP* **01** (2017) 096, [1612.05492]. 160

[212] L. Calibbi, F. Goertz, D. Redigolo, R. Ziegler and J. Zupan, *Minimal axion model from flavor*, *Phys. Rev. D* **95** (2017) 095009, [1612.08040]. 160

[213] T. Gherghetta, V. V. Khoze, A. Pomarol and Y. Shirman, *The Axion Mass from 5D Small Instantons*, *JHEP* **03** (2020) 063, [2001.05610]. 160

[214] A. R. Zhitnitsky, *On Possible Suppression of the Axion Hadron Interactions. (In Russian)*, *Sov. J. Nucl. Phys.* **31** (1980) 260. 160

[215] M. Dine, W. Fischler and M. Srednicki, *A Simple Solution to the Strong CP Problem with a Harmless Axion*, *Phys. Lett. B* **104** (1981) 199–202. 160

[216] S. Raby, *Supersymmetric Grand Unified Theories: From Quarks to Strings via SUSY GUTs*, vol. 939. Springer, 2017, 10.1007/978-3-319-55255-2. 186

Associated Publications

- L. Da Rold and F. Lamagna,*Composite Higgs and leptoquarks from a simple group*, *JHEP* **03** (2019) 135, [1812.08678]
- L. Da Rold and F. Lamagna, *A vector leptoquark for the B-physics anomalies from a composite GUT*, *JHEP* **12** (2019) 112, [1906.11666]
- L. Da Rold and F. Lamagna, *A model for the Singlet-Triplet Leptoquarks*, *Phys. Rev. D* **103** (2021) 115007, [2011.10061]
- L. Da Rold and F. Lamagna, *A composite Froggatt-Nielsen model of flavor*, *Phys. Rev. D* **105** 115020, [2112.14600]